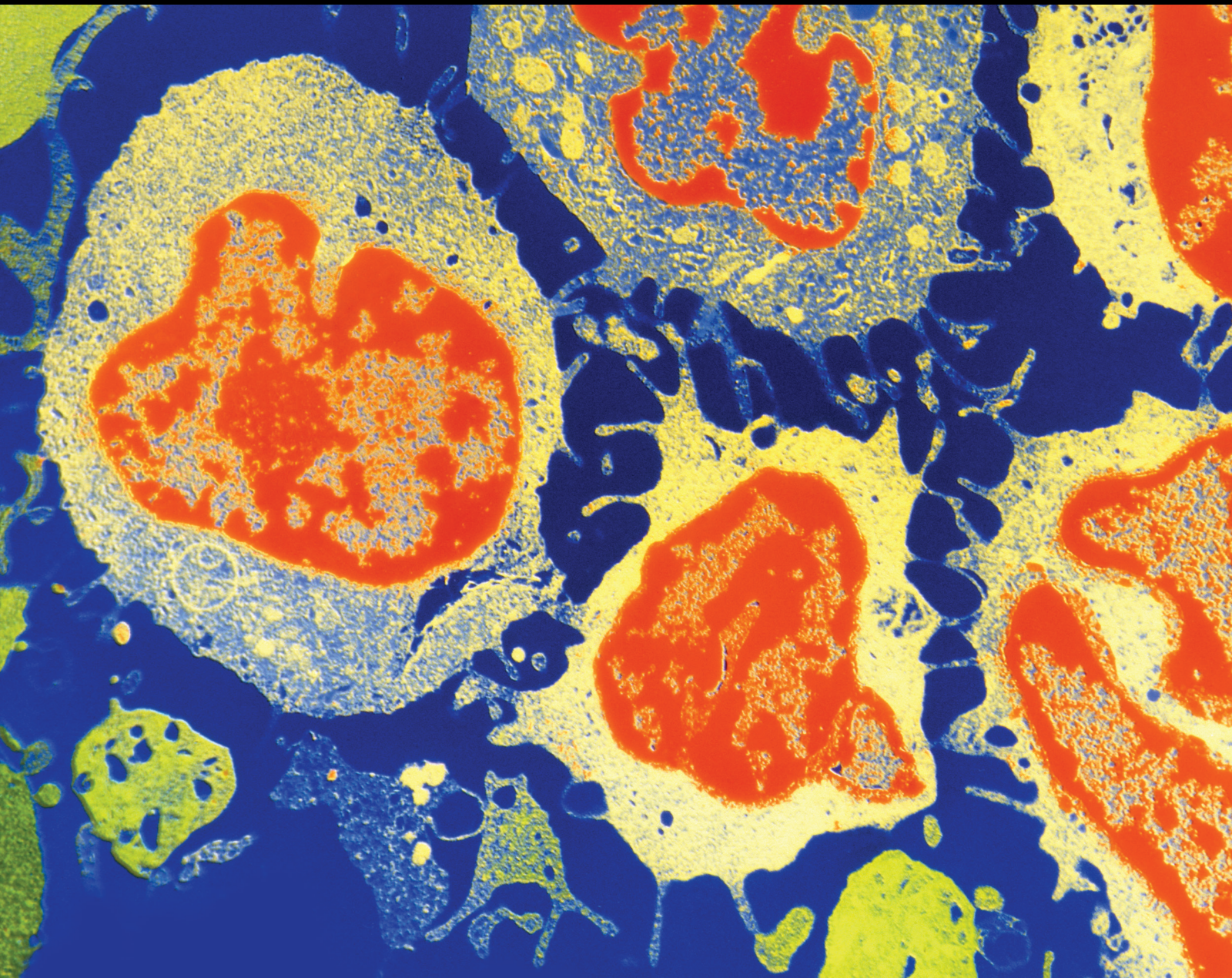# Competing Endogenous RNAs (ceRNAs): Emerging Regulators of Cancer

Lead Guest Editor: Zhiqian Zhang
Guest Editors: Baotong Zhang, Fangfang Tao, and Li-Bin Wang

Competing Endogenous RNAs (ceRNAs): Emerging Regulators of Cancer

Competing Endogenous RNAs (ceRNAs): Emerging Regulators of Cancer

Lead Guest Editor: Zhiqian Zhang
Guest Editors: Baotong Zhang, Fangfang Tao, and Li-Bin Wang

Contents

Chidamide and Radiotherapy Synergistically Induce Cell Apoptosis and Suppress Tumor Growth and Cancer Stemness by Regulating the MiR-375-EIF4G3 Axis in Lung Squamous Cell Carcinomas

Xu Huang (iD), Nan Bi (iD), Jingbo Wang (iD), Hua Ren (iD), Desi Pan (iD), Xianping Lu (iD), and Luhua Wang (iD)

Research Article

Correlation between Genes of the ceRNA Network and Tumor-Infiltrating Immune Cells and Their Biomarker Screening in Kidney Renal Clear Cell Carcinoma

Aoran Kong,[1,2] Hui Dong,[3] Guangwen Zhang,[4] Shuang Qiu,[5] Mengyuan Shen,[6] Xiaohan Niu,[7] and Lixin Wang [1]

[1] *Center of Laboratory Medicine, General Hospital of Ningxia Medical University, Yinchuan 750004, China*
[2] *Clinical Laboratory, XiangYang Hospital of Traditional Chinese Medicine, Xiangyang, Hubei 441000, China*
[3] *Institute of Medical Sciences, General Hospital of Ningxia Medical University, Yinchuan 750004, China*
[4] *Department of Radiology, Xijing Hospital, Fourth Military Medical University, Xi'an, Shaanxi, China*
[5] *Clinical Laboratory, Yichang Central Hospital, Yichang, Hubei 443000, China*
[6] *Clinical Laboratory, ShangHai Changzheng Hospital, Shanghai 200003, China*
[7] *Department of Medical Examination, The People's Hospital of West Coast, Qingdao, Shangdong 2664000, China*

Correspondence should be addressed to Lixin Wang; 13895630916@nyfy.com.cn

This study aimed to using bioinformatics tools, qPCR, and the immunohistochemical analysis to find out factors related to the early diagnosis and prognosis of kidney renal clear cell carcinoma (KIRC). The expression profiles of lncRNA, miRNA, and mRNA of KIRC were downloaded from The Cancer Genome Atlas database. A ceRNA regulatory network was constructed based on the interaction between these three differentially expressed genes. The CIBERSORT deconvolution algorithm was used to analyze the differential distribution of 22 types of immune cells. The Kaplan–Meier survival and Cox analyses were used to screen genes of the ceRNA network and also immune cell subtypes related to the clinical and prognostic prediction of KIRC. Co-expression regulatory relationships were found among LINC01426, LINC00894, CCNA2, L1 cell adhesion molecule (L1CAM), and T follicular helper cells, which served as potential biomarkers. The results of quantitative reverse transcriptase-polymerase chain reaction showed that LINC01426 was upregulated while L1CAM was downregulated in KIRC, but no difference was found in the expression levels of LINC00894 and CCNA2 in cancer and adjacent samples. The immunohistochemical analysis showed that T follicular helper cells were more concentrated in core tissues and metastases of KIRC. In a word, co-expression relationships were found among LINC01426, L1CAM, and T follicular helper cells, and they may serve as biomarkers for early diagnosis and prognostic evaluation of KIRC.

1. Introduction

Kidney renal clear cell carcinoma (KIRC) originates from proximal tubular epithelial cells [1]. It is the most common and aggressive subtype of renal cancer, accounting for approximately 75%–80% [2]. Most patients are diagnosed in the advanced stage because the initial clinical symptoms and signs of KIRC are relatively hidden [3]. Compared with other subtypes of kidney cancer, KIRC has a higher recurrence rate and metastasis rate. Although surgical treatment, molecular-targeted therapy (sorafenib and sunitinib), immunotherapy (interleukin-2), and other treatments developed in recent years have greatly improved the survival time of patients; the 5-year survival rate is still less than 10% [4, 5]. Therefore, a biomarker that can detect KIRC early and predict its prognosis needs to be identified.

Salmena et al. formulated a hypothesis about ceRNA in 2011; they believed that long noncoding RNAs (lncRNAs)

use some core seed sequences to adsorb the corresponding miRNA, thereby interfering with the abundance of target gene mRNA and affecting gene expression [6]. A large number of studies have shown that ceRNA played a vital role in the occurrence, development, and prognosis of tumors [7]. For example, Wang et al. experimentally proved that lncRNA UCA1 was used as the ceRNA of miR-182-5p to positively regulate the expression of Delta-like4 (DLL4), thereby promoting the malignant phenotype of renal cancer cells and playing a carcinogenic role in the pathogenesis of renal cancer [8]. Human immune surveillance is an important immune function of the body to prevent tumors, and evading the destruction of the body's immune function is one of the important mechanisms of tumors [9, 10]. In recent years, the distribution and density of local immune cells have received wide attention from scholars in tumor diagnosis and prognostic evaluation [11]. Studies have shown differences in infiltrating immune cells in different types of sarcoma [12]. Liang et al. found that Janus Kinase 3 (JAK3) moderately to strongly positively correlated with the abundance of B cells, CD8+ T cells, CD4+ T cells, neutrophils, and dendritic cells in KIRC, which may become potential biomarkers of KIRC [13]. Although a large number of studies have explored the correlation between infiltrating immune cells and tumor occurrence, development, prognosis, and so on, the specific mechanism of action in tumors has not yet been clearly elucidated.

This topic analyzed the potential roles of the ceRNA network and tumor-infiltrating immune cells in KIRC in tumorigenesis, metastasis, and prognosis. A flowchart explaining this process is given in Figure 1. In conclusion, this study might offer new ideas for prognostic monitoring of patients with KIRC and research on new treatment methods.

2. Materials and Methods

2.1. Data Acquisition and Differential Expression Analysis of Genes. Metadata files, manifest files, and cart files of KIRC transcriptome and miRNA and patient clinical information were downloaded from The Cancer Genome Atlas (TCGA) database. After decompressing the cart file, the Perl script was run to obtain the original transcriptome and miRNA matrix files. The gene names were converted using the human. gtf file downloaded from the Ensembl database and the mature. fa file downloaded from the miRBase database. DESeq2 package in R4.0.2 software was used for differential expression analysis to obtain differentially expressed lncRNAs, miRNAs, and mRNA ((false discovery rate, FDR) < 0.05, |log (fold change)| > 2).

2.2. Construction of the ceRNA Network. LncRNA–miRNA and miRNA–mRNA interactions predicted from the miRcode [14] and StarBase [15] databases, respectively, showing significant results in hypergeometric testing and correlation analysis, were selected for the visualization of the ceRNA network using the Cytoscape 3.7.2 software.

2.3. Clinical Significance of the ceRNA Network in KIRC. Single-factor Cox regression, lasso regression, and multifactor Cox regression analyses were performed on all genes in the ceRNA network, and a risk scoring model was built for the selected genes. The diagnostic value of the model was assessed through the risk survival curve and receiver operating characteristic (ROC) curve. The Kaplan–Meier survival method was employed to perform the survival analysis of all genes in the network in batches.

2.4. Abundance Analysis and Differential Expression Analysis of Infiltrating Immune Cells. The gene expression feature set of 22 types of immune cell subtypes was downloaded from the CIBERSORT website. Based on the gene expression profile, the e1071 package was run to obtain the abundance of infiltrating immune cells and statistical accuracy (P value) of 22 types of immune cells in each sample (the number of permutations was set to 1000). The samples with $P < 0.05$ were retained for subsequent analysis. The difference in immune cells between KIRC tissue and adjacent tissues was analyzed by a two independent-sample t test.

2.5. Survival Correlation Analysis of Infiltrating Immune Cells in KIRC. Single-factor Cox regression, lasso regression, and multifactor Cox regression analyses were conducted on infiltrating immune cells to build a risk assessment model. The risk survival curve and ROC curve were drawn to evaluate the diagnostic value of the model. The correlation between immune cell subtypes and clinical metastasis was predicted using the Wilcoxon rank-sum test (The clinical research objects are all T staging in TNM). The Kaplan–Meier survival method was used to analyze the survival of all immune cells with different distributions.

2.6. Co-expression Analysis of Genes in the ceRNA Network and Immune Cells. The relationship between ceRNAs and 22 types of immune cells was investigated using Pearson's correlation coefficient.

2.7. Quantitative Reverse Transcriptase–Polymerase Chain Reaction. Quantitative reverse transcriptase-polymerase chain reaction (qRT-PCR) was used to quantitatively express key genes in the ceRNA network. Clinical tissue cDNA chips were purchased from Shanghai Outdo Biotech Co., Ltd. The chip lot number was cDNA-HKidE030CS01 (15 cases of renal clear cell carcinoma, 1 spot on the cancer/ adjacent, the RNA of the frozen sample was reverse-transcribed into cDNA and spotted on a 96-well plate, and the samples covered clinical stage 1, stage 2, and stage 3.). The relative expression levels of lncRNA and mRNA in cancer and adjacent cancer samples of KIRC were detected using the PerfectStart Green qPCR SuperMix (TransGen Biotech, China) following manufacturer's instructions. Primers for lncRNA and mRNA are shown in Table 1. The reaction conditions were predenaturation at 94°C for 30 seconds; 94°C for 5 seconds, 60°C for 30 seconds, 40 cycles; finally, the temperature was lowered to 37°C for 20 min until
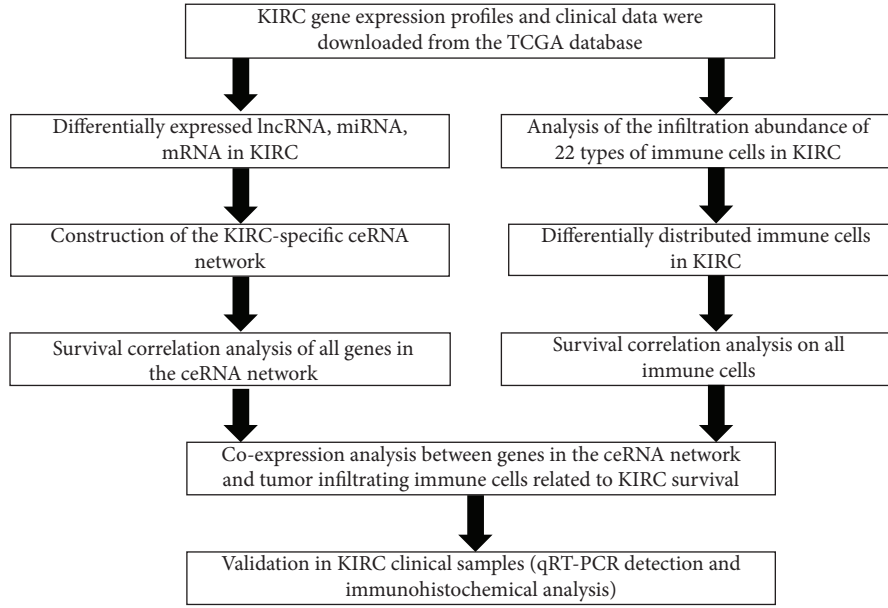
FIGURE 1: A flowchart depicting the analytical process.

TABLE 1: Primers for lncRNA and mRNA.

Gene		Primer sequence (5′-3′)
LINC01426	F	ACTGTCCCTTTATCACCCTT
	R	CGTTGAAGCTCCTTGCCTAT
LINC00894	F	GCTCCTGGGACCACATTA
	R	TAGTACAAGCTGAGGCAAA
L1CAM	F	TGGGAATGTAAATACACCGTGAC
	R	GCACAGGCATACAGGGAGG
CCNA2	F	ATGAGCATGTCACCGTTCC
	R	AAGCCAGGGCATCTTCACG

F : forward, R : reverse.

the reaction was completed. The gene expression profiles downloaded from TCGA database were statistically analyzed in the R software (GDCRNATools, ggplot2, DESeq2, survival, glmnet, survminer). The results of qRT-PCR were analyzed by $2^{-\triangle\triangle Ct}$ and independent t test in IBM SPSS statistics 25.0.

2.8. Immunohistochemistry in Clinical Tissues. Clinical tissue chips were purchased from Shanghai Outdo Biotech Co., Ltd. The chip lot number was KidE085CS01 (26 cases of renal clear cell carcinoma, one spot on the carcinoma/adjacent/distal, and 7 metastases, one site per metastases, and the samples covered clinical stage 1, stage 2, and stage 3). Immunohistochemical (IHC) staining was performed using a Leica BOND-MAX auto-stainer (Leica Instrument Co., Ltd., Germany), and the CD4 (EP204) rabbit mAb (48274, Cell Signaling Technology, China) was diluted to 1 : 200. The marker of T follicular helper cells was CD4, respectively [16]. IHC was performed as follows. Briefly, 4μm thick tissue

sections were cut with a microtome, deparaffinized in xylene, dehydrated through graded ethanol (100% and 95%), and rinsed with water. Subsequently, the sections were subjected to heat-induced antigen retrieval and finally loaded onto the Benchmark auto-stainer, and the detection was performed using a bond polymer refine detection kit (Leica Instrument Co., Ltd.).

2.9. Immunohistochemical Digital Pathological Analysis. The expression levels of CD4 were estimated by QuPath (open source software for Quantitative Pathology, version 0.2.0) [17]. Each slice included 26 cores of tumor tissues, corresponding peritumor normal renal tissue, distal normal renal tissue, and 7 cores of metastatic renal carcinoma. Digitized IHC microarrays of CD4 were acquired at 100× magnification using an Olympus slide scanner (Olympus motorized BX61VS). The annotation of each core was manually delineated on the pathological slice, while the peritumoral region of the tumoral core and nonspecific staining was excluded. Then, cells within the annotations were detected. The positive cell ratio, Allred score, and H score of each core were calculated to assess the expression levels of CD4. The process of digital analysis of IHC is shown in Supplemental Material 3.

2.10. Statistical Analysis. All statistical analyses of the gene expression profiles downloaded from the TCGA database and the immune cells obtained by the CIBERSORT algorithm were performed using the R version 4.0.2 software. The qRT-PCR results were calculated using the $2^{-\triangle\triangle Cq}$ method and the paired samples t test, and the IHC results were analyzed using nonparametric tests. The

FIGURE 2: ceRNA network in KIRC.

(a)

(b)

FIGURE 3: Continued.
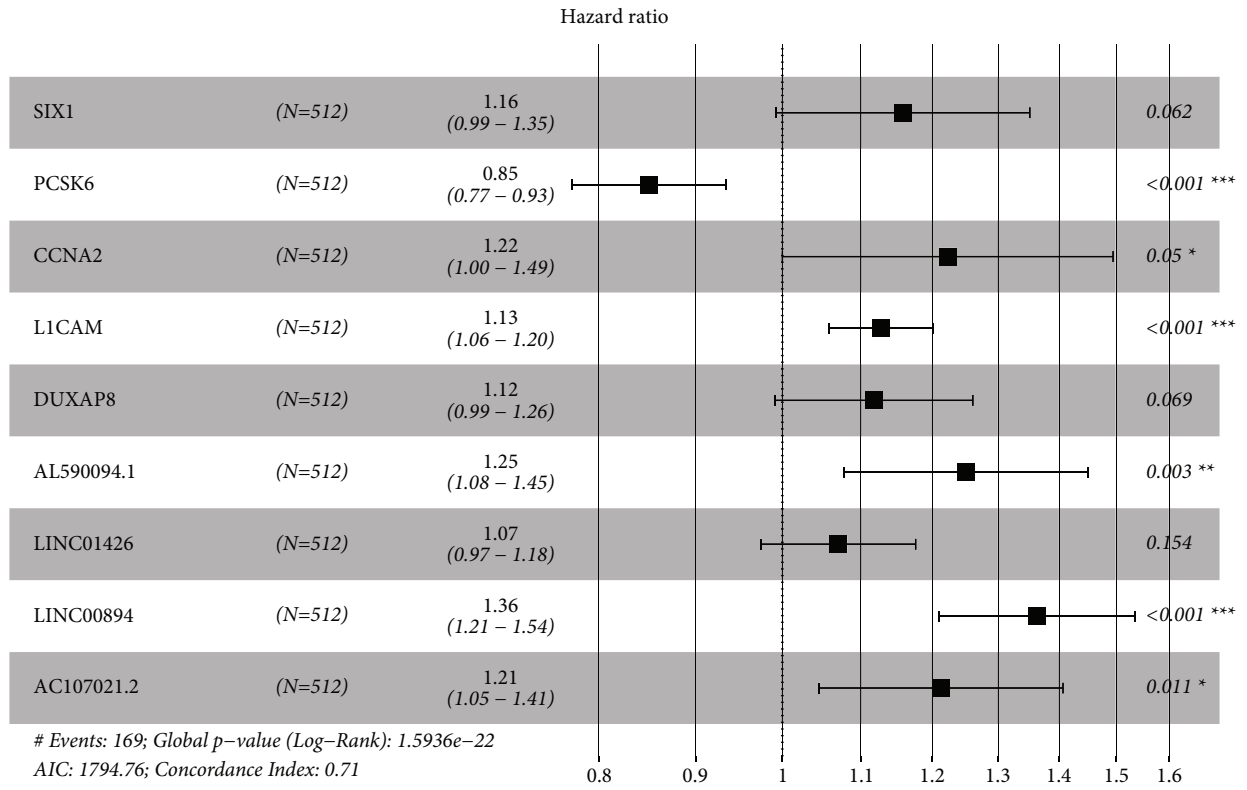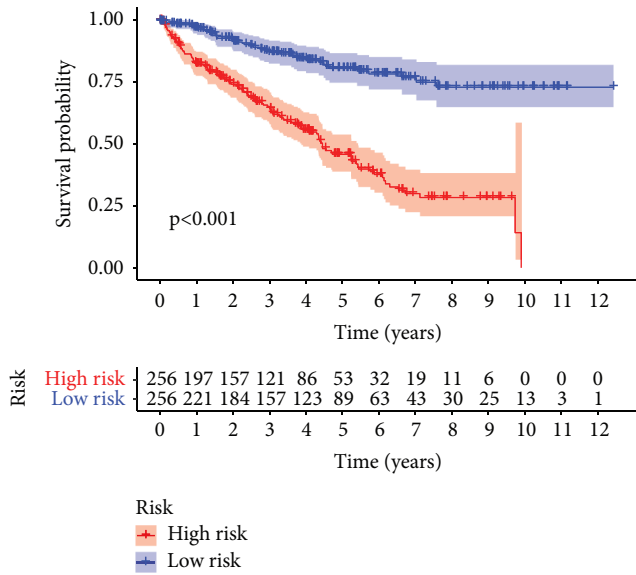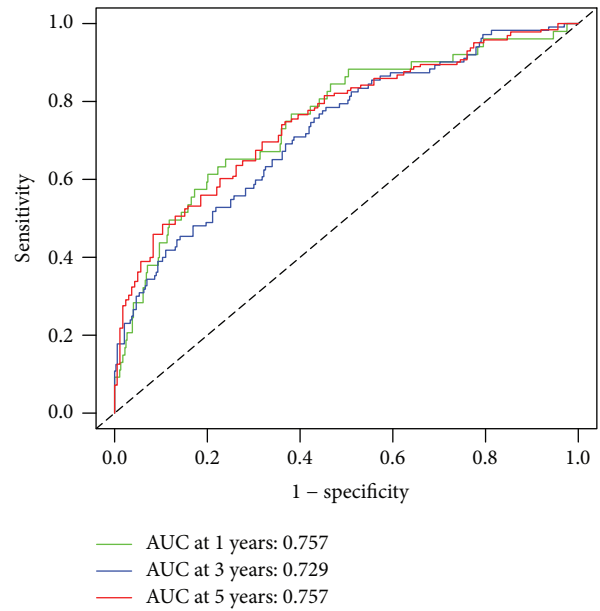
FIGURE 3: Screening of key genes. ((a)–(c)) Construction of the risk scoring model. (d) Kaplan–Meier risk survival curve of patients with KIRC. (e) ROC curve assessed the diagnostic efficacy of the model.
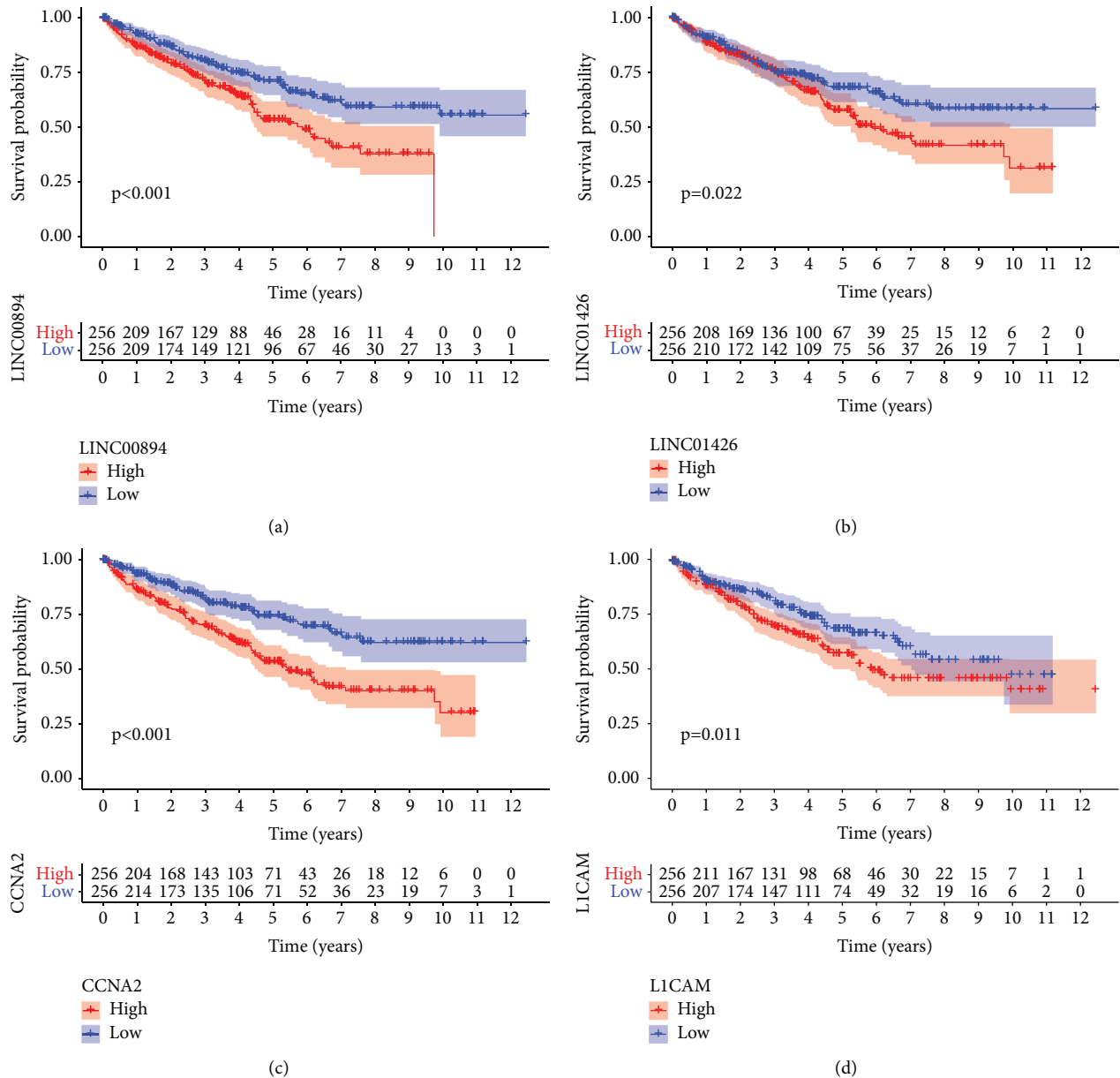
Figure 4: Kaplan–Meier survival curve of key genes. (a) Kaplan–Meier survival curve of LNC00894. (b) Kaplan–Meier survival curve of LINC01426. (c) Kaplan–Meier survival curve of CCNA2. (d) Kaplan–Meier survival curve of L1CAM.

aforementioned analysis was performed using the IBM SPSS statistics 25.0 software. Only the two-sided P value <0.05 was considered to be of statistical significance.

3. Results and Discussion

3.1. Identification of Differentially Expressed Genes. KIRC transcriptome data of 611 cases (72 cases in the normal group and 539 cases in the cancer group) and miRNA data of 616 cases (71 cases in the normal group and 545 cases in the cancer group) were downloaded from the TCGA database. Gene differential expression analysis revealed 126 DElncRNAs (119 upregulated and 7 downregulated), 25

DEmiRNAs (12 upregulated and 13 downregulated), and 957 DEmRNAs (688 upregulated and 269 downregulated). See Supplementary Material 1 for all differential gene names.

3.2. Construction of the ceRNA Network Based on Differentially Expressed Genes. A ceRNA network, composed of 97 pairs of lncRNA–miRNA and 41 pairs of miRNA–mRNA predicted from the miRcode and StarBase databases, respectively, was constructed (Figure 2), which included 57 lncRNAs, 7 miRNAs, and 34 mRNAs. The lncRNA, miRNA, and mRNA gene names in the ceRNA network are listed in Supplementary Material 2.
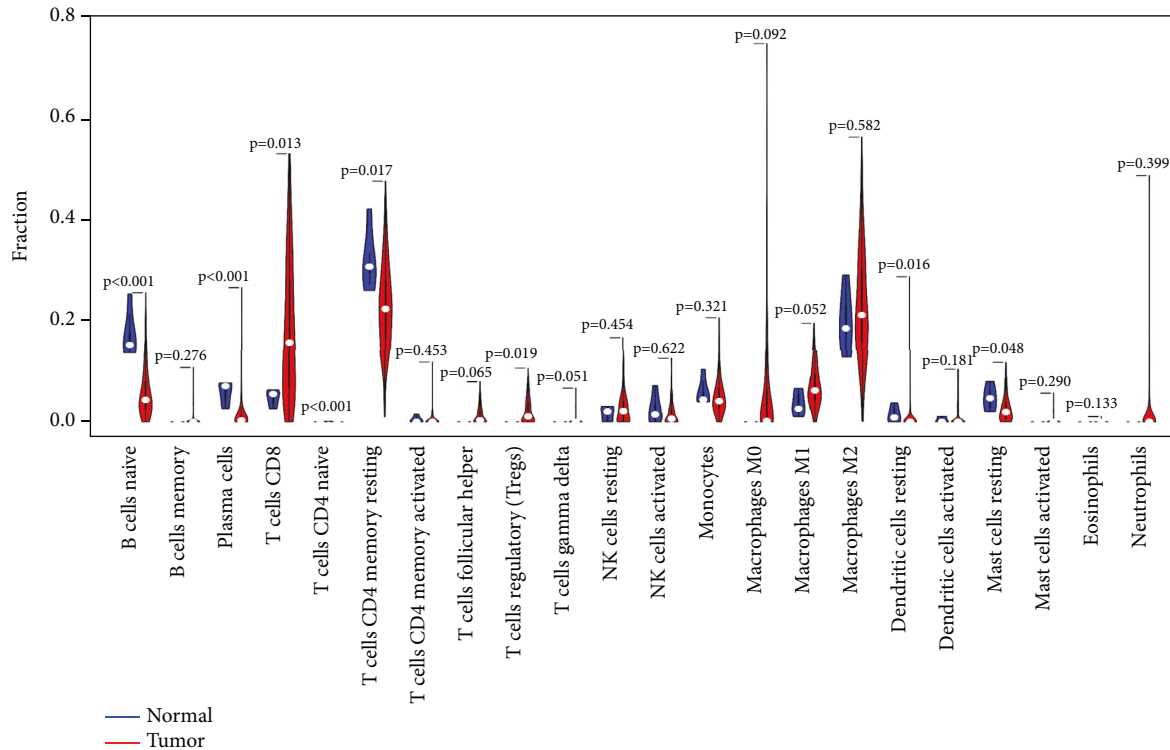
FIGURE 5: Difference in the proportions of 22 types of immune cells in cancer and adjacent cancer samples.

3.3. Survival Analysis of the ceRNA Network in KIRC. After performing Cox regression analysis on the ceRNA network, nine genes (SIX1, PCSK6, CCNA2, L1 cell adhesion molecule (L1CAM), DUXAP8, AL590094.1, LINC01426, LINC00894, and AC107021.2) were obtained to construct a risk scoring model (Figures 3(a)–3(c)). The risk survival curve indicated that the survival rate of the high-risk group was significantly lower compared with the low-risk group ($P < 0.001$) (Figure 3(d)). The area under the curve (AUC) (1-, 3-, and 5-year survival was 0.757, 0.729, and 0.757, respectively) of the ROC curve indicated a higher diagnostic efficiency of the model (Figure 3(e)). The Kaplan–Meier survival analysis showed that LINC00894, LINC01426, CCNA2, and L1CAM were significant to patients with KIRC (Figures 4(a)–4(d)).

3.4. Composition of Immune Cells in KIRC. The CIBERSORT algorithm was used to obtain the immune cell infiltration abundance of all samples, and 223 samples with $P < 0.05$ were retained for subsequent analysis. The heatmap and the violin map showed the difference in the distribution of immune cells between cancer and adjacent cancer samples (Figure 5).

3.5. Clinical Correlation Analysis of Immune Cells in KIRC. Three potential prognostic biomarkers (T-cell CD4 memory activated, T follicular helper cells, and resting mast cells) were regarded as key members among 22 types of immune cells and were integrated into a new multivariable model (Figures 6(a)–6(c)). The risk survival curve suggested that the survival rate of the high-risk group was considerably higher than that of the low-risk group ($P = 0.006$) (Figure 6(d)). The ROC curve (AUC of 1-, 3-, and 5-year survival was 0.587, 0.642, and 0.616, respectively) demonstrated the sensitivity and specificity of the model (Figure 6(e)).

The Wilcoxon rank-sum test suggested that resting mast cells had significant differences in T stage and stage (Figures 7(a) and 7(b)). The results of the Kaplan–Meier survival analysis showed that plasma cells (Figure 7(c)), T follicular helper cells (Figure 7(d)), and regulatory T cells (Figure 7(e)) correlated with the survival of patients with KIRC.

3.6. Co-Expression Analysis. Important co-expression patterns between immune cells (Figure 8(a)), key members of the ceRNA network, and co-expression of some important co-expression patterns of key members of immune cells (Figure 8(b)) were analyzed. The results showed a positive correlation between CCNA2 and T follicular helper cells ($R = 0.37$, $P < 0.001$) (Figure 8(c)), between L1CAM and T follicular helper cells ($R = 0.30$, $P < 0.001$) (Figure 8(d)), between LINC00894 and T follicular helper cells ($R = 0.35$, $P < 0.001$) (Figure 8(e)), and between LINC01426 and T follicular helper cells ($R = 0.24$, $P < 0.001$) (Figure 8(f)). These results indicated that their relationship might be a biomarker for the diagnosis and prognosis of KIRC.
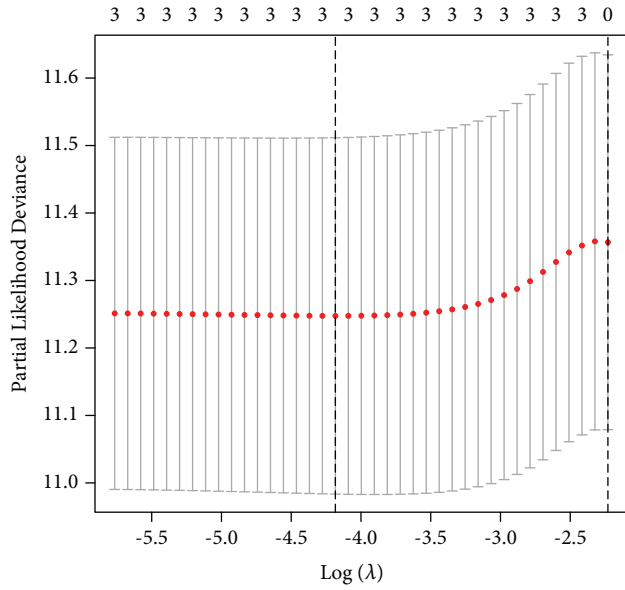
(a)
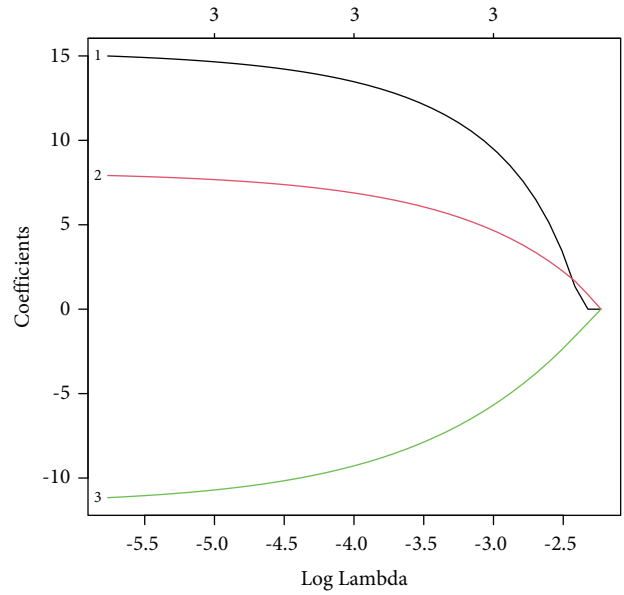
(b)
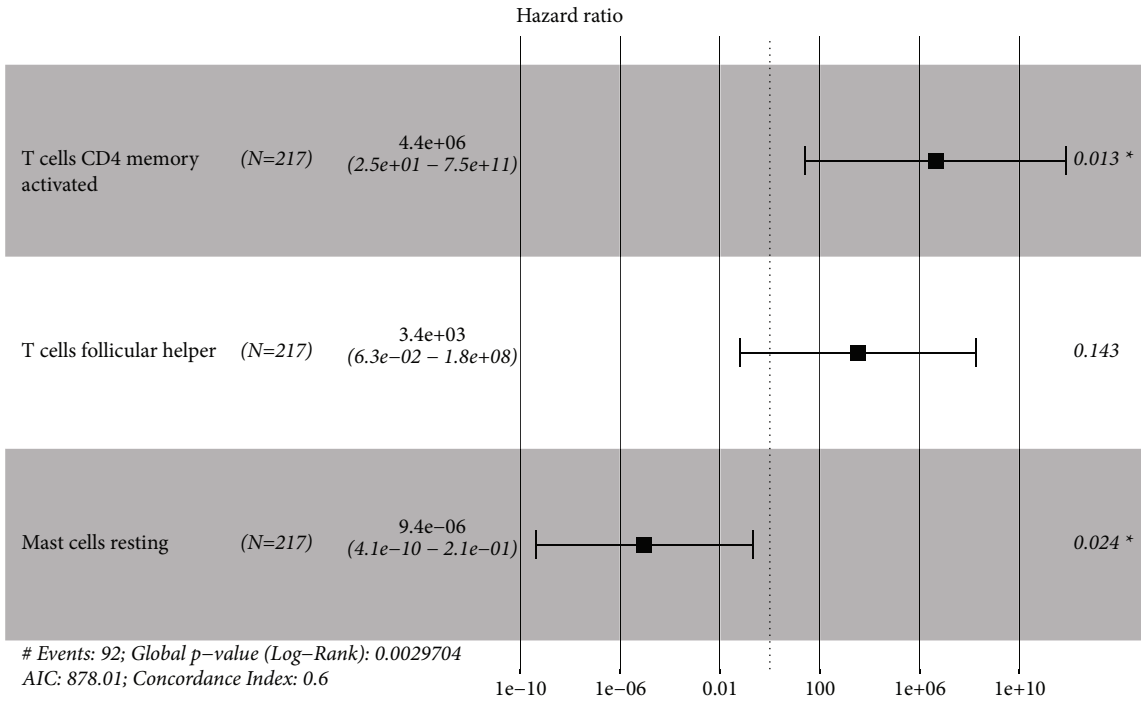
(c)

FIGURE 6: Continued.

(d)

(e)
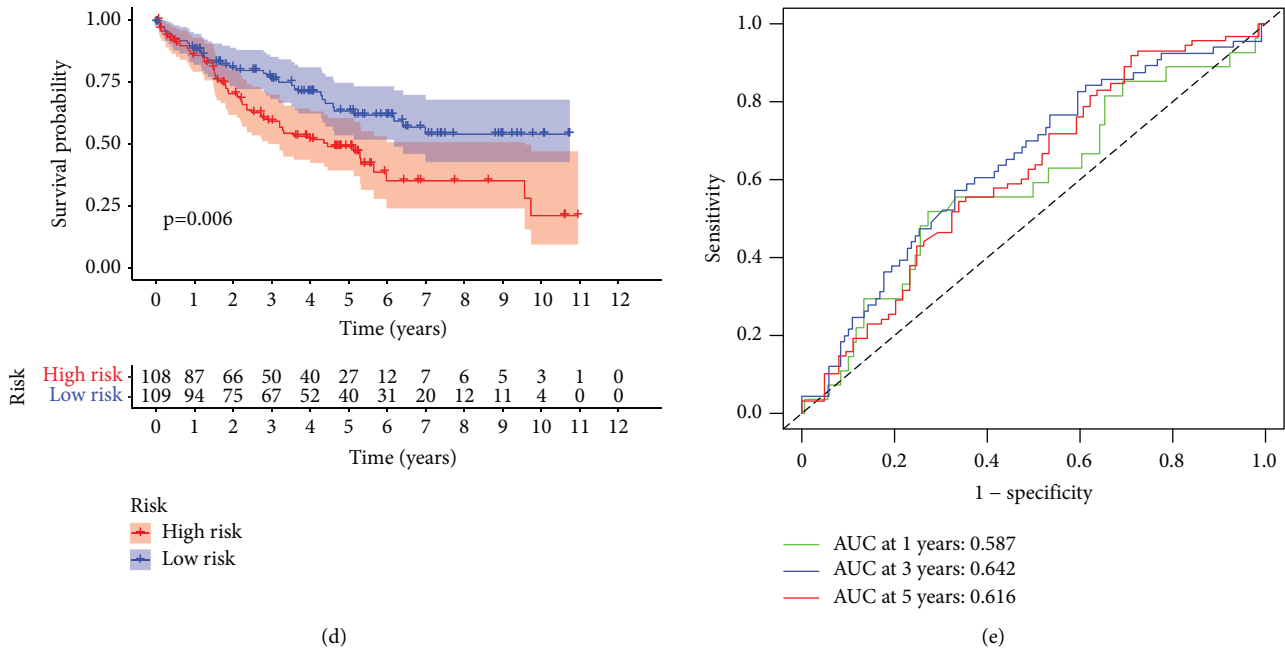
Figure 6: Identification of significant immune cells. ((a)–(c)) Lasso and Cox regression analyses. (d) Risk survival curve of the high- and low-risk groups. (e) ROC curve analysis for predicting the 1-, 3-, and 5-year survival.

(a)

(b)

Figure 7: Continued.

(c)

(d)

(e)
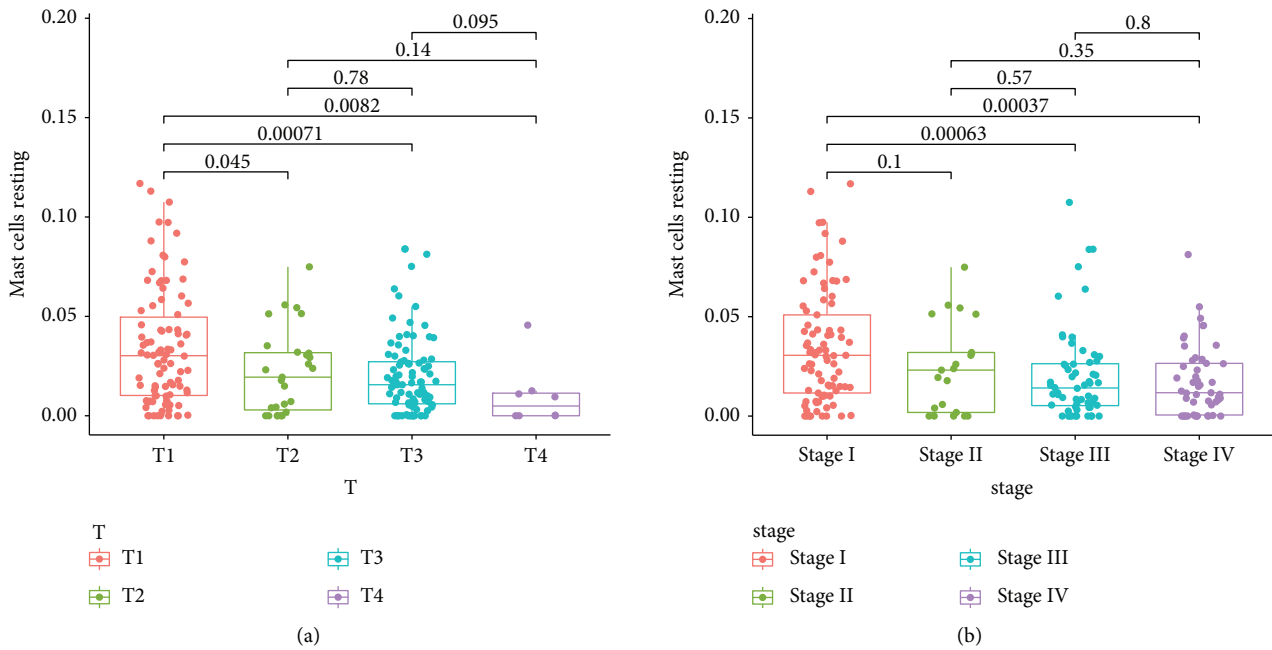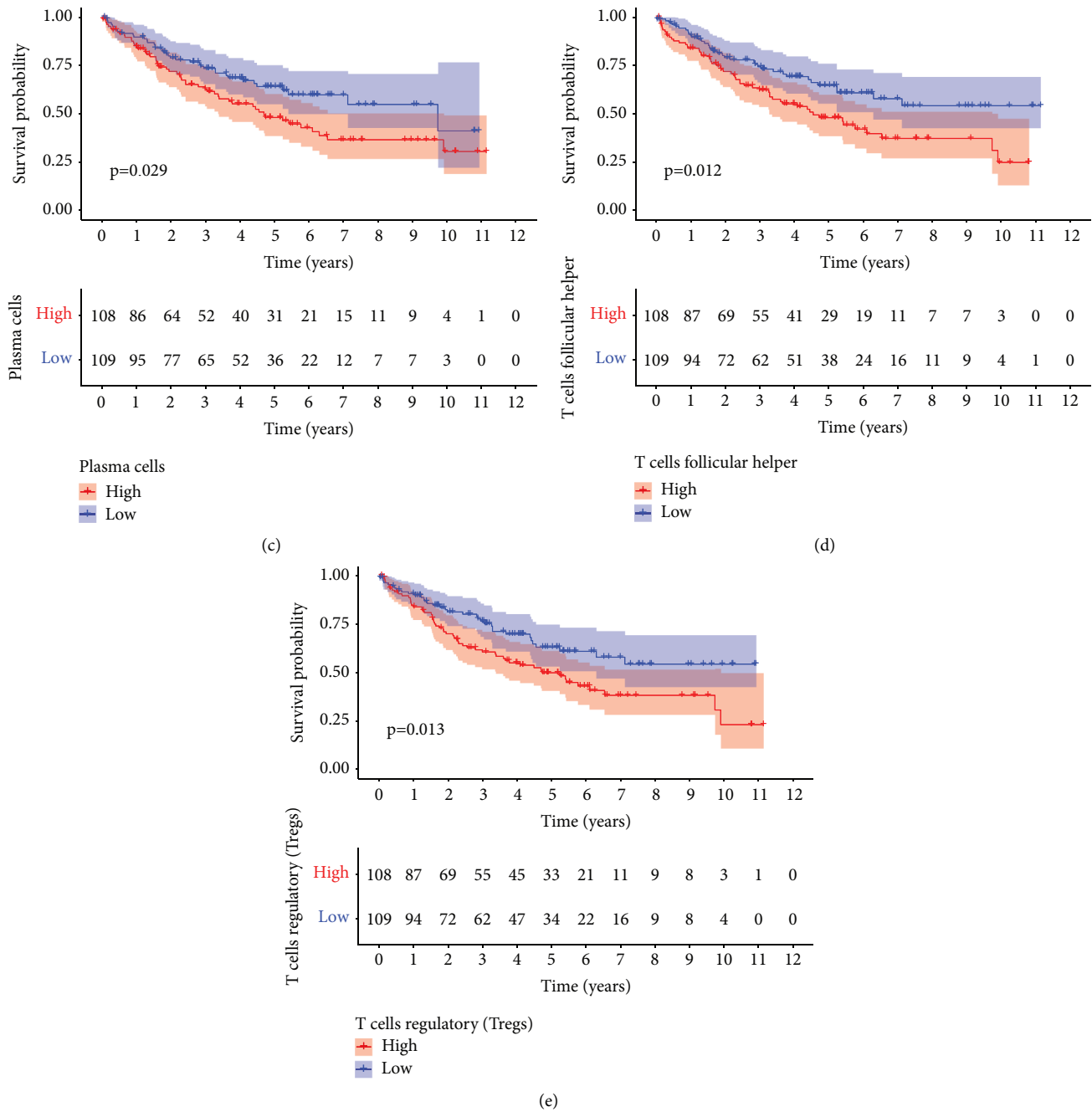
FIGURE 7: The relationship between significant immune cells and tumor stage and survival. (a) Box plots of T stages of resting mast cells. (b) Box plots of the stage of resting mast cells. (c) Kaplan–Meier survival analysis of plasma cells. (d) Kaplan–Meier survival analysis of T follicular helper cells. (e) Kaplan–Meier survival analysis of regulatory T cells.

4. Results of Clinical Tissue Specimen Verification

The qRT-PCR results showed that lncRNA LINC01426 was upregulated while mRNA L1CAM was downregulated in kidney cancer tissues, which was consistent with the expression pattern in the TCGA database ($P < 0.05$) (Figures 9(a) and 9(b)). However, there was no difference in expression levels of lncRNA LINC00894 and CCNA2 mRNA in renal cancer tissue and adjacent tissue ($P > 0.05$)

(Figures 9(c) and 9(d)). The IHC results showed that the level of T follicular helper cells (CD4 marker positive) was the highest in the core of tumor tissues, which was significantly different from the corresponding normal renal tissue adjacent to cancer, distal normal renal tissue and metastatic renal cancer core tissue ($P < 0.05$). The level of T-follicular helper cells is the second highest in the metastatic renal cell carcinoma core tissue, which was a significant difference between adjacent normal renal tissues and distal normal renal tissue ($P < 0.05$) (Figures 9(e) and 9(f)). The results demonstrated
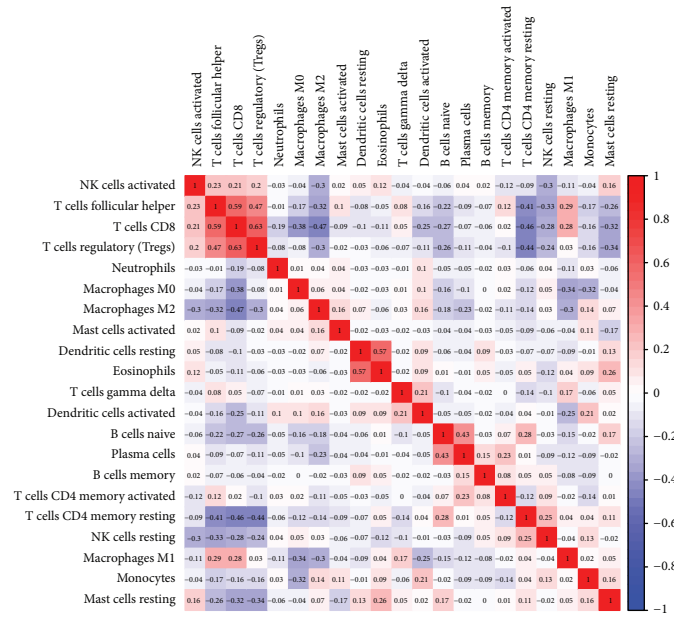
(a)
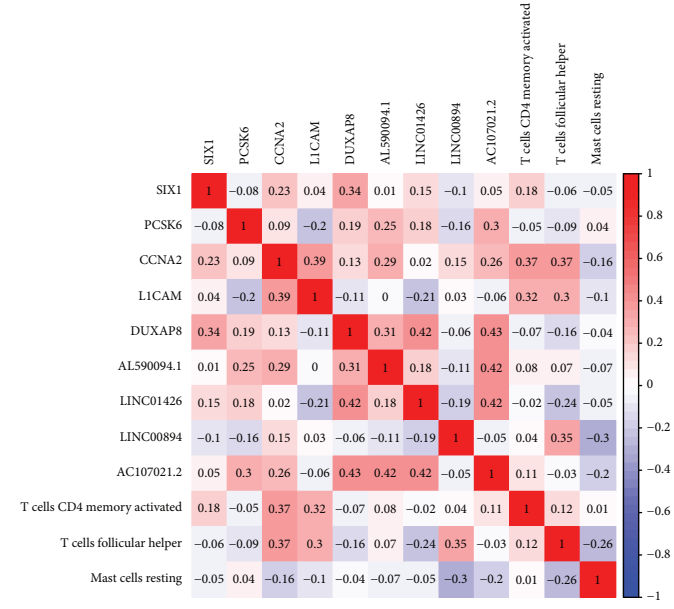
(b)

Figure 8: Continued.

(c)

(d)

(e)

(f)
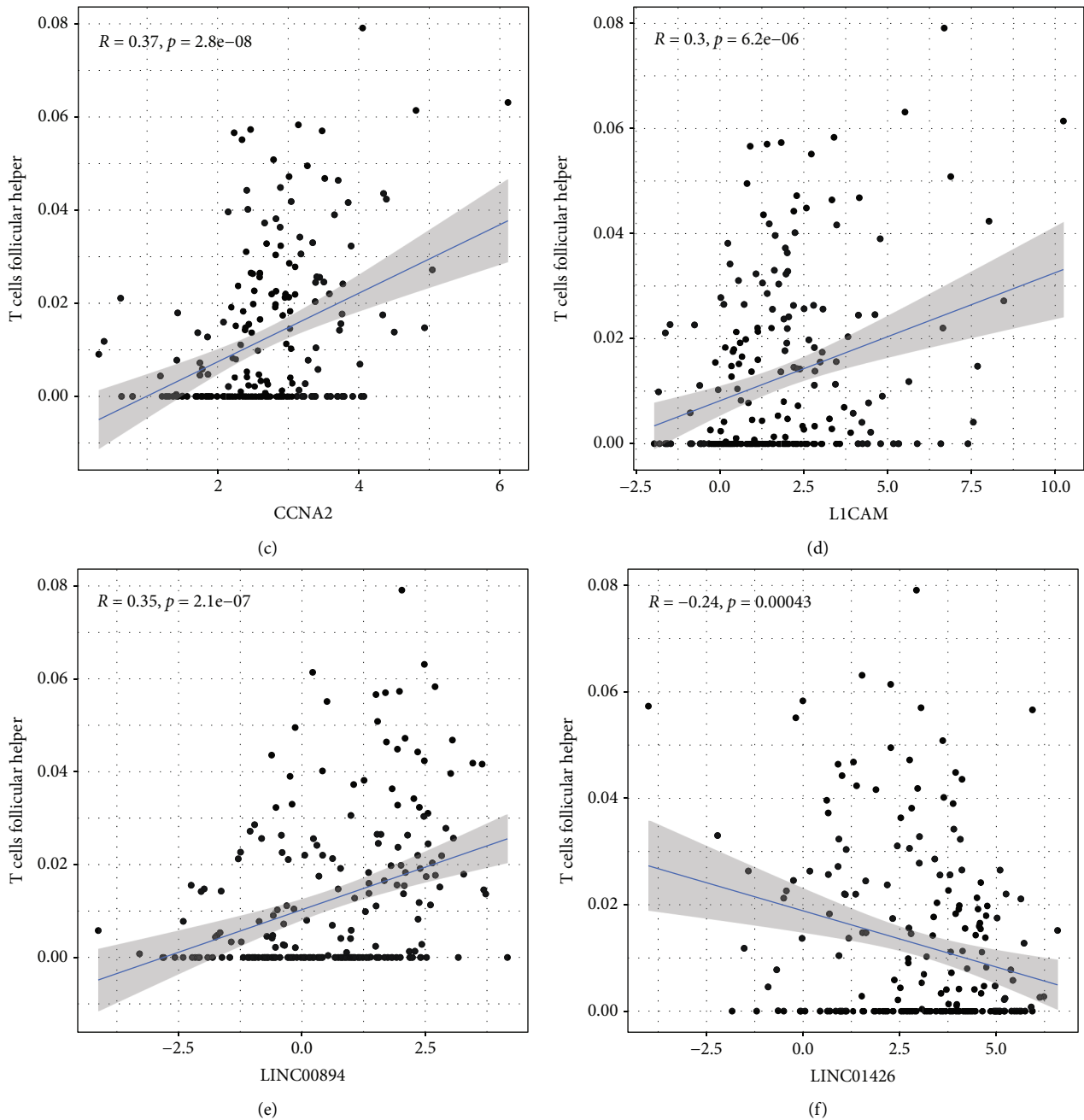
FIGURE 8: Co-expression analysis between tumor-infiltrating immune cells and key members of the ceRNA network. (a) Co-expression heatmap among immune cells. (b) Co-expression heatmap among two risk scoring models. (c) A positive correlation was found between CCNA2 and T follicular helper cells ($R = 0.37$, $P < 0.001$). (d). A positive correlation was found between L1CAM and T follicular helper cells ($R = 0.30$, $P < 0.001$). (e) A positive correlation was found between LINC00894 and T follicular helper cells ($R = 0.35$, $P < 0.001$) 0.001. (f) A negative correlation was found between LINC01426 and T follicular helper cells ($R = -0.24$, $P < 0.001$).

that the expression characteristics of lncRNA LINC01426 and mRNA L1CAM as well as T follicular helper cells were verified in clinical specimens. This suggested that a co-expression relationship existed between LINC01426, L1CAM, and T follicular helper cells, and they might be used as biomarkers for early diagnosis and prognostic evaluation of KIRC.

(a)

(b)

(c)

(d)

(e)

(f)
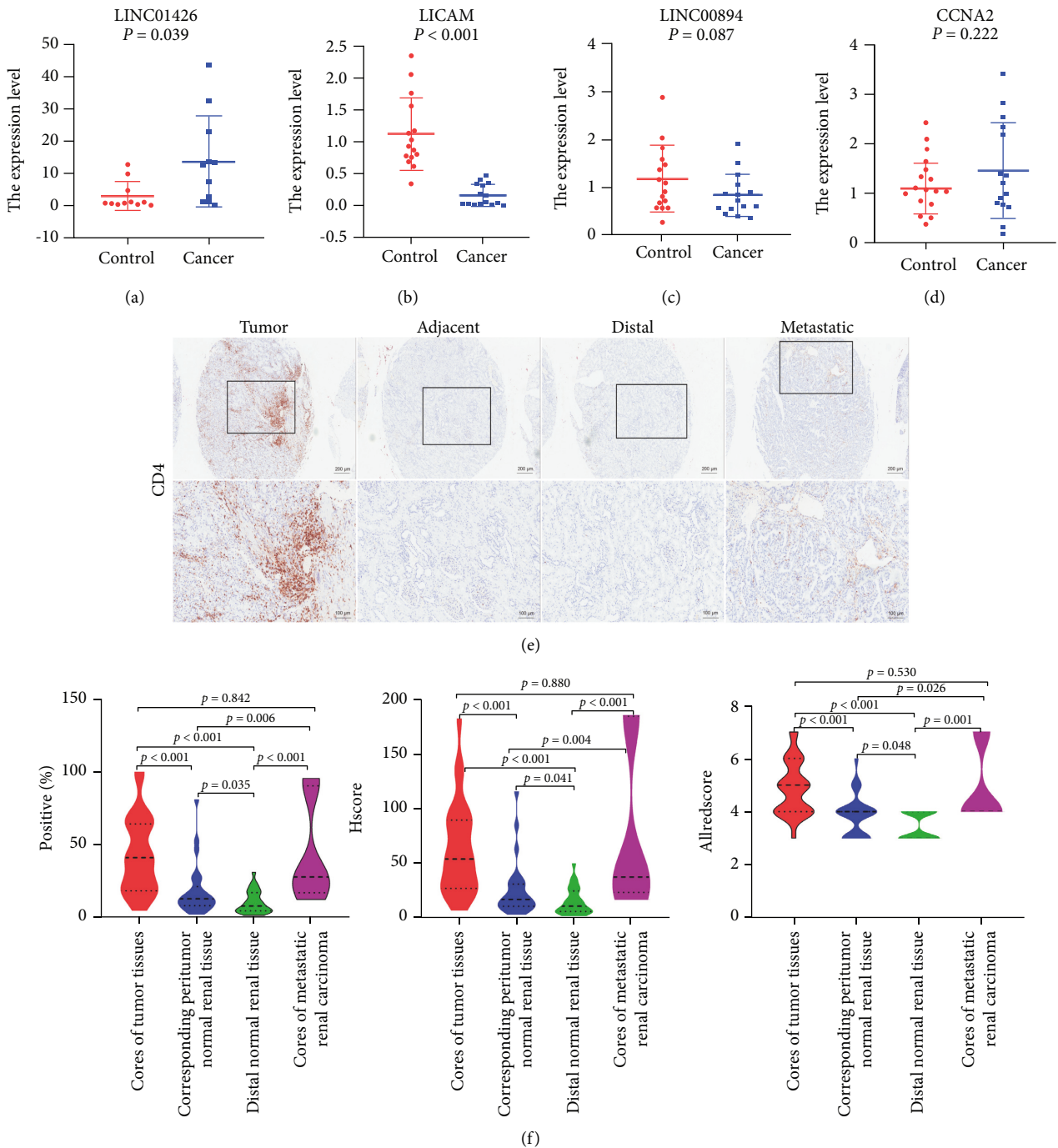
FIGURE 9: Verification in clinical samples. ((a)-(d)) Differentially expressed CCNA2, L1CAM, LINC01426, and LINC00894 in the cancerous and paracancerous groups. LINC01426 was upregulated, L1CAM was downregulated in kidney cancer tissues ($P < 0.05$), LINC00894 and CCNA2 had no difference ($P > 0.05$). (e) IHC results (including 26 cores of tumor tissues, corresponding to peritumor normal renal tissue, distal normal renal tissue, and seven cores of metastatic renal carcinoma). (f) IHC results using nonparametric tests. T follicular helper cells (CD4 marker positive) displayed difference in the core of the tumor tissues, and the corresponding normal kidney tissue adjacent to the cancer, the distal normal kidney tissue, and the core of metastatic renal cancer ($P < 0.05$).

5. Conclusions

At present, many patients with KIRC whose diagnoses were mainly based on the clinical symptoms and imaging methods have already developed distant metastases at this time; the recurrence rate after surgical radical treatment was high [18]. In recent years, a large number of researchers have focused on exploring the mechanism of genes, tumor-infiltrating immune cells, and the interaction between the two in the occurrence, development, metastasis, and prognosis of KIRC, indicating that genes and immune cells were closely related to tumors, and provided direction for

the diagnosis and treatment of KIRC in the future [19–22]. For example, Zhengyan Chang et al. separately constructed the risk scoring model of the ceRNA network and infiltrating immune cells in colon cancer and found that T follicular helper cells and hsa-miR-125b-5p, macrophages M0 and hsa-miR-125b, and macrophages M0 and FAS might become potential biomarkers through co-expression analysis, and this conclusion was verified in clinical tissues [23]. This research model based on bone metastatic melanoma, gastric cancer, breast cancer bone metastasis, mesothelioma bone metastasis, and other tumors has been adopted by various studies [24–26]. The present study also used this model and used bioinformatics analysis to identify co-expression regulation relationships among LINC01426, LINC00894, CCNA2, L1CAM, and T follicular helper cells. These key members might become KIRC diagnostic and therapeutic potential biomarkers.

LINC01426 was upregulated in renal clear cell carcinoma tissues and its overexpression was correlated with a disappointing prognosis [27]. So far, the data on L1CAM expression in renal clear cell carcinoma were contradictory; studies have shown that cell adhesion, metastasis, and invasion abilities were significantly increased with the upregulation of L1CAM expression in KIRC, and in turn, the downregulation of LICAM expression decreased the proliferation of renal cancer cell and reduced the expression of cyclin D1 [28, 29]. However, this just illustrated the importance of L1CAM in the progression of KIRC. T follicular helper cells are a specialized subset of CD4+ T cells that were first identified in tonsils in humans. They play an essential role in forming germinal centers, and Xiaoliang Hua et al. found that tumors from high-risk patients had a higher relative abundance of T follicular helper cells [30]. The present study confirmed the high expression of LINC01426, L1CAM, and tumor infiltration of T follicular helper cells because these cells were closely related to the clinical and prognostic prediction of KIRC. Thus, these cells were found more likely to be KIRC biomarkers.

In conclusion, the present bio-report analysis indicated a relationship among LINC01426, L1CAM, and T follicular helper cells, which was meaningful. As it is difficult to detect the patient's immune cells, the abundance of T follicular helper cells in KIRC was determined by detecting the expression levels of LINC01426 and L1CAM, which have a co-expression relationship to provide new prospects for the early diagnosis of KIRC so as to develop new therapeutic drugs.

Data Availability

The datasets used and/or analyzed in the present study are available from the corresponding author on reasonable request.

Ethical Approval

This study was approved by the Ethics committee of General Hospital of Ningxia Medical University adhering to the tenets of the Declaration of Helsinki. All tissue and cDNA

microarrays purchased by Shanghai Outdo Biotech Co., Ltd. meet ethical requirements.

Conflicts of Interest

There are no conflicts of interest regarding the publication of this paper.

Authors' Contributions

Aoran Kong and Hui Dong contributed equally to this work.

Acknowledgments

Supplementary Materials

Differentially expressed lncRNA, miRNAs, and mRNAs were put in Supplementary Material 1. Gene ID of lncRNAs, miRNAs and mRNAs in the ceRNA network were displayed in Supplementary Material 2. For a comprehensive digital IHC image analysis with Qupath, please refer to the protocol in Supplementary Material 3. (*Supplementary Materials*)

References

[1] S. A. Padala, A. Barsouk, K. C. Thandra et al., "Epidemiology of renal cell carcinoma," *World Journal of Oncology*, vol. 11, no. 3, pp. 79–87, 2020.

[2] D. J. Sanchez and M. C. Simon, "Genetic and metabolic hallmarks of clear cell renal cell carcinoma," *Biochimica et Biophysica Acta (BBA) - Reviews on Cancer*, vol. 1870, no. 1, pp. 23–31, 2018.

[3] K. Gupta, J. D. Miller, J. Z. Li, M. W. Russell, and C. Charbonneau, "Epidemiologic and socioeconomic burden of metastatic renal cell carcinoma (mRCC): a literature review," *Cancer Treatment Reviews*, vol. 34, no. 3, pp. 193–205, 2008.

[4] P. C. Barata and B. I. Rini, "Treatment of renal cell carcinoma: current status and future directions," *CA: A Cancer Journal for Clinicians*, vol. 67, no. 6, pp. 507–524, 2017.

[5] B. Shuch, A. Amin, A. J. Armstrong et al., "Understanding pathologic variants of renal cell carcinoma: distilling therapeutic opportunities from biologic complexity," *European Urology*, vol. 67, no. 1, pp. 85–97, 2015.

[6] L. Salmena, L. Poliseno, Y. Tay, L. Kats, and P. P. Pandolfi, "A ceRNA hypothesis: the Rosetta Stone of a hidden RNA language?" *Cell*, vol. 146, no. 3, pp. 353–358, 2011.

[7] Y. Bai, J. Long, Z. Liu et al., "Comprehensive analysis of a ceRNA network reveals potential prognostic cytoplasmic lncRNAs involved in HCC progression," *Journal of Cellular Physiology*, vol. 234, no. 10, pp. 18837–18848, 2019.

[8] W. Wang, W. Hu, Y. Wang et al., "Long non-coding RNA UCA1 promotes malignant phenotypes of renal cancer cells by modulating the miR-182-5p/DLL4 axis as a ceRNA," *Molecular Cancer*, vol. 19, no. 1, p. 18, 2020.

[9] C. Mascaux, M. Angelova, A. Vasaturo et al., "Immune evasion before tumour invasion in early lung squamous carcinogenesis," *Nature*, vol. 571, no. 7766, pp. 570–575, 2019.

[10] G. Klein and E. Klein, "Surveillance against tumors--is it mainly immunological?" *Immunology Letters*, vol. 100, no. 1, pp. 29–33, 2005.

[11] D. Bruni, H. K. Angell, and J. Galon, "The immune contexture and Immunoscore in cancer prognosis and therapeutic efficacy," *Nature Reviews Cancer*, vol. 20, no. 11, pp. 662–680, 2020.

[12] A. Dufresne, T. Lesluyes, C. Ménétrier-Caux et al., "Specific immune landscapes and immune checkpoint expressions in histotypes and molecular subtypes of sarcoma," *OncoImmunology*, vol. 9, no. 1, Article ID 1792036, 2020.

[13] F. Liang, H. Liang, Z. Li, and P. Huang, "JAK3 is a potential biomarker and associated with immune infiltration in kidney renal clear cell carcinoma," *International Immunopharmacology*, vol. 86, Article ID 106706, 2020.

[14] A. Jeggari, D. S. Marks, and E. Larsson, "miRcode: a map of putative microRNA target sites in the long non-coding transcriptome," *Bioinformatics*, vol. 28, no. 15, pp. 2062-2063, 2012.

[15] J. H. Li, S. Liu, H. Zhou, L. H. Qu, and J. H. Yang, "starBase v2.0: decoding miRNA-ceRNA, miRNA-ncRNA and protein-RNA interaction networks from large-scaleCLIP-Seq data," *Nucleic Acids Research*, vol. 42, pp. D92–D97, 2014.

[16] S. Crotty, "Follicular helper CD4 T cells (TFH)," *Annual Review of Immunology*, vol. 29, no. 1, pp. 621–663, 2011.

[17] P. Bankhead, M. B. Loughrey, J. A. Fernández et al., "QuPath: open source software for digital pathology image analysis," *Scientific Reports*, vol. 7, no. 1, Article ID 16878, 2017.

[18] J. M. Harvey, G. M. Clark, C. K. Osborne, and D. C. Allred, "Estrogen receptor status by immunohistochemistry is superior to the ligand-binding assay for predicting response to adjuvant endocrine therapy in breast cancer," *Journal of Clinical Oncology*, vol. 17, no. 5, pp. 1474–1481, 1999.

[19] H. Zhao, Y. Cao, Y. Wang et al., "Dynamic prognostic model for kidney renal clear cell carcinoma (KIRC) patients by combining clinical and genetic information," *Scientific Reports*, vol. 8, no. 1, Article ID 17613, 2018.

[20] Y. Ye, F. Zhang, Q. Chen, Z. Huang, and M. Li, "LncRNA MALAT1 modified progression of clear cell kidney carcinoma (KIRC) by regulation of miR-194-5p/ACVR2B signaling," *Molecular Carcinogenesis*, vol. 58, no. 2, pp. 279–292, 2019.

[21] S. Li and W. Xu, "Mining TCGA database for screening and identification of hub genes in kidney renal clear cell carcinoma microenvironment," *Journal of Cellular Biochemistry*, vol. 121, no. 8-9, pp. 3952–3960, 2019.

[22] L. Yin, W. Li, G. Wang et al., "NR1B2 suppress kidney renal clear cell carcinoma (KIRC) progression by regulation of LATS 1/2-YAP signaling," *Journal of Experimental & Clinical Cancer Research*, vol. 38, no. 1, p. 343, 2019.

[23] Z. Chang, R. Huang, W. Fu et al., "The construction and analysis of ceRNA network and patterns of immune infiltration in colon adenocarcinoma metastasis," *Frontiers in Cell and Developmental Biology*, vol. 8, p. 688, 2020.

[24] S. Liu, A. Song, X. Zhou et al., "ceRNA network development and tumour-infiltrating immune cell analysis of metastatic breast cancer to bone," *Journal of Bone Oncology*, vol. 24, Article ID 100304, 2020.

[25] R. Huang, J. Wu, Z. Zheng et al., "The construction and analysis of ceRNA network and patterns of immune infiltration in mesothelioma with bone metastasis," *Frontiers in Bioengineering and Biotechnology*, vol. 7, p. 257, 2019.

[26] R. Huang, Z. Zeng, G. Li et al., "The construction and comprehensive analysis of ceRNA networks and tumor-infiltrating immune cells in bone metastatic melanoma," *Frontiers in Genetics*, vol. 10, p. 828, 2019.

[27] Y. Jiang, H. Zhang, W. Li, Y. Yan, X. Yao, and W. Gu, "LINC01426 contributes to clear cell renal cell carcinoma progression by modulating CTBP1/miR-423-5p/FOXM1 axis via interacting with IGF2BP1," *Journal of Cellular Physiology*, vol. 236, no. 1, pp. 427–439, 2021.

[28] Y. Wang, D. Fu, J. Su et al., "C1QBP suppresses cell adhesion and metastasis of renal carcinoma cells," *Scientific Reports*, vol. 7, no. 1, p. 999, 2017.

[29] K. Doberstein, A. Wieland, S. B. B. Lee et al., "L1-CAM expression in ccRCC correlates with shorter patients survival times and confers chemoresistance in renal cell carcinoma cells," *Carcinogenesis*, vol. 32, no. 3, pp. 262–270, 2011.

[30] X. Hua, J. Chen, Y. Su, and C. Liang, "Identification of an immune-related risk signature for predicting prognosis in clear cell renal cell carcinoma," *Aging (Albany NY)*, vol. 12, no. 3, pp. 2302–2332, 2020.

Research Article

LncSNHG1 Promoted CRC Proliferation through the miR-181b-5p/SMAD2 Axis

Qi Huang [ID],[1] Zhi Yang [ID],[2] Jin-hai Tian [ID],[1] Pei-dong You [ID],[1] Jia Wang [ID],[1] Rong Ma [ID],[1] Jingjing Yu [ID],[1] Xu Zhang [ID],[1] Jia Cao [ID],[1] Jie Cao [ID],[2] and Li-bin Wang [ID][1]

[1]*The Biochip Research Center of General Hospital of Ningxia Medical University, Yinchuan 750004, China*
[2]*Guangzhou First People's Hospital, Guangzhou 510180, China*

Correspondence should be addressed to Jie Cao; eycaojie@scut.edu.cn and Li-bin Wang; wanglibin007@126.com

Objective. To investigate the effects of LncRNA SNHG1 on the proliferation, migration, and epithelial-mesenchymal transition (EMT) of colorectal cancer cells (CRCs). *Methods*. 4 pairs of CRC tissue samples and their corresponding adjacent samples were analyzed by the human LncRNA microarray chip. The expression of LncSNHG1 in CRC cell lines was verified by qRT-PCR. Colony formation assays and CCK8 assays were applied to study the changes in cell proliferation. The transwell assay and wound healing experiments were used to verify the cell invasion and migration. EMT progression was confirmed finally. *Results*. LncSNHG1 was overexpressed both in CRC tissues and cell lines, while the miR-181b-5p expression was decreased in CRC cell lines. After knock-down of LncSNHG1, the proliferation, invasion, and migration of HT29 and SW620 cells were all decreased. Meanwhile, LncSNHG1 enhanced EMT progress through regulation of the miR-181b-5p/SMAD2 axis. *Conclusion*. LncSNHG1 promotes colorectal cancer cell proliferation and invasion through the miR-181b-5p/SMAD2 axis.

1. Introduction

Colorectal cancer (CRC) is one of the most common gastrointestinal malignant tumors and the second leading cause of cancer mortality worldwide [1]. In spite of multiple treatment such as surgery, radiotherapy, and chemotherapy, the 5-year subsistence rate of CRC remained around 55% while metastasis and recurrence are the leading causes of death [2, 3]. Accordingly, exploring the molecular mechanisms associated with the incidence of CRC may be of great help to seek effective treatment strategies and improve the prognosis. Although 80% of human genes may be transcribed into RNA, more than 98% are non-protein-coding RNAs (ncRNAs). Long noncoding RNAs (LncRNAs) are a kind of noncoding RNA which has about 200 nucleotides. LncRNAs have been improved to associated with diverse diseases such as Parkinson's disease and various cancers [4, 5]. Long noncoding RNA small nucleolar RNA host gene 1 (LncRNA SNHG1 and LncSNHG1), which localized at 11q12.3 region and has 11 exons, was reported to play an important role in enhancing cell proliferation, invasion, apoptosis, and epithelial-mesenchymal transition (EMT) in several cancers, including colorectal cancer, non-small-cell lung cancer, and gastric cancer [6–9]. The increased expression of LncSNHG1 is an effective marker in predicting a poor outcome in CRC patients [10]. LncRNAs have been reported to function through competition for microRNA (miRNA) binding, resulting in imposing posttranscriptional regulation in CRC cells [11].

MicroRNAs (miRNAs) are a group of noncoding RNAs which have 21–24 nucleotides in length. miRNAs often play their function in the posttranscriptional regulation through ceRNA with LncRNA [12]. The expression change of miRNA has been related with different cancers. Fridrichova et al. have reported that miRNAs are involved in regulating invasive processes, cell-cell adhesion junctions, cancer cell-extracellular matrix interactions, and cancer cell stem abilities in breast cancer [13]. Cao et al. proved that miRNA-124 and miR-552 regulate tumor cell proliferation and migration in hepatocellular carcinoma and CRC [14, 15].

miR-181b is a member of miR-181 family and positioned at chr9q3.33 [16]. It has been reported that miR-181b could inhibit the progression of human colon cancer cell proliferation [17]. However, the molecular mechanism by which miR-181b mediates CRC progression still needs further study.

In this study, we used TargetScan software to search the potential miRNA sites that complement the untranslated area (UTR) of the SNHG1 3 'end. miR-181 b-5p was upregulated more than 2 times with LncSNHG1 silencing. miR-181 b directly binds to the $3'$ untranslated regions (UTRs) of both LncSNHG1 and SMAD2 in CRC cells. Furthermore, the TGF-β/SMAD2 pathway was activated abnormally and closely related to cell proliferation, EMT progress, chemoresistance, and poor prognosis in CRC [18].

Epithelial-mesenchymal transition (EMT) is defined as the transformation of an epithelial cell into mesenchymal cells. Accompanying the process was the loss of membrane E-cadherin expression and the gain of mesenchymal marker positivity [19]. EMT has been shown to be an essential process during CRC invasion and metastasis since 1995 [20]. Previous studies have shown the association between LncSNHG1 and EMT in different cancers. Liu et al. have shown that the overexpression of LncSNHG1 enhances the EMT process via the miR-15b/DCLK1/Notch1 axis and promotes the metastasis in GC cells [9]. LncSNHG1 also plays a vital role in the promotion of the cell cycle, migration, and EMT progression of hepatocellular carcinoma [21]. Although LncSNHG1 can indicate CRC deterioration by cooperating with miR-497/miR-195-5p to modify the EMT process, the molecular mechanism mediated by LncSNHG1 in CRC progression remains unknown [22].

Based on the abovementioned background, we assumed the LncSNHG1 promoted the CRC progress via miR-181b-5p binding. In this study, we aim to present in vitro results to certificate the change of LncSNHG1, miR-181b-5p, and SMAD2 in CRC to provide a potential application for the treatment of CRC.

2. Materials and Methods

2.1. Clinical Samples Collection. Approval for this research was given by the General Hospital of Ningxia Medical University Ethics Committee. All the patients involved have signed informed consent forms. We recollected 24 paired colorectal tissues and adjacent normal samples from the oncology surgery department of the General Hospital of Ningxia Medical University. All of the tissue specimens were confirmed for diagnosis based on hematoxylin-eosin and pathological examination. 4 pairs of cancer tissues and adjacent tissues were randomly selected for differentially expressed LncRNA screening (LncRNA chip hybridization, Biochip, China).

2.2. Microarray Analysis. 4 pairs of cancer tissues and adjacent normal tissues were used for the microarray analysis. Human LncRNA Array v2 microarray (Beijing Capital Bio Biotechnology Corporation, China) has been used for LncRNA microarray profiling analysis. The LncRNA array

data were analyzed by GeneSpring 13.0 (Agilent) software. Bioanalyzer 2100 (Agilent Technologies, USA) was used for the RNA integrity analysis. RNA digestion, amplification, and labelling were performed according to protocol. The microarray contained 162351 human LncRNA probes. With the filter criteria fold-change ≥2, Pvalue < 0.05, fluorescence value ≥ 100, differentially expressed LncRNAs were detected and separated.

2.3. Cell Line and Cell Culture. The human colorectal cancer cell lines HCT116, HT29, LOVO, and SW620 and human colon epithelial cells NCM460 were purchased from the cell bank of the Chinese Academy of Sciences. The cells were cultured with high glucose DMEM medium (HyClone, Logan, USA) supplemented with 1% penicillin-streptomycin solution and 10% fetal bovine serum (Gibco, Australia). The cells were incubated at 37 °C with 5% CO_2.

2.4. Plasmids and Cell Transfection. shRNA for LncSNHG1 and negative control shRNA-NC plasmid, miR-181b-5p inhibitor and negative control (NC) vector were all designed and synthesized from HanBio Company (China). HT29 and SW620 cells were cultured in 6-well plates. When the cell density reaches 70%–80% confluence, a 2.5 μg plasmid vector was transfected to the cells using Lipofectamine 3000 (Invitrogen, CA, USA) according to the manufacturer's protocol. Fluorescence microscope, qRT-PCR, and western blot assays were used for observing the cell transfection efficiency.

2.5. Real-Time Quantitative Reverse Transcription-PCR (qRT-PCR). Following the manufacturer's protocol, the total RNA was extracted from tissues and cells by using TRIzol reagent (Invitrogen, CA, USA). cDNA was synthesized with the TaKaRa verse transcription kit (TaKaRa, Shanghai, China). The PCR amplification was performed with specific primer sat Prism 7900 system (ABI, USA). GAPDH served as internal control. Using $2^{-\Delta\Delta Ct}$ methods, we calculated the relative expression of each gene.

2.6. Dual-Luciferase Reporter Assay. Based on the TargetScan database, LncSNHG1 has binding sites with miR-181b-5p at the 3'-UTR. To identify it, the wt-Lnc SNHG1 and mut-LncSNHG1 luciferase expression vectors were constructed from GeneChem Co. and incubated into the vector and cells in a 24-well plate (5×10^3 cells per well). When the cells fusioned to 80%, the wt-LncSNHG1 and mut-LncSNHG1 groups were transfected into miR-NC and miR-181b-5p, respectively. The double luciferase reporting experiment was carried out using the luciferase reporter kit. The ratio of luciferase activity was statistically analyzed. All the experiments was repeated three times.

2.7. Cell Migration and Invasion Assay. To determine the cell migration and invasion, wound healing assay was used. $1 Ч 10^5$ HT29 and SW620 cells were seeded in a 6-well plate and transfected with an interfering vector for 48 h. The cell

was wounded with a 200 μl pipet tip scraping across the monolayer. After that, the speed of the wound's recovery was photographed. The cell mobility was assessed by calculating the wound width.

2.8. Colony Formation Assay.

After being transfected with an interfering or overexpressing vector, the HT29 and SW620 cells were seeded in a 6-well plate. The medium was exchanged every three days. Two weeks later, the cells were fixed with 100% methanol for 15 min. Then, it was stained with crystal violet for 10 min. The colony numbers of representative areas were observed and calculated. All experiments were performed three times.

2.9. Flow Cytometry.

The HT29 and SW620 cells were seeded in a 6-well plate after being transfected with an interfering or overexpressing vector for 48 h. Then, the cells were digested with trypsin and 1×10^6 cells were counted for analysis. The cells were washed with cold PBS three times. They were then collected and suspended into a single cell in a binding buffer. According to the instructions of the apoptosis detection kit (Best Bio, Shanghai, China), the cells were stained with Annexin V-APC for 10 min and propidium iodide (PI) for 10 min. A BD flow cytometer examined the samples, and FlowJo software (Tree Star Corporation, Ashland, OR, USA) analyzed the data.

2.10. Western Blot.

The total protein of each group was extracted and the protein concentration was detected by the BCA protein reagent kit (Thermo Fisher Scientific, Inc.). The protein samples were separated with 10% SDS-PAGE and transferred to a PVDF membrane. The membranes were blocked with 5% defatted milk in TBST at 25°C for 1 h. The membrane was incubated with a specific primary antibody (1 : 1 000) at 4°C overnight. Then, the HRP-conjugated secondary antibodies were incubated at 25 °C for 2 h. After washing the membrane with TBST 3 times, the protein bands were detected and scanned by Bio Imaging Systems (BIO-RAD, CA, USA). The absorbance of the protein bands in each group was measured by Quantity One gel analysis software. The protein expression level is assessed by the ratio of the target band to the GAPDH band. Each protein sample was applied with 3 repeats.

2.11. Statistical Analysis.

Statistical analysis was carried out using SPSS 20.0 software. The mean ± standard deviation ($x \pm s$) was used to measure the data expression. The T test was performed between the two groups. A single factor variance analysis was used to analyze the variance between the two groups. P value < 0.05 indicated that the difference has the significance of statist.

3. Result

3.1. Expression Analysis of LncRNAs and Its Verification in CRC Tissues and Cells.

To screen for specific LncRNA in colorectal cancer, we selected 4 CRC tissue samples (CA1-CA4) and adjacent normal samples (AP1-AP4) for investigating the expression of LncRNAs by microarray profiles. The cluster analysis displayed the different expression of LncRNAs between the two groups (Figure 1(a)). Based on the different fluorescence signal values, the variation in LncRNA expression between the CRC and adjacent normal tissues is described in the volcano plot (Figure 1(b)). As illustrated in Figure 1, 13198 differentially expressed LncRNAs were separated. Taking the fold-change ≥5 or ≤ -5, the P value <0.01 and the processed signal ≥100 as screening criteria, 18 candidate LncRNAs were selected including 8 upregulation and 10 downregulation. Among them, LncSNHG1 was significantly highly expressed in CRC tissues.

To further verify the selected LncSNHG1 with CRC, qRT-PCR explored the LncSNHG1 expression in CRC tissues and cell lines. The results showed the expression of LncSNHG1 in 24CRC was 4.45 ± 2.11, which was higher than that in para cancerous tissues (Figure 1(c); (p) < 0.05). Compared with human normal colorectal cancer NCM460 cells, LncSNHG1 was highly expressed in SW620, HT29, HCT116, and LOVO cell lines (Figure 1(d); P < 0.05). Based on the results, we selected HT29 and SW620 cell lines for the following experiments.

3.2. LncSNHG1 Promoted CRC Cells Proliferation and Migration.

To investigate the effect of LncSNHG1 on CRC cell growth, we constructed siRNA for LncSNHG1 and transfected it into HT29 and SW620 cells. After 48 h, all cell proliferation was significantly inhibited, while cell mobility was decreased (Figure 2(a)–2(d)). The results demonstrated that sh-SNHG1 had anticancer effects on CRC cells. The results of colony formation assays showed that the colony numbers were smaller and fewer when treated with sh-SNHG1 (Figure 2(e)). These results illustrated that LncSNHG1has the function of promoting CRC cell proliferation.

3.3. Downregulation of LncSNHG1 Influence the Cell Cycle and Promoted Apoptosis of HT29 and SW620 Cells.

With the flow cytometry analysis, the effects of LncSNHG1 on the cell cycle and apoptosis were evaluated. The results showed that the G0/G1 phrases were all increased after being treated with sh-SNHG1 in HT29 and SW620 cells. Meanwhile, the cells' S phrases were all decreased. The results proved that inhibition of LncSNHG1 enhanced the cells G0/G1 accumulation (Figures 3(a) and 3(b)).

Compared with the control and NC groups, the apoptosis rate in the sh-SNHG1 group was significantly increased both in HT29 and SW620 cells. The results indicated that inhibition of LncSNHG1 promoted apoptosis of CRC cells (Figure 3(c) and 3(d)).

3.4. miR-181b-5pas ceRNA to LncSNHG1 in CRC Cells.

A large body of research literature has proved that LncRNA is an important factor to regulate the expression of miRNA. In this study, we identified the target miRNA of LncSNHG1 through starBase database (http://starbase.sysu.edu.cn/) and searched for potential sites that complement the

(a)

(b)

(c)

(d)
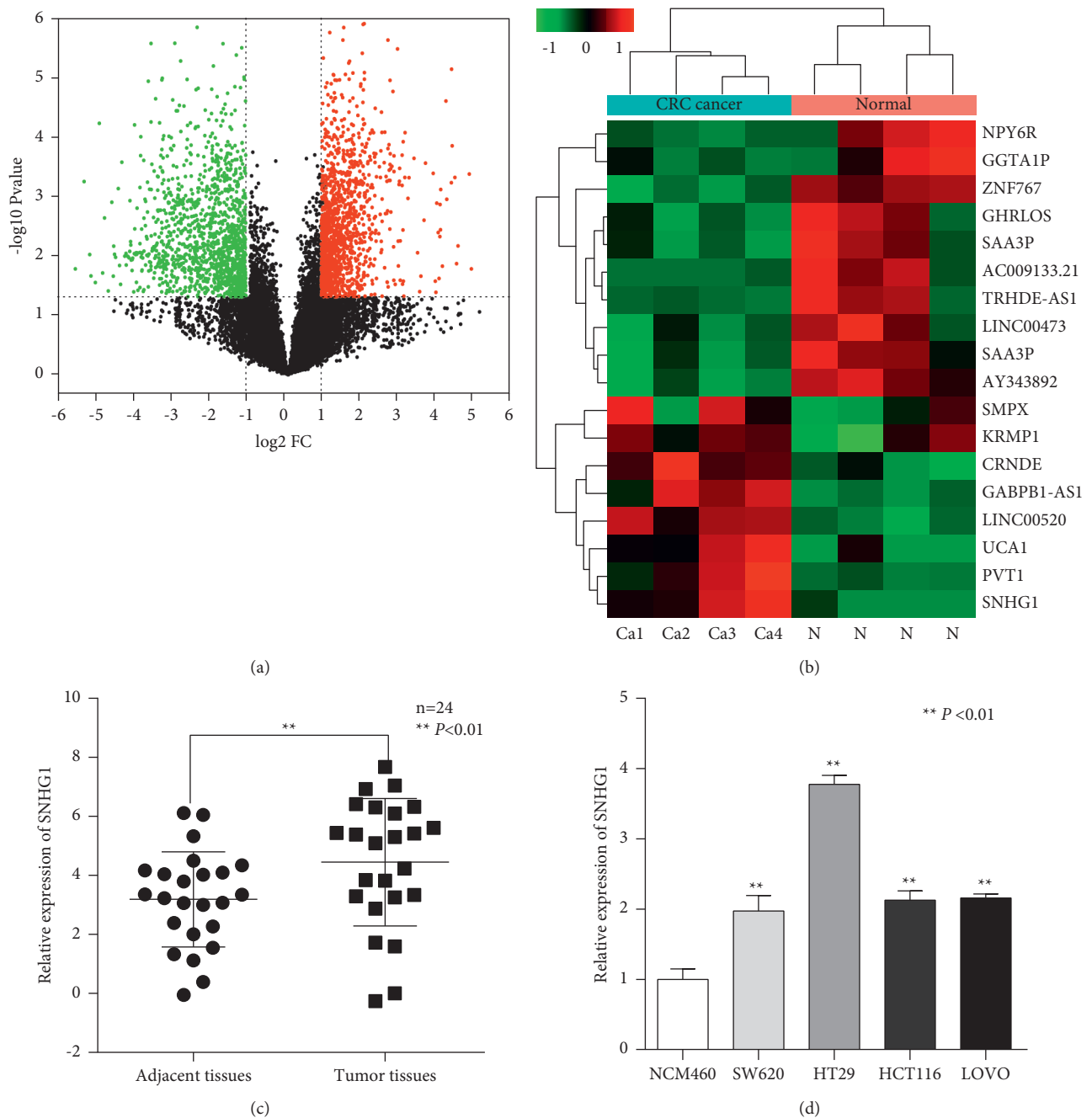
Figure 1: LncRNAs expression analysis in CRC tissues and cells. (a, b) Cluster and volcano plot analysis of different expression of LncRNAs between CRC tissues samples (CA1–CA4) and adjacent normal samples (N) based on the microarray profiles. The expression levels are presented in red and green, which indicated upregulated and downregulated LncRNAs. (C, D) The expression of LncSNHG1 in CRC tissues (c) and cell lines (d) ($^*P < 0.05$ and $^{**}P < 0.01$).

untranslated area (UTR) of theSNHG1 3 ′end with Tar-getScan software. Based on the bioinformatic analyses, we selected 10 miRNAs which matched to LncSNHG1 (Figure 4(a)). The expression of 10 miRNAs was measured in HT29 and SW620 cells after LncSNHG1 silencing. The results proved that the expression of miR-181b-5p was significantly decreased in the cell lines (Figure 4(b)). In order to confirm the binding site of LncSNHG1 to miR-181b-5p, luciferase reporter assays were used. We found that in the LncSNHG1-wt report vector transfer group, miR-181b-5p

mimic could reduce the activity of luciferase. But there is no difference between LncSNHG1 mutation and the miR-181b-5p mimic group. The results proved that there was a direct combination between LncSNHG1 3'UTR and miR-181b-5p (Figure 4(c)).

To further identify the specific target genes that are regulated by LncSNHG1 in CRC, RNA transcriptome sequencing was carried out. Based on the results, the most highly expressed genes such as ATP6V1C2, CLDN2, SMAD2, ITGA2, FOSL1, FBXO34, and others are selected.

(a)

(b)

(c)

(d)

(e)
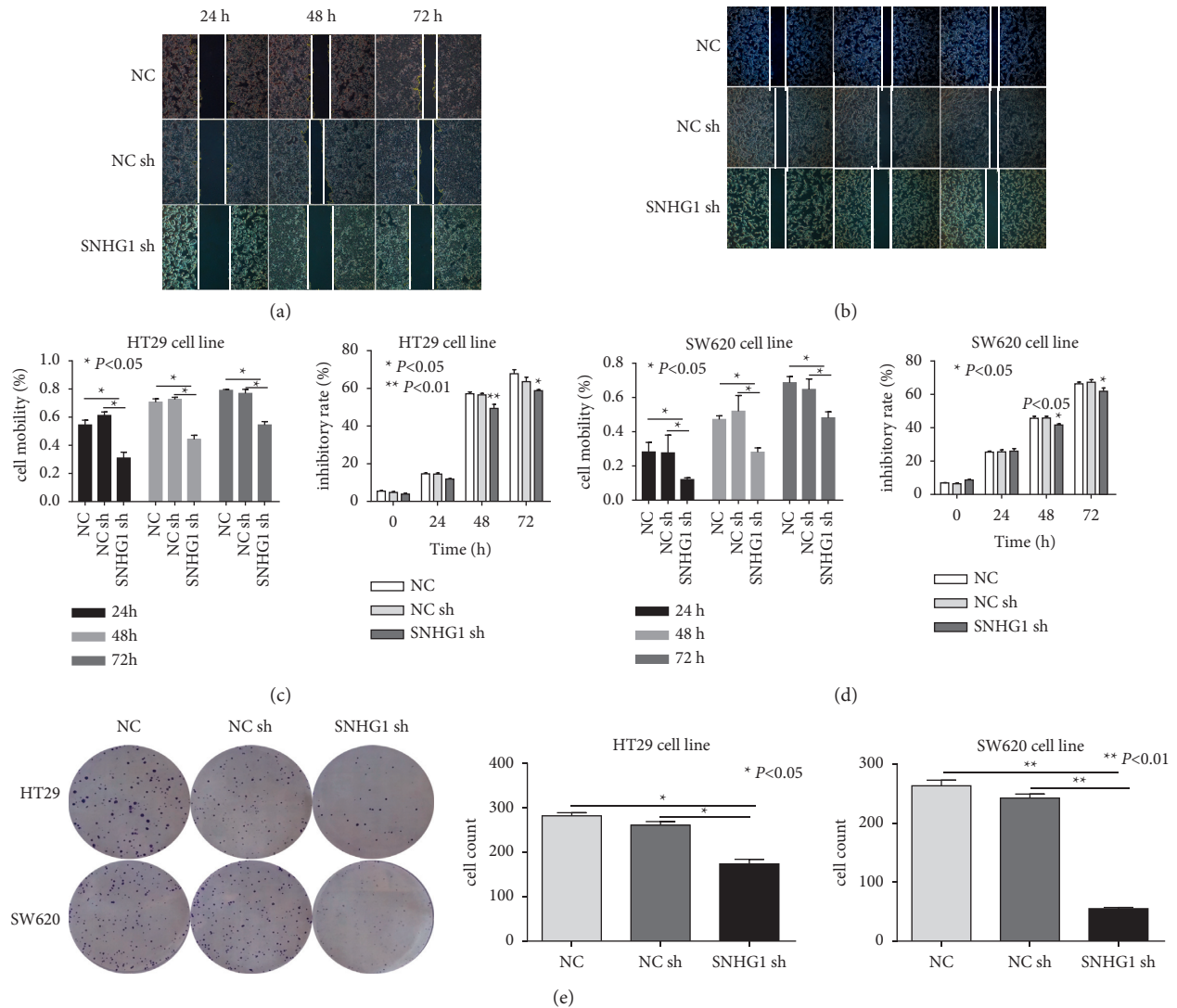
FIGURE 2: LncSNHG1 promoted CRC cells proliferation and migration. (A–D) The migration assays showed the cell mobility and inhibition rate of HT29 (A, C) and SW620 cells (B, D) after downregulation of lncSNHG1. (E) Colony formation assay showed the cell self-renewal in HT29 and SW620 cells after downregulation of SNHG1 ($^*P < 0.05$ and $^{**}P < 0.01$).

qRT-PCR were used to verify these genes, the results showed that SMAD2 was high expressed in HT29 and SW620 cells (Figure 4(d)). Bioinformatics analysis showed that there were seven complementary bases in the miR-181b-5p and SMAD2 3'UTR regions. Luciferase reporter assays proved that of the wild type SMAD2 and the miR-181b-5p mimic group was significantly lower than that of the miR-NC group. But the luciferase activity between the miR-NC and miR-181b-5p mimic groups was no significant difference (Figure 4(e)).

3.5. LncSNHG1 Induced CRC EMT through miR-181b-5p/SMAD2. To identify the relationship between LncSNHG1 and miR-181b-5p and the EMT regulated by the ceRNA in CRC, western blot was used. After transfecting miR-181b-5p mimics and inhibitor into the cells, SMAD2, BCL-2, and BAX were tested. The results proved that SMAD2 and the apoptosis related protein Bax were

remarkably decreased in the miR-181b-5p inhibitor group, while the apoptosis stimulating protein Bcl-2 showed a reduction. When the cells were treated with sh-SNHG1, SMAD2 and Bax expression were increased. Combined treated the cells with sh-SNHG1 and 181b-5p inhibitor could reverse the expression meanwhile (Figure 5(a) and 5(b)).

EMT is a process which often occurs in different cancer oncogenesis. Previous research has proved that SMAD2 could induce EMT and influence CRC progression. To verify the results, we tested the EMT-related protein after being transfected with 181b-5p and sh-SNHG1. Western blot results proved that N-cadherin, vimentin, and slug was increased while E-cadherin was decreased in the 181b-5p inhibitor group as well as in the sh-SNHG1 group.

When treated the cells with 181b-5p inhibitor combined with sh-SNHG1, all the protein expression would be reversed (Figure 6(a) and 6(b)). These results suggested that inhibiting miR-181b could reverse the anticancer effect of sh-SNHG1 on CRC cells through SMAD2.

(a)

(b)

(c)

(d)
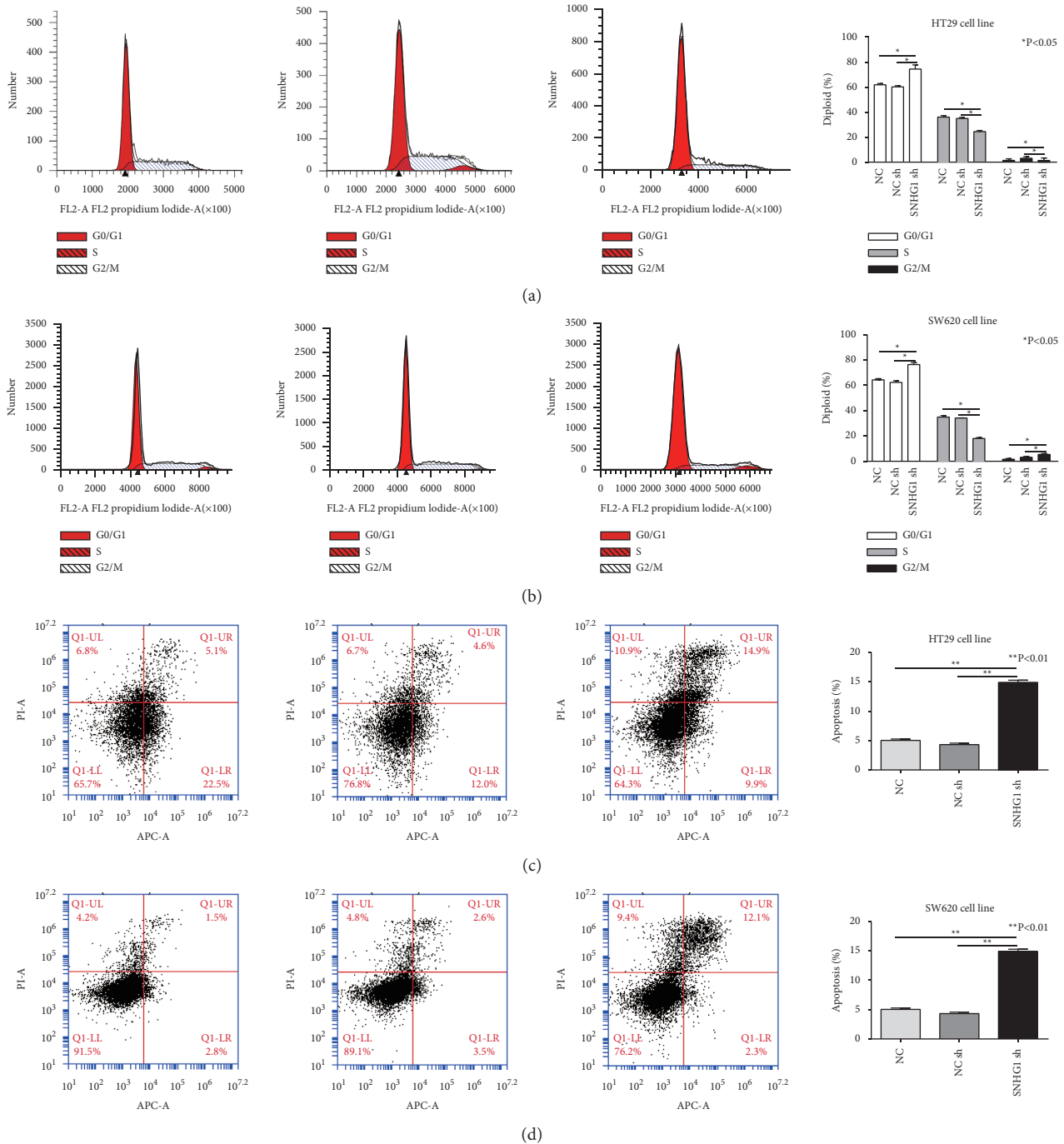
FIGURE 3: The effects of LncSNHG1 on HT29 and SW620 cell cycle and inhibited apoptosis. (A, B) The cell cycle changed after down-regulation of LncSNHG1 in HT29 and SW620 cells. (C, D) The cells apoptosis being promoted by downregulation of LncSNHG1 ($^*P < 0.05$ and $^{**}P < 0.01$).

4. Discussion

Due to the lack of effective methods for the early diagnosis of CRC and its unoptimistic survival rate, the study of the incidence and mechanism of CRC has been a hotspot these years. Plenty of LncRNAs and miRNAs have been indicated to be in association with CRC development, via kinds of pathways such as Wnt/β-catenin or TGF-β/Smad2/3 [11, 16, 23]. The essential finding of this

research is that we identified LncSNHG1 plays an important role in proliferation, migration, invasion, and EMT progress by acting as a molecular sponge for miR-181b in CRC processing.

LncRNAs are transcribed by RNA polymerase II (PoII) but not translated into protein. Although they have been thought to be junk genes, LncRNAs have been identified as key regulatory elements in multiple physiological processes, such as cell cycle and proliferation, with the development of

(a)

(b)

(c)

(d)

(e)
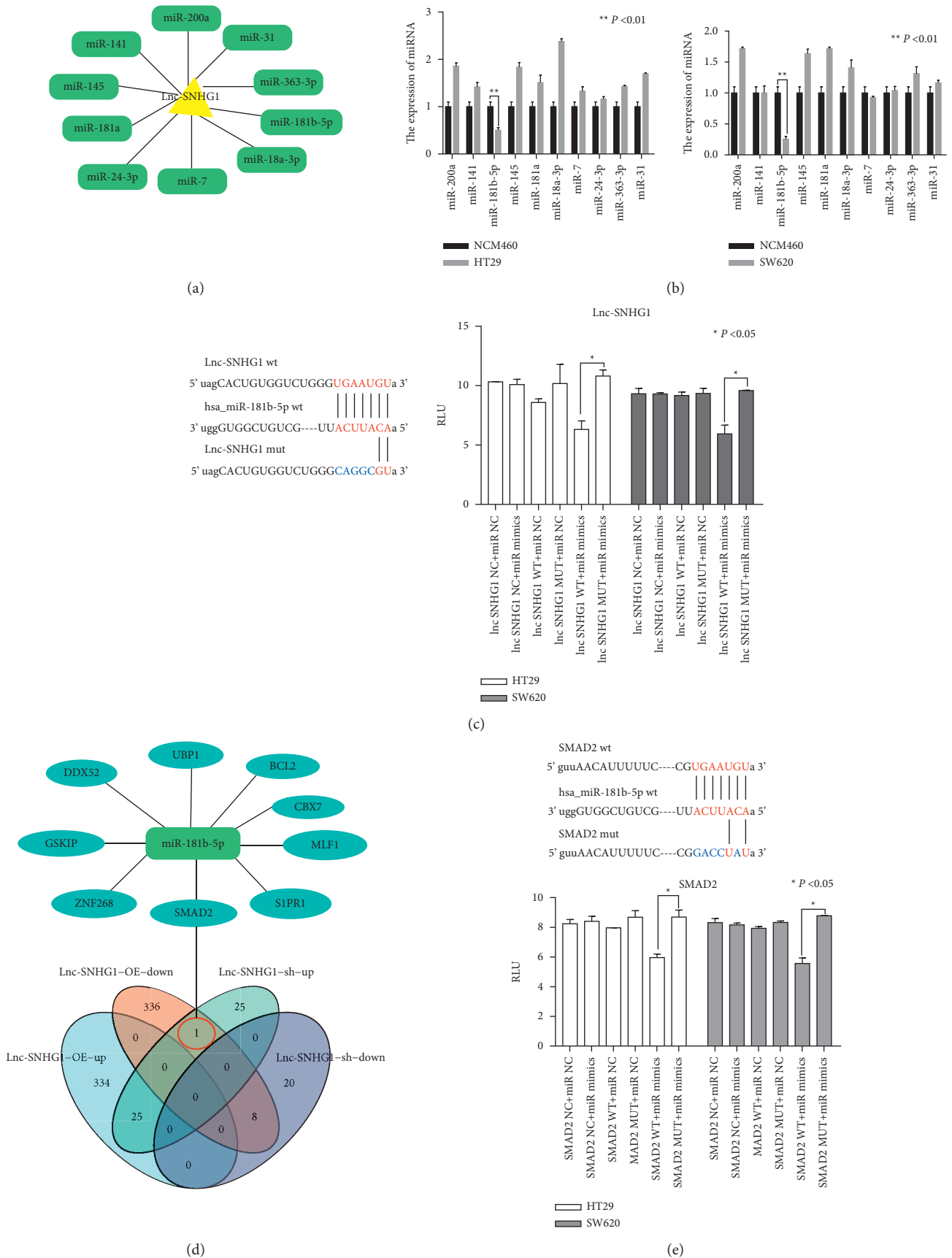
Figure 4: miR-181b-5pas ceRNA to LncSNHG1 in CRC cells. (A, B) Target miRNA prediction and identify in HT29 and SW620 cells. (C) Luciferase reporter assays tested the direct combination between LncSNHG1 3'UTR and miR-181b-5p. (D, E) Prediction and identification of SMAD2 as miR-181b-5p target gene through RNA transcriptome sequence and luciferase reporter assay ($**P < 0.05$).

(a)

(b)
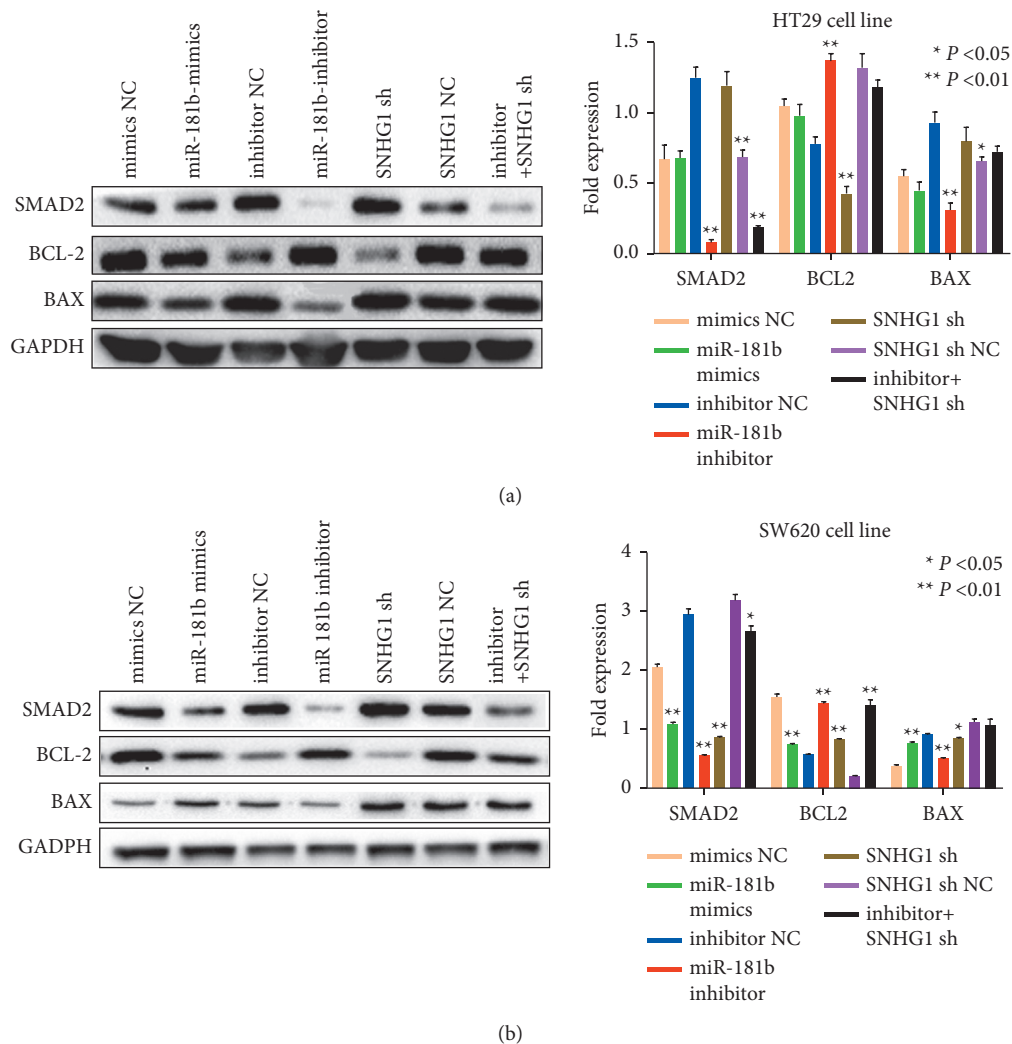
FIGURE 5: The relationship between LncSNHG1, miR-181b-5p, SMAD2, and apoptosis. (A, B) The expression of SMAD2 and apoptosis-related proteins Bcl-2 and Bax after treated with sh-SNHG1 and 181b-5p inhibitor in HT29 and SW620 cells.

high-throughput technologies nowadays [24]. LncRNAs have been associated with a variety of malignant tumors progression [25]. Meanwhile, LncSNHG1 involvement in gene transcription, invasion, cell migration, metastasis, tumorigenesis, and chemoresistance of multiple cancers has been reported widely [26]. By analyzing the RNA-Seq and miR-Seq and corresponding clinical data of CRC from the TCGA database, A. Poursheikhani et al. reported that SNHG1 was one of the significant diagnostic LncRNAs in CRC development [23]. In our research, we utilized the Human LncRNA Microarray chip to determine that LncSNHG1 was upregulated in CRC tissue and was qualified by qRT-PCR. This finding was consistent with previous studies, while the relationship between poor prognosis of CRC patients and high level LncSNHG1 had been reported [10, 11, 27–29]. In our gain-of-function and loss-of-function experiments, LncSNHG1 was verified to enhance proliferation, migration, EMT progress, cell cycle progression, and inhibition of apoptosis in CRC cells. These results which were in accordance with forepassed literature identified that

LncSNHG1 might serve as an oncogene in CRC development [7, 22, 29].

Most LncRNAs are involved in gene regulation mechanisms by acting as competing endogenous RNAs (ceRNAs) by miRNA recognition elements (MREs) [30, 31]. A couple of miRNAs (such as miR-154-5p and miR-137) mediate the part of LncSNHG1 in modulating CRC development have been demonstrated [10, 29]. The miR-181b family had been implicated in the progression of kinds of malignant tumor such as glioblastoma, osteosarcoma, pancreatic cancer, breast cancer, and colorectal cancer [14, 15, 32–36]. Interestingly, the miR-181b family may act as oncogenes [32, 33] or tumor suppressors [36, 37] in different cancer types. Moreover, whether the miR-181b family in cancer tissue is upregulated or downregulated in prostate cancer [38–40] and gastric carcinoma [41, 42] remains a controversy. The function of miR-181b depend on not only the type of tumor but also the cellular circumstances may be the cause [43, 44]. A similar situation emerged in the research studies about the miR-181b family in CRC. miR-181b in CRC has been
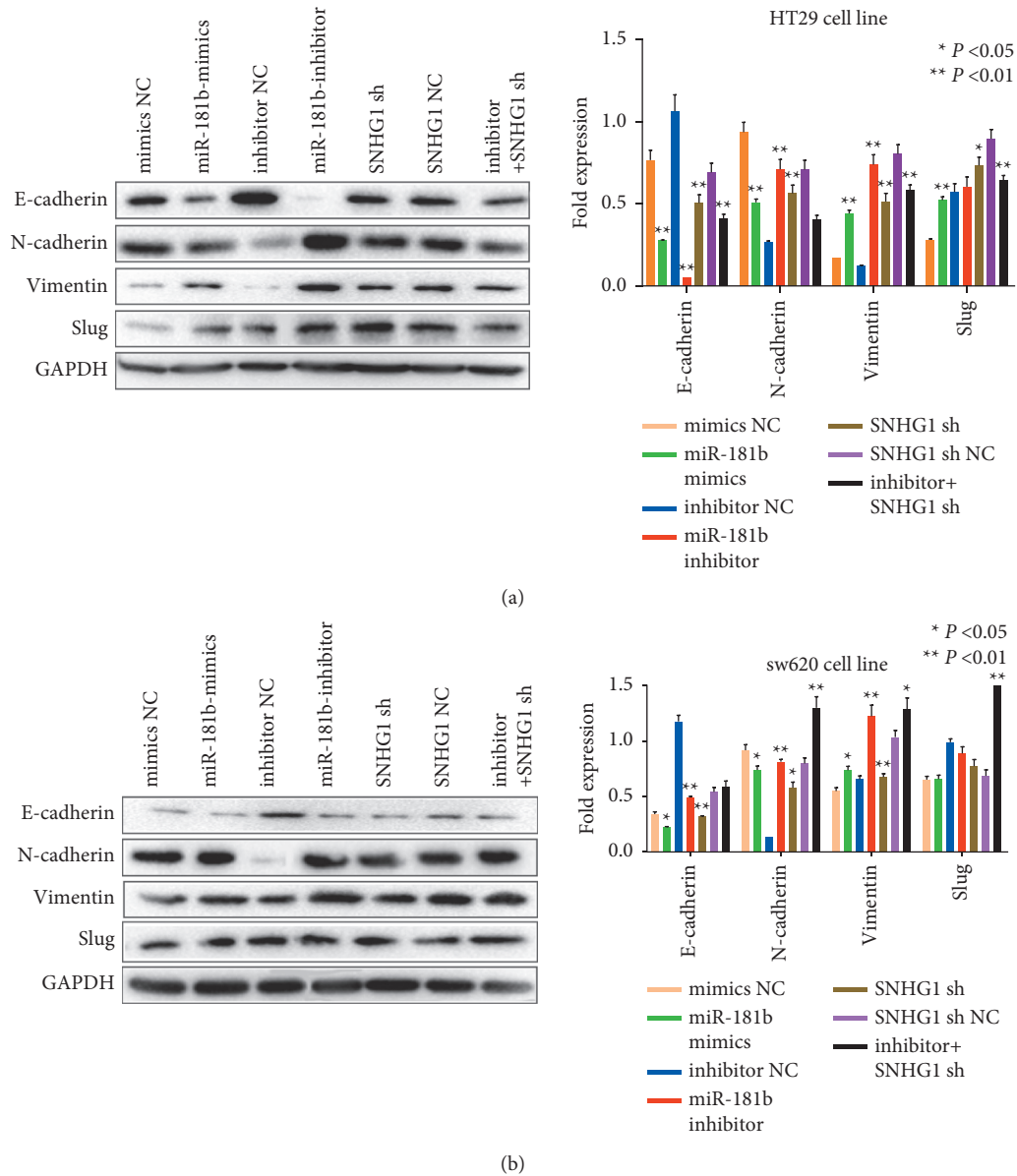
FIGURE 6: EMT induced by LncSNHG1 in CRC cells. (A, B) The different expression of EMT related protein after treated with 181b-5p and sh-SNHG1 in HT29 and SW620 cells.

reported to be an oncomiRNA and the probable mechanism could be that association with the mutation status of the p53 gene [45], Warburg effect promotion [46], cylindromatosis (CYLD) expression suppression, PDCD4 suppression [35],and the NF-κB signaling pathway [15] inhibition. But LUN-DE ZHAO and others and Si Chen, et al. showed that miR-181b could act as a tumor suppressor in CRC by targeting RASSF1A [34] and regulating TUSC3 [14], respectively. In our research, we verified that LncSNHG1 positively regulated proliferation, migration, invasion, and EMT by competing with miR-181b-5p in CRC cells. The result is similar with the previous one [14], and we are the only two reports in LncRNA-miR181b-CRC while the first study figured out the LncRNA-miR181b-EMT in CRC development until now. Every cloud has a silver lining; the different effects miR-181b would exert in CRC development might be decided by upstream factors such as LncRNAs. Further studies on the function of the miR-181b family in CRC processing are needed.

LncSNHG1 can act as an oncogene by regulating Wnt/β-catenin signaling, the PI3K/AKT signaling pathway, and the HIF-1α/VEGF signal pathway in different tumor progression [28, 47, 48]. In our research, the positive correlation between LncSNHG1 and SMAD2 was verified by the in vitro assays. The TGF-β was demonstrated to act as both tumor suppressor (in the early stage) and progression promoter (in the advanced stage) by multifaceted impacts in cancer progression [49]. Smad2 is located at 18q21. It belongs to the Smad superfamily that transmit signals of TGF-β from receptors on cell membranes to the nucleus [50]. The role of TGF-β/Smad2 in colon cancer has been reported in various studies. Xinke Wang, et al. reported that LncRNA SNHG6

was a promoter in CRC progression by activating TGF-β/Smad signaling pathway [51]. While Xuning Shen, et al. proved the role of LncRNA TUG1 in CRC metastasis by TGF-β promotion [52]. In the current study, we report the function of LncRNA SNHG1 in TGF-β/SMAD2 signal way regulation in cancer development, which was similar with the previous study [51], indicating that the LncRNA SNHG family may regulate CRC progression in a similar way. Although EMT via the TGF-β/Smad pathway is a fundamental process for cancer metastasis and chemoresistance in CRC [17, 51], the literature about LncRNA SNHG1 in EMT is limited. Liu ZQ and others discovered the mechanism of SNHG1 in promoting EMT in gastric cancer cells [9]. Meng XF and others proved SNHG1 could mediate the proliferation, invasion, and EMT of prostate cancer by regulating miR-195-5p expression [53]. In our research, compared with the cells transfected with sh-SNHG1, the E-cadherin was reduced and the N-cadherin and vimentin were increased. These results suggested that inhibiting miR-181b-5p could reverse the anticancer effect of silent SNHG1 on CRC cells.

In brief, this study first proved that LncSNHG1 regulated the biological behavior of miR-181b-5p-miediated cells in colorectal cancer. Targeting the LncSNHG1 may present a promising therapeutic target for CRC, while more detailed research is still needed in near future [54, 55].

Data Availability

The colorectal cancer LncRNA expression array data used to support the findings of this study are included within the supplementary information file (s).

Ethical Approval

Approval for this research was given by the General Hospital of Ningxia Medical University Ethics Committee.

Consent

All the patients involved have signed informed consent forms.

Conflicts of Interest

The authors declare that there are no conflicts of interest.

Acknowledgments

Supplementary Materials

Colorectal cancer differentially expressed LncRNAs. (*Supplementary Materials*)

References

[1] H. Sung, J. Ferlay, R. L. Siegel et al., "Global Cancer Statistics 2020: GLOBOCAN estimates of incidence and mortality worldwide for 36 Cancers in 185 countries," *CA: A Cancer Journal for Clinicians*, vol. 71, no. 3, pp. 209–249, 2021.

[2] A. M. D. Wolf, E. T. H. Fontham, T. R. Church et al., "Colorectal cancer screening for average-risk adults: 2018 guideline update from the American Cancer Society," *CA: A Cancer Journal for Clinicians*, vol. 68, no. 4, pp. 250–281, 2018.

[3] B. Tang, W. Liang, Y. Liao, Z. Li, Y. Wang, and C. Yan, "PEA15 promotes liver metastasis of colorectal cancer by upregulating the ERK/MAPK signaling pathway," *Oncology Reports*, vol. 41, no. 1, pp. 43–56, 2019.

[4] C. Qian, Y. Ye, H. Mao et al., "Downregulated lncRNA-SNHG1 enhances autophagy and prevents cell death through the miR-221/222/p27/mTOR pathway in Parkinson's disease," *Experimental Cell Research*, vol. 384, no. 1, Article ID 111614, 2019.

[5] M. Hu, Y. Han, Y. Zhang, Y. Zhou, and L. Ye, "Retracted article: lncRNA TINCR sponges miR-214-5p to upregulate ROCK1 in hepatocellular carcinoma," *BMC Medical Genetics*, vol. 21, no. 1, p. 2, 2020.

[6] M. Zhang, W. Wang, T. Li et al., "Long noncoding RNA SNHG1 predicts a poor prognosis and promotes hepatocellular carcinoma tumorigenesis," *Biomedicine & Pharmacotherapy*, vol. 80, pp. 73–79, 2016.

[7] Y. Zhao, Z. S. Qin, Y. Feng, X. J. Tang, T. Zhang, and L. Yang, "Long non-coding RNA (lncRNA) small nucleolar RNA host gene 1 (SNHG1) promote cell proliferation in colorectal cancer by affecting P53," *European Review for Medical and Pharmacological Sciences*, vol. 22, no. 4, pp. 976–984, 2018.

[8] Y. Cui, F. Zhang, C. Zhu, L. Geng, T. Tian, and H. Liu, "Upregulated lncRNA SNHG1 contributes to progression of non-small cell lung cancer through inhibition of miR-101-3p and activation of Wnt/β-catenin signaling pathway," *Oncotarget*, vol. 8, no. 11, pp. 17785–17794, 2017.

[9] Z.-Q. Liu, W.-F. He, Y.-J. Wu et al., "LncRNA SNHG1 promotes EMT process in gastric cancer cells through regulation of the miR-15b/DCLK1/Notch1 axis," *BMC Gastroenterology*, vol. 20, no. 1, p. 156, 2020.

[10] M. Xu, X. Chen, K. Lin et al., "The long noncoding RNA SNHG1 regulates colorectal cancer cell growth through interactions with EZH2 and miR-154-5p," *Molecular Cancer*, vol. 17, no. 1, p. 141, 2018.

[11] Y. Zhu, B. Li, Z. Liu et al., "Up-regulation of lncRNA SNHG1 indicates poor prognosis and promotes cell proliferation and metastasis of colorectal cancer by activation of the Wnt/β-catenin signaling pathway," *Oncotarget*, vol. 8, no. 67, pp. 111715–111727, 2017.

[12] T. Tian, R. Qiu, and X. Qiu, "SNHG1 promotes cell proliferation by acting as a sponge of miR-145 in colorectal cancer," *Oncotarget*, vol. 9, no. 2, pp. 2128–2139, 2018.

[13] I. Fridrichova and I. Zmetakova, "MicroRNAs contribute to breast cancer invasiveness," *Cells*, vol. 8, no. 11, p. 1361, 2019.

[14] J. Cao, J. Qiu, X. Wang et al., "Identification of microRNA-124 in regulation of Hepatocellular carcinoma through BIRC3 and the NF-κB pathway," *Journal of Cancer*, vol. 9, no. 17, pp. 3006–3015, 2018.

[15] C. Jia, X. Yan, T. Liu et al., "MicroRNA-552 promotes tumor cell proliferation and migration by directly targeting DACH1 via the Wnt/β-catenin signaling pathway in colorectal cancer [J]," *Oncology Letters*, vol. 14, pp. 3795–3802, 2017.

[16] J. Yin, Z. Shi, W. Wei et al., "MiR-181b suppress glioblastoma multiforme growth through inhibition of SP1-mediated glucose metabolism," *Cancer Cell International*, vol. 20, no. 1, p. 69, 2020.

[17] X. Yang, Y. Sun, Y. Zhang, and S. Han, "Downregulation of miR181b inhibits human colon cancer cell proliferation by targeting CYLD and inhibiting the NF-κB signaling pathway," *International Journal of Molecular Medicine*, vol. 46, no. 5, pp. 1755–1764, 2020.

[18] H. Li, Z. Zhang, L. Chen et al., "Cytoplasmic Asporin promotes cell migration by regulating TGF-β/Smad2/3 pathway and indicates a poor prognosis in colorectal cancer," *Cell Death & Disease*, vol. 10, no. 2, p. 109, 2019.

[19] S. Gurzu, C. Silveanu, A. Fetyko, V. Butiurca, Z. Kovacs, and I. Jung, "Systematic review of the old and new concepts in the epithelial-mesenchymal transition of colorectal cancer," *World Journal of Gastroenterology*, vol. 22, no. 30, pp. 6764–6775, 2016.

[20] E. D. Hay, "An overview of epithelio-mesenchymal transformation," *Cells Tissues Organs*, vol. 154, no. 1, pp. 8–20, 1995.

[21] B. Li, A. Li, Z. You, J. Xu, and S. Zhu, "Epigenetic silencing of CDKN1A and CDKN2B by SNHG1 promotes the cell cycle, migration and epithelial-mesenchymal transition progression of hepatocellular carcinoma," *Cell Death & Disease*, vol. 11, no. 10, p. 823, 2020.

[22] J. Bai, J. Xu, J. Zhao, and R. Zhang, "lncRNA SNHG1 cooperated with miR-497/miR-195-5p to modify epithelial-mesenchymal transition underlying colorectal cancer exacerbation," *Journal of Cellular Physiology*, vol. 235, no. 2, pp. 1453–1468, 2020.

[23] A. Poursheikhani, M. R. Abbaszadegan, N. Nokhandani, and M. A. Kerachian, "Integration analysis of long non-coding RNA (lncRNA) role in tumorigenesis of colon adenocarcinoma," *BMC Medical Genomics*, vol. 13, no. 1, p. 108, 2020.

[24] F. Kopp and J. T. Mendell, "Functional classification and experimental dissection of long noncoding RNAs," *Cell*, vol. 172, no. 3, pp. 393–407, 2018.

[25] W.-X. Peng, P. Koirala, and Y.-Y. Mo, "LncRNA-mediated regulation of cell signaling in cancer," *Oncogene*, vol. 36, no. 41, pp. 5661–5667, 2017.

[26] K. Z. Thin, J. C. Tu, and S. Raveendran, "Long non-coding SNHG1 in cancer," *Clinica Chimica Acta*, vol. 494, pp. 38–47, 2019.

[27] X. Sun, Z. Wang, and W. Yuan, "Down-regulated long noncoding RNA SNHG1 inhibits tumor genesis of colorectal carcinoma," *Cancer Biomarkers*, vol. 20, no. 1, pp. 67–73, 2017.

[28] H. Qi, J. Wang, F. Wang, and H. Ma, "Long non-coding RNA SNHG1 promotes cell proliferation and tumorigenesis in colorectal cancer via Wnt/beta-catenin signaling," *Die Pharmazie*, vol. 72, no. 7, pp. 395–401, 2017.

[29] Y. Fu, Y. Yin, S. Peng et al., "Small nucleolar RNA host gene 1 promotes development and progression of colorectal cancer through negative regulation of miR-137," *Molecular Carcinogenesis*, vol. 58, no. 11, pp. 2104–2117, 2019.

[30] L. Salmena, L. Poliseno, Y. Tay, L. Kats, and P. P. Pandolfi, "A ceRNA hypothesis: the Rosetta Stone of a hidden RNA language?" *Cell*, vol. 146, no. 3, pp. 353–358, 2011.

[31] M. D. Paraskevopoulou, I. S. Vlachos, D. Karagkouni et al., "DIANA-LncBase v2: indexing microRNA targets on noncoding transcripts," *Nucleic Acids Research*, vol. 44, no. D1, pp. D231–D238, 2016.

[32] J. Wan, F. Long, C. Zhang, and Y. Liu, "miR181bp53 negative feedback axis regulates osteosarcoma cell proliferation and invasion," *International Journal of Molecular Medicine*, vol. 45, no. 6, pp. 1803–1813, 2020.

[33] Y. An, X.-m. Chen, Y. Yang et al., "LncRNA DLX6-AS1 promoted cancer cell proliferation and invasion by attenuating the endogenous function of miR-181b in pancreatic cancer," *Cancer Cell International*, vol. 18, no. 1, p. 143, 2018.

[34] L.-D. Zhao, W.-W. Zheng, G.-X. Wang et al., "Epigenetic silencing of miR-181b contributes to tumorigenicity in colorectal cancer by targeting RASSF1A," *International Journal of Oncology*, vol. 48, no. 5, pp. 1977–1984, 2016.

[35] Y. Liu, R. Uzair-ur-Rehman, Y. Guo et al., "miR-181b functions as an oncomiR in colorectal cancer by targeting PDCD4," *Protein & Cell*, vol. 7, no. 10, pp. 722–734, 2016.

[36] Y. Xu, S. Ye, N. Zhang et al., "The FTO/miR-181b-3p/ARL5B signaling pathway regulates cell migration and invasion in breast cancer," *Cancer Communications*, vol. 40, no. 10, pp. 484–500, 2020.

[37] B. Cui, B. Li, Q. Liu, and Y. Cui, "lncRNA CCAT1 promotes glioma tumorigenesis by sponging miR-181b," *Journal of Cellular Biochemistry*, vol. 118, no. 12, pp. 4548–4557, 2017.

[38] T. Tao, M. Chen, R. Jiang et al., "Involvement of EZH2 in aerobic glycolysis of prostate cancer through miR-181b/HK2 axis," *Oncology Reports*, vol. 37, no. 3, pp. 1430–1436, 2017.

[39] K. Pelka, K. Klicka, T. M. Grzywa et al., "miR-96-5p, miR-134-5p, miR-181b-5p and miR-200b-3p heterogenous expression in sites of prostate cancer versus benign prostate hyperplasia-archival samples study," *Histochemistry and Cell Biology*, vol. 155, no. 3, pp. 423–433, 2021.

[40] A. Schaefer, M. Jung, H. J. Mollenkopf et al., "Diagnostic and prognostic implications of microRNA profiling in prostate carcinoma," *International Journal of Cancer*, vol. 126, no. 5, pp. 1166–1176, 2010.

[41] X. Li, Y. Zhang, H. Zhang et al., "miRNA-223 promotes gastric cancer invasion and metastasis by targeting tumor suppressor EPB41L3," *Molecular Cancer Research*, vol. 9, no. 7, pp. 824–833, 2011.

[42] Y. Gao, Z. Xu, F. Yuan, and M. Li, "Correlation of expression levels of micro ribonucleic ccid-10b (miR-10b) and micro ribonucleic acid-181b (miR-181b) with gastric cancer and its diagnostic significance," *Medical Science Monitor*, vol. 24, pp. 7988–7995, 2018.

[43] G. A. Calin and C. M. Croce, "MicroRNA signatures in human cancers," *Nature Reviews Cancer*, vol. 6, no. 11, pp. 857–866, 2006.

[44] J. Winter and S. Diederichs, "MicroRNA biogenesis and cancer," *MicroRNA and Cancer*, vol. 676, pp. 3–22, 2011.

[45] Y. Xi, A. Formentini, M. Chien et al., "Prognostic values of microRNAs in colorectal cancer," *Biomarker Insights*, vol. 2, pp. 113–121, 2006.

[46] X. Pan, J. Feng, Z. Zhu et al., "A positive feedback loop between miR-181b and STAT 3 that affects Warburg effect in colon cancer via regulating PIAS 3 expression," *Journal of*

Cellular and Molecular Medicine, vol. 22, no. 10, pp. 5040–5049, 2018.

[47] Q. Du and J. Chen, "SNHG1 promotes proliferation, migration and invasion of bladder cancer cells via the PI3K/AKT signaling pathway," *Experimental and Therapeutic Medicine*, vol. 20, no. 5, p. 110, 2020.

[48] S. Liang, K. Ren, B. Li et al., "LncRNA SNHG1 alleviates hypoxia-reoxygenation-induced vascular endothelial cell injury as a competing endogenous RNA through the HIF-1alpha/VEGF signal pathway," *Molecular and Cellular Biochemistry*, vol. 465, no. 1-2, pp. 1–11, 2020.

[49] D. R. Principe, J. A. Doll, J. Bauer et al., "TGF: duality of function between tumor prevention and carcinogenesis," *JNCI Journal of the National Cancer Institute*, vol. 106, no. 2, p. djt369, 2014.

[50] Y. Shi and J. Massagué, "Mechanisms of TGF-β signaling from cell membrane to the nucleus," *Cell*, vol. 113, no. 6, pp. 685–700, 2003.

[51] X. Wang, Q. Lai, J. He et al., "LncRNA SNHG6 promotes proliferation, invasion and migration in colorectal cancer cells by activating TGF-β/Smad signaling pathway via targeting UPF1 and inducing EMT via regulation of ZEB1," *International Journal of Medical Sciences*, vol. 16, no. 1, pp. 51–59, 2019.

[52] X. Shen, X. Hu, J. Mao et al., "The long noncoding RNA TUG1 is required for TGF-β/TWIST1/EMT-mediated metastasis in colorectal cancer cells," *Cell Death & Disease*, vol. 11, no. 1, p. 65, 2020.

[53] X. F. Meng, A. D. Liu, and S. L. Li, "SNHG1 promotes proliferation, invasion and EMT of prostate cancer cells through miR-195-5p," *European Review for Medical and Pharmacological Sciences*, vol. 24, no. 19, pp. 9880–9888, 2020.

[54] C. Lin, J. Zhang, Y. Lu et al., "NIT1 suppresses tumour proliferation by activating the TGFβ1-Smad2/3 signalling pathway in colorectal cancer," *Cell Death & Disease*, vol. 9, no. 3, p. 263, 2018.

[55] M. Cheng, Y. Jiang, H. Yang, D. Zhao, L. Li, and X. Liu, "FLNA promotes chemoresistance of colorectal cancer through inducing epithelial-mesenchymal transition and smad2 signaling pathway," *American journal of cancer research*, vol. 10, no. 2, pp. 403–423, 2020.

Hindawi

Research Article

Prognostic Lnc-S100B-2 Affects Cell Apoptosis and Microenvironment of Colorectal Cancer through MLLT10 Signaling

Jianmei Yi,[1] **Feng Peng,**[1] **Jingli Zhao,**[2] **and Xiaosong Gong** ⓘ[1]

[1]*Department of General Surgery 2, Zhuzhou Central Hospital, Zhuzhou 412007, China*
[2]*Operating Room, Zhuzhou Central Hospital, Zhuzhou 412007, China*

Correspondence should be addressed to Xiaosong Gong; gongxiaosong0418@163.com

Long noncoding RNA (LncRNA) is closely associated with the development of colorectal cancer (CRC). The chip data and clinical information of GSE104364 and GSE151021 were downloaded by GEOquery. Limma and Kaplan–Meier analysis were performed. Lnc-S100B-2 was obtained, and high expression of Lnc-S100B-2 was predicted to be associated with a lower survival rate. Online software was adopted to predict downstream regulatory genes, and miR-331-3p and Mixed Lineage Leukemia Translocated to 10 (MLLT10) were screened and verified. After silencing Lnc-S100B-2 and MLLT10, the proliferative activity of CRC cells decreased, and the apoptosis rate increased. At the gene and protein levels, the expressions of PCNA, Ki67, and Bcl-2 were decreased in the sh-Lnc-S100B-2 group, sh-MLLT10 group, and sh-Lnc-S100B-2 + sh-MLLT10 group, while the expressions of cleaved caspase 3, caspase 9, and Bax were increased. *In vivo*, the volume and mass of the tumor decreased in the sh-Lnc-S100B-2 + sh-MLLT10 group. Proliferation and apoptosis-related index (PCNA, Ki67, cleaved caspase 3, caspase 9, Bax, and Bcl-2) expression level was also altered. Meanwhile, the infiltration of immune cells (CD3 (-), CD16 (+), and CD11b (+) cells) decreased. The expressions of epithelial-mesenchymal transformation (EMT) related indicators (E-cadherin, N-cadherin, Vimentin, β-catenin, Snail, and Slug) were changed. E-cadherin and β-catenin were increased in the sh-Lnc-S100B-2 + sh-MLLT10 group, while N-cadherin, vimentin, snail, and slug were decreased. In conclusion, our study found that the expression of Lnc-S100B-2 was dysregulated in CRC. Lnc-S100B-2 could affect cell apoptosis and the microenvironment of CRC through regulating MLLT10.

1. Introduction

Colorectal cancer (CRC) is one of the most common malignant tumors in humans and the fourth deadliest cancer in the world, with nearly 900,000 deaths every year [1]. CRC has become a major global public health problem [2]. As previously described, CRC might develop in patients with distinct intestinal diseases such as inflammatory bowel diseases, microscopic colitis, and irritable bowel syndrome [3]. It might bring some difficulties to the diagnosis of CRC. Studies have shown that some progress has been made in diagnosing, treating, and preventing CRC. For example, colonoscopy's targeted screening and surveillance policy will curb the rising incidence of CRC [4]. Allium constituents are shown to modify the risk of colon cancer and reduce the

mortality rates associated with this malignancy [5]. The poor prognosis of CRC patients remains a major problem [6]. CRC patients are usually diagnosed as advanced, with a poor prognosis and a low 5-year survival rate [7]. Previous studies have shown that the poor prognosis of CRC is related to molecular and gene changes [8]. Differential genes and molecules have essential research value in CRC [9,10].

Long noncoding RNAs (LncRNAs) are more than 200 nucleotides in length without protein-coding potential. LncRNAs are involved in regulating biological processes such as cell proliferation, differentiation, migration, and invasion [11–13] via mediating interactions between DNA and proteins, adsorbing microRNAs, and binding to proteins as decoys [14,15]. In recent years, studies on LncRNAs have attracted widespread attention. LncRNA interacts with

cell metabolism (glucose metabolism, mitochondrial function, and oxidative stress) to affect cancer development [16]. In breast cancer and bladder cancer studies, LncRNAs can be used as prognostic markers for patients [17,18]. Similarly, in studies on CRC, prognostic LncRNAs have been found to promote or inhibit the growth, metastasis, invasion, and affect the microenvironment of CRC [9,19,20]. However, the role of Lnc-S100B-2 played in CRC cells, and the CRC microenvironment has never been reported previously.

Mixed Lineage Leukemia Translocated to 10 (MLLT10) is a transcriptional activator of gene expression. MLLT10 rearrangement is closely related to the development of leukemia. MLLT10 is one of the most common fusion partners of mixed-lineage leukemia (MLL, also known as KMT2A) in acute leukemia [21]. MLLT10 and IL3 are involved in gene rearrangement in patients with early T-cell precursor acute lymphoblastic leukemia [22]. Meanwhile, MLLT10 might be involved in the metastasis of non-small cell lung cancer [23]. The expression of MLLT10 is different in CRC [24]. However, the regulatory pathway of MLLT10 in CRC remains unclear.

In the study, we aimed to obtain prognostic LncRNA and their downstream regulatory genes through database screening and bioinformatics prediction. The expression of genes and their interrelationships were verified by experiments. Its functions were verified by *in vitro* and *in vivo* experiments. The study was expected to provide a biomarker and a promising therapeutic target for the treatment of CRC.

2. Methods

2.1. CRC Dataset and Bioinformatics Analysis.
CRC datasets (GSE104364 and GSE151021) were downloaded from Gene Expression Omnibus (GEO) (http://www.ncbi.nlm.nih.gov/geo/). Among them, the GSE104364 dataset included CRC patients ($N = 12$) and normal controls ($N = 6$). The GSE151021 dataset included CRC patients ($N = 4$) and normal controls ($N = 4$). The original chip expression data and the corresponding clinical information were downloaded by GEOquery.

Limma was used to analyze LncRNA differentially expressed on chip data [25], selection criteria for $|\,logFC\,| > 1$ and $P < 0.05$. The R-package pheatmap was used to cluster the expression patterns of differentially expressed LncRNAs in the two groups, and a heatmap was drawn for visualization.

2.2. Clinical Specimens.
CRC samples ($N = 5$) and matched adjacent tissues ($N = 5$) were randomly collected from Zhuzhou Central Hospital. Before participation, we obtained the informed consent of the study subjects.

2.3. Cell Culture and Transfection.
Human CRC cell line HCT116 was purchased from Shanghai Zhong Qiao Xin Zhou Biotechnology Co., Ltd. Cells were cultured in DMEM medium containing 10% FBS with 1% penicillin-streptomycin solution (C0222, Beyotime, China) in an incubator at 37°C, 5% CO_2, and saturated humidity.

The silenced plasmid (NC), Lnc-S100B-2 silenced plasmid (sh-Lnc-S100B-2), Lnc-S100B-2 overexpressed plasmid (oe-Lnc-S100B-2), and MLLT10 silenced plasmid (sh-MLLT10) were purchased from HonorGene. Briefly, $5\,\mu g$ plasmid was added to $250\,\mu L$ serum-free medium and mixed. Lipofectamine 2000 (Invitrogen, USA) was used for transfection according to the manufacturer's instructions. The specific groups were as follows: a control group (without any treatment), an NC group (NC was transfected), a sh-Lnc-S100B-2 group (sh-Lnc-S100B-2 was transfected), a sh-MLLT10 group (sh-MLLT10 was transfected), and a sh-Lnc-S100B-2+sh-MLLT10 group (sh-Lnc-S100B-2 and sh-MLLT10 were transfected).

2.4. RNA Isolation and Quantitative Real-Time PCR (qRT-PCR).
The Trizol method was used to isolate the total RNA from tissues and HCT116 cells. Briefly, 0.02 g tissues or 5×10^6 cells were lysed with 1 mL Trizol. Isopropyl alcohol and ethanol were successively added for extraction and separation. $30\,\mu L$ sterile enzyme-free water was used to dissolve RNA precipitates. After detecting the RNA concentration, HiFiScript cDNA Synthesis Kit (CW2569 M, CWBIO, China) and miRNA cDNA Synthesis Kit (CW2141S, CWBIO, China) were used reverse transcription with a $20\,\mu L$ reverse transcription reaction system. SYBR-Green PCR Master Mix (CW2601S, CWBIO, China) was used for PCR amplification using the $30\,\mu L$ amplification system. 40 cycles were amplified. $2^{-\Delta\Delta Ct}$ was applied to calculate RNA expression levels. The sequences of primers used in the study were listed at Table 1. The expression of U6 and β-actin was applied as control.

2.5. Plate Clone Formation Assay.
As previously described, the plate clone formation assay was adopted to detect cell proliferation [26]. Briefly, cells were digested with 0.25% trypsin (C0201, Beyotime) and cultured for 14 days. The cells were fixed with 4% paraformaldehyde ((N1012, NCM Biotech) for 15 min and stained with crystal violet (G1062, Solarbio) for 30 min. A microplate reader (MB-530, HEALES) was adopted to measure the cell colony number, and pictures were taken.

2.6. Western Blot.
The RIPA buffer (P0013 B, Beyotime) was used to extract proteins by lysing cells and tissues. The SDS-PAGE gel was used to separate the proteins. The proteins were transferred to the nitrocellulose membrane. 5% skimmed milk was used to block the membrane at 4°C overnight. The membranes were incubated with primary antibodies or secondary antibodies at room temperature (RT) for 90 min. The antibodies used were as follows: anti-β-actin (1 : 5000, 66009-1-Ig, proteintech), anti-PCNA (1 : 2000, 10205-1-AP, proteintech), anti-Ki67 (1 : 1000, 27309-1-AP, proteintech), anti-cleaved caspase 3 (1 : 1000, 9664S, CST), anti-caspase 9 (1 : 500, bs-20773R, Bioss Antibodies), anti-Bax (1 : 1000, ab32503, abcam), anti-Bcl-2 (1 : 1000, 12789-1-AP, proteintech), anti-E-cadherin (1 : 1000, 20874-1-AP, proteintech), anti-β-catenin (1 : 1000, bs-1165R, Bioss

TABLE 1: The primers sequences in the study.

Name		Sequences (5'-3')	
Hsa-miR-331-3p	F	GCCCCTGGGCCTATCCTAGAA	
	RT	GCTGTCAACGATACGCTACGTAAC	
U6	F	CTCGCTTCGGCAGCACA	Product length 94 bp
	R	AACGCTTCACGAATTTGCGT	
Lnc-S100B-2	F	AAGCGACAACCCCTACGAG	Product length 172 bp
	R	CTCCCCACAACAGAAACGTCA	
MLLT10	F	ATGTTCAGGGGAATTTTAAAGTCAA	Product length 100 bp
	R	TGTTACAGAATAACAACCAGTGGG	
Ki67	F	AAGAAGCCCATGAAGACCTCC	Product length 170 bp
	R	CTCTTCTGCCCTCCGCTCT	
Caspase3	F	TGGCAACAGAATTTGAGTCCT	Product length 161 bp
	R	ACCATCTTCTCACTTGGCAT	
Caspase9	F	AAGCCAACCCTAGAAAACCTTACCC	Product length 126 bp
	R	AGCACCGACATCACCAAATCCTC	
Bcl-2	F	AGCTGCACCTGACGCCCTT	Product length 147 bp
	R	ACATCTCCCGGTTGACGCTCT	
PCNA	F	TAGCTCCAGCGGTGTAAACCT	Product length 243 bp
	R	ACTTTCTCCTGGTTTGGTGCTT	
Bax	F	TCACTGAAGCGACTGATGTCCC	Product length 96 bp
	R	ACTCCCGCCACAAAGATGGTC	
N-cadherin	F	TGCCCCTCAAGTGTTACCTC	Product length 182 bp
	R	CAAAATCACCATTAAGCCGAGT	
E-cadherin	F	ATTTTTCCCTCGACACCCGAT	Product length 109 bp
	R	TCCCAGGCGTAGACCAAGA	
Vimentin	F	CCCTTGACATTGAGATTGCCACC	Product length 166 bp
	R	ACCGTCTTAATCAGAAGTGTCCT	
β-Catenin	F	ATTCTTGGCTATTACGACAGACT	Product length 176 bp
	R	AGCAGACAGATAGCACCTT	
Snail	F	CGTCCTTCTCCTCTACTTCAGTC	Product length 125 bp
	R	CTTTCGAGCCTGGAGATCCTT	
Slug	F	AGGACACATTAGAACTCACACGG	Product length 196 bp
	R	TACACAGCAGCCAGATTCCTC	
β-Actin	F	ACCCTGAAGTACCCCATCGAG	Product length 224 bp
\	R	AGCACAGCCTGGATAGCAAC	

Antibodies), anti- N-cadherin (1 : 2000, 22018-1-AP, proteintech), anti-vimentin (1 : 2000, 10366-1-AP, proteintech), anti-Snail (1 : 1000, 13099-1-AP, proteintech), anti-Slug (1 : 1000, #9585, CST), HRP goat anti-mouse IgG (1 : 5000, SA00001-1, proteintech), and HRP goat anti-rabbit IgG (1 : 6000, SA00001-2, proteintech). Proteins were detected by Western Bright ECL kit (K-12045-D50, advansta). The expression of β-actin was applied as control.

2.7. Flow Cytometry. Apoptosis analysis was as follows. The cells were digested by trypsin without EDTA. Cells were washed twice by PBS and centrifuged at 2000 rpm for 5 min. 500μL binding buffer was added to resuspend cells. After being mixed with 5μL Annexin V-FITC, 5μL propidium iodide (PI) was added to the cells and mixed and incubated for 10 min in the dark at RT. Flow cytometry (A00-1-1102, Beckman Coulter, USA) was used for observation and analysis.

Cell-cycle analysis was as follows. The cells were digested by trypsin and centrifuged at 800 rpm for 5 min. After being resuspended with 400μL PBS, 1.2 mL of 100% precooled ethanol was added, and the cells were placed at 4℃ overnight. Cells were washed twice with 1 mL precooled PBS.

Then, cells were fixed with 150μL PI staining solution and incubated for 30 min in the dark at 4℃. Flow cytometry (A00-1-1102, Beckman Coulter, USA) was applied to analyze the cell cycle.

Identification of CD3 (-) CD16 (+) cells and CD11b (+) cells was as follows. 1×10^{6} cells were resuspended with 200μL PBS volume. Cells were incubated with 5μL CD3 (12-0038-42, eBioscience), CD16 (17-0168-42, eBioscience), or CD11b (12-0118-42, eBioscience) for 30 min in the dark. Cells were washed twice by 1 mL PBS. 200μL PBS was added to resuspend cells. After filtration with a nylon net, flow cytometry was used to detect the percent of CD3 (-) CD16 (+) cells and CD11b (+) cells.

2.8. Dual-Luciferase Reporter Assay. The online software miRDB (http://mirdb.org/index.html) was used to predict the target gene of miR-331-3p. Dual-luciferase reporter assay was used to identify the correlation between miR-331-3p and its target gene MLLT10. Briefly, 293A cells, MLLT10-wt plasmids, and MLLT10-Mut plasmids were purchased from HonorGene. MiR-331-3p mimics and mimic NC were purchased from Shanghai GenePharma Co., Ltd. The MLLT10-wt or MLLT10-Mut or miR-331-3p mimics or

mimic NC were cotransfected into precultured 293A cells using Lipofectamine 2000. After 48 h, the luciferase activity was analyzed with the Dual Luciferase Reporter Assay System (Promega, USA).

2.9. Animal Experiments. Male BALB/*c* nude mice ($N = 24$) were purchased from Human SJA Laboratory Animal Co., Ltd. As previously mentioned [27], animal models were constructed. Briefly, mice were fed adaptively for a week with normal food, water, and light. Stable HCT116 cells were cultured after NC, sh-MLLT10, and sh-Lnc-S100B-2 transfection. After the cells had grown to about 80% fusion, they were digested with trypsin and counted. $200 \mu L$ PBS containing 2×10^6 HCT116 cells was injected into the right lower flank of 6–8 weeks old mice. They were randomly divided into four groups: the NC group, the sh-MLLT10 group, the sh-Lnc-S100B-2 group, and the sh-Lnc-S100B-2 + sh-MLLT10 group, with 6 rats in each group. After 35 days of normal feeding, the mice were euthanized humanely. The tumor body was taken, and the tumor volume was measured (volume = (widths × width × length)/2).

2.10. Immunohistochemistry (IHC). Briefly, after 12 hours of baking at 60°C, the paraffin slices were dewaxed. After heating for antigenic repair, 1% periodic acid was used to inactivate endogenous enzyme activity. After incubation with anti-caspase 3 (1 : 200, 19677-1-AP, proteintech) at 4°C overnight, $100 \mu L$ anti-rabbit IgG was inoculated at 37°C for 30 min. After DAB color development, the hematoxylin was counterstained for 10 min. Then, the sections were sealed with the neutral resin and observed with a light microscope.

2.11. Immunofluorescence (IF) Assay. The expression of CD3, E-cadherin, and vimentin in tissues was determined by IF. Briefly, after heating for antigenic repair, the sample was treated with hydrogen boride solution and Sudan black dye. 10% serum and 5% BSA were used to seal the sample for 60 min. Anti-CD3 (1 : 50, 17617-1-AP, proteintech), anti-E-cadherin (1 : 50, 20874-1-AP, proteintech), and anti-vimentin (1 : 50, 10366-1-AP, proteintech) were incubated overnight at 4°C, and anti-rabbit -IgG labeled fluorescent antibodies were incubated at 37°C for 90 min. Nuclear DNA was labeled with DAPI (blue). Cells were analyzed with a fluorescence microscope.

2.12. Statistics Analysis. Data were analyzed using the GraphPad Prism 8.0.1 and presented as the mean ± SD. Kaplan–Meier analysis and log-rank test were adopted to analyze the survival time of patients. Correlation between the expression of miR-331-3p and Lnc-S100B-2 was analyzed by Pearson's correlation analysis. Paired *t*-test, one-way ANOVA or two-way ANOVA with Tukey's multiple comparisons test were performed to evaluate the statistical significance. $P < 0.05$ was considered to indicate a statistically significant difference.

3. Results

3.1. Lnc-S100B-2 Is Highly Expressed with a Poor Prognosis in CRC. To obtain differential LncRNAs in CRC, we analyzed the expression profiles of LncRNAs in the GSE104364 and GSE151021 datasets. We found a series of differentially expressed LncRNAs in CRC (Figure 1(a). Kaplan–Meier analysis showed that the survival curve of Lnc-CA14-1, Lnc-FABP2-4, Lnc-MYH11-1, and Lnc-S100B-2 was $P < 0.05$ (Figure 1(b)). Higher Lnc-S100B-2 level was associated with poorer survival. These results suggested that Lnc-S100B-2 might be involved in the prognosis of CRC.

3.2. Lnc-S100B-2 Affects the Proliferation and Apoptosis of HCT116 Cells. We randomly collected 5 pairs of tumor and matched adjacent tissues. Clinical samples were used to verify the level of Lnc-S100B-2. The paired *t*-test (Figure 2(a)) were consistent with those of predicting results (Figure 1(a)). The expression of Lnc-S100B-2 was significantly upregulated in tumor tissues. The results of plate clone formation assay showed that the activity of HCT116 cells was decreased when Lnc-S100B-2 was inhibited (Figure 2(b)). Apoptosis results proved that Lnc-S100B-2 was positively correlated with CRC cell activity (Figure 2(c)). Knockdown of Lnc-S100B-2 resulted in cell stagnation in the G2 phase (Figure 2(d)). Expression of proliferation (PCNA and Ki67) and apoptosis-related indicators (cleaved caspase 3, Bax, and Bcl-2) at the gene and protein levels was identified (Figure 2(e) and 2(f)). Expressions of PCNA, Ki67, and Bcl-2 decreased in the sh-Lnc-S100B-2 group compared to the control group, while cleaved caspase 3 and Bax were the opposite. Combined with the above results, the expression of Lnc-S100B-2 in CRC might affect cell proliferation and apoptosis.

3.3. Lnc-S100B-2 Regulates MLLT10 in CRC. Next, we validated the expression of the downstream gene of Lnc-S100B-2. MiR-331-3p was decreased in cancer tissue (Figure 3(a)). Pearson's analysis showed that the levels of miR-331-3p were significantly negatively correlated with Lnc-S100B-2 (Figure 3(b)). The expression of miR-331-3p increased or decreased with the decrease or increase of Lnc-S100B-2 (Figures 3(c) and 3(d)). These results hinted that Lnc-S100B-2 could regulate the levels of miR-331-3p. Meanwhile, the expression of MLLT10 was higher in tumors than in adjacent mucosa (Figure 3(e)). The online software miRDB (http://mirdb.org/index.html) was used to predict the target gene of miR-331-3p. Dual-luciferase reporter assay results showed that miR-331-3p targeted MLLT10 (Figure 3(f)). The above experimental results suggested that Lnc-S100B-2 might regulate the expression of MLLT10 through miR-331-3p.

3.4. MLLT10 Could Promote HCT116 Cell Apoptosis. To verify the role of MLLT10 in CRC, we stably transfected sh-MLLT10 in HCT116 cells. qRT-PCR results showed that sh-MLLT10 had good efficacy (Figure 4(a)). The expression of apoptosis-related indexes (cleaved caspase 3, caspase 9, Bax,

(a)

(b)
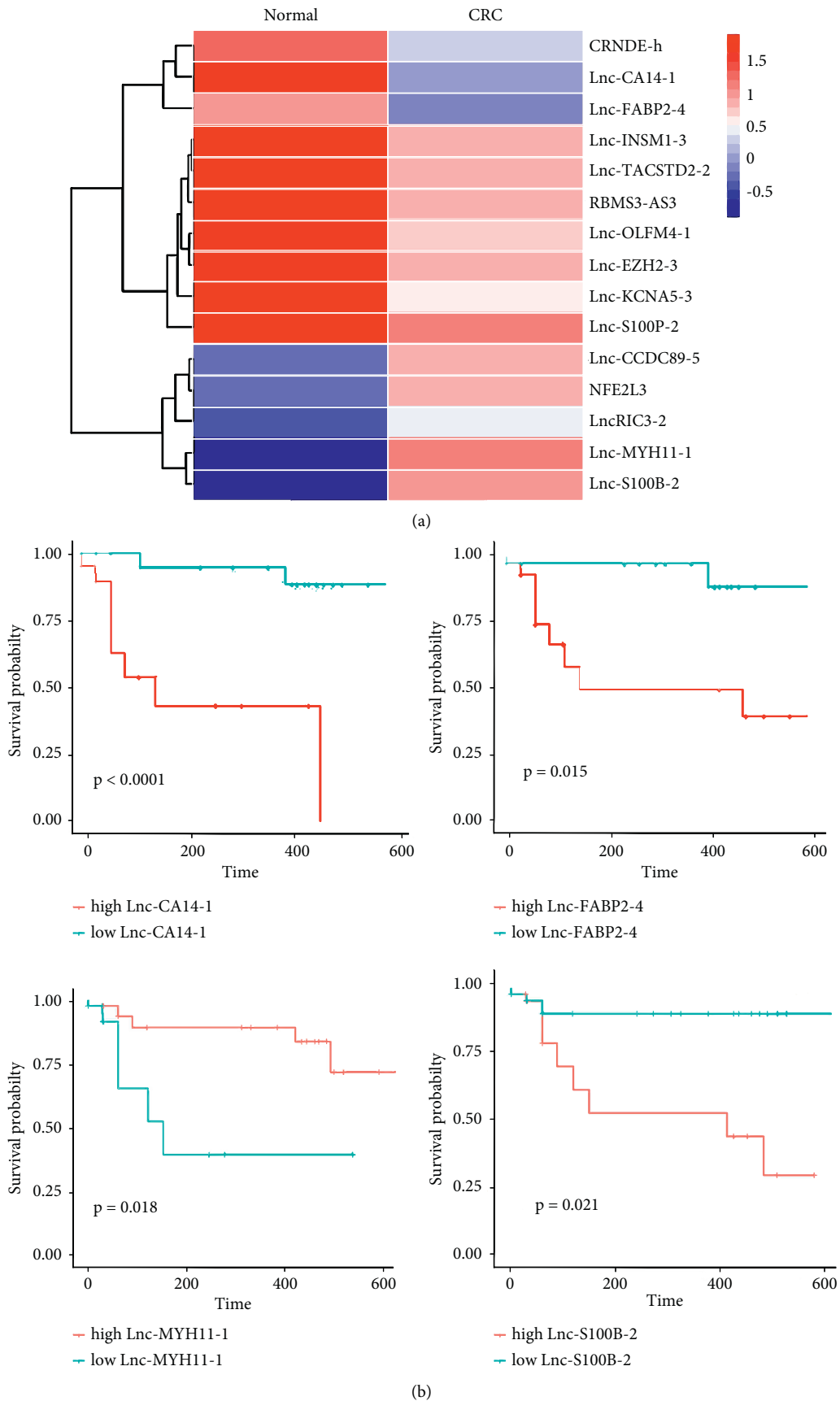
FIGURE 1: Expressions of differential LncRNA and prognosis in CRC. (a) The expression of differential LncRNAs in GEO. Blue turns red, indicating increased gene abundance. (b) Survival prediction analysis of the Lnc-CA14-1, Lnc-FABP2-4, Lnc-MYH11-1, and Lnc-S100B-2 in high and low groups.

(a)

(b)

(c)

(d)

Figure 2: Continued.

(e)

(f)
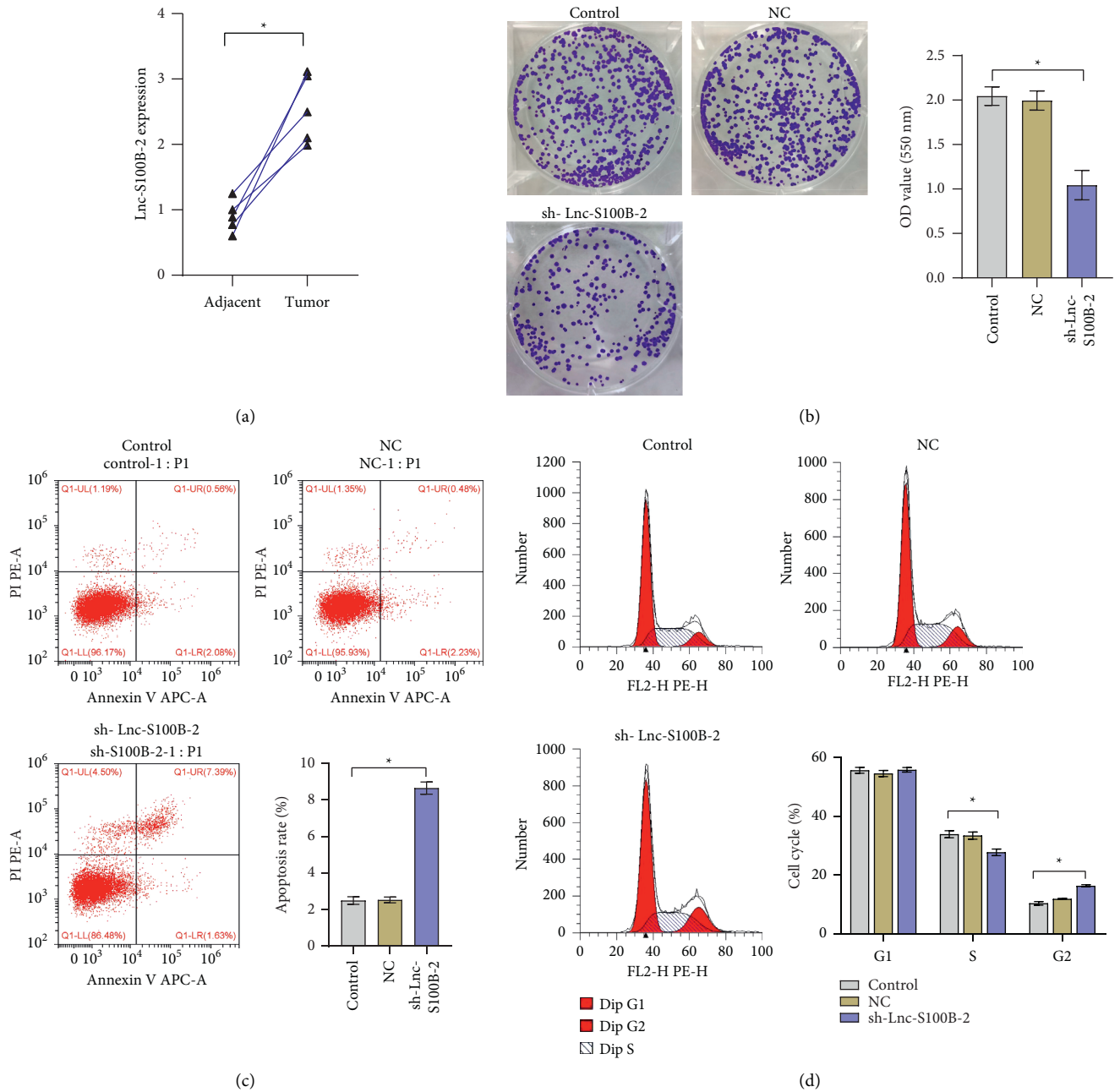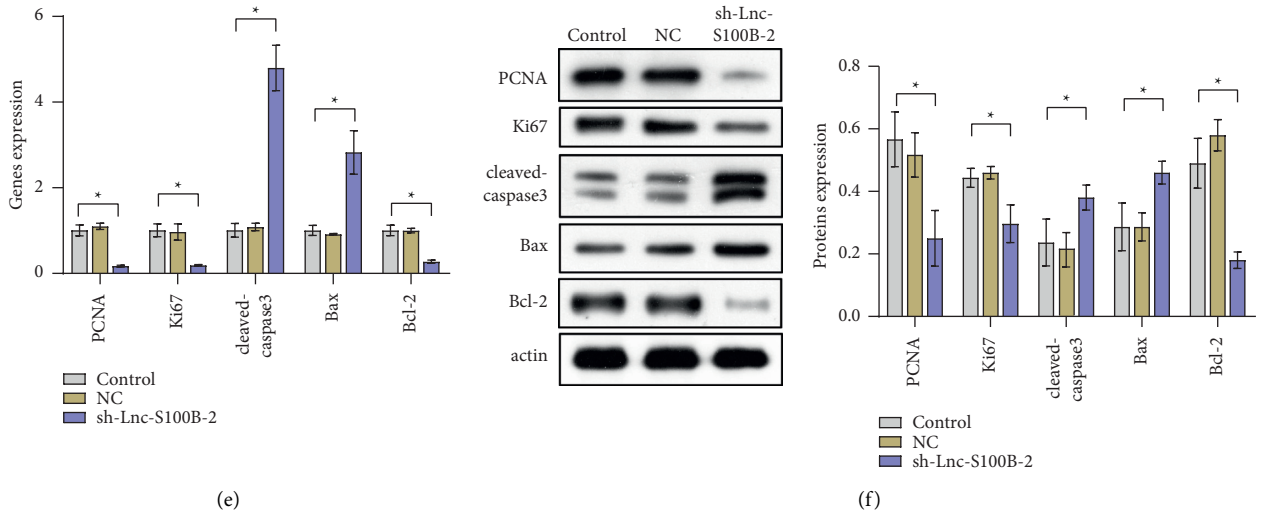
FIGURE 2: Effects of Lnc-S100B-2 in CRC cells. (a) Expression of Lnc-S100B-2 between adjacent and tumor tissues. (b) The proliferation of HCT116 cells by plate clone formation assay. (c) The apoptosis rate of HCT116 cells. (d) Cell cycle analysis of HCT116 cells. (e), (f) Expressions of PCNA, Ki67, cleaved caspase 3, Bax, and Bcl-2 at the gene and protein levels. $^*P < 0.05$, paired t-test and one-way ANOVA.

(a)

(b)

(c)

(d)

(e)

(f)
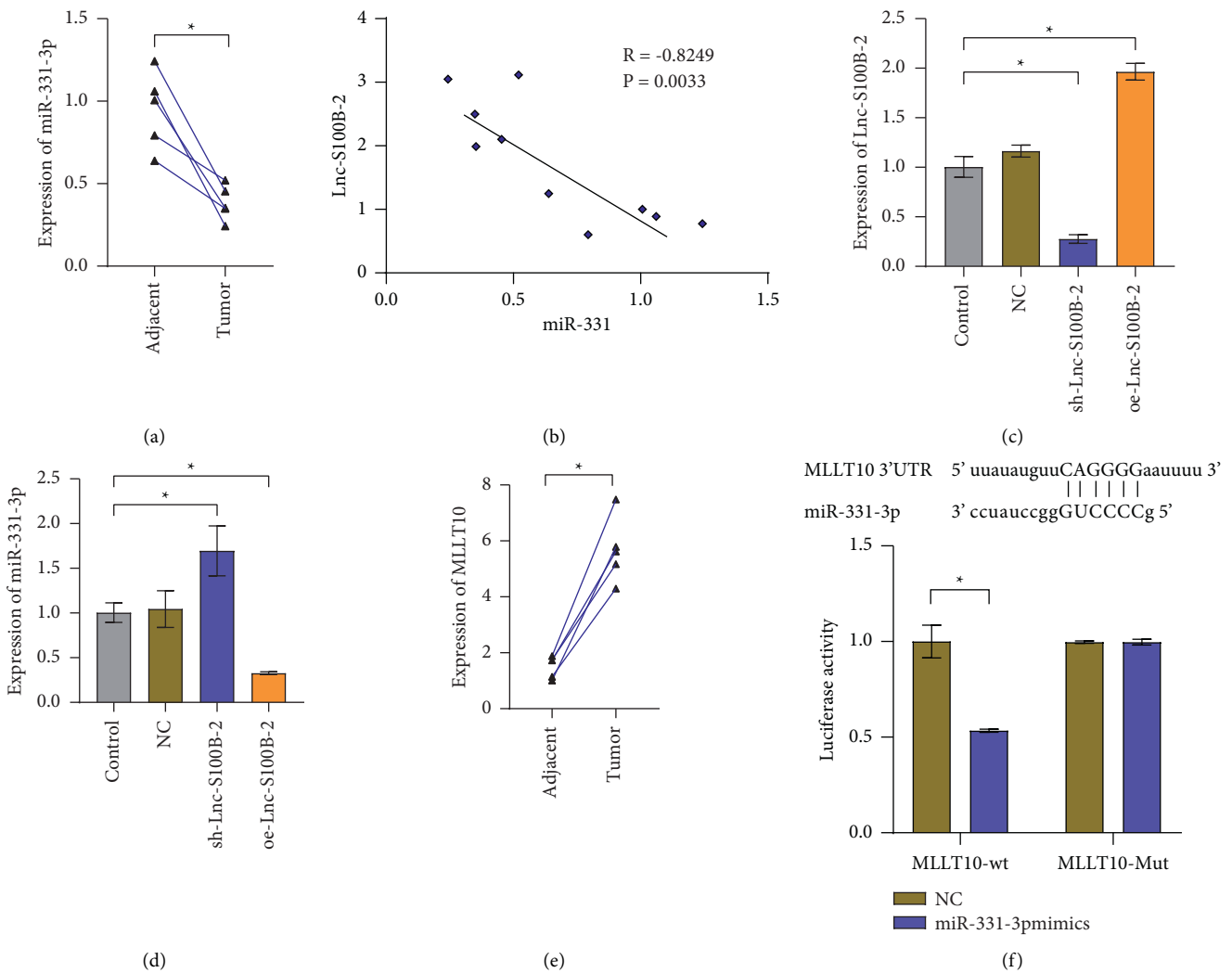
FIGURE 3: Lnc-S100B-2 regulates the expression of MLLT10 by miR-331-3p. (a) Expression of miR-331-3p between adjacent and tumor tissues. (b) Pearson's correlation analyzed the correlation between miR-331-3p and Lnc-S100B-2. (c), (d) Expression of Lnc-S100B-2 and miR-331-3p. (e) Expression of MLLT)10 between adjacent and tumor tissues. (f) Dual-luciferase reporter analysis of miR-331-3p and MLLT10. $^*P < 0.05$, paired t-test and one-way ANOVA.

(a)

(b)

(c)

(d)
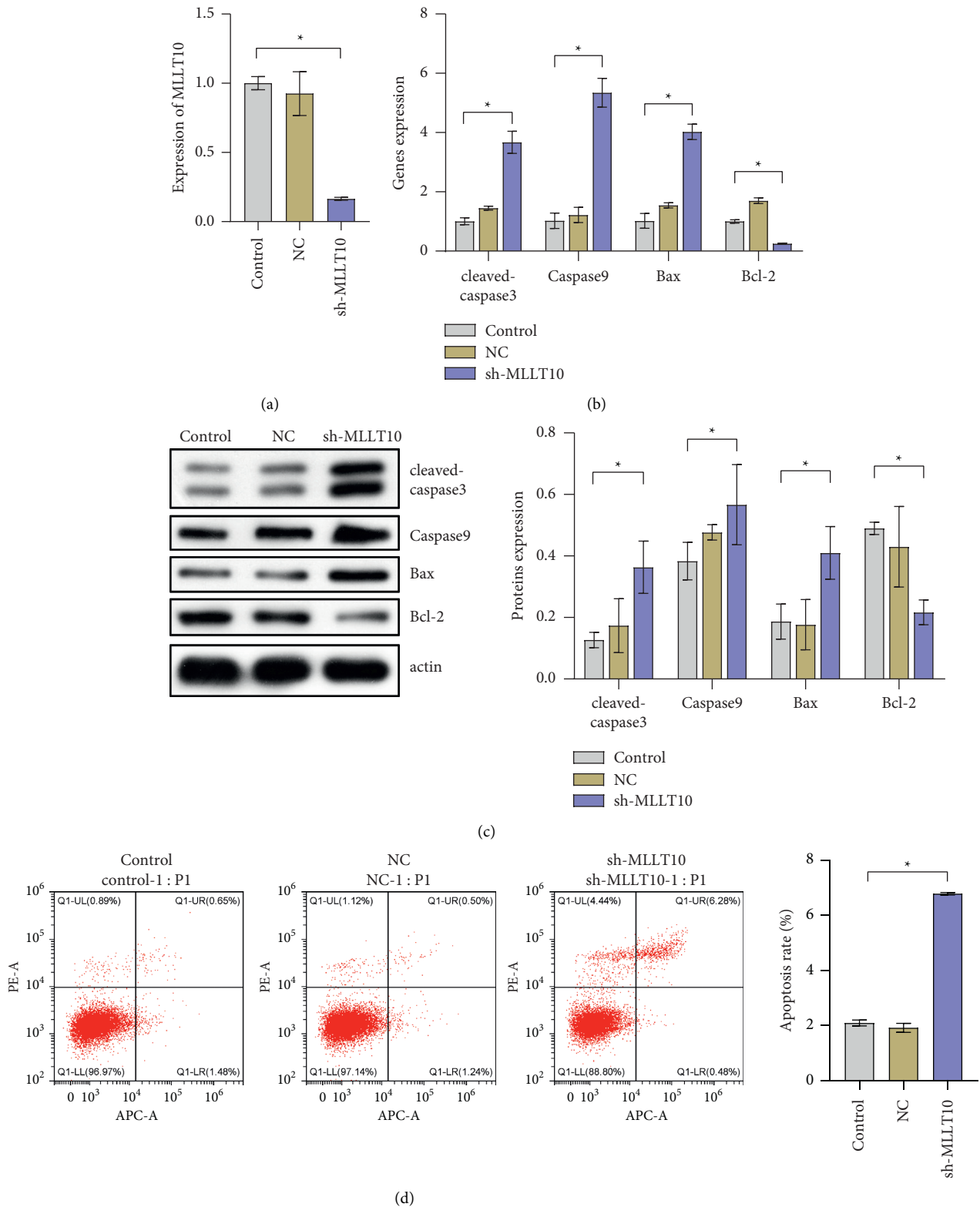
FIGURE 4: The expression of MLLT10 could affect cell apoptosis in CRC. (a) Expression of MLLT10. (b), (c) The expressions of cleaved caspase 3, caspase 9, Bax, and Bcl-2 at the gene and protein levels. (d) The apoptosis rate of HCT116 cells. $^{*}P < 0.05$, one-way ANOVA.

and Bcl-2) significantly changed in the sh-MLLT10 group (Figure 4(b) and 4(c)). Meanwhile, the apoptosis rate of HCT116 cells also indicated that the expression of MLLT10 was negatively correlated with the apoptosis rate (Figure 4(d)). These results suggested that the levels of MLLT10 in CRC could affect cell apoptosis.
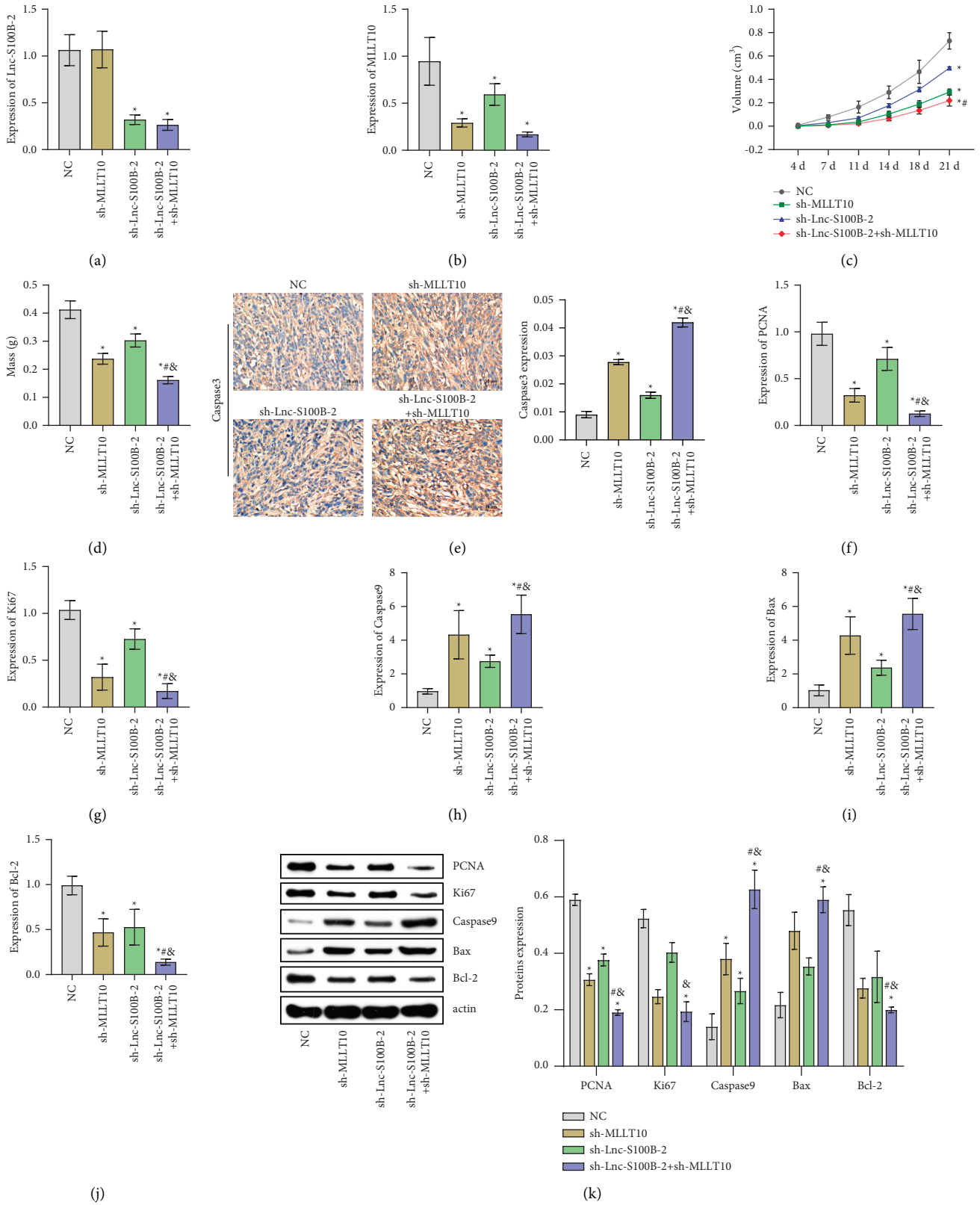
FIGURE 5: Effects of Lnc-S100B-2 and MLLT10 *in vivo*. (a, b) Expression of Lnc-S100B-2 and MLLT10. (c, d) Tumor volume and mass. (e) Expression of caspase 3 by IHC. (f–k) The expression of PCNA, Ki67, caspase 9, Bax, and Bcl-2 at the gene and protein levels. $^*P < 0.05$ versus NC group, $^\#P < 0.05$ versus sh-MLLT10 group, and $^\&P < 0.05$ versus sh-Lnc-S100B-2 group, one-way ANOVA and two-way ANOVA.
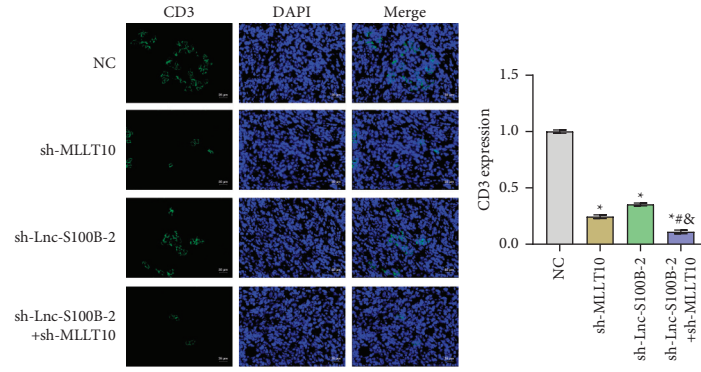
(a)
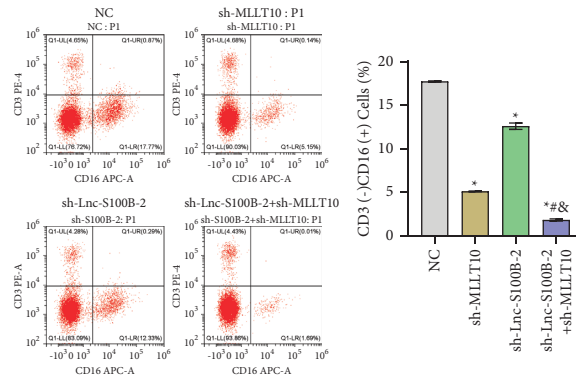
(b)
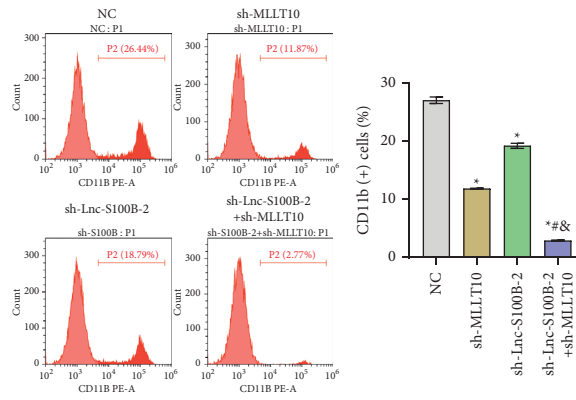
(c)
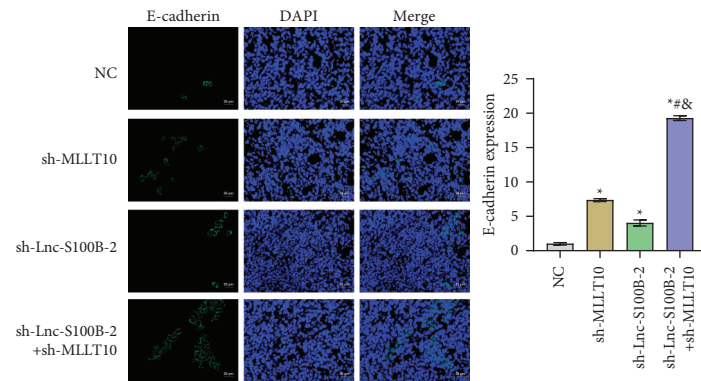
(d)

Figure 6: Continued.

(e)

(f)

(g)

(h)

(i)

(j)

(k)

(l)
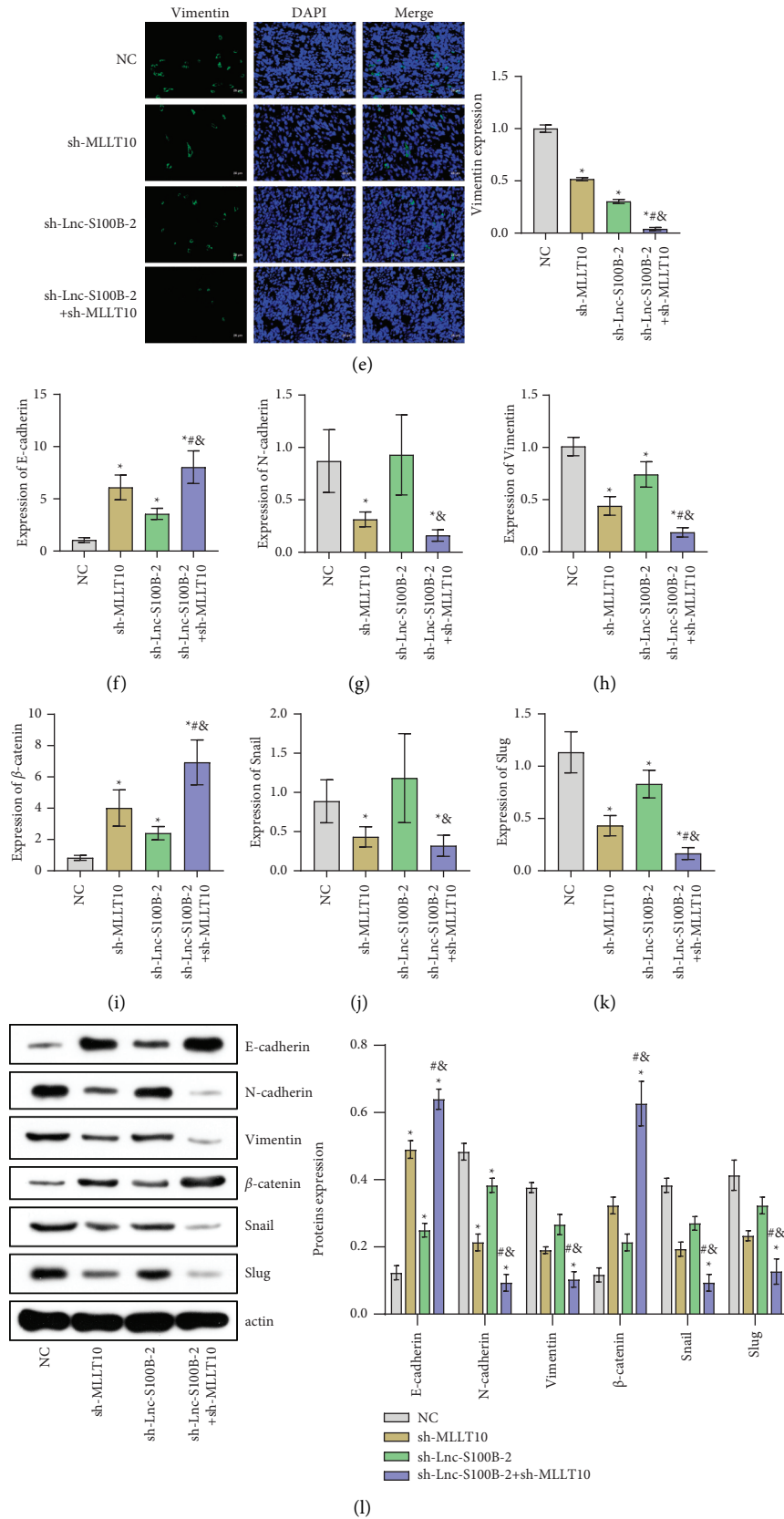
FIGURE 6: Effects of Lnc-S100B-2 and MLLT10 on the tumor microenvironment. (a) The expressions of CD3 were detected by IF assay. (b) The percent of CD3 (-) CD16 (+) cells was detected by flow cytometry. (c) The percent of CD11b (+) cells was analyzed by flow cytometry. (d, e) The expression E-cadherin and vimentin was analyzed by IF assay. (f–l) The expressions of E-cadherin, N-cadherin, vimentin, β-catenin, snail, and slug were detected by qRT-PCR and Western blot. $^{*}P < 0.05$ versus NC group, $^{\#}P < 0.05$ versus sh-MLLT10 group, $^{\&}P < 0.05$ versus sh-Lnc-S100B-2 group, and one-way ANOVA.

3.5. Effects of Lnc-S100B-2 and MLLT10 on the Development of CRC. Then, HCT116 cells transfected with NC, sh-MLLT10, sh-Lnc-S100B-2, or sh-Lnc-S100B-2+ sh-MLLT10 were subcutaneously injected into nude mice. The expression of Lnc-S100B-2 and MLLT10 was altered in the tumor (Figures 5(a) and 5(b)). Tumor volume and mass were significantly reduced after inhibition of Lnc-S100B-2 and MLLT10 (Figures 5(c) and 5(d)). After IHC staining of the tumor (Figure 5(e)), the expression of caspase 3 was significantly increased after sh-Lnc-S100B-2 and sh-MLLT10 treatment. Meanwhile, the sh-Lnc-S100B-2 + sh-MLLT10 group was markedly higher than the sh-MLLT10 group. These results suggested that Lnc-S100B-2 might regulate the expression of MLLT10 to affect cell apoptosis. At the gene and protein levels, the levels of proliferation (PCNA and Ki67) and apoptosis-related indexes (cleaved caspase 3, Bax, and Bcl-2) further suggested that Lnc-S100B-2 could affect the development of CRC by regulating the expression of MLLT10 (Figures 5(f)–5(k)). These results indicated that Lnc-S100B-2 might affect the proliferation and apoptosis of CRC cells by regulating MLLT10.

3.6. Effects of Lnc-S100B-2 and MLLT10 on Immune Cell Invasion and EMT in CRC. Immune cell invasion and EMT are two essential components of the tumor microenvironment. To further explore the role of Lnc-S100B-2 and MLLT10 in CRC, we investigated the immune cell invasion and the degree of EMT in the tumor. CD3 expression was significantly decreased after sh-Lnc-S100B-2 and sh-MLLT10 treatment (Figure 6(a)). It suggested that the infiltration degree of lymphocytes in the tumor tissue was reduced. The number of CD3 (-) CD16 (+) cells and CD11b (+) cells were also significantly decreased with the silencing of Lnc-S100B-2 and MLLT10 (Figures 6(b) and 6(c)). These results suggested that regulation of Lnc-S100B-2 and MLLT10 might affect the abundance of immune cells in tumor tissues. In addition, the expression of E-cadherin was significantly increased in the sh-MLLT10 group compared with the other three groups. Vimentin is the opposite (Figure 6(e)). We examined the expression levels of EMT-related indicators (E-cadherin, N-cadherin, vvimentin, β-catenin, snail, and slug) at the gene and protein levels. The results showed (Figures 6(f)–6(l)) that E-cadherin and β-catenin were significantly increased in the sh-Lnc-S100B-2+sh-MLLT10 group, compared with the sh-Lnc-S100B-2 group and the sh-MLLT10 group, while N-cadherin, vimentin, snail, and slug were decreased considerably. It is suggested that Lnc-S100B-2 might affect the EMT of tumor cells through MLLT10, at least partially. Combined with the above experimental results, we found that the regulation of Lnc-S100B-2 and MLLT10 could affect the immune cell invasion and EMT in the tumor.

4. Discussion

In our study, Lnc-S100B-2 has obtained through Limma and Kaplan–Meier analysis in the CRC datasets (GSE104364 and GSE151021). At the cellular and animal levels, the effects of

Lnc-S100B-2 and its downstream MLLT10 signaling on CRC have been identified.

Lnc-S100B-2 is a long noncoding RNA. Our study found that Lnc-S100B-2 was overexpressed in CRC. The expression of Lnc-S100B-2 could affect the proliferation, apoptosis, and EMT of CRC cells. The prognosis of CRC is closely related to EMT. Kaplan–Meier analysis showed that the over-expression of Lnc-S100B-2 predicted a poor prognosis in CRC. EMT is closely associated with poor prognosis of cancer patients, including gastric cancer [28], glioma [29], and bile duct cancer [30]. In bladder cancer, Cao *R.* et al. found that EMT, as a negative independent prognostic factor, had a tumor-promoting effect due to its related genetic characteristics [31]. These findings suggest that EMT in CRC may affect patient prognosis. At the same time, this verified our results from the side that Lnc-S100B-2 affected the prognosis of CRC through EMT of CRC cells.

Our study found that Lnc-S100B-2 might regulate the expression of MLLT10 through miR-331-3p. miRNA is also involved in CRC development and prognosis [32]. Lin et al. showed that miR-195-5p/NOTCH2 signaling could affect the polarization of M2-like tumor-associated macrophages by mediating tumor cell EMT [33]. Zhang Y et al. found that miR-17-5P could activate cancer-associated fibroblasts by regulating RUNX3/MYC/TGF-β1 signaling, influencing tumor microenvironment and promoting CRC development [34]. These results suggest that miRNA might influence the tumor microenvironment and CRC development by regulating the expression of downstream target genes.

Studies have shown that MLLT10 is often observed in acute myeloid and lymphoid leukemia, affecting its treatment and prognosis [35,36]. Previous studies have shown that inhibition of MLLT10 expression can affect the proliferation, migration, and invasion of non-small cell lung cancer cells [23]. It is similar to our findings. MLLT10 could affect the apoptosis level of CRC cells. The expression of apoptosis-related indicators (cleaved caspase 3, caspase 9, Bax, and Bcl-2) was altered with the silence of MLLT10. MLLT10 also has a particular regulatory effect on cell EMT and immune cell infiltration. After inhibiting the expression of MLLT10, the expression levels of EMT-related indicators (E-cadherin, N-cadherin, vimentin, β-catenin, snail, and Slug) changed. EMT is involved in the migration, invasion, and metastasis of cancer cells [37]. EMT is closely related to cell apoptosis. A negative correlation between apoptosis and EMT has been reported in ovarian cancer [38]. Vimentin can affect the apoptosis of SMMC-7721 cells in liver cancer studies [39]. Regulation of Snail1 expression can restore EMT and prevent ethanol-induced apoptosis of neural crest cells [40]. All these proved from the side that MLLT10 affects CRC cell apoptosis and EMT, with sure accuracy. Jing et al.'s study further proved our results, knockdown of MLLT10 could also inhibit EMT and affect the development of colorectal cancer [24].

In our study, MLLT10 expression could affect the degree of infiltration of immune cells. After regulating the expression of MLLT10, the proportion of CD16 and CD11b positive cells decreased. The abundance of tumor-infiltrating immune cells is highly correlated with the progression of

CRC [41]. Our study found that the proportion of CD3 positive cells (T cells) decreased after MLLT10 silencing. It is suggested that MLLT10 could affect the infiltration degree of T cells in CRC. Studies have shown that the proportions of T cells, NK cells, and macrophages in CRC are higher than those in normal tissues [41]. CD3 (-) CD16 (+) are cytotoxic natural killer cells (NK) that can directly kill tumor cells [42]. In the peripheral blood of CRC patients, it was identified that CRC patients with high CD16 (+) NKT-like cells had shorter disease-free survival [43]. That is, relative CD16 (+) NKT-like cells are reduced in patients with high survival. These findings are similar to ours. Low levels of MLLT10 have a low degree of immune cell infiltration.

5. Conclusion

Lnc-S100B-2 was screened out in this study, which is closely associated with a poor prognosis of CRC. Regulation of Lnc-S100B-2 and its downstream MLLT10 can affect CRC cell apoptosis. Lnc-S100B-2 and MLLT10 are associated with EMT and immune cell infiltration in CRC cells. It might provide a potential biomarker for CRC prognosis.

Data Availability

The data used to support the findings of this study are available from the corresponding author upon request.

Conflicts of Interest

The authors declare that there are no conflicts of interest regarding the publication of this study.

Acknowledgments

References

[1] E. Dekker, P. J. Tanis, J. L. A. Vleugels, P. M. Kasi, and M. B. Wallace, "Colorectal cancer," *The Lancet*, vol. 394, no. 10207, pp. 1467–1480, 2019.

[2] A. Jemal, F. Bray, M. M. Center, J. Ferlay, E. Ward, and D. Forman, "Global cancer statistics," *CA: A Cancer Journal for Clinicians*, vol. 61, no. 2, pp. 69–90, 2011.

[3] M. El-Salhy, "The prevalence of inflammatory bowel diseases, microscopic colitis, and colorectal cancer in patients with irritable bowel syndrome," *Gastroenterology Insights*, vol. 3, no. 1, pp. 7–10, 2011.

[4] E. Ray-Offor and F. B. Abdulkareem, "Screening colonoscopy in port harcourt, Nigeria," *Gastroenterology Insights*, vol. 10, no. 1, pp. 1–4, 2019.

[5] A. Forma, Z. Chilimoniuk, J. Januszewski, and R. Sitarz, "The potential application of allium extracts in the treatment of gastrointestinal cancers," *Gastroenterology Insights*, vol. 12, no. 2, pp. 136–146, 2021.

[6] B. Gong, "Identification of hub genes related to carcinogenesis and prognosis in colorectal cancer based on integrated bioinformatics," *Mediators Inflammatory*, vol. 2020, Article ID 5934821, 2020.

[7] J. M. E. Walsh and J. P. Terdiman, "Colorectal cancer screening," *Journal of the American Medical Association*, vol. 289, no. 10, pp. 1288–1296, 2003.

[8] A. Sadanandam, C. A. Lyssiotis, K. Homicsko et al., "A colorectal cancer classification system that associates cellular phenotype and responses to therapy," *Nature Medicine*, vol. 19, no. 5, pp. 619–625, 2013.

[9] R. Tang, J. Chen, M. Tang et al., "LncRNA SLCO4A1-AS1 predicts poor prognosis and promotes proliferation and metastasis via the EGFR/MAPK pathway in colorectal cancer," *International Journal of Biological Sciences*, vol. 15, no. 13, pp. 2885–2896, 2019.

[10] N. Li, R. Babaei-Jadidi, F. Lorenzi et al., "An FBXW7-ZEB2 axis links EMT and tumour microenvironment to promote colorectal cancer stem cells and chemoresistance," *Oncogenesis*, vol. 8, no. 3, p. 13, 2019.

[11] J. Li, Z Li, W Zheng et al., "LncRNA-ATB: an indispensable cancer-related long noncoding RNA," *Cell Proliferation*, vol. 50, no. 6, 2017.

[12] Y. Xin, Z. Li, J. Shen, M. T. V. Chan, and W. K. K. Wu, "CCAT1: a pivotal oncogenic long non-coding RNA in human cancers," *Cell Proliferation*, vol. 49, no. 3, pp. 255–260, 2016.

[13] R. Mehra, A. M. Udager, T. U. Ahearn et al., "Overexpression of the long non-coding RNA SChLAP1 independently predicts lethal prostate cancer," *European Urology*, vol. 70, no. 4, pp. 549–552, 2016.

[14] S. Lee, F Kopp, T. C Chang et al., "Noncoding RNA NORAD regulates genomic stability by sequestering PUMILIO proteins," *Cell*, vol. 164, no. 1-2, pp. 69–80, 2016.

[15] S. Carpenter, D. Aiello, M. K. Atianand et al., "A long noncoding RNA mediates both activation and repression of immune response genes," *Science*, vol. 341, no. 6147, pp. 789–792, 2013.

[16] Y. H. Lin, "Crosstalk of lncRNA and cellular metabolism and their regulatory mechanism in cancer," *International Journal of Molecular Sciences*, vol. 21, no. 8, 2020.

[17] A. He, S. He, D. Peng et al., "Prognostic value of long noncoding RNA signatures in bladder cancer," *Aging*, vol. 11, no. 16, pp. 6237–6251, 2019.

[18] Y. Shen, X. Peng, and C. Shen, "Identification and validation of immune-related lncRNA prognostic signature for breast cancer," *Genomics*, vol. 112, no. 3, pp. 2640–2646, 2020.

[19] M. Xu, X. Xu, B. Pan et al., "LncRNA SATB2-AS1 inhibits tumor metastasis and affects the tumor immune cell microenvironment in colorectal cancer by regulating SATB2," *Molecular Cancer*, vol. 18, no. 1, p. 135, 2019.

[20] X. Wang, G. Jiang, W. Ren, B. Wang, C. Yang, and M. Li, "LncRNA NEAT1 regulates 5-fu sensitivity, apoptosis and invasion in colorectal cancer through the MiR-150-5p/CPSF4 Axis," *OncoTargets and Therapy*, vol. 13, pp. 6373–6383, 2020.

[21] J. F. Peterson, W. R. Sukov, B. A. Pitel et al., "Acute leukemias harboring KMT2A/MLLT10 fusion: a 10-year experience from a single genomics laboratory," *Genes, Chromosomes and Cancer*, vol. 58, no. 8, pp. 567–577, 2019.

[22] M. A. K. Othman, J. B. Melo, I. M. Carreira et al., "MLLT10 and IL3 rearrangement together with a complex four-way translocation and trisomy 4 in a patient with early T-cell precursor acute lymphoblastic leukemia: a case report," *Oncology Reports*, vol. 33, no. 2, pp. 625–630, 2015.

[23] Q.-Q. Tian, J. Xia, X. Zhang, B.-Q. Gao, and W. Wang, "miR-331-3p inhibits tumor cell proliferation, metastasis, invasion by targeting MLLT10 in non-small cell lung cancer," *Cancer Management and Research*, vol. 12, pp. 5749–5758, 2020.

[24] X. Jing, H. Wu, X. Cheng et al., "MLLT10 promotes tumor migration, invasion, and metastasis in human colorectal cancer," *Scandinavian Journal of Gastroenterology*, vol. 53, no. 8, pp. 964–971, 2018.

[25] M. E. Ritchie, B. Phipson, D. Wu et al., "Limma powers differential expression analyses for RNA-sequencing and microarray studies," *Nucleic Acids Research*, vol. 43, no. 7, p. e47, 2015.

[26] Z. Zheng, J.-Q. Qu, H.-M. Yi et al., "MiR-125b regulates proliferation and apoptosis of nasopharyngeal carcinoma by targeting A20/NF-κB signaling pathway," *Cell Death & Disease*, vol. 8, no. 6, Article ID e2855, 2017.

[27] V. Huang, R. F. Place, V. Portnoy et al., "Upregulation of Cyclin B1 by miRNA and its implications in cancer," *Nucleic Acids Research*, vol. 40, no. 4, pp. 1695–1707, 2012.

[28] M. A. Kim, H. S. Lee, H. E. Lee, J. H. Kim, H.-K. Yang, and W. H. Kim, "Prognostic importance of epithelial-mesenchymal transition-related protein expression in gastric carcinoma," *Histopathology*, vol. 54, no. 4, pp. 442–451, 2009.

[29] J. Zhang, H. Cai, L. Sun et al., "LGR5, a novel functional glioma stem cell marker, promotes EMT by activating the Wnt/β-catenin pathway and predicts poor survival of glioma patients," *Journal of Experimental & Clinical Cancer Research*, vol. 37, no. 1, p. 225, 2018.

[30] R. Sun, Z. Liu, B. Qiu et al., "Annexin10 promotes extrahepatic cholangiocarcinoma metastasis by facilitating EMT via PLA2G4A/PGE2/STAT3 pathway," *EBioMedicine*, vol. 47, pp. 142–155, 2019.

[31] R. Cao, L. Yuan, B. Ma, G. Wang, W. Qiu, and Y. Tian, "An EMT-related gene signature for the prognosis of human bladder cancer," *Journal of Cellular and Molecular Medicine*, vol. 24, no. 1, pp. 605–617, 2020.

[32] A. Fateh, "Prognostic and predictive roles of microRNA-383 in colorectal cancer," *Gastroenterology Insights*, vol. 7, no. 1, pp. 26–29, 2016.

[33] X. Lin, S. Wang, M. Sun et al., "miR-195-5p/NOTCH2-mediated EMT modulates IL-4 secretion in colorectal cancer to affect M2-like TAM polarization," *Journal of Hematology & Oncology*, vol. 12, no. 1, p. 20, 2019.

[34] Y. Zhang, S. Wang, Q. Lai et al., "Cancer-associated fibroblasts-derived exosomal miR-17-5p promotes colorectal cancer aggressive phenotype by initiating a RUNX3/MYC/TGF-β1 positive feedback loop," *Cancer Letters*, vol. 491, pp. 22–35, 2020.

[35] J. L. Deutsch and J. L. Heath, "MLLT10 in benign and malignant hematopoiesis," *Experimental Hematology*, vol. 87, pp. 1–12, 2020.

[36] M. O. Forgione, *MLLT10 Rearranged Acute Leukemia: Incidence, Prognosis, and Possible Therapeutic Strategies*, Genes Chromosomes Cancer, New York, NY, USA, 2020.

[37] B. D. Craene and G. Berx, "Regulatory networks defining EMT during cancer initiation and progression," *Nature Reviews Cancer*, vol. 13, no. 2, pp. 97–110, 2013.

[38] H. Yan, H. Li, M. A. Silva et al., "LncRNA FLVCR1-AS1 mediates miR-513/YAP1 signaling to promote cell progression, migration, invasion and EMT process in ovarian cancer," *Journal of Experimental & Clinical Cancer Research*, vol. 38, no. 1, p. 356, 2019.

[39] Y. Wei, B. Lv, J. Xie et al., "Plumbagin promotes human hepatoma SMMC-7721 cell apoptosis via caspase-3/vimentin signal-mediated EMT," *Drug Design, Development and Therapy*, vol. 13, pp. 2343–2355, 2019.

[40] Y. Li, F. Yuan, T. Wu et al., "Sulforaphane protects against ethanol-induced apoptosis in neural crest cells through restoring epithelial-mesenchymal transition by epigenetically modulating the expression of Snail1," *Biochimica et Biophysica Acta - Molecular Basis of Disease*, vol. 1865, no. 10, pp. 2586–2594, 2019.

[41] P. Ge, W. Wang, L. Li et al., "Profiles of immune cell infiltration and immune-related genes in the tumor microenvironment of colorectal cancer," *Biomedicine & Pharmacotherapy*, vol. 118, Article ID 109228, 2019.

[42] M. Shevtsov and G. Multhoff, "Immunological and translational aspects of NK cell-based antitumor immunotherapies," *Frontiers in Immunology*, vol. 7, p. 492, 2016.

[43] D. Krijgsman, N. L. de Vries, A. Skovbo et al., "Characterization of circulating T-, NK-, and NKT cell subsets in patients with colorectal cancer: the peripheral blood immune cell profile," *Cancer Immunology, Immunotherapy*, vol. 68, no. 6, pp. 1011–1024, 2019.

Research Article

Identification of Differentially Expressed and Prognostic lncRNAs for the Construction of ceRNA Networks in Lung Adenocarcinoma

Yimeng Cui, Yaowen Cui, Ruixue Gu, Yuechao Liu, Xin Wang, Lulu Bi, Shuai Zhang, Weina Fan, Fanglin Tian, Yuning Zhan, Ningzhi Zhang, Ying Xing ⓘ, and Li Cai ⓘ

The Fourth Department of Medical Oncology, Harbin Medical University Cancer Hospital, 150 Haping Road, Harbin 150040, China

Correspondence should be addressed to Ying Xing; xingying0618@163.com and Li Cai; caili@ems.hrbmu.edu.cn

Background. Long noncoding RNAs (lncRNAs) could function as competitive endogenous RNAs (ceRNAs) to competitively adsorb microRNAs (miRNAs), thereby regulating the expression of their target protein-coding mRNAs. In this study, we aim to identify more effective diagnostic and prognostic markers for lung adenocarcinoma (LUAD). *Methods.* We obtained differentially expressed lncRNAs (DElncRNAs), miRNAs (DEmiRNAs), and mRNAs (DEmRNAs) for LUAD by using The Cancer Genomes Atlas (TCGA) portal. Weighted gene coexpression network analysis (WGCNA) was performed to unveil core gene modules associated with LUAD. The Cox proportional hazards model was performed to determine the prognostic significance of DElncRNAs. The diagnostic and prognostic significance of DElncRNAs was further verified based on the receiver operating characteristic curve (ROC). Cytoscape was used to construct the ceRNA networks comprising the lncRNAs-miRNAs-mRNAs axis based on the correlation obtained from the miRcode, miRDB, and TargetScan. *Results.* Compared with normal lung tissues, 2355 DElncRNAs, 820 DEmiRNAs, and 17289 DEmRNAs were identified in LUAD tissues. We generated 8 WGCNA core modules in the lncRNAs coexpression network, 5 modules in the miRNAs, and 12 modules in the mRNAs coexpression network, respectively. One lncRNA module (blue) consisting of 441 lncRNAs, two miRNA modules (blue and turquoise) containing 563 miRNAs, and one mRNA module (turquoise), which consisted of 15162 mRNAs, were mostly significantly related to LUAD status. Furthermore, 67 DEmRNAs were found to be tumor-associated as well as the target genes of the DElncRNAs-DEmiRNAs axis. Survival analyses showed that 6 lncRNAs (LINC01447, WWC2-AS2, OGFRP1, LINC00942, LINC01168, and AC005863.1) were significantly correlated with the prognosis of LUAD patients. Ultimately, the potential ceRNA networks including 6 DElncRNAs, 4 DEmiRNAs, and 22 DEmRNAs were constructed. *Conclusion.* Our study indicated that 6 DElncRNAs had the possibilities as diagnostic and prognostic biomarkers for LUAD. The lncRNA-mediated ceRNA networks might provide novel insights into the molecular mechanisms of LUAD progression.

1. Introduction

Lung cancer is the leading cause of cancer-related death worldwide, of which lung adenocarcinoma (LUAD) is the dominant histological subtype, accounting for 40% of all cases [1, 2]. Statistics show that a dismal 5-year survival rate is less than 20% despite recent advances in therapies [3]. The major factors in unfavorable prognosis of LUAD are diagnosis at terminal cancer and the propensity for metastasis

[4]. Hence, there is an urgent need to identify new biomarkers to predict diagnosis and prognosis at an early stage and explore novel therapeutic targets for LUAD [5].

High-throughput genome sequencing and microarrays have indicated that 75% of the human genomes are transcribed into noncoding RNAs with the exception of protein-coding genes [6, 7]. Long noncoding RNAs (LncRNAs) are a class of RNA transcripts with a length of more than 200 nucleotides without protein-coding ability [8]. LncRNAs are
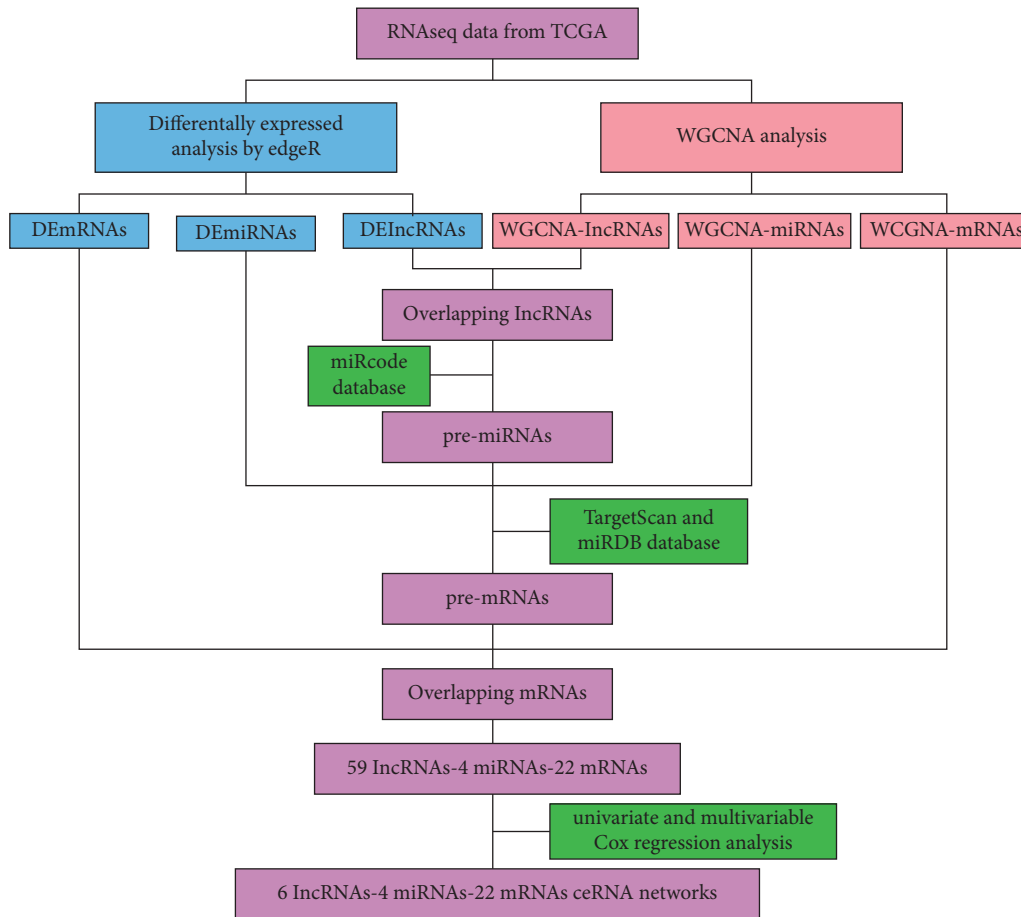
FIGURE 1: Research diagram of the ceRNA networks in LUAD.

broadly perceived for their functions in regulating biological processes through different mechanisms in various cancer types and have held substantial promise as novel biomarkers for cancer therapy [9–11]. MicroRNAs (miRNAs) have also been confirmed to play an important role in cancer progression over the past decades [12, 13]. Intriguingly, increasing evidence supports that lncRNAs act as endogenous molecular sponges that recognize and competitively bind to miRNAs by sharing miRNA response elements (MREs), indirectly regulating target mRNAs at a post-transcriptional level [14, 15]. Besides, the hypothesis that the complicated ceRNA networks participate in tumor development has been verified [16, 17]. For instance, the lncRNA ITGB8-AS1-miR-33b-5p-ITGA3 axis was reported to promote invasion and migration in colorectal cancer [18]. LncRNA PVT1, as a ceRNA for miR-143, upregulated HK2 expression and promoted proliferation of gallbladder cancer cells [19].

Weighted gene coexpression network analysis (WGCNA) lied in the construction of scale-free gene coexpression networks to identify crucial modules of highly correlated genes that are associated with specific clinical features [20, 21]. The advantage of WGCNA is that it can identify and cluster highly correlated genes into the same module. At present, WGCNA plays a significant role in multiple fields, such as cancer, nervous system, and genetic data analysis, which is extremely useful for identifying

potential candidate biomarkers or novel treatment targets [22–25].

In the current study, we identified differently expressed lncRNAs (DElncRNAs), miRNAs (DEmiRNAs), and mRNAs (DEmRNAs) and obtained the key modules relevant to LUAD traits by using WGCNA. Six diagnostic and prognostic DElncRNAs and 6 lncRNAs-4 miRNAs-22 mRNAs ceRNA networks may provide a useful basis for formulating early diagnosis and individualized treatments in LUAD.

2. Methods

2.1. Research Process Design. The bioinformatics scheme design of the study is shown in Figure 1.

2.2. Data Collection and Processing. The transcriptome profiling data and clinical data of patients with LUAD (tumor = 534; normal = 59) were obtained from the TCGA database (https://portal.gdc.cancer.gov/) (Supplementary Table S3). LncRNA-seq data were extracted by comparing lncRNA annotation according to Genecode (https://www.gencodegenes.org/). We performed data analysis based on 'Level 3' read count. TMM (trimmed mean of *M* value) normalization and differential expression analysis were

implemented with the *R* package edgeR ($|\log FC| > 1.5$ and *p* value < 0.05). Volcano maps were created using ggplot2 on Sangerbox (https://sangerbox.com/). The Venn diagram was performed using the Venny website (https://bioinfogp.cnb. csic.es/tools/venny/index.html).

2.3. Construction of the Weighted Gene Coexpression Network and Identification of Module Eigengenes. We incorporated RPKM (Reads Per Kilobase per Million) files of lncRNAs, miRNAs, and mRNAs into WGCNA analysis and constructed gene coexpression networks using the WGCNA *R* package [26]. The process included the following key steps [20, 21]: Firstly, the outliers were removed using the abline function for the clustered samples. Secondly, the established similarity matrix was converted into an adjacency matrix based on the β value. On this foundation, a topological overlap matrix (TOM) was constructed which was used to carry out the corresponding dissimilarity, and the hierarchical clustering tree of genes (dendrogram) was generated through hierarchical clustering to implement module detection. Finally, Module Members (MMs) and Gene Significance (GS) were counted and further investigated for module signature genes that were closely associated with cancer progression.

The construction process among lncRNA, miRNA, and mRNA coexpression networks was similar with the exception of some parameters: in the selection of soft power values, β values of lncRNAs, miRNAs, and mRNAs were 4, 3, and 1, respectively. The height cutoff MEDissThres of lncRNA, miRNA, and mRNA settings of similar modules was 0.5, 0.8, and 0.4, respectively. In terms of recognizing dynamic modules, 3 kinds of RNAs had the same conditions (deepSplit = 2, minModuleSize = 30).

2.4. Prediction of lncRNAs-miRNAs-mRNAs Networks. Forecasting target genes for lncRNAs and miRNAs through website tools: first of all, the overlapping lncRNA-targeted miRNAs (pre-miRNAs) were predicted via the miRcode website (https://www.mircode.org/) from which we obtained miRNA response element (MRE) information. The mRNAs (pre-mRNAs) targeted by shared miRNAs were predicted by TargetScan (https://www.targetscan.org/vert_72/) and miRDB databases (https://mirdb.org/). Genes with the same targeting relationship were extracted to construct the lncRNAs-miRNAs-mRNAs ceRNA networks using Cytoscape for visualization.

2.5. Survival Analysis. In combination with clinical information of TCGA-LUAD samples, univariate and multivariate Cox regression analysis were performed using survival *R* package Coxph function to clarify the relationship between characteristic lncRNAs and overall survival (OS), and forest maps were drawn using forestplot *R* package for visualization. LncRNAs significantly associated with prognosis were involved in the construction of the ceRNA regulatory networks. The area under the curve (AUC) for 1-year, 3-year, and 5-year OS was calculated by the 'timeROC' *R* package to assess the predictive accuracy of prognosis. In addition, diagnostic ROC curves were plotted with IBM SPSS Statistics 26 for the lncRNA signature. $P < 0.05$ was considered statistically significant.

3. Results

3.1. Identification of DElncRNAs, DEmiRNAs, and DEmRNAs in LUAD. TCGA-LUAD mRNA expression data, including 534 LUAD samples and 59 normal samples, were downloaded and matched with Genecode v38 for obtaining lncRNA expression data. The expression profiles of miRNAs in 521 tumor samples and 46 normal samples were explored. Original count data were standardized, and differential expression analysis was implemented with the *R* package edgeR. In total, 641 DElncRNAs, 224 DEmiRNAs, and 5000 DEmRNAs were screened out ($|\log FC| > 1.5$ and $p < 0.05$) (Supplementary Table S1). Volcano plots presented that 109 lncRNAs were downregulated, 48 miRNAs and 536 mRNAs were downregulated, and 532 lncRNAs, 176 miRNAs, and 4464 mRNAs were upregulated in LUAD samples (Figures 2(a)–2(c)).

3.2. Construction of Gene Coexpression Networks to Obtain Hub Modules. WGCNA, a systematic biological approach, was conducted to certify clinical phenotype in relation to coexpressed genes in networks. Selection of soft threshold power was a critical step in constructing WGCNA. To determine the relative balance between scale independence and average connectivity, we analyzed network topologies with soft threshold power ranging from 1 to 20. When the power value (β) was confirmed to 4 (lncRNAs), 3 (miRNAs), and 1 (mRNAs), the corresponding fitting index reached 0.9, and the coexpression network satisfied the scale-free distribution (Supplementary Figures S1(a)-S1(c)). We generated 8, 5, and 12 key modules (noted by different colors) in lncRNA, miRNA, and mRNA coexpression networks through the dynamic tree cutting method (Figures 3(a)–3(f)). Each module was color coded, but the genes in the gray module did not belong to any other module. Notably, we also identified the relationship of each module with the LUAD phenotype.

The results showed that there was a significant association between the blue module and tumor phenotype in the lncRNAs coexpression networks (weighted correlation of module features = 0.78) (Figure 3(b)). Meanwhile, the turquoise module was obviously correlated with tumor characteristics in the mRNAs coexpression networks (module trait weighted correlation = 0.71) (Figure 3(f)). For miRNA coexpression networks, both blue and turquoise modules were significantly correlated with the tumor phenotype (module trait weighted correlation = 0.59/0.56) (Figure 3(d)). The genes in the core module were extracted for further analysis (WGCNA-lncRNAs = 441, WGCNA-miRNAs = 563, and WGCNA-mRNAs = 15162) (Figures 4(a), 4(c), 4(d), and 4(f)).

(a)

(b)

(c)
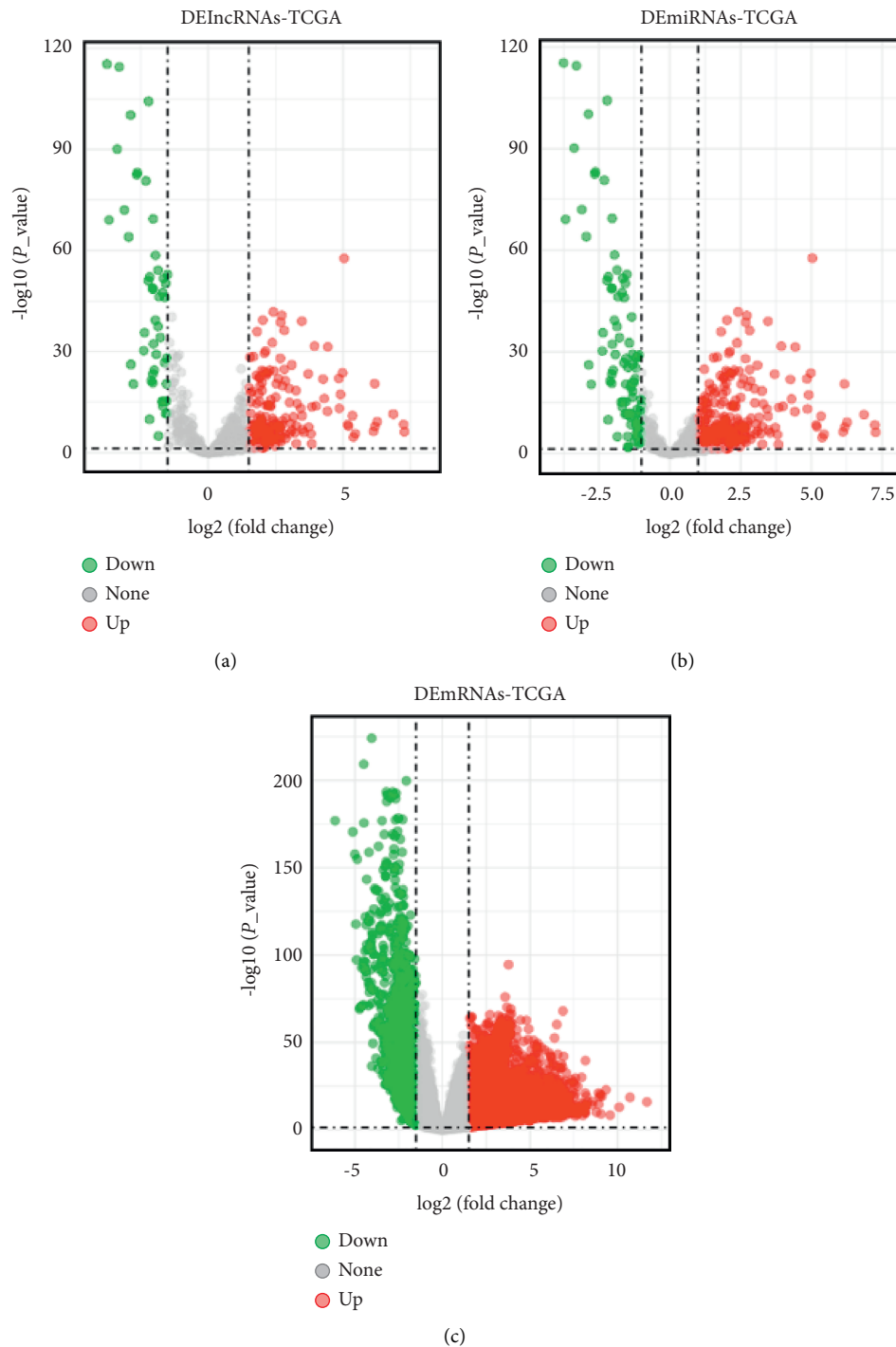
Figure 2: Identification of DElncRNAs, DEmiRNAs, and DEmRNAs in TCGA-LUAD. (a) Volcano plot of DElncRNAs from the TCGA database. (b) Volcano plot of DEmiRNAs from the TCGA database. (c) Volcano plot of DEmRNAs from the TCGA database. The x-axis and y-axis stood for log2 (fold change) of gene expression and lg-transformed p value, respectively. Red dots: the significantly overexpressed genes, green dots: downregulated genes, and gray dots: not significantly differentially expressed genes. |log2FC| > 1.5 and $p < 0.05$ were the cutoff criteria. Volcano maps were created using ggplot2 on the Sangerbox website (https://www.sangerbox.com/tool).

3.3. Prediction of lncRNAs-miRNAs and miRNAs-mRNAs Pairs. At first, we screened out 197 lncRNAs through matching the DElncRNAs with WGCNA-lncRNAs using the Venny website (Figure 4(b)). The predicted potential miRNAs (pre-miRNAs) that interacted with 197 lncRNAs were obtained using the miRcode database and identified a total of 7770 lncRNAs-miRNAs pairs, including 150 lncRNAs and 282 miRNAs. Taking the intersection of 24 DEmiRNAs, 282 pre-miRNAs, and 563 WGCNA-miRNAs, 10 miRNAs were ultimately included (Figure 4(e)). Then,

(a)

(b)

(c)

(d)

(e)

(f)
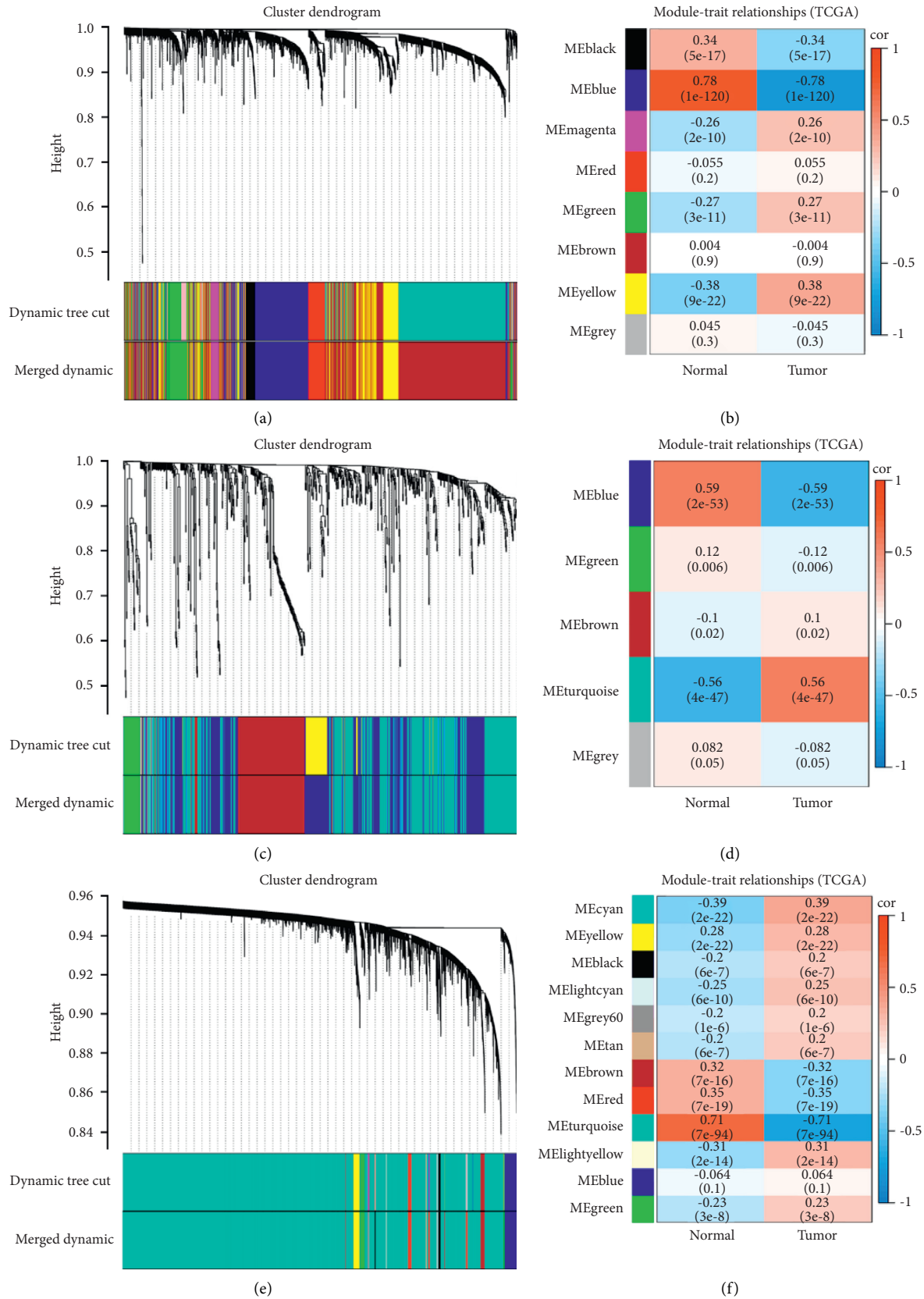
FIGURE 3: Drawing hierarchical clustering dendrograms of identified coexpressed genes and assessing the associations between module traits and the LUAD phenotype. Clustering dendrograms of lncRNAs (a), miRNAs (b), and mRNAs (c). *Note.* Each short vertical line corresponded to a gene and an expression module of genes that was highly interconnected (labeled on each branch). Two coloured rows below the dendrograms separately represented the original modules and merged modules. Analysis of module-trait relationships of LUAD based on lncRNA data (d), miRNA data (e), and mRNA data (f). *Note.* Each row corresponded to a module eigengene, and each column corresponded to a trait. Each cell contained the corresponding correlation (first line) and *p* value (second line). Color coding the table was according to the correlation of the color legend. *P* value < 0.05 represented statistical significance.
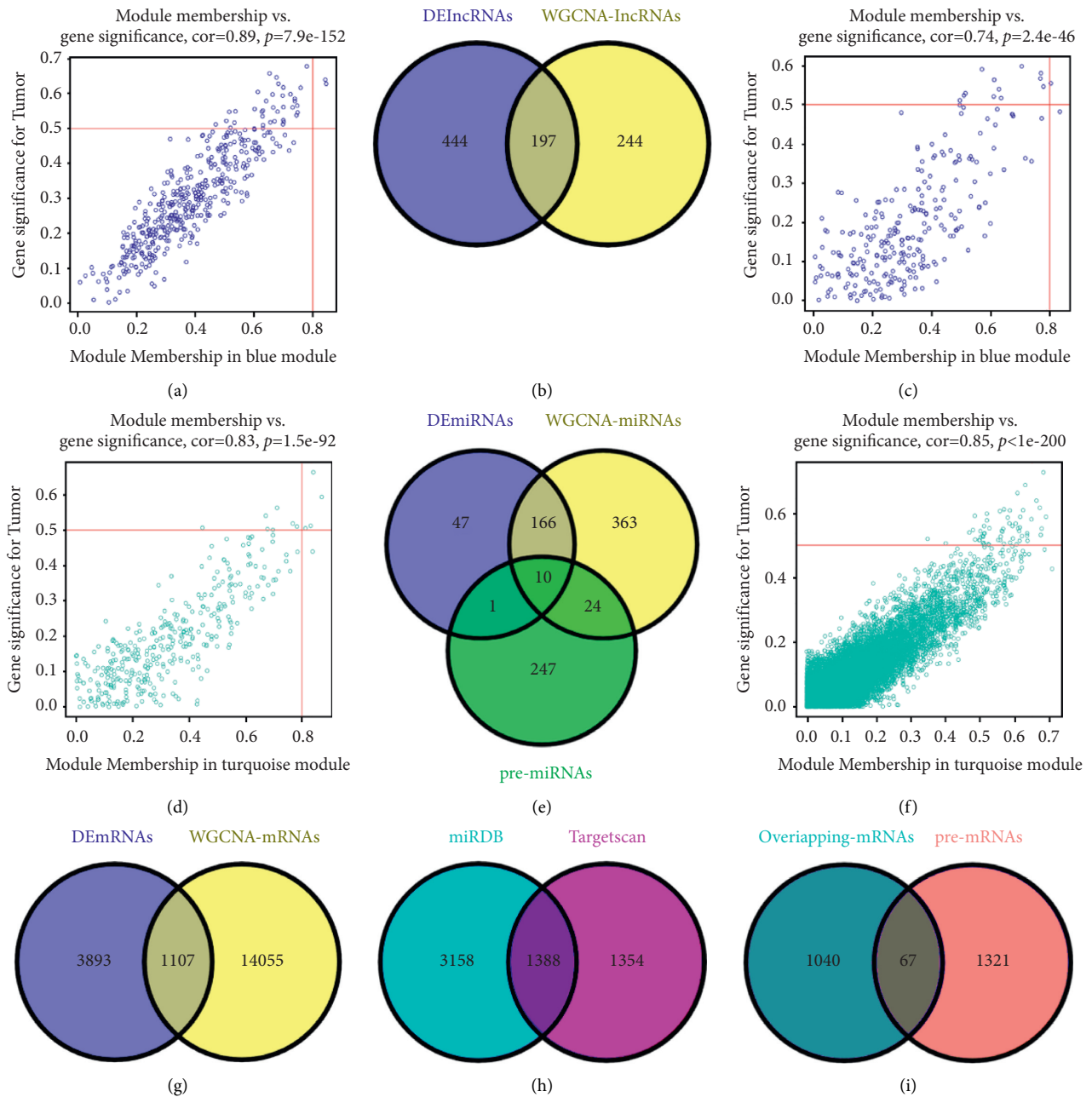
FIGURE 4: Scatter plots of gene significance (GS) and module membership (MM) in tumor-specific coexpression modules were displayed, and lncRNAs, miRNAs, and mRNAs were preliminarily screened for further analysis. Association between the vital modules included module eigengenes and tumor phenotypes in the coexpression network of (a) lncRNAs (weighted correlation of blue module characteristics = 0.89), (c, d) miRNAs (blue and turquoise modules trait weighted correlation = 0.74/0.83), and (f) mRNAs (turquoise module trait weighted correlation = 0.85). (b) The overlapping lncRNAs shared by DElncRNAs and WGCNA-lncRNAs. (e) The Venn diagram showed the intersection of DEmiRNAs, WGCNA-miRNAs, and pre-miRNAs (the target miRNAs of lncRNAs predicted by miRcode online prediction tools). (g) Venn diagram presented 1107 common mRNAs by intersecting DEmRNAs and WGCNA-mRNAs. (h) Based on the TargetScan and miRDB website, 1388 target genes of miRNAs were mostly overlapped. (i) The Venn diagram showed the unique correlation of genes among DEmRNAs, WGCNA-mRNAs, and pre-mRNAs.

1107 mRNAs were selected by taking the intersection of 5000 DEmRNAs and 15162 WGCNA-mRNAs (Figure 4(g)). Next, 10 intersectional miRNAs were predicted by TargetScan and miRDB online target gene prediction tools for their target genes (Figure 4(e)). No targeted genes were predicted for miR-142-3p at the TargetScan website, and

results of the remaining 9 miRNAs showed that 3074 miRNAs-mRNAs pairs included 2742 target genes; 6121 miRNAs-mRNAs pairs were retrieved on the miRDB website, containing 2742 target genes. There were 1388 mRNAs that were duplicated in both sites (Figure 4(h)). Finally, 67 target mRNAs were selected from DEmRNAs,
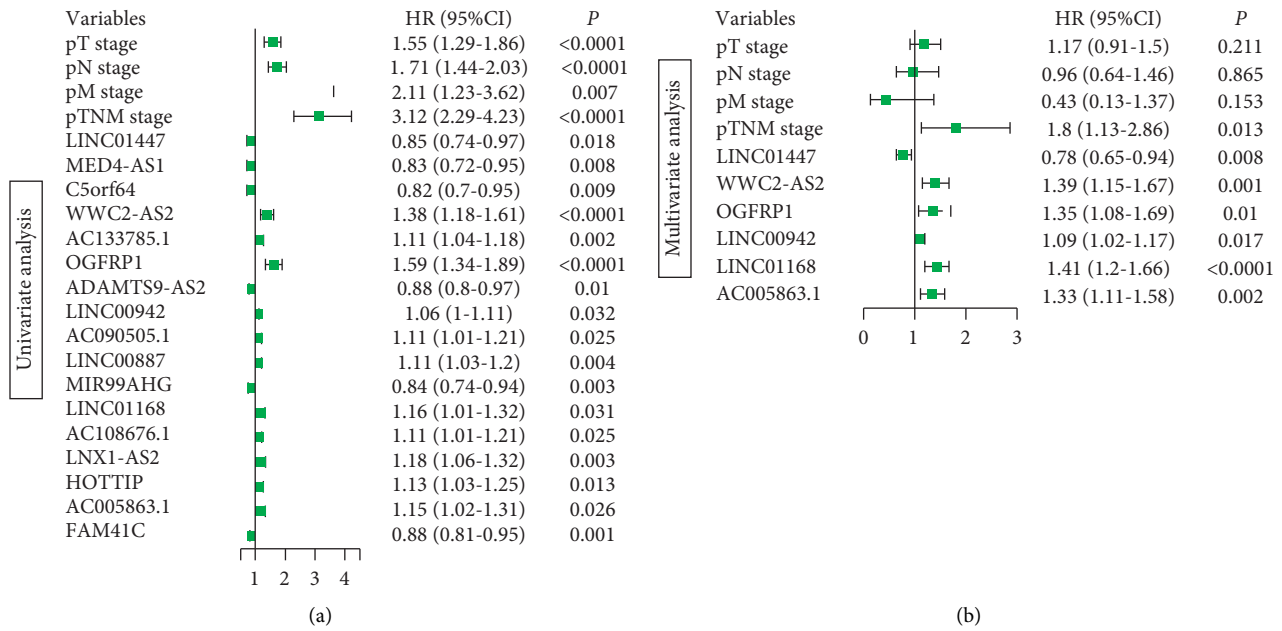
FIGURE 5: Univariate and multivariate Cox regression analysis. (a) The forest plot showed the prognostic factors associated with overall survival rates using univariate analysis. (b) Six lncRNAs were independent prognostic factors for patients with LUAD by performing multivariate Cox regression analysis. Hazard ratios (HRs) > 1 indicated a factor with poor prognosis, whereas HRs < 1 were related to favorable prognosis. All the variables shown were statistically significant with p value < 0.05.

mRNAs in the WGCNA core module, and predicted mRNAs (pre-mRNAs) (Figures 4(g) and 4(i)) (Supplementary Table S2). We performed reverse inferences based on 67 target genes and received 38 pairs of miRNAs-mRNAs (including 6 miRNAs and 38 mRNAs). The interaction effect between 6 miRNAs and 99 lncRNAs was also concluded at length.

3.4. Construction of lncRNAs-miRNAs-mRNAs Networks for LUAD. When miRNA binds to MRE on lncRNAs, mRNA expression is not inhibited; hence, miRNAs are mostly negatively correlated with lncRNA and mRNA expression (Supplementary Figure S2) [27]. Therefore, we screened for negatively associated genes, which included 59 lncRNAs, 4 miRNAs, and 22 mRNAs. Clinical data were downloaded from TCGA-LUAD, of which 512 samples had complete clinical information. Clinicopathological features of pT stage, pN stage, pM stage, and pTNM stage were incorporated into analysis, and the Coxph function in the survival R package was used to perform univariate and multivariate Cox regression analysis (Supplementary Tables S4 and S5.). As a consequence, 6 lncRNAs were identified as crucial prognostic factors (WWC2-AS2, OGFRP1, LINC00942, LINC01168, and AC005863.1 were risk factors, and only LINC01447 belonged to protective factor) (Figures 5(a) and 5(b)) (Supplementary Table S6). Cox regression analysis was performed to obtain risk scores of each sample which were used for ROC analysis of the prognosis classification utilizing the 'timeROC' R package. As shown in Supplementary Figure S3(a), the lncRNA signature is an independent predictor which reached an optimism-corrected AUC of 0.79 (1 year), 0.79 (3 years), and 0.77 (5 years). Meanwhile, diagnostic ROC curves further demonstrated the superior

clinical utility of the prognostic lncRNA model (AUC = 0.728) (Supplementary Figure S3(b)). Eventually, we constructed ceRNA networks for 6 lncRNAs, 4 miRNAs, and 22 mRNAs, that were visualized using Cytoscape v3.7.2 software and an alluvial plot (Figures 6(a) and 6(b)).

4. Discussion

Due to the unfavorable prognosis and high mortality rate of LUAD, it is necessary to improve the strategy of diagnosis and treatment. The lncRNA-mediated ceRNA hypothesis proposed that lncRNA functions as a ceRNA to regulate the gene expression by influencing miRNA activity. A previous study suggested that lncRNA-KRTAP5-AS1 and lncRNA-TUBB2A could serve as ceRNA to reinforce proliferation, invasion, and EMT function of Claudin-4 [28]. HOXD-AS1 was bound to miR-130a-3p in a competitive manner, which activated the expression of EZH2 and MMP2 and facilitated liver cancer metastasis [29]. Previous studies suggested that lncRNA as ceRNA played an important biological function in LUAD, but the tumor-specific ceRNA networks launched by lncRNAs remained largely unknown [30, 31]. Different from lncRNA-regulated ceRNA networks in LUAD established by Wu et al., six distinct lncRNAs were exhibited in our ceRNA networks. The reason may be that different bioinformatics tools and concerns were applied (i.e., we used the WGCNA analysis and conducted Cox regression analysis to identify cancer-related prognostic lncRNAs).

In the present study, we identified 6 differentially expressed and prognostic lncRNAs. Among them, LINC01447, LINC01168, and AC005863.1 have not been

(a)

(b)
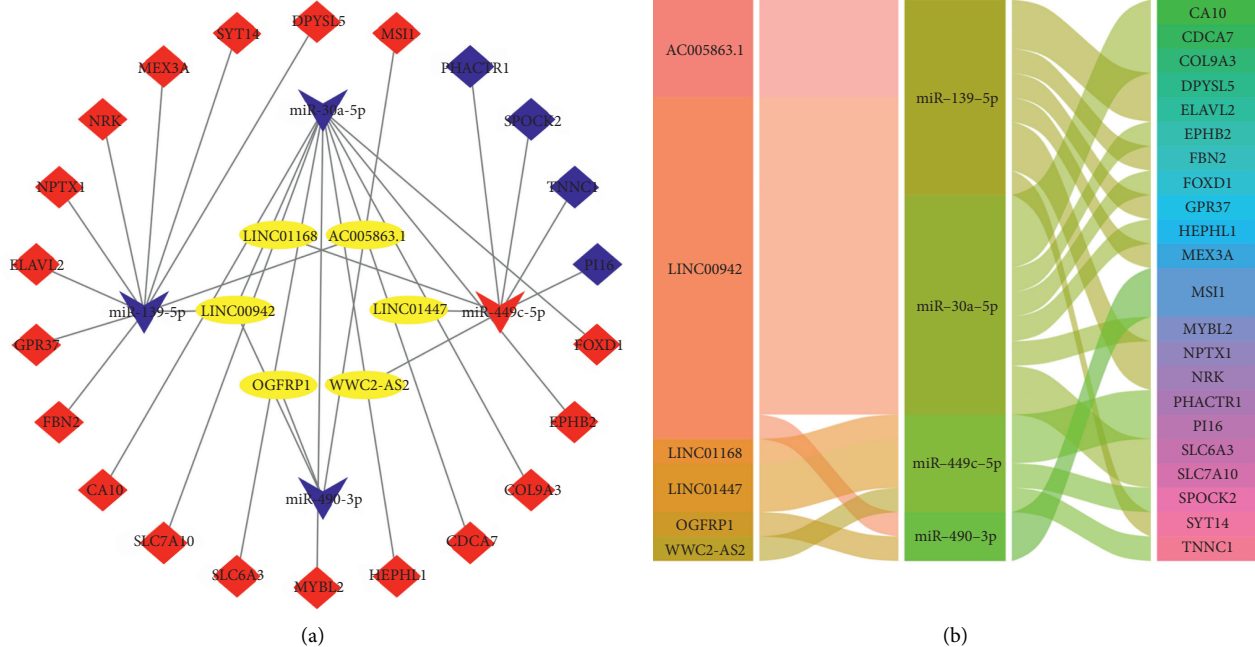
FIGURE 6: Visualization of ceRNAs networks. (a) Construction of 6 lncRNAs-4 miRNAs-22 mRNAs ceRNAs networks. *Note.* Diamonds denoted miRNAs, squares represented mRNAs, and yellow round rectangles represented lncRNAs. Red and blue indicated upregulated and downregulated genes in LUAD. (b) The alluvial plot of 6 lncRNAs-4 miRNAs-22 mRNAs ceRNA regulatory networks consisted of 3 columns (lncRNAs-miRNAs-mRNAs).

reported to date. It is interesting to explore the biofunctional role in the development and progression of LUAD for these three lncRNAs. The other three were lncRNA OGFRP1, LINC00942, and WWC2-AS2, which were both reported in the field of malignant tumors [32–36]. OGFRP1 promoted tumor progression by increasing the activity of the AKT/mTOR pathway or directly interacting with miR-4640-5p [32, 33]. Recent studies have shown that LINC00942 potentiated breast cancer cell proliferation and progression by affecting METTL14-mediated m6A methylation [34]. WWC2-AS2 and LINC00942 were involved in the construction of a prognostic lncRNA signature in cervical cancer and lung adenocarcinoma [35, 36]. In the current study, high expression of OGFRP1, LINC00942, and WWC2-AS2 was associated with poor prognosis of LUAD patients, which was in line with the abovereported results. Nevertheless, all these lncRNAs associated with molecular events still need further experimental validation in LUAD.

Four predicted miRNAs in ceRNA networks stand out in our study. These DEmiRNAs are as follows: miR-139-5p (downregulated), miR-30a-5p (downregulated), miR-490-3p (downregulated), and miR-449c-5p (upregulated). Consistently, miR-139-5p was downregulated in LUAD and exerted the ability to inhibit proliferation, migration, and invasion of cancer cells by targeting MAD2L1 [37]. Moreover, several studies have found that miR-30a-5p inhibited the proliferation of multiple cancers, such as breast cancer, glioma, and lung squamous cell carcinoma [38–40]. It is reported that miR-490-3p overexpression significantly inhibited the proliferation, invasion, and migration of hepatocellular carcinoma cells by activating BCYRN1 [41]. MiR-449c-5p was a hub for circ-NOTCH1 to promote

metastasis and stemness of gastric cancer cells, leading to the disease progression of gastric cancer [42]. These DEmiRNAs might serve as putative targets for LUAD diagnosis and therapy.

In the established ceRNA networks, the 22 DEmRNAs attracted the researchers' attention, and they found that they were effective regulators during cancer progression [43–49]. EPHB2 has been associated with cancer stemness and acquired sorafenib resistance via the β-catenin/TCF1 axis [43]. CXCL5 as a tumor angiogenic factor promoted the expression of FOXD1 by activating the AKT/NF-κB pathway in colorectal cancer [44]. High expression of CDCA7 promoted tumorigenesis and predicted poorer prognosis in patients with TNBC and ESCC [45, 46]. Downregulation of TNNC1 (Troponin C1) expression accelerated tumor formation and increased mortality in LUAD patients [47]. Glioma cells with low SYT14 (Synaptotagmin 14) expression were observed to suppress the proliferation capacity [48]. Upregulation of SPOCK2 negatively regulated MMP2 gene expression, which in turn inhibited the invasion and metastasis of prostate cancer cells [49]. These studies indicated these potent cancer regulators involved in the present ceRNA networks.

5. Conclusions

We used bioinformatics methods to construct the LUAD-specific lncRNA-mediated ceRNA regulatory networks. We also identified 6 DElncRNAs as prognostic biomarkers which might play critical roles in tumorigenesis and development of lung cancer. Further experimental verification

is needed to elucidate the underlying regulatory mechanism in the future.

Data Availability

All data generated or analyzed during this study are included in this published article and its supplementary information files.

Conflicts of Interest

The authors declare no conflicts of interest.

Authors' Contributions

Yimeng Cui, Yaowen Cui, and Ruixue Gu contributed equally to this work.

Supplementary Materials

Supplementary Figure S1. Analysis of network topology for soft thresholding powers (weighting coefficient, β) in lncRNAs, miRNAs, and mRNAs. The x-axis represented different soft thresholding powers. Upper: assessment for R^2 of $\log(k)$ and $\log(p(k))$ correlation coefficients corresponding to different β values in the network. The red line indicated a scale-free topology fitting index R^2 of 0.9. Lower: analysis of the mean connectivity for various β values. Supplementary Figure S2. Correlation analysis of lncRNAs, miRNAs, and mRNAs in the ceRNA network. (a) LncRNAs were negatively correlated with miRNAs. (b) Negative correlation among mRNAs and miRNAs. (c) LncRNAs had a positive correlation with mRNAs. Supplementary Figure S3. ROC plots of the prognostic lncRNA signature in the TCGA-LUAD dataset. (a) Survival-dependent ROC curves attested the prognostic significance of DElncRNAs. The area under the red line represented the 1-year AUC; the area under the blue line represented the 3-year AUC; and the area under the black line represented the 5-year AUC. (b) ROC curve analysis showed the application value of DElncRNAs in the diagnosis. Supplementary Table S1. The summarized data of DERNAs. Supplementary Table S2. The integrated results of DERNAs via differential expression analysis, WGCNA, and website prediction. Supplementary Table S3. Baseline clinicopathological characteristics of the TCGA-LUAD cohort. ($n = 513$). Supplementary Table S4. Univariate Cox regression analysis of factors associated with overall survival in the TCGA-LUAD dataset. Supplementary Table S5. Multivariable Cox regression analysis of factors associated with overall survival in the TCGA-LUAD dataset. Supplementary Table S6. 6 prognostic lncRNA-mediated ceRNA networks. (*Supplementary Materials*)

References

[1] H. Sung, J. Ferlay, R. L. Siegel et al., "Global cancer Statistics 2020: GLOBOCAN estimates of incidence and mortality worldwide for 36 cancers in 185 countries," *CA: A Cancer Journal for Clinicians*, vol. 71, no. 3, pp. 209–249, 2021.

[2] R. L. Siegel, K. D. Miller, H. E. Fuchs, and A. Jemal, "Cancer Statistics, 2021," *CA: A Cancer Journal for Clinicians*, vol. 71, no. 1, pp. 7–33, 2021.

[3] P. Khan, J. A. Siddiqui, I. Lakshmanan et al., "RNA-based therapies: a cog in the wheel of lung cancer defense," *Molecular Cancer*, vol. 20, no. 1, p. 54, 2021.

[4] J. Yang, Q. Qiu, X. Qian et al., "Long noncoding RNA LCAT1 functions as a ceRNA to regulate RAC1 function by sponging miR-4715-5p in lung cancer," *Molecular Cancer*, vol. 18, no. 1, p. 171, 2019.

[5] Z. Cong, Y. Diao, Y. Xu et al., "Long non-coding RNA linc00665 promotes lung adenocarcinoma progression and functions as ceRNA to regulate AKR1B10-ERK signaling by sponging miR-98," *Cell Death & Disease*, vol. 10, no. 2, Article ID 84, 2019.

[6] R. Elkon and R. Agami, "Characterization of noncoding regulatory DNA in the human genome," *Nature Biotechnology*, vol. 35, no. 8, pp. 732–746, 2017.

[7] B. S. Gloss and M. E. Dinger, "Realizing the significance of noncoding functionality in clinical genomics," *Experimental & Molecular Medicine*, vol. 50, no. 8, pp. 1–8, 2018.

[8] S. Chen and X. Shen, "Long noncoding RNAs: functions and mechanisms in colon cancer," *Molecular Cancer*, vol. 19, no. 1, p. 167, 2020.

[9] L. Statello, C.-J. Guo, L.-L. Chen, and M. Huarte, "Gene regulation by long non-coding RNAs and its biological functions," *Nature Reviews Molecular Cell Biology*, vol. 22, no. 2, pp. 96–118, 2021.

[10] X. Qian, J. Zhao, P. Y. Yeung, Q. C. Zhang, and C. K. Kwok, "Revealing lncRNA structures and interactions by sequencing-based approaches," *Trends in Biochemical Sciences*, vol. 44, no. 1, pp. 33–52, 2019.

[11] E. M. McCabe and T. P. Rasmussen, "lncRNA involvement in cancer stem cell function and epithelial-mesenchymal transitions," *Seminars in Cancer Biology*, vol. 75, pp. 38–48, 2020.

[12] A. R. Paliouras, T. Monteverde, and M. Garofalo, "Oncogene-induced regulation of microRNA expression: implications for cancer initiation, progression and therapy," *Cancer Letters*, vol. 421, pp. 152–160, 2018.

[13] T. Fehlmann, M. Kahraman, N. Ludwig et al., "Evaluating the use of circulating MicroRNA profiles for lung cancer detection in symptomatic patients," *JAMA Oncology*, vol. 6, no. 5, pp. 714–723, 2020.

[14] C. Glenfield and A. McLysaght, "Pseudogenes provide evolutionary evidence for the competitive endogenous RNA hypothesis," *Molecular Biology and Evolution*, vol. 35, pp. 2886–2899, 2018.

[15] M. Zhao, J. Feng, and L. Tang, "Competing endogenous RNAs in lung cancer," *Cancer Biology and Medicine*, vol. 18, no. 1, pp. 1–20, 2021.

[16] X. Qi, Y. Lin, J. Chen, and B. Shen, "Decoding competing endogenous RNA networks for cancer biomarker discovery," *Briefings in Bioinformatics*, vol. 21, no. 2, pp. 441–457, 2020.

[17] X. Qi, Y. Lin, J. Chen, and B. Shen, "The landscape of emerging ceRNA crosstalks in colorectal cancer: systems biological perspectives and translational applications," *Clinical and Translational Medicine*, vol. 10, Article ID e153, 2020.

[18] X. Lin, S. Zhuang, X. Chen et al., "lncRNA ITGB8-AS1 functions as a ceRNA to promote colorectal cancer growth and migration through integrin-mediated focal adhesion signaling," *Molecular Therapy*, 2021, In press.

[19] J. Chen, Y. Yu, H. Li et al., "Long non-coding RNA PVT1 promotes tumor progression by regulating the miR-143/HK2 axis in gallbladder cancer," *Molecular Cancer*, vol. 18, no. 1, Article ID 33, 2019.

[20] J. Long, S. Huang, Y. Bai et al., "Transcriptional landscape of cholangiocarcinoma revealed by weighted gene coexpression network analysis," *Briefings in Bioinformatics*, vol. 22, 2021.

[21] M. Niemira, F. Collin, A. Szalkowska et al., "Molecular signature of subtypes of non-small-cell lung cancer by large-scale transcriptional profiling: identification of key modules and genes by weighted gene co-expression network analysis (WGCNA)," *Cancers*, vol. 12, 2019.

[22] L. Chen, L. Yuan, Y. Wang et al., "Co-expression network analysis identified FCER1G in association with progression and prognosis in human clear cell renal cell carcinoma," *International Journal of Biological Sciences*, vol. 13, no. 11, pp. 1361–1372, 2017.

[23] Y. Luo, D. Shen, L. Chen et al., "Identification of 9 key genes and small molecule drugs in clear cell renal cell carcinoma," *Aging*, vol. 11, no. 16, pp. 6029–6052, 2019.

[24] H. Spiers, E. Hannon, L. C. Schalkwyk et al., "Methylomic trajectories across human fetal brain development," *Genome Research*, vol. 25, no. 3, pp. 338–352, 2015.

[25] Q. Liu, C. Jiang, J. Xu et al., "Genome-wide temporal profiling of transcriptome and open chromatin of early cardiomyocyte differentiation derived from hiPSCs and hESCs," *Circulation Research*, vol. 121, no. 4, pp. 376–391, 2017.

[26] Y. Yao, T. Zhang, L. Qi et al., "Integrated analysis of co-expression and ceRNA network identifies five lncRNAs as prognostic markers for breast cancer," *Journal of Cellular and Molecular Medicine*, vol. 23, no. 12, pp. 8410–8419, 2019.

[27] J. Jiang, Y. Bi, X. P. Liu et al., "To construct a ceRNA regulatory network as prognostic biomarkers for bladder cancer," *Journal of Cellular and Molecular Medicine*, vol. 24, no. 9, pp. 5375–5386, 2020.

[28] Y.-x. Song, J.-x. Sun, J.-h. Zhao et al., "Non-coding RNAs participate in the regulatory network of CLDN4 via ceRNA mediated miRNA evasion," *Nature Communications*, vol. 8, no. 1, Article ID 289, 2017.

[29] H. Wang, X. Huo, X.-R. Yang et al., "STAT3-mediated upregulation of lncRNA HOXD-AS1 as a ceRNA facilitates liver cancer metastasis by regulating SOX4," *Molecular Cancer*, vol. 16, no. 1, Article ID 136, 2017.

[30] X. Wu, Z. Sui, H. Zhang, Y. Wang, and Z. Yu, "Integrated analysis of lncRNA-mediated ceRNA network in lung adenocarcinoma," *Frontiers in Oncology*, vol. 10, Article ID 554759, 2020.

[31] D. Jin, Y. Song, Y. Chen, and P. Zhang, "Identification of three lncRNAs as potential predictive biomarkers of lung adenocarcinoma," *BioMed Research International*, vol. 2020, Article ID 7573689, 13 pages, 2020.

[32] J. Zhang, X. Xu, J. Yin et al., "lncRNA OGFRP1 promotes tumor progression by activating the AKT/mTOR pathway in human gastric cancer," *Aging*, vol. 13, no. 7, pp. 9766–9779, 2021.

[33] X. Liu, N. Niu, P. Li et al., "LncRNA OGFRP1 acts as an oncogene in NSCLC via miR-4640-5p/eIF5A axis," *Cancer Cell International*, vol. 21, no. 1, Article ID 425, 2021.

[34] T. Sun, Z. Wu, X. Wang et al., "LNC942 promoting METTL14-mediated m6A methylation in breast cancer cell proliferation and progression," *Oncogene*, vol. 39, no. 31, pp. 5358–5372, 2020.

[35] Y. Cui, Z. Zhou, Y. Chai, X. Che, and Y. Zhang, "Identification of a nomogram from ferroptosis-related long noncoding RNAs signature to analyze overall survival in patients with bladder cancer," *Journal of Oncology*, vol. 2021, Article ID 8533464, 2021.

[36] L. Lu, L. P. Liu, Q. Q. Zhao, R. Gui, and Q. Y. Zhao, "Identification of a ferroptosis-related LncRNA signature as a novel prognosis model for lung adenocarcinoma," *Frontiers in Oncology*, vol. 11, Article ID 675545, 2021.

[37] J. Li, X. He, X. Wu, X. Liu, Y. Huang, and Y. Gong, "miR-139-5p inhibits lung adenocarcinoma cell proliferation, migration, and invasion by targeting MAD2L1," *Computational and Mathematical Methods in Medicine*, vol. 2020, Article ID 2953598, 10 pages, 2020.

[38] C. Chen, J. Tang, S. Xu, W. Zhang, and H. Jiang, "miR-30a-5p inhibits proliferation and migration of lung squamous cell carcinoma cells by targeting FOXD1," *BioMed Research International*, vol. 2020, Article ID 2547902, 2020.

[39] P. O. Editors, "Retraction: MiR-30a-5p antisense oligonucleotide suppresses glioma cell growth by targeting SEPT7," *PLoS One*, vol. 15, Article ID e0228340, 2020.

[40] L. Li, L. Kang, W. Zhao et al., "miR-30a-5p suppresses breast tumor growth and metastasis through inhibition of LDHA-mediated Warburg effect," *Cancer Letters*, vol. 400, pp. 89–98, 2017.

[41] S. Ding, Y. Jin, Q. Hao, Y. Kang, and R. Ma, "LncRNA BCYRN1/miR-490-3p/POU3F2, served as a ceRNA network, is connected with worse survival rate of hepatocellular carcinoma patients and promotes tumor cell growth and metastasis," *Cancer Cell International*, vol. 20, no. 1, Article ID 6, 2020.

[42] X. Zhao, Q. Zhong, X. Cheng et al., "miR-449c-5p availability is antagonized by circ-NOTCH1 for MYC-induced NOTCH1 upregulation as well as tumor metastasis and stemness in gastric cancer," *Journal of Cellular Biochemistry*, vol. 121, no. 10, pp. 4052–4063, 2020.

[43] H. W. Leung, C. O. N. Leung, E. Y. Lau et al., "EPHB2 activates β-catenin to enhance cancer stem cell properties and drive sorafenib resistance in hepatocellular carcinoma," *Cancer Research*, vol. 81, no. 12, pp. 3229–3240, 2021.

[44] C. Chen, Z.-Q. Xu, Y.-P. Zong et al., "CXCL5 induces tumor angiogenesis via enhancing the expression of FOXD1 mediated by the AKT/NF-κB pathway in colorectal cancer," *Cell Death & Disease*, vol. 10, no. 3, p. 178, 2019.

[45] H. Li, Y. Weng, S. Wang et al., "CDCA7 facilitates tumor progression by directly regulating CCNA2 expression in esophageal squamous cell carcinoma," *Frontiers in Oncology*, vol. 11, Article ID 734655, 2021.

[46] L. Ye, F. Li, Y. Song et al., "Overexpression of CDCA7 predicts poor prognosis and induces EZH2-mediated progression of triple-negative breast cancer," *International Journal of Cancer*, vol. 143, no. 10, pp. 2602–2613, 2018.

[47] S. Kim, J. Kim, Y. Jung et al., "Characterization of TNNC1 as a novel tumor suppressor of lung adenocarcinoma," *Molecules and Cells*, vol. 43, pp. 619–631, 2020.

[48] B. Sheng, Y. Jiang, D. Wu et al., "RNAi-mediated SYT14 knockdown inhibits the growth of human glioma cell line U87MG," *Brain Research Bulletin*, vol. 140, pp. 60–64, 2018.

[49] G. Liu, F. Ren, and Y. Song, "Upregulation of SPOCK2 inhibits the invasion and migration of prostate cancer cells by regulating the MT1-MMP/MMP2 pathway," *PeerJ*, vol. 7, Article ID e7163, 2019.

Review Article

The Role of miR-23b in Cancer and Autoimmune Disease

Yu-Xin Guo [ID],[1] **Na Wang** [ID],[2] **Wen-Cheng Wu** [ID],[1] **Cui-Qin Li** [ID],[1] **Rui-Heng Chen** [ID],[3] **Yuan Zhang** [ID],[1] **and Xing Li** [ID][1]

[1]*National Engineering Laboratory for Resource Development of Endangered Crude Drugs in Northwest China,*
Key Laboratory of Medicinal Resources and Natural Pharmaceutical Chemistry (Shaanxi Normal University),
The Ministry of Education, College of Life Sciences, Shaanxi Normal University, Xi'an, Shaanxi 710119, China
[2]*Surgical Oncology Department, The First People's Hospital of Tianshui, Tianshui, Gansu 741000, China*
[3]*The High School Affiliated to Shaanxi Normal University, Xi'an, Shaanxi 710119, China*

Correspondence should be addressed to Yuan Zhang; yuanzhang_bio@126.com and Xing Li; xingli_xian@126.com

Received 27 May 2021; Accepted 18 October 2021; Published 3 November 2021

Academic Editor: Alessandro Granito

Short-stranded miRNAs are single-stranded RNA molecules involved in the regulation of gene expression. miRNAs are involved in a variety of cellular physiological processes, including cell proliferation, differentiation, and apoptosis. miR-23b have been identified to act both as oncogenes and as tumor suppressors. In addition, miR-23b is related to inflammation resistance to various autoimmune diseases and restrained inflammatory cell migration. The characterization of the specific alterations in the patterns of miR-23b expression in cancer and autoimmune disease has great potential for identifying biomarkers for early disease diagnosis, as well as for potential therapeutic intervention in various diseases. In this review, we summarize the ever-expanding role of miR-23b and its target genes in different models and offer insight into how this multifunctional miRNA modulates tumor cell proliferation and apoptosis or inflammatory cell activation, differentiation, and migration.

1. Introduction

According to GLOBOCAN 2020, an assessment of cancer morbidity and mortality, it is reported that the number of new cancer cases reached 19.3 million worldwide, and almost 10 million people died from cancer [1]. Moreover, breast cancer in women has overtaken lung cancer as the primary cause of cancer incidence worldwide in 2020 [1, 2]. Then, lung cancer is the second most frequently occurring cancer and the leading cause of cancer death [1]. Moreover, changes in incidence and trends are closely related to the prevalence of tobacco [3, 4]. So, men are more likely to suffer from this disease. Among male cancers, liver cancer is also a high incidence disease, ranking second in male mortality, and the incidence of primary liver cancer has continued to rise since 2020 [4, 5]. Gastric cancer is a significant disease worldwide. Notably, in the United States, Canada, and the United Kingdom, the incidence of gastric cancer has increased in both low- and high-risk young adults (younger than 50 years) [6]. At present, the treatment of tumors can be divided into drug therapy and surgical treatment [7]. Drug therapy refers to using drugs to destroy cancer cells, which is often used in clinical treatment. However, while killing tumor cells, it will kill normal cells, so it often brings a series of side effects, and chemotherapy does not have specificity for tumor tissue [8]. Thus, most drug therapy has side effects. In addition, surgical treatment has adverse effects such as postoperative recurrence and slow healing. Importantly, their pathogenesis is also unclear [9]. These factors lead to limited treatment options. Therefore, clarifying the specific mechanism of the disease is of great significance for the treatment of the disease.

Autoimmune disease refers to a disease in which the body's immune response to its antigen causes damage to its own tissues [10]. Multiple sclerosis (MS) is an autoimmune demyelinating central nervous system (CNS) disease, in which immune cells infiltrate into the central nervous system from the periphery, activate microglia and astrocytes, and inhibit the differentiation of oligodendrocytes into oligodendrocytes, resulting in pathological features such as

demyelination of myelin and axon [11, 12]. However, its exact molecular mechanisms remain unclear. Besides, rheumatoid arthritis (RA), also a chronic autoimmune disease, affects nearly 0.5%–1% of the population in the world [13]. The most common clinicopathological features of RA patients are cartilage degeneration and bone erosion of large and small joints, leading to mobility difficulties and even disability in severe cases [14, 15]. Although there is some genetic and environmental correlation, the specific pathogenesis is not clear [16]. Systemic lupus erythematosus (SLE) is also a chronic multisystem autoimmune disorder. Although the cause of SLE is unknown, both genetic and environmental elements are relevant to the disease mechanism [17]. Infection and environmental elements have been hypothesized to cause cell damage, promote the exposure of autoantigens to the immune system, and cause B- and T-cell activation [18]. Indeed, clarifying the pathogenesis plays a critical role in the diagnosis and timely treatment of diseases.

Small endogenous regulatory RNAs, also known as short-strand ribonucleic acid microRNAs (miRNAs), are critical posttranscriptional regulators of gene expression and were first identified in *C. elegans* [19–21]. There are many kinds of miRNAs, among which miRNA-23b belongs to miR-23b/27b/24-1 cluster [22]. miR-23b possessed regulatory roles, especially in the development of cancer and autonomic immune diseases [23]. In conclusion, this review reveals miR-23b in various diseases, including cancer and autoimmune diseases, and its role in disease progression.

2. miRNA

MicroRNA (miRNAs), which belonged to a category of single-stranded RNA molecular, is not involved in coding with a role in regulating gene expression [24, 25]. The formation of miRNA includes the multistage process. Firstly, in the nucleus, RNA polymerase II or III transcripts miRNA-related genes into primary miRNAs (pri-miRNAs), where miRNAs are several thousand nucleotides (nt) long [26–28]. Subsequently, the microprocessing complex Drosha-DGCR8, consisting of the RNA binding protein DiGeorge syndrome critical region gene8 (DGCR8) and the ribonuclease type III RNase Drosha, splits the precursor miRNA (pre-miRNA), which forms the hairpin structure [29, 30]. This process is carried out in the nucleus. Then, in the cytoplasm, the RNA Dicer enzyme decomposed per-miRNA into mature miRNA, and the miRNA was still in the double-stranded state [29]. Finally, the double-stranded miRNA combined with Argonaute2 (AGO2) to form RISC (RNA-induced silencing complex) [31]. One strand of the miRNA double strand is preserved in the RISC complex, while the other strand is expelled from the complex and rapidly degrades [30]. In the cytoplasm, miRNAs exert various biological functions by RISC [32]. miRNAs processing and loading into RISC is performed by specific RNA-biding proteins (RBPs), which exert cotranscriptional and posttranscriptional regulation of miRNA transcription product [33]. Moreover, a number of miRNAs can have different nuclear functions independently of RISC [33].

MicroRNA regulation commonly occurs based on microRNA binding to the $3'$ untranslated region ($3'$-UTR) of target mRNA [34]. MicroRNAs inhibit the expression of target genes by $3'$-UTR combining with target RNAs [35]. Therefore, different miRNA biological processes occur at different sites in the cell, including RNA transcription, processing, transport, and RISC binding. Importantly, miRNAs are critical for cell proliferation, differentiation, and apoptosis [36]. miRNAs have been involved in many cancers and neurodegenerative diseases, such as multiple sclerosis, Parkinson's disease, and Alzheimer's disease [37, 38]. Overall, miRNAs play an essential part in the occurrence and development of diseases [39].

3. miR-23b Research Progress

The miR-23b is due to the chromosomal region 9q22,32 encoding mi-23b/27b/24-1 [23]. The biogenetic process of miR-23b is similar when miRNA is cut into miRNA double strand by Dicer enzyme-containing protein complex. One strand is a passenger strand that will be degraded, and the other is miR-23b. miR-23b is involved in regulating normal physiological function, cell differentiation, and cellular immunity [40]. Thus, when the miR-23b homeostasis is damaged, the normal physiological function of the cell will also be affected, and then diseases will occur. miR-23b can induce a complex network of responses by directly targeting multiple transcripts. To be specific, the changes of miR-23b expression were closely related to various transcription factors, such as TAB2, TAB3, NF-κB, tumor suppressor P53, estrogen receptor ER-α, mitogen-activated protein kinase MAPK, activation protein AP-1, reactive oxygen species ROS, and CCL7 [19, 41, 42]. It has been reported that miR-23b is closely related to the occurrence and development of a variety of diseases, including tumors and autoimmune diseases [23]. This review summarized tumor-related diseases such as breast cancer, lung cancer, gastric cancer, and liver cancer [43–45] and autoimmune diseases such as multiple sclerosis, systemic lupus erythematosus, and arthritis [46–48]. The above studies indicated that miR-23b is mainly involved in a variety of physiological processes such as cell proliferation, migration, and adhesion [49, 50].

4. The Role of miR-23b in Cancer

4.1. Breast Cancer. miR-23b is a pathogenic gene in the course of the occurrence of breast tumors. Because miR-23b expression changes abnormally in breast cancer, it is considered a biomarker for breast cancer development. The expression rate of miR-23b in breast cancer tissues was significantly higher than that in benign breast fibroadenomas. Through KEGG pathway enriching analysis, it is found that miR-23b is involved in the metabolism and cellular pathway of breast cancer, such as EGFR and c-Met signaling pathways [51, 52]. In addition, the function of miR-23b at the cellular and molecular level has also been extensively studied. The CRISPR/Cas9 system was able to knock out miR-23b and miR-27b thoroughly; therefore, some researchers used this system to knock out the miR-23b gene in

MCF-7 cells. The results showed that the cell behaviors were changed, such as cell growth rate and colony formation, and significantly decreased [53, 54]. Moreover, miR-23b expression is regulated by multiple factors. A study shows that the membrane receptor tyrosine kinase (HER2/neu) can induce miR-23b by regulating its downstream transcription factor NF-□B, promoting the growth of breast cancer cells [55]. On the other hand, miR-23b blockades tumor cell invasion by inhibiting the expression of B-lymphocyte-induced maturation protein-1 (Blimp1) [43, 56]. Cas/ErbB2 MCF10A.B2 represents invasive human mammary epithelial cells with characteristics of overexpression p130Cas and activation of ErbB2. miR-23b can directly reversely mediate Blimp1 and increase its level of expression [43].

4.2. Lung Cancer. miR-23b is identified to be related to lung cancer according to a variety of validation methods, including PCR array, logistic regression, and receiver operating characteristics curve analyses; mir-23b is determined to be closely related to the formation of lung cancer [57]. By performing an MTT assay, it was demonstrated that, in the H1838 lung cancer cell line, the overexpression of miR-23b significantly improved cell viability. In H1437 and H1944 lung cancer cell lines, inhibiting the expression of miR-23b significantly reduced the ability of cell proliferation [45]. The specific mechanisms of action indicate that, by increasing the expression of miR-23b, it acts on myeloid leukemia 1 short (Mcl-1S) gene to enhance the proliferation, migration, and invasion ability of A549 cells [58]. Mcl-1S has a proapoptosis effect, which is a short splicing variant of antiapoptosis protein Mcl-1 [59]. This may be the main reason that miR-23b can promote the growth of lung cancer cells. A new study proved that kinectin1 antisense RNA 1 (KTN1-AS1) is negatively correlated with miR-23b in NSCLC (non-small-cell lung cancer) cells, and the overexpression of KTN1-AS1 can significantly reduce the expression level of miR-23b. Administration of KTN1-AS1 can restore the proliferation and growth of NSCLC cells [60]. KTN1-AS1 contributes to facilitating NSCLC progression by inhibiting miR-23b [60].

4.3. Liver Cancer. There is a critical relationship between liver cancer and immunity [61, 62]. The liver acts as an immune organ, maintaining immune homeostasis and containing many immune cells, such as DC cells and T cells [61]. Tregs are an immunosuppressive subset of CD4+ T cells. Tregs have an important feature; that is, they have both activating and inhibitory receptors. Blocking activated receptors and/or stimulating inhibitory receptors shifts the balance to inhibiting Tregs, treating tumors and chronic infectious diseases. Furthermore, Tregs play a crucial role during tumor development and progression by regulating other immune cells. Notably, Tregs work with neutrophils to reduce the incidence of liver cancer [63]. On the contrary, the therapeutic effects of Treg can be achieved by blocking the inhibitory receptors or stimulating the activation receptors in autoimmune diseases [62]. According to the reports, autoimmune liver disease is related to the number and functional defects of Tregs. Therefore, the treatment of autoimmune liver disease aims to restore the sufficient number and function of Treg [64, 65].

In hepatocellular carcinoma (HCC) cells, miR-23b possessed important functions [66]. miR-23b may possess a dual function of oncogenic and inhibitory effect on the tumor. Because the expression of miR-23b is detected in 125 HCC patients, 48 of them were upregulated, and 77 were downregulated [67]. In Cao's research, it was shown that the expression of miR-23b in HCC tissues was remarkably decreased, which was positively correlated with metastasis of HCC [44]. Intriguingly, body fat is also associated with the progression of liver cancer. Compared with HCC patients with low body fat percentage, the study has found that serum exosomes of HCC patients with a high body fat ratio express a high level of miR-23b [68]. Besides, hepatocellular carcinoma cell line SMMC-7721 demonstrated that miR-23b could promote tumor cell growth by targeting suppression of tumorigenicity 7 like (ST7L) [66]. Proline-rich tyrosine kinase 2 (PYK2) is a nonreceptor tyrosine kinase belonging to the adhesion-focused kinase family [69]. PYK2 plays an essential role in regulating cell proliferation and migration in various cancer cells [70, 71], and miR-23b inhibits the HCC cell line MHCC97L by targeting Pyk2 [72].

4.4. Gastric Cancer. The high expression of miR-23b, a typical feature of gastric cancer, is believed to facilitate this disease's aggressive progression [73]. Moreover, miR-23b in plasma expression is correlated with a poor prognosis of gastric cancer [74]. miR-23b is one of the critical factors in the initiation and progression of gastric cancer. By performing experiments in a gastric cancer xenograft mouse model and gastric cancer cells MKN-45 and AGS, results can identify that miR-23b could target programmed cell death (PDCD4) and promote tumor growth [75]. Besides, it has demonstrated that miR-23b and long noncoding RNA, tumor suppressor candidate 7 (TUSC7), inhibited each other. Contrary to the effect of miR-23b, TUSC7 suppressed the growth of gastric cancer cells AGS and MKN-45 [76]. The latest clinical data has shown that miR-23b encapsulated in the exosomes can also be used as a biomarker to predict the recurrence and prognosis of gastric cancer patients at different stages [77].

The mechanism of miR-23b in breast cancer, lung cancer, liver cancer, and gastric cancer is shown in Figure 1.

5. The Role of miR-23b in Autoimmune Disease

5.1. MS/EAE. Abnormal expression of a series of microRNAs can be used as potential therapeutic targets for EAE, assessed in the plasma and spinal cord tissue of EAE mice [78]. In addition to the dysregulation of miR-23b in the tumor diseases mentioned above, miR-23b also reflected abnormal expression in autoimmune diseases. The analysis of a miRNA-microarray found that, with the aggravation of EAE, the expression of miR-23b gradually increased. This result is considered to be one of the biomarkers of the disease [79]. Moreover, several studies have reported that miR-23b
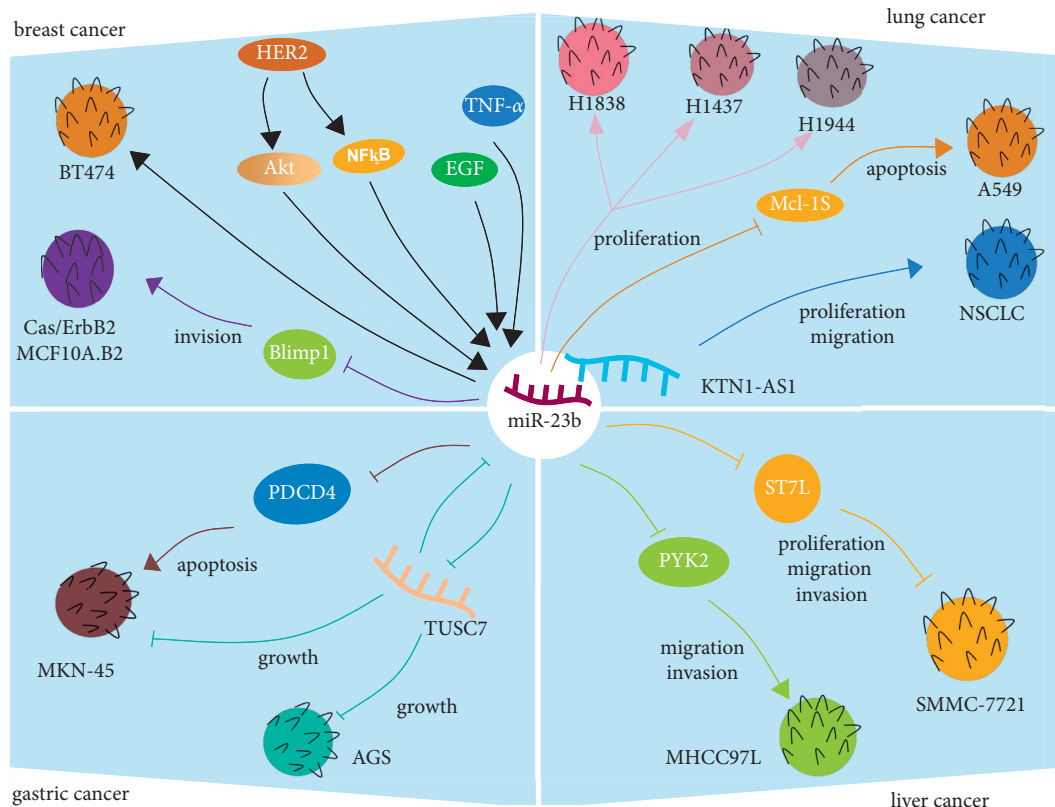
FIGURE 1: The mechanism of miR-23b in cancers. (1) Breast cancer: HER2, EGF, and TNF-α promote the growth of BT474 cells by promoting the upregulation of miR-23b. Cas/ErbB2 MCF10A.B2 represents overexpression p130Cas with activation of ErbB2. miR-23b impairs Cas/ErbB2 MCF10A.B2 cell invasion by downmodulating Blimp1 expression. (2) Lung cancer: miR-23b promotes H1838, H1437, and H1944 lung cancer cell proliferation. It is beneficial for the growth of A549 by Mcl-1S. In addition, KTN1-AS1 promotes NSCLC proliferation by inhibiting miR-23b. (3) Liver cancer: miR-23b boosts the proliferation of H1838, H1437, and H1944 lung cancer cell lines. It is useful for the expansion of A549 by Mcl-1S. Furthermore, KTN1-AS1 accelerates NSCLC proliferation by inhibiting miR-23b. (4) Gastric cancer: miR-23b modulates tumor growth by targeting PDCD4. Moreover, as a potential target of miR-23b, TUSC7 also regulates the growth of gastric cancer cells AGS and MKN-45.

regulates autoimmune disease pathogenesis by targeting different protein molecules, such as TAB2, TAB3, IKK-α, and CCL-7.

Bone marrow mesenchymal stem cells (BMSCs), adult pluripotent stem cells, exert the immunoregulatory role by carrying miRNA. BMSCs combined with miR-23b had a better synergistic effect and could effectively alleviate EAE [46]. BMSC loading overexpression miR-23b inhibits Th17 cell differentiation, blocks the secretion of inflammatory factor IL-17, on the contrary promotes the secretion of tumor growth factor-beta 1 (TGF-β1), and ultimately inhibits the development of EAE [46]. In addition to analyzing the effect of miR-23b on EAE verification from the perspective of inflammatory subset cells Th17, the research focuses on the effect of inflammatory chemokine CCL7. Similar to the effect of miR-23b in Th17 cells, miR-23b inhibits Th1 and Th17 cells and diminishes the infiltration of encephalitogenic T cells into the central nervous system contributing to halting EAE by binding with CCL7 in the 3'-UTR site [41]. In addition, miR-23b could alleviate the severity of EAE by targeting TAB2, TAB3, and IKK-α [42].

5.2. RA. RA chronically damages the heart, skin, and many other organs, accompanied by pathological characteristics of erosive changes in joint surfaces that lead to the destruction of the joints [80]. Besides its specific expression in MS, miR-23b is also expressed explicitly in arthritis. It is therefore considered to be a biomarker of RA [47]. The identification of miR-23b expression shows downregulation in inflammatory lesions from RA individuals and related mouse models compared with healthy controls [42]. It is well known that RA is more common in old age [81]. However, juvenile idiopathic arthritis will also occur in a high proportion, which is very detrimental to the growth of children [82]. The study has shown that miR-23b helps in the diagnosis and monitoring of RA [83]. miR-23b is negatively related to inflammation in RA [47]. Similarly, the negative correlation between IL-17 and miR-23b is verified in comparing RA patients and healthy subjects [42]. In addition, Zhu et al. found that (TAB2), TAB3, and nuclear factor k-B kinase subunit α (IKK-α) were down-regulated after transfection of miR-23b in fibroblast-like synovial cells (FLSs), which were obtained from synovial joint tissues of individuals with

knee joint injury. [42]. Therefore, it is implied that miR-23b can target TAB2, TAB3, and IKK-α to alleviate disease.

5.3. SLE. SLE is an autoimmune disease in women with features of multiple tissues and systems [84]. Moreover, brain tissue is often the target organ of this disease. Due to the long-term and widespread existence of intracranial vascular inflammation, part of the gray matter shows ischemia, infarction, atrophy, and several demyelinations of white matter areas [85]. The injury of the gray and white matter directly affects nerve function and leads to abnormal clinical symptoms. The incidence of SLE is increasing year by year, with facial erythema, joint pain, fever, and fatigue as the primary manifestations. Using the mouse model of SLE, the research has verified that the treatment of adipose-derived stem cells (ADSCs) can effectively alleviate the progression of the disease. Specifically, it reduces the expression of inflammatory factor IL-17, which may be related to the upregulation of miR-23b [48]. Additionally, through RNA differential analysis of renal biopsy samples from several patients with SLE, it is found that miR-23b is downregulated in the inflammatory sites of SLE patients [42]. Similar to RA, miR-23b also inhibited the development of SLE upon inhibiting TAB2, TAB3, and IKK-α [42]. All in all, the high expression of miR-23b will be helpful for the relief of SLE.

The mechanism of action of miR-23b in EAE, RA, and SLE is summarized in Figure 2.

6. Treatment

miRNAs are abnormally expressed in various pathological processes. Restoring miRNA normal levels might be regarded as a promising therapy. Up to date, miRNA inhibitors have been frequently used in the study of miRNA function and mechanism. It is common to use artificial inhibitors, including anti-miRNA oligonucleotide (AMO) and miRNA sponges [86]. AMO is a short-stranded RNA oligonucleotide that is complementary to natural miRNAs [87]. AMO has been used in various cancers [88–91]. Artificial miRNA sponge is constructed by inserting tandemly arrayed miRNA sites into 3′-terminus (3′ 3′-UTRs) of a reporter gene [92]. This type of miRNA sponge is characterized by inductive and stable expression, driven by the most potent promoters in mammalian systems, such as U6 or cytomegalovirus (CMV) [93]. MicroRNA (miRNA) sponges are transcripts with repeated miRNA antisense sequences that can sequester miRNAs from the endogenous target, leading to miRNA translation inhibition or mRNA degradation to fail [94]. The microRNA sponge can play a role in cancer treatment. For example, there have been studies based on the bladder cancer xenograft model of BALB/c nude mice, and lentivirus-transduced miR-130b/miR-494 sponge inhibits tumor growth [95]. Besides, the miRNA sponge also has excellent potential in the treatment of liver cancer. To be specific, miR-17-3p, miR-181b-5p, and miR-9 sponges all demonstrated the ability to inhibit the growth of liver cancer cells [96–98]. Interestingly, the team identified a circRNA that is highly expressed in
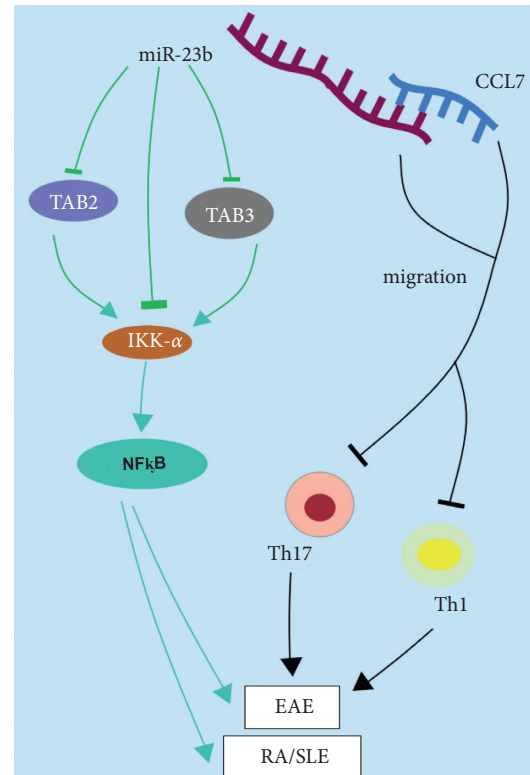
Figure 2: The mechanism of miR-23b in MS, RA, and SLE. IKK-α could promote the expression of inflammatory factor NF-□B, which contributes to the occurrence of autoimmune diseases RA, SLE, and MS/EAE. Additionally, miR-23b could alleviate these diseases by inhibiting TAB2 and TAB3, which are beneficial for IKK-α. Besides, the binding of miR-23b to CCL7 can inhibit the migration of inflammatory cells Th1 and Th17 and ultimately inhibit disease development.

human and mouse brains and later showed that this circRNA could act as a sponge for miRNAs [99, 100]. For example, circHIPK3 is the sponge of miR-558 inhibiting bladder cancer development both in vivo and in vitro [101]. Notably, miR-23b sponge is also applied to liver cancer cells and glioma cells, and the results show that it has a good effect in inhibiting the disease [102, 103]. In addition to the above methods for regulating miRNA levels, RNA mimics can be used as well. miRNA mimics are double-stranded RNA molecules, which modulate miRNA level [25]. miRNA mimic is a strategy to restore miRNA function. Even viral vectors can transfect miRNA into cells, but they have genome integration and the potential danger of immunogenicity [104]. For example, miR-125b-5p mimic has been demonstrated to inhibit acute liver injury in vivo [105]. Therefore, miRNA mimic does not integrate into the genome, making it a good prospect in disease treatment [104]. In conclusion, the AMO, sponge, and mimic of miR-23b can potentially treat cancers and autoimmune diseases.

7. Conclusion

miR-23b is frequently upregulated in a variety of tumors and human cancer cell lines and exerts a vital function in

tumorigenesis. The expression level of miR-23b is induced by the HER2/neu, EGF, TNF-α, and Blimp1, constitutively activated in breast cancer [43, 55]. In studies on lung cancer cell lines and NSCLC cells, miR-23b has been shown to promote cancer development. Therefore, miR-23b is a potential clinical pathologic marker in lung cancer [57]. In addition, miR-23b can be used as a novel therapeutic target. Studies in liver cancer have shown that ST7L, as the direct target of miR-23b, plays a regulatory role in liver cancer cells and can act as an oncogene [66]. Finally, for gastric cancer, miR-23b promotes tumor development by targeting PDCD4 [75]. It has been shown to antagonize TUSC7, a tumor inhibitor [76]. However, the regulatory role of miR-23b looks paradox in different cancer. In conclusion, miRNA-23b expression profiles differ between disease states and normal tissue, and the abnormal regulation of miR-23b can be used as a warning for tumors in tumor studies. However, its regulatory effects on a variety of proteins make it a very challenging target for cancer therapy. In general, for tumors, miR-23b often has different roles in divergent systems or environments. It is consistent with previous research illustrating that one of the frustrating aspects of microRNA research is that individual microRNAs have opposite functions in different systems, suggesting that microRNA communication is environment-dependent [34]. Some examples demonstrate that miR-125b is downregulated in various cancers such as hepatocellular carcinoma and breast cancer and overexpressed in colon cancer and hepatocellular tumors [106]. Furthermore, future work should build on the study of how miR-23b participates in the tumor suppressor pathway or promotion pathway to lay a theoretical foundation for tumor therapy.

The discovery of miRNAs has expanded the knowledge of human diseases, including autoimmune diseases. Here, we have summarized the crucial functions of miR-23b as an anti-inflammatory gene in MS/EAE, RA, and SLE. Hundreds of cell- and animal-based studies agree on the inflammatory-suppressive role of miR-23b and suggest recovery of miR-23b level as a potential therapeutic approach. In autoimmune diseases, the overexpression of miR-23b primarily reflects the ability to inhibit the differentiation of th17 cells, reduce inflammatory cytokines, and block the infiltration of inflammatory cells into the lesion. The benefit of miR-23b-based therapy is the chance to suppress multiple proinflammatory cytokines and chemokines production concurrently in EAE [41, 42]. As a marker of RA, studies have shown that it can help diagnose and detect the disease. Moreover, it can downregulate Tab2, Tab3, and IKK-α. In SLE studies, studies in animal models have shown that overexpression of miR-23b can inhibit the inflammatory factor IL-17 and alleviate SLE. Next, miR-23b inhibitors can be administrated to observe whether they can consistently inhibit inflammatory factors secretion and disease development in animal models of SLE. Furthermore, a more detailed understanding of mechanisms underlying how miR-23b modulates therapeutic effect might be a study focus in the future.

Although miR-23b functions based on multiple pathways and multiple targets in the disease's pathological process, it is inevitable that the expression of miR-23b is abnormal and undulatory during the occurrence of the disease. Regulating miR-23b to its normal level is a new potential therapeutic strategy for treating related diseases. So far, the application of miRNA sponges, AMOS, and mimics has provided favorable conditions for regulating abnormal miR-23b expression.

Conflicts of Interest

The authors declare that they have no conflicts of interest.

Authors' Contributions

All authors listed have made substantial contributions to the work and have approved to publish it.

Acknowledgments

References

[1] H. Sung, J. Ferlay, and R. L. Siegel, M. Laversanne, I. Soerjomataram, A. Jemal, and F. Bray, Global cancer statistics 2020: GLOBOCAN estimates of incidence and mortality worldwide for 36 cancers in 185 countries," *CA: A Cancer Journal for Clinicians*, vol. 71, 2021.

[2] W. Cao, H.-Da Chen, Yi-W. Yu, Ni Li, and W.-Q. Chen, "Changing profiles of cancer burden worldwide and in China: a secondary analysis of the global cancer statistics 2020," *Chinese Medical Journal*, vol. 134, 2021.

[3] M. Thun, R. Peto, J. Boreham, and A. D. Lopez, "Stages of the cigarette epidemic on entering its second century," *Tobacco Control*, vol. 21, no. 2, pp. 96–101, 2012.

[4] R. Alonso, M. Piñeros, M. Laversanne et al., "Lung cancer incidence trends in Uruguay 1990-2014: an age-period-cohort analysis," *Cancer epidemiology*, vol. 55, pp. 17–22, 2018.

[5] J. L. Petrick, A. A. Florio, A. Znaor et al., "International trends in hepatocellular carcinoma incidence, 1978-2012," *International Journal of Cancer*, vol. 147, no. 2, pp. 317–330, 2020.

[6] M. Arnold, J. Y. Park, M. C. Camargo, N. Lunet, D. Forman, and I. Soerjomataram, "Is gastric cancer becoming a rare disease? A global assessment of predicted incidence trends to 2035," *Gut*, vol. 69, no. 5, pp. 823–829, 2020.

[7] E. J. Mun, H. M. Babiker, U. Weinberg, E. D. Kirson, and D. D. Von Hoff, "Tumor-treating fields: a fourth modality in cancer treatment," *Clinical Cancer Research*, vol. 24, no. 2, pp. 266–275, 2018.

[8] P. Kumari, B. Ghosh, and S. Biswas, "Nanocarriers for cancer-targeted drug delivery," *Journal of Drug Targeting*, vol. 24, no. 3, pp. 179–191, 2016.

[9] L. L. Bu, J. Yan, Z. Wang et al., "Advances in drug delivery for post-surgical cancer treatment," *Biomaterials*, vol. 219, Article ID 119182, 2019.

[10] D. McGonagle and M. F. McDermott, "A proposed classification of the immunological diseases," *PLoS Medicine*, vol. 3, no. 8, Article ID e297, 2006.

[11] F. Piancone, F. La Rosa, I. Marventano, M. Saresella, and M. Clerici, "The role of the inflammasome in neurodegenerative diseases," *Molecules*, vol. 26, no. 4, 2021.

[12] M. Prinz and J. Priller, "The role of peripheral immune cells in the CNS in steady state and disease," *Nature Neuroscience*, vol. 20, no. 2, pp. 136–144, 2017.

[13] G. J. Tobón, P. Youinou, and A. Saraux, "The environment, geo-epidemiology, and autoimmune disease: rheumatoid arthritis," *Journal of Autoimmunity*, vol. 35, no. 1, pp. 10–14, 2010.

[14] M. Zaiss, H.-J. J. Wu, D. Mauro, G. Schett, and F. Ciccia, "The gut-joint axis in rheumatoid arthritis," *Nature Reviews. Rheumatology*, vol. 17, 2021.

[15] J. S. Smolen, D. Aletaha, A. Barton et al., "Rheumatoid arthritis," *Nature Reviews. Disease Primers*, vol. 4, p. 18001, 2018.

[16] A. Myngbay, L. Manarbek, S. Ludbrook, and J. Kunz, "The role of collagen triple helix repeat-containing 1 protein (CTHRC1) in rheumatoid arthritis," *International Journal of Molecular Sciences*, vol. 22, no. 5, 2021.

[17] H. Liu, Y. Zou, C. Chen, Y. Tang, and J. Guo, "Current understanding of circular RNAs in systemic lupus erythematosus," *Frontiers in Immunology*, vol. 12, Article ID 628872, 2021.

[18] E. Gianchecchi, D. Delfino, and A. Fierabracci, "Natural killer cells: potential biomarkers and therapeutic target in autoimmune diseases?" *Frontiers in Immunology*, vol. 12, Article ID 616853, 2021.

[19] M. Donadelli, I. Dando, C. Fiorini, and M. Palmieri, "Regulation of miR-23b expression and its dual role on ROS production and tumour development," *Cancer Letters*, vol. 349, no. 2, pp. 107–113, 2014.

[20] S. P. O'Hara, J. L. Mott, P. L. Splinter, G. J. Gores, and N. F. LaRusso, "MicroRNAs: key modulators of posttranscriptional gene expression," *Gastroenterology*, vol. 136, no. 1, pp. 17–25, 2009.

[21] M. Ha and V. N. Kim, "Regulation of microRNA biogenesis," *Nature Reviews Molecular Cell Biology*, vol. 15, no. 8, pp. 509–524, 2014.

[22] Y. Jiang, Y.-Y. Man, Y. Liu et al., "Loss of miR-23b/27b/24-1 cluster impairs glucose tolerance via glycolysis pathway in mice," *International Journal of Molecular Sciences*, vol. 22, no. 2, 2021.

[23] W. Wang, Y. Wang, W. Liu, and A. J. van Wijnen, "Regulation and biological roles of the multifaceted miRNA-23b (MIR23B)," *Gene*, vol. 642, pp. 103–109, 2018.

[24] J. Arzuaga-Mendez, M. Lopez-Santillan, J. C. Garcia-Ruiz, E. Lopez-Lopez, and I. Martin-Guerrero, "Systematic review of the potential of MicroRNAs in the management of patients with follicular lymphoma," *Critical Reviews in Oncology/hematology*, vol. 159, Article ID 103247, 2021.

[25] T. X. Lu and M. E. Rothenberg, "MicroRNA," *The Journal of Allergy and Clinical Immunology*, vol. 141, no. 4, pp. 1202–1207, 2018.

[26] J. Winter, S. Jung, S. Keller, R. I. Gregory, and S. Diederichs, "Many roads to maturity: microRNA biogenesis pathways and their regulation," *Nature Cell Biology*, vol. 11, no. 3, pp. 228–234, 2009.

[27] J. M. Thomson, M. Newman, J. S. Parker, E. M. Morin-Kensicki, T. Wright, and S. M. Hammond, "Extensive posttranscriptional regulation of microRNAs and its implications for cancer," *Genes & Development*, vol. 20, no. 16, pp. 2202–2207, 2006.

[28] Y. Lee, M. Kim, J. Han et al., "MicroRNA genes are transcribed by RNA polymerase II," *The EMBO Journal*, vol. 23, no. 20, pp. 4051–4060, 2004.

[29] Y. Lee, C. Ahn, J. Han et al., "The nuclear RNase III Drosha initiates microRNA processing," *Nature*, vol. 425, no. 6956, pp. 415–419, 2003.

[30] I. Baskara-Yhuellou and J. Tost, "The impact of microRNAs on alterations of gene regulatory networks in allergic diseases," *Advances in Protein Chemistry and Structural Biology*, vol. 120, pp. 237–312, 2020.

[31] D. Cifuentes, H. Xue, D. W. Taylor et al., "A novel miRNA processing pathway independent of Dicer requires Argonaute2 catalytic activity," *Science*, vol. 328, no. 5986, pp. 1694–1698, 2010.

[32] T. Kawamata and Y. Tomari, "Making RISC," *Trends in Biochemical Sciences*, vol. 35, no. 7, pp. 368–376, 2010.

[33] C. Catalanotto, C. Cogoni, and G. Zardo, "MicroRNA in control of gene expression: an overview of nuclear functions," *International Journal of Molecular Sciences*, vol. 17, no. 10, 2016.

[34] A. M. Mohr and J. L. Mott, "Overview of microRNA biology," *Seminars in Liver Disease*, vol. 35, no. 1, pp. 3–11, 2015.

[35] B. Bae and P. Miura, "Emerging roles for 3' UTRs in neurons," *International Journal of Molecular Sciences*, vol. 21, no. 10, 2020.

[36] T. Siddika and I. U. Heinemann, "Bringing MicroRNAs to light: methods for MicroRNA quantification and visualization in live cells," *Frontiers in Bioengineering and Biotechnology*, vol. 8, Article ID 619583, 2020.

[37] L. Moreno-García, T. López-Royo, A. C. Calvo et al., "Competing endogenous RNA networks as biomarkers in neurodegenerative diseases," *International Journal of Molecular Sciences*, vol. 21, no. 24, 2020.

[38] M. Cantile, M. Di Bonito, M. T. De Bellis, and G. Botti, "Functional interaction among lncRNA HOTAIR and MicroRNAs in cancer and other human diseases," *Cancers*, vol. 13, no. 3, 2021.

[39] F. Precazzini, S. Detassis, A. S. Imperatori, M. A. Denti, and P. Campomenosi, "Measurements methods for the development of MicroRNA-based tests for cancer diagnosis," *International Journal of Molecular Sciences*, vol. 22, no. 3, 2021.

[40] V. Viswanathan, J. Fields, and B. M. Boman, "The miRNA23b-regulated signaling network as a key to cancer development--implications for translational research and therapeutics," *Journal of Molecular Medicine*, vol. 92, no. 11, pp. 1129–1138, 2014.

[41] Y. Zhang, J.-J. Han, X.-Y. Liang et al., "miR-23b suppresses leukocyte migration and pathogenesis of experimental autoimmune encephalomyelitis by targeting CCL7," *Molecular Therapy*, vol. 26, no. 2, pp. 582–592, 2018.

[42] S. Zhu, W. Pan, X. Song et al., "The microRNA miR-23b suppresses IL-17-associated autoimmune inflammation by targeting TAB2, TAB3 and IKK-α," *Nature Medicine*, vol. 18, no. 7, pp. 1077–1086, 2012.

[43] M. Sciortino, M. d. P. Camacho-Leal, F. Orso et al., "Dysregulation of Blimp1 transcriptional repressor unleashes p130Cas/ErbB2 breast cancer invasion," *Scientific Reports*, vol. 7, no. 1, p. 1145, 2017.

[44] J. Cao, J. Liu, J. Long et al., "microRNA-23b suppresses epithelial-mesenchymal transition (EMT) and metastasis in hepatocellular carcinoma via targeting Pyk2," *Biomedicine & Pharmacotherapy*, vol. 89, pp. 642–650, 2017.

[45] S. Begum, M. Hayashi, T. Ogawa et al., "An integrated genome-wide approach to discover deregulated microRNAs in non-small cell lung cancer: clinical significance of miR-23b-3p deregulation," *Scientific Reports*, vol. 5, Article ID 13236, 2015.

[46] R. Hu, W. Lv, S. Zhang et al., "Combining miR-23b exposure with mesenchymal stem cell transplantation enhances therapeutic effects on EAE," *Immunology Letters*, vol. 229, pp. 18–26, 2021.

[47] X. Liu, S. Ni, C. Li et al., "Circulating microRNA-23b as a new biomarker for rheumatoid arthritis," *Gene*, vol. 712, Article ID 143911, 2019.

[48] X. He, Y. Zhang, A. Zhu et al., "Suppression of interleukin 17 contributes to the immunomodulatory effects of adipose-derived stem cells in a murine model of systemic lupus erythematosus," *Immunologic Research*, vol. 64, no. 5-6, pp. 1157–1167, 2016.

[49] L. Pellegrino, J. Stebbing, V. M. Braga et al., "miR-23b regulates cytoskeletal remodeling, motility and metastasis by directly targeting multiple transcripts," *Nucleic Acids Research*, vol. 41, no. 10, pp. 5400–5412, 2013.

[50] I. P. Michael, S. Saghafinia, and D. Hanahan, "A set of microRNAs coordinately controls tumorigenesis, invasion, and metastasis," *Proceedings of the National Academy of Sciences*, vol. 116, no. 48, pp. 24184–24195, 2019.

[51] M. Taha, N. Mitwally, A. S. Soliman, and E. Yousef, "Potential diagnostic and prognostic utility of miR-141, miR-181b1, and miR-23b in breast cancer," *International Journal of Molecular Sciences*, vol. 21, no. 22, 2020.

[52] T. Chiyomaru, N. Seki, S. Inoguchi et al., "Dual regulation of receptor tyrosine kinase genes EGFR and c-Met by the tumor-suppressive microRNA-23b/27b cluster in bladder cancer," *International Journal of Oncology*, vol. 46, no. 2, pp. 487–496, 2015.

[53] H. Chang, B. Yi, R. Ma, X. Zhang, H. Zhao, and Y. Xi, "CRISPR/cas9, a novel genomic tool to knock down microRNA in vitro and in vivo," *Scientific Reports*, vol. 6, Article ID 22312, 2016.

[54] B. N. Hannafon, A. Cai, C. L. Calloway et al., "miR-23b and miR-27b are oncogenic microRNAs in breast cancer: evidence from a CRISPR/Cas9 deletion study," *BMC Cancer*, vol. 19, no. 1, p. 642, 2019.

[55] L. Jin, O. Wessely, E. G. Marcusson, C. Ivan, G. A. Calin, and S. K. Alahari, "Prooncogenic factors miR-23b and miR-27b are regulated by Her2/Neu, EGF, and TNF-α in breast cancer," *Cancer Research*, vol. 73, no. 9, pp. 2884–2896, 2013.

[56] M. Boi, E. Zucca, G. Inghirami, and F. Bertoni, "PRDM1/BLIMP1: a tumor suppressor gene in B and T cell lymphomas," *Leukemia and Lymphoma*, vol. 56, no. 5, pp. 1223–1228, 2015.

[57] Y. Zhu, T. Li, G. Chen et al., "Identification of a serum microRNA expression signature for detection of lung cancer, involving miR-23b, miR-221, miR-148b and miR-423-3p," *Lung Cancer*, vol. 114, pp. 6–11, 2017.

[58] L. Wang, Z. Hu, Q. Guo, L. Yang, Y. Pang, and W. Wang, "MiR-23b functions as an oncogenic miRNA by downregulating Mcl-1S in lung cancer cell line A549," *Journal of Biochemical and Molecular Toxicology*, vol. 34, no. 7, Article ID e22494, 2020.

[59] J. Bae, C. P. Leo, S. Y. Hsu, and A. J. W. Hsueh, "MCL-1S, a splicing variant of the antiapoptotic BCL-2 family member MCL-1, encodes a proapoptotic protein possessing only the BH3 domain," *Journal of Biological Chemistry*, vol. 275, no. 33, pp. 25255–25261, 2000.

[60] C. Liu, X. Li, Y. Hao et al., "STAT1-induced upregulation of lncRNA KTN1-AS1 predicts poor prognosis and facilitates non-small cell lung cancer progression via miR-23b/DEPDC1 axis," *Aging*, vol. 12, no. 9, pp. 8680–8701, 2020.

[61] X. Ficht and M. Iannacone, "Immune surveillance of the liver by T cells," *Science Immunology*, vol. 5, no. 51, 2020.

[62] A. Granito, L. Muratori, C. Lalanne et al., "Hepatocellular carcinoma in viral and autoimmune liver diseases: role of CD4+ CD25+ Foxp3+ regulatory T cells in the immune microenvironment," *World Journal of Gastroenterology*, vol. 27, no. 22, pp. 2994–3009, 2021.

[63] H. Wang, H. Zhang, Yu Wang et al., "Regulatory T cell and neutrophil extracellular trap interaction contributes to carcinogenesis in non-alcoholic steatohepatitis," *Journal of Hepatology*, vol. S0168-S8278, no. 21, p. 01962, 2021.

[64] S. Ferri, M. S. Longhi, C. De Molo et al., "A multifaceted imbalance of T cells with regulatory function characterizes type 1 autoimmune hepatitis," *Hepatology*, vol. 52, no. 3, pp. 999–1007, 2010.

[65] M. S. Longhi, F. Meda, P. Wang et al., "Expansion and de novo generation of potentially therapeutic regulatory T cells in patients with autoimmune hepatitis," *Hepatology*, vol. 47, no. 2, pp. 581–591, 2008.

[66] L. Zhuang, X. Wang, Z. Wang et al., "MicroRNA-23b functions as an oncogene and activates AKT/GSK3β/β-catenin signaling by targeting ST7L in hepatocellular carcinoma," *Cell Death & Disease*, vol. 8, no. 5, p. e2804, 2017.

[67] M. Hayashi, S. Yamada, K. Kurimoto et al., "miR-23b-3p plays an oncogenic role in hepatocellular carcinoma," *Annals of Surgical Oncology*, vol. 28, 2020.

[68] Y. Liu, J. Tan, S. Ou, J. Chen, and L. Chen, "Adipose-derived exosomes deliver miR-23a/b to regulate tumor growth in hepatocellular cancer by targeting the VHL/HIF axis," *Journal of Physiology and Biochemistry*, vol. 75, no. 3, pp. 391–401, 2019.

[69] N. Vrachnis, P. Belitsos, S. Sifakis et al., "Role of adipokines and other inflammatory mediators in gestational diabetes mellitus and previous gestational diabetes mellitus," *International Journal of Endocrinology*, vol. 2012, Article ID 549748, 2012.

[70] B.-H. Kuang, M.-Q. Zhang, L.-H. Xu et al., "Proline-rich tyrosine kinase 2 and its phosphorylated form pY881 are novel prognostic markers for non-small-cell lung cancer progression and patients' overall survival," *British Journal of Cancer*, vol. 109, no. 5, pp. 1252–1263, 2013.

[71] M. K. Wendt, B. J. Schiemann, J. G. Parvani, Y.-H. Lee, Y. Kang, and W. P. Schiemann, "TGF-β stimulates Pyk2 expression as part of an epithelial-mesenchymal transition program required for metastatic outgrowth of breast cancer," *Oncogene*, vol. 32, no. 16, pp. 2005–2015, 2013.

[72] P. Assunção, E. Cardoso da Conceição, L. Luiz Borges, J. Abadia, and M. de Paula, "Eugenia unifloraDevelopment and validation of a HPLC-UV method for the evaluation of ellagic acid in liquid extracts of L. (Myrtaceae) leaves and its ultrasound-assisted extraction optimization," *Evidence-Based Complementary and Alternative Medicine*, vol. 2017, Article ID 1501038, 2017.

[73] G. Ma, W. Dai, A. Sang, X. Yang, and C. Gao, "Upregulation of microRNA-23a/b promotes tumor progression and confers poor prognosis in patients with gastric cancer," *International Journal of Clinical and Experimental Pathology*, vol. 7, no. 12, pp. 8833–8840, 2014.

[74] K. Zhuang, K. Han, H. Tang et al., "Up-regulation of plasma miR-23b is associated with poor prognosis of gastric cancer," *Medical Science Monitor*, vol. 22, pp. 356–361, 2016.

[75] X. Hu, Y. Wang, H. Liang et al., "miR-23a/b promote tumor growth and suppress apoptosis by targeting PDCD4 in gastric cancer," *Cell Death & Disease*, vol. 8, no. 10, p. e3059, 2017.

[76] P. Qi, M.-d. Xu, X.-H. Shen et al., "Reciprocal repression between TUSC7 and miR-23b in gastric cancer," *International Journal of Cancer*, vol. 137, no. 6, pp. 1269–1278, 2015.

[77] Y. Kumata, H. Iinuma, Y. Suzuki et al., "Exosome-encapsulated microRNA-23b as a minimally invasive liquid biomarker for the prediction of recurrence and prognosis of gastric cancer patients in each tumor stage," *Oncology Reports*, vol. 40, no. 1, pp. 319–330, 2018.

[78] B. Martinez and P. V. Peplow, "MicroRNAs as disease progression biomarkers and therapeutic targets in experimental autoimmune encephalomyelitis model of multiple sclerosis," *Neural Regeneration Research*, vol. 15, no. 10, pp. 1831–1837, 2020.

[79] S. H. Venkatesha, S. Dudics, Y. Song, A. Mahurkar, and K. D. Moudgil, "The miRNA expression profile of experimental autoimmune encephalomyelitis reveals novel potential disease biomarkers," *International Journal of Molecular Sciences*, vol. 19, no. 12, 2018.

[80] M. Cassotta, T. Y. Forbes-Hernandez, D. Cianciosi et al., "Nutrition and rheumatoid arthritis in the "omics" era," *Nutrients*, vol. 13, no. 3, 2021.

[81] T. Uhlig, T. K. Kvien, A. Glennås, L. M. Smedstad, and O. Førre, "The incidence and severity of rheumatoid arthritis, results from a county register in Oslo, Norway," *Journal of Rheumatology*, vol. 25, no. 6, pp. 1078–1084, 1998.

[82] A. Ravelli and A. Martini, "Juvenile idiopathic arthritis," *The Lancet*, vol. 369, no. 9563, pp. 767–778, 2007.

[83] K. Orczyk and E. Smolewska, "The potential importance of MicroRNAs as novel indicators how to manage patients with juvenile idiopathic arthritis more effectively," *Journal of Immunology Research*, vol. 2021, Article ID 9473508, 2021.

[84] Z. Zhuo, L. Su, Y. Duan et al., "Different patterns of cerebral perfusion in SLE patients with and without neuropsychiatric manifestations," *Human Brain Mapping*, vol. 41, no. 3, pp. 755–766, 2020.

[85] M. Wigren, E. Svenungsson, I. Y. Mattisson et al., "Cardiovascular disease in systemic lupus erythematosus is associated with increased levels of biomarkers reflecting receptor-activated apoptosis," *Atherosclerosis*, vol. 270, pp. 1–7, 2018.

[86] R. O. Bak and J. G. Mikkelsen, "miRNA sponges: soaking up miRNAs for regulation of gene expression," *Wiley Interdisciplinary Reviews: RNA*, vol. 5, no. 3, pp. 317–333, 2014.

[87] J. Krützfeldt, N. Rajewsky, R. Braich et al., "Silencing of microRNAs in vivo with "antagomirs"," *Nature*, vol. 438, no. 7068, pp. 685–689, 2005.

[88] D. Shu, H. Li, Y. Shu et al., "Systemic delivery of anti-miRNA for suppression of triple negative breast cancer utilizing RNA nanotechnology," *ACS Nano*, vol. 9, no. 10, pp. 9731–9740, 2015.

[89] D. W. Binzel, Y. Shu, H. Li et al., "Specific delivery of MiRNA for high efficient inhibition of prostate cancer by RNA nanotechnology," *Molecular Therapy*, vol. 24, no. 7, pp. 1267–1277, 2016.

[90] S. Gao, H. Tian, Y. Guo et al., "miRNA oligonucleotide and sponge for miRNA-21 inhibition mediated by PEI-PLL in breast cancer therapy," *Acta Biomaterialia*, vol. 25, pp. 184–193, 2015.

[91] L. Xu, Y. Huang, D. Chen et al., "Downregulation of miR-21 increases cisplatin sensitivity of non-small-cell lung cancer," *Cancer Genetics*, vol. 207, no. 5, pp. 214–220, 2014.

[92] M. S. Ebert, J. R. Neilson, and P. A. Sharp, "MicroRNA sponges: competitive inhibitors of small RNAs in mammalian cells," *Nature Methods*, vol. 4, no. 9, pp. 721–726, 2007.

[93] M. S. Ebert and P. A. Sharp, "Emerging roles for natural microRNA sponges," *Current Biology*, vol. 20, no. 19, pp. R858–R861, 2010.

[94] M. A. Iqbal, S. Arora, G. Prakasam, G. A. Calin, and M. A. Syed, "MicroRNA in lung cancer: role, mechanisms, pathways and therapeutic relevance," *Molecular Aspects of Medicine*, vol. 70, pp. 3–20, 2019.

[95] Q. Lu, T. Liu, H. Feng et al., "Circular RNA circSLC8A1 acts as a sponge of miR-130b/miR-494 in suppressing bladder cancer progression via regulating PTEN," *Molecular Cancer*, vol. 18, no. 1, p. 111, 2019.

[96] J. Yu, Q.-g. Xu, Z.-g. Wang et al., "Circular RNA cSMARCA5 inhibits growth and metastasis in hepatocellular carcinoma," *Journal of Hepatology*, vol. 68, no. 6, pp. 1214–1227, 2018.

[97] D. Han, J. Li, H. Wang et al., "Circular RNA circMTO1 acts as the sponge of microRNA-9 to suppress hepatocellular carcinoma progression," *Hepatology*, vol. 66, no. 4, pp. 1151–1164, 2017.

[98] D. Li, J. Zhang, and J. Li, "Role of miRNA sponges in hepatocellular carcinoma," *Clinica Chimica Acta*, vol. 500, pp. 10–19, 2020.

[99] T. B. Hansen, E. D. Wiklund, J. B. Bramsen et al., "miRNA-dependent gene silencing involving Ago2-mediated cleavage of a circular antisense RNA," *The EMBO Journal*, vol. 30, no. 21, pp. 4414–4422, 2011.

[100] T. B. Hansen, T. I. Jensen, B. H. Clausen et al., "Natural RNA circles function as efficient microRNA sponges," *Nature*, vol. 495, no. 7441, pp. 384–388, 2013.

[101] Y. Li, F. Zheng, X. Xiao et al., "CircHIPK3 sponges miR-558 to suppress heparanase expression in bladder cancer cells," *EMBO Reports*, vol. 18, no. 9, pp. 1646–1659, 2017.

[102] Y. Sun, Q. Zhou, J. Li, C. Zhao, Z. Yu, and Q. Zhu, "LncRNA RP11-422N16.3 inhibits cell proliferation and EMT, and induces apoptosis in hepatocellular carcinoma cells by sponging miR-23b-3p," *OncoTargets and Therapy*, vol. 12, pp. 10943–10961, 2019.

[103] L. Chen, K. Zhang, Z. Shi et al., "A lentivirus-mediated miR-23b sponge diminishes the malignant phenotype of glioma cells in vitro and in vivo," *Oncology Reports*, vol. 31, no. 4, pp. 1573–1580, 2014.

[104] T. Nogimori, K. Furutachi, K. Ogami, N. Hosoda, and S.-i. Hoshino, "A novel method for stabilizing microRNA mimics," *Biochemical and Biophysical Research Communications*, vol. 511, no. 2, pp. 422–426, 2019.

[105] D. Yang, Q. Yuan, A. Balakrishnan et al., "MicroRNA-125b-5p mimic inhibits acute liver failure," *Nature Communications*, vol. 7, no. 1, Article ID 11916, 2016.

[106] J. Banzhaf-Strathmann and D. Edbauer, "Good guy or bad guy: the opposing roles of microRNA 125b in cancer," *Cell Communication and Signaling*, vol. 12, no. 1, p. 30, 2014.

Research Article

High Expression Levels of SLC38A1 Are Correlated with Poor Prognosis and Defective Immune Infiltration in Hepatocellular Carcinoma

Yun Liu ,[1] **Yong Yang** ,[2] **Linna Jiang** ,[3] **Hongrui Xu** ,[4] **and Junwei Wei** [5,6]

[1]*Department of General Surgery, First Hospital of Handan City, Handan, Hebei 056000, China*
[2]*Department of General Surgery, Cixian Cancer Hospital, Handan, Hebei 056000, China*
[3]*Pathology Department, First Hospital of Handan City, Handan, Hebei 056000, China*
[4]*Translational Medicine Center, Huaihe Hospital of Henan University, Kaifeng, Henan 475000, China*
[5]*Department of Gastroenterology, First Hospital of Handan City, Handan, Hebei 056000, China*
[6]*Department of Infectious Diseases, Third Affiliated Hospital of Hebei Medical University, Shijiazhuang, Hebei 050000, China*

Correspondence should be addressed to Junwei Wei; 20191523@stu.hebmu.edu.cn

Solute Carrier Family 38 Member 1 (SLC38A1) is a principal transporter of glutamine and plays a crucial role in the transformation of neoplastic cells. However, the correlation between SLC38A1 expression, prognosis, and immune infiltration in hepatocellular carcinoma (HCC) has yet to be elucidated. We used two independent patient cohorts, namely, a *Cancer* Genome Atlas (TCGA) cohort and a Clinical Proteomic Tumor Analysis Consortium (CPTAC) cohort, to analyze the role of SLC38A1 in HCC at the mRNA and protein levels, respectively. In these two cohorts, SLC38A1 mRNA and protein expression levels were higher in HCC tissues than in adjacent nontumor tissues. Both SLC38A1 mRNA and protein expression were positively associated with clinicopathological characteristics (clinical stage, *T* stage, pathological grade, tumor size, and tumor thrombus), were negatively associated with survival, and were independent prognostic factors in HCC patients. Functional enrichment analyses further indicated that SLC38A1 was involved in multiple pathways related to amino acid metabolism, tumors, and immunity. High expression levels of SLC38A1 were inversely proportional to CD8+ T cells and directly proportional to macrophages M0, neutrophils, programmed cell death-1/programmed cell death ligand 1 (PD-1/PD-L1), and cytotoxic T lymphocyte-associated protein 4 (CTLA-4). Moreover, we used immunohistochemical analysis of tissue samples and other online databases to further validate the expression levels and prognostic significance of SLC38A1 in HCC. Collectively, our study demonstrated that the upregulated expression of SLC38A1 was related to an unfavorable prognosis and defective immune infiltration in HCC.

1. Introduction

Hepatocellular carcinoma (HCC) is the most common primary tumor of the liver and the fourth leading cause of global cancer-related deaths [1]. A previous study that was based on the Surveillance, Epidemiology, and End Results Program (SEER) registry project indicated that the incidence of HCC will continue to rise in the future and is expected to peak in the year 2030 [2]. While treatment strategies for liver cancer have expanded with the emergence of new therapies, the prognoses of patients in advanced stages of HCC are still

relatively unsatisfactory [3]. Therefore, it is of great significance to identify an effective biomarker that could predict prognosis and could be used as a therapeutic target for HCC patients [4].

The Solute Carrier Family 38 (SLC38) is the principal transporter for glutamine and plays a major role in maintaining homeostasis in the body [5]. Glutamine has a large number of vital functions in mammalian cells; consequently, the dysregulation of the SLC38 transporter may result in tumorigenesis and the progression of cancers [6]. The SLC38 transporter has been described as having the functional

nature and regulatory mode of system A and system N transport activities [7]. As the first member of system A, SLC38A1 is predominantly expressed in the placenta and the brain [8]. Like other family members, the main function of SLC38A1 is to regulate the transport of short chain neutral amino acids, including glutamine. Although the upregulation of SLC38A1 expression has been demonstrated in a variety of tumors [9–12], the prognostic significance of SLC38A1 expression has not been reported in HCC. Furthermore, immunotherapy has been considered as a promising treatment for cancers, including HCC. It is also possible that tumor-infiltrating lymphocytes may influence the efficacy of immunotherapy. However, the correlation between SLC38A1 expression and immune infiltration in HCC has yet to be determined.

In the present study, we used various public databases to comprehensively analyze the expression of SLC38A1 and evaluate its prognostic significance at the mRNA and protein levels. We further validated the differential expression levels of SLC38A1 between HCC and adjacent nontumor tissue by performing immunohistochemistry (IHC) on our tissue samples. We also performed multiple enrichment analysis to explore the potential molecular mechanisms that might be mediated by SLC38A1 in HCC. In addition, we investigated the correlations between SLC38A1 expression and tumor-infiltrating immune cells (TIICs) or immune checkpoints. These analyses demonstrated that SLC38A1 was expressed at higher levels in HCC and associated with an unfavorable prognosis and defective immune infiltration.

2. Materials and Methods

2.1. mRNA Expression and Clinical Data from the TCGA Database. We used The *Cancer* Genome Atlas (TCGA) database to investigate the mRNA expression patterns of SLC38A1 in HCC. We downloaded transcriptome and corresponding clinical data for HCC patients from the Genomic Data Commons Data Portal (https://portal.gdc. cancer.gov/). The TCGA RNAseq data consisted of 424 samples, with 374 samples of HCC tissues and 50 samples of adjacent hepatic tissues. We selected HCC samples with a complete set of clinical information for the subsequent analysis of clinical significance. The clinicopathological characteristics included age, sex, pathological grade, clinical stage, tumor stage (T), lymphatic metastasis (N), distant metastasis (M), survival time, and survival status.

2.2. Protein Expression and Clinical Data from the CPTAC Database. We used the Clinical Proteomic Tumor Analysis Consortium (CPTAC) database to explore the protein expression profiles of SLC38A1 in HCC. The CPTAC database is a centralized data repository of proteomics data sets and clinical data for a variety of cancers (https://proteomics. cancer.gov/data-portal). We downloaded and extracted protein expression data relating to SLC38A1 and corresponding clinical data from the CPTAC-HCC proteome, including 159 samples of tumor tissue and adjacent hepatic tissue. The unshared log-ratio value was defined as the

protein expression value. The clinicopathological characteristics included age, sex, tumor differentiation, medical history of liver cirrhosis, tumor size, tumor thrombus, tumor encapsulation, and survival time.

2.3. The Analysis of Other Online Databases. The Oncomine database combines 715 datasets and 86733 samples into one comprehensive database that aims to help researchers design better experiments and obtain more robust results (https:// www.oncomine.org/) [13]. We performed meta-analysis of SLC38A1 RNA expression using the Oncomine database with a threshold of $p \leq 0.01$ and a fold change (FC) ≥ 1.5. The Hepatocellular Carcinoma Expression Atlas Database (HCCDB) is an online resource for comprehensively annotating liver cancer gene expression and includes 15 public HCC expression datasets from 4000 samples (http://lifeome. net/database/hccdb/home.html) [14]. We used this database to further confirm whether the mRNA expression of SLC38A1 in HCC tissues was higher than that in nontumor tissues. The Kaplan–Meier plotter database offers a convenient way to assess the impact of multiple genes on survival in patients with 21 different cancer types (http://kmplot. com/analysis/) [15]. In the present study, we used this database to validate the correlation of SLC38A1 expression with the prognosis of HCC patients.

2.4. Immunohistochemistry. We retrospectively collected 30 pairs of paraffin-embedded HCC tissues and adjacent nontumor tissue samples from surgeries taking place between May 2019 and December 2020 at the Third Hospital of Hebei Medical University. This study was approved by the Ethics Committee of the Third Hospital of Hebei Medical University and carried out in accordance with the principles of the Declaration of Helsinki. The need for informed consent was waived by the Ethics Committee of the Third Hospital of Hebei Medical University given the retrospective nature of the study.

The paraffin-embedded tissue samples were sectioned, deparaffinized, hydrated, and boiled in a pressure cooker for antigen retrieval. The sections were then incubated with 3% hydrogen peroxide to inactivate endogenous peroxidase activity. Next, the samples were blocked in 10% goat serum and incubated overnight with a rabbit anti-human primary SLC38A1 antibody (Proteintech, China) at 4°C. Next, the sections were incubated with goat anti-rabbit horseradish peroxidase (HRP) conjugated secondary antibody (ZSGB-Bio, China) at 37°C. Finally, the sections were incubated with 3,3′-diaminobenzidine (DAB) and stained with hematoxylin. Two experienced pathologists independently assessed the samples. Each tissue sample was scored according to the intensity of staining and the proportion (%) of tumor cells that were stained. The scores ranged from 0 to 3; a score of 0–1 was considered as a negative stain while a score of 2–3 was considered as a positive stain.

2.5. Gene Set Enrichment Analysis (GSEA). We used GSEA software (version 4.1.0) to explore the potential signaling pathways by which SLC38A1 may be involved in HCC. In

this study, we categorized samples as either high- or low-SLC38A1 phenotypes in accordance with the median value of SLC38A1 expression from the TCGA database. Annotated gene sets (c2.cp.kegg.v7.3.symbols.gmt) were used as internal gene sets. The phenotypic enrichment pathways were sorted based on the nominal p value and normalized enrichment score (NES) [16]. Nominal p value and false discovery rate (FDR) q-value less than 0.05 were considered to be statistically significant.

2.6. Gene Coexpression and GO/KEGG Enrichment Analysis. We screened the genes that were coexpressed with SLC38A1 from the CPTAC database. Those with an absolute value of Pearson's correlation coefficient $|R| \geq 0.4$ and a p value < 0.001 were selected as the screening threshold. Then, we performed Gene Ontology (GO) and Kyoto Encyclopedia of Genes and Genomes (KEGG) enrichment analysis of the coexpression genes by the R package "clusterProfiler" (version 3.18.1) which used multiple databases, including Disease Ontology database, Network of *Cancer* Gene database, Gene Ontology database, KEGG database, and Reactome Pathway database [17]. Before performing enrichment analysis, gene symbol codes were converted to Entrez ID by using human genome annotation package "org.Hs.eg.db." Adjusted p values that were <0.05 were considered to be statistically significant.

2.7. Analysis of the Immune Landscape Related to the Expression Level of SLC38A1. CIBERSORT is a tool for deconvolving the expression matrix of immune cell subtypes based on the principle of linear support vector regression (http://cibersort.stanford.edu/) [18]. Using CIBERSORT analysis, it is possible to estimate the proportion of tumor-infiltrating immune cells (TIICs). In this study, we calculated the proportion of 22 TIICs in all HCC samples from the TCGA dataset. Tumor samples with a p value < 0.05 were chosen for subsequent analysis. Then, we carried out differential and correlation analysis to evaluate the correlation between SLC38A1 expression and TIICs or immune checkpoints. In the differential analysis, we divided the samples into high- and low-SLC38A1 expression groups in line with the median level of SLC38A1 expression. For the correlation analysis, our screening criteria were an $|R| \geq 0$ and p value < 0.05.

2.8. Statistical Analysis. Statistical analyses were performed on the IHC data using SPSS software (version 23.0) and McNemar's test. All statistical analyses from the TCGA and CPTAC datasets were performed with R software (version 4.0.3). The median level of SLC38A1 expression was considered as a cutoff value. The association of clinicopathological characteristics with SLC38A1 expression was analyzed by Wilcoxon's rank sum test or the Kruskal–Wallis rank sum test and logistic regression. The effect of SLC38A1 expression on survival was evaluated by the Kaplan–Meier method, followed by the log-rank test. The effects of SLC38A1 expression and other clinicopathological characteristics on survival were compared by using univariate and multivariate Cox regression. Receiver Operating Characteristic (ROC) curves and the area under the curve (AUC) were used to compare the predictive accuracy of SLC38A1 expression with other clinicopathological characteristics. Correlation analysis of gene expression was evaluated by Spearman's correlation coefficient and statistical significance. A p value or FDR <0.05 was considered to be statistically significant.

3. Results

3.1. The Expression Levels of SLC38A1 Were Upregulated in HCC. The analytical process used in the present study is shown in Figure 1. We first performed a meta-analysis of SLC38A1 mRNA levels from the Oncomine database which included four HCC studies that used the same thresholds as described above [19–21]. Our analyses demonstrated that the mRNA expression of SLC38A1 in the tumor group was significantly higher than that in the nontumor group (Figure 2(a)). Then, we analyzed the mRNA and protein expression of SLC38A1 from the TCGA and CPTAC databases, respectively. Our results showed that both the mRNA and protein expression of SLC38A1 was upregulated in tumor samples when compared to adjacent nontumor samples (Figures 2(b) and 2(c)). Furthermore, the online HCCDB database showed consistent results based on data from the Gene Expression Omnibus (GEO) and the International *Cancer* Genome Consortium (ICGC) datasets. Further details were given in Supplementary Table 1. Moreover, the IHC staining results from 30 paired HCC tissues in our hospital further confirmed the significantly higher protein levels of SLC38A1 in tumor tissues (76.7% vs. 46.7%, $p < 0.05$). Representative immunohistochemical images of SLC38A1 protein expression are shown in Figure 2(d). Collectively, these data indicated that SLC38A1 expression was upregulated in HCC.

3.2. The Upregulation of SLC38A1 Expression Predicted a Worse Prognosis in HCC Patients. First, we evaluated the impact of SLC38A1 expression on survival using the TCGA dataset. We found that high expression levels of SLC38A1 were significantly associated with poor overall survival (OS), progression-free survival (PFS), and disease-specific survival (DSS) ($p = 0.002$, $p = 0.003$, $p = 0.009$, respectively; Figures 3(a) and 3(c)). Then, we used the online Kaplan–Meier plotter database to validate the prognostic value of SLC38A1 in HCC and obtained results that were consistent with the TCGA database (Figures 3(d) and 3(e)). We also used the CPTAC database to further verify the relationship between the expression level of SLC38A1 protein and prognosis; the higher the expression level of SLC38A1, the worse the prognosis for HCC patients ($p = 0.004$, Figure 3(f)).

3.3. The Expression Level of SLC38A1 Was Associated with the Clinicopathological Characteristics of HCC Patients. As shown in Figures 4(a) and 4(c), the upregulated mRNA
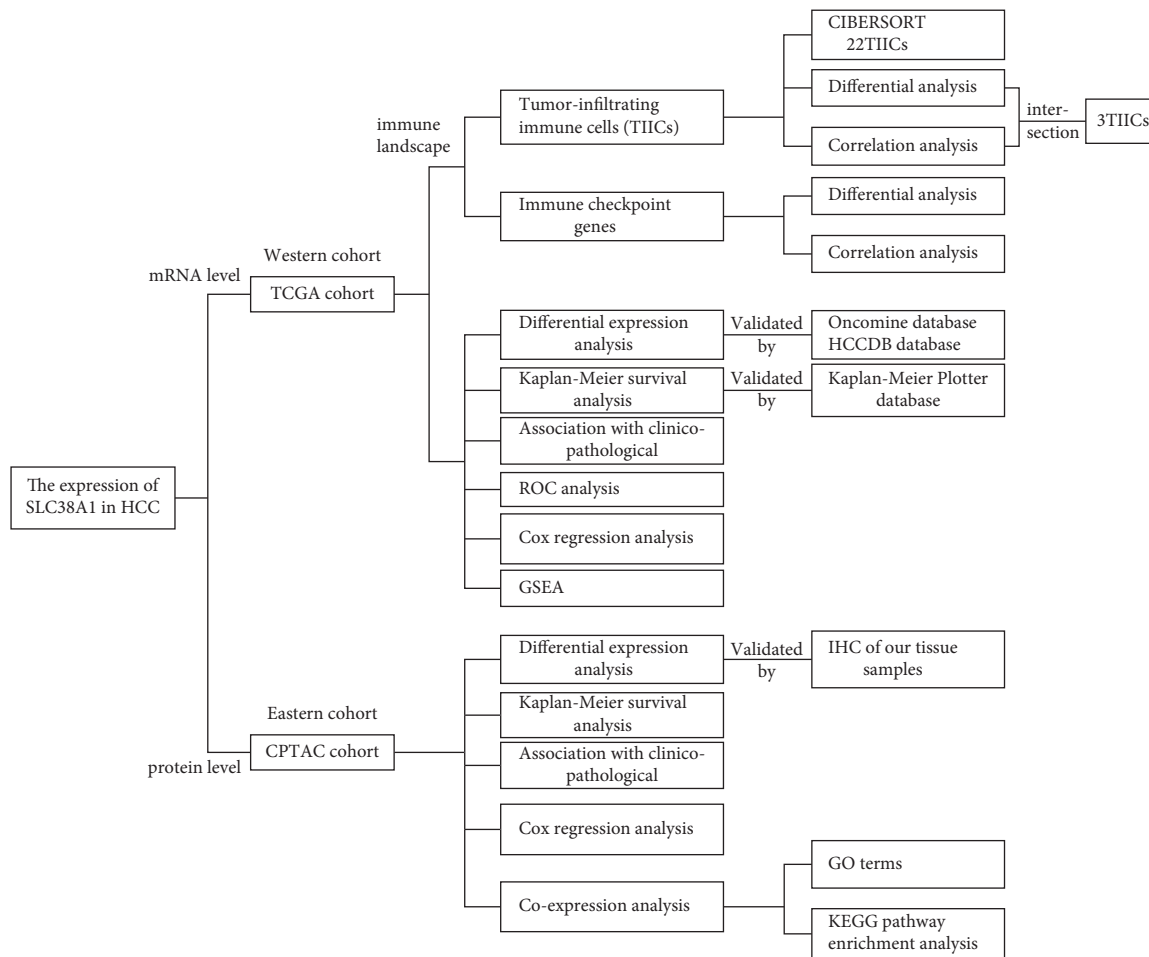
FIGURE 1: Analytical workflow of this study. GSEA, gene set enrichment analysis; GO, gene ontology; HCC, hepatocellular carcinoma; IHC, immunohistochemistry; KEGG, Kyoto Encyclopedia of Genes and Genomes; ROC, receiver operating characteristic.

expression of SLC38A1 was significantly correlated with the pathological grade of tumors ($p = 8.124\text{E-}04$), clinical stage ($p = 0.001$), and T stage ($p = 6.295\text{E-}04$), based on the TCGA database. Figures 4(d) and 4(f) show that high protein levels of SLC38A1 were significantly associated with tumor differentiation ($p = 0.028$), tumor size ($p = 0.026$), and tumor thrombus ($p = 0.003$), as based on the CPTAC database. Univariate logistic regression analysis further showed that the upregulation of SLC38A1 expression in HCC was significantly correlated with high pathological grade, clinical stage, T stage, tumor differentiation, and tumor thrombus (Tables 1 and 2). These results further revealed that the upregulation of SLC38A1 expression was significantly associated with poor clinicopathological characteristics and suggested that HCC patients with high levels of SLC38A1 expression are more likely to progress to advanced stages than those with low levels of SLC38A1 expression.

3.4. SLC38A1 Represents an Independent Prognostic Predictor for Patients with HCC. As shown in Figures 5(a) and 5(b), the univariate cox regression analysis showed that high

levels of SLC38A1 expression were significantly associated with a poor OS (hazard ration [HR]: 1.482, 95% confidence interval [CI]: 1.232–1.784, $P < 0.001$; HR: 2.305, 95% CI:1.466–3.623, $P < 0.001$, from the TCGA and CPTAC databases, respectively). Although other clinicopathological characteristics including clinical stage, T stage, M stage, differentiation, tumor size, and tumor thrombus, were also related to OS, as based on univariate cox regression analysis, only the expression levels of SLC38A1 remained associated with OS when we performed multivariate cox regression analysis (HR: 1.397, 95% CI: 1.144–1.705, $P < 0.001$; HR: 1.766, 95%CI: 1.061–2.940, $P = 0.029$, respectively), as shown in Figures 5(c) and 5(d). Therefore, our univariate and multivariate Cox regression analysis demonstrated that the expression level of SLC38A1 was an independent prognostic factor for HCC patients. To further evaluate the predictive accuracy of SLC38A1 expression, we performed ROC. Compared to other predictive factors (age, sex, tumor pathological grade, clinical stage, T stage, N stage and M stage), the AUC for SLC38A1 expression was greater (AUC = 0.734, Figure 6).

Comparison of SLC38A1 Across 4 Analyses

over-expression

Median Rank	p–Value	Gene
2287.0	9.03E-4	SLC38A1

Legend

1. Hepatocellular Carcinoma vs. Normal
Chen Liver, Mol Biol Cell, 2002

2. Hepatocellular Carcinoma vs. Normal
Roessoer Liver, Cancer Res, 2010

3. Hepatocellular Carcinoma vs. Normal
Roessoer Liver 2, Cancer Res, 2010

4. Hepatocellular Carcinoma vs. Normal
Wurmbach Liver, Hepatology, 2007

1 5 10 25   25 10 5 1   Not measured

%

The rank for a gene is the median rank for that gene across each of the analyses.
The p-Value for a gene is its p-Value for the median-ranked analysis.

(a)

(b)

(c)

(d)

FIGURE 2: The expression levels of SLC38A1 in HCC. (a) Meta-analysis of SLC38A1 expression levels in HCC tissues relative to nontumor tissues, as determined by the Oncomine database. (b) Comparison of SLC38A1 mRNA expression level in HCC tissues and adjacent nontumor tissue, as determined by the TCGA database. (c) Comparison of SLC38A1 protein expression levels in HCC tissues and adjacent nontumor tissues, as determined by the CPTAC database. (d) Representative immunohistochemical images of SLC38A1 protein expression in adjacent nontumor tissues and HCC tissues from our hospital (scale bars = 200 μm).
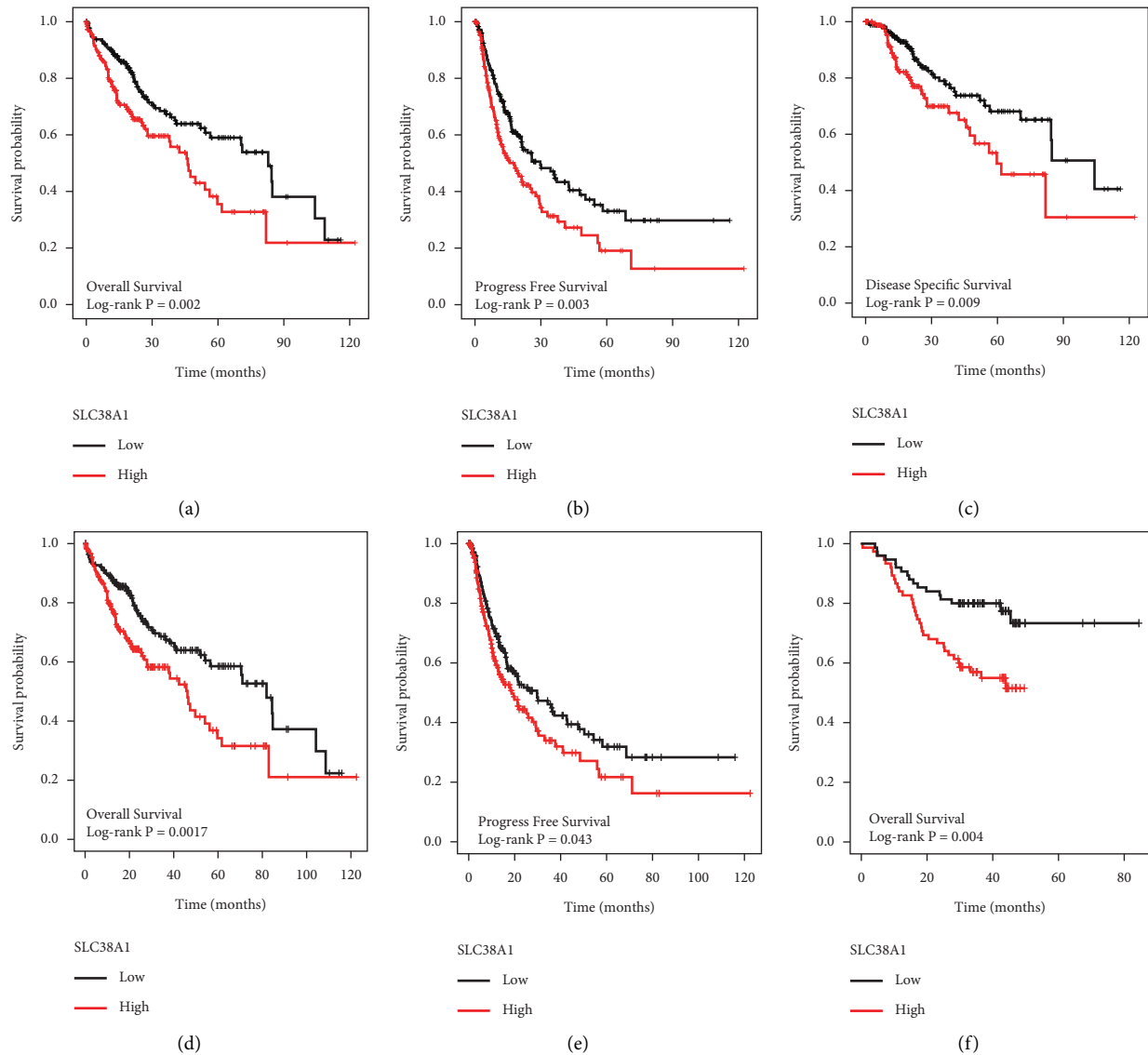
FIGURE 3: The effect of SLC38A1 expression on survival in HCC patients. (a) OS in TCGA. (b) PFS in TCGA. (c) DSS in TCGA. (d) OS in K-M plotter. (e) PFS in K-M plotter. (f) OS in CPTAC. OS, overall survival; PFS, progression-free survival; DSS, disease-specific survival.

3.5. The Potential Molecular Mechanisms That Might Be Mediated by SLC38A1 in HCC

3.5.1. GSEA.
We performed GSEA between high- and low-SLC38A1 expression phenotypes to explore potential signaling pathways based on the TCGA dataset. According to NES and FDR values, we selected significantly enriched KEGG signaling pathways. We identified a total of 85 signaling pathways that were differentially enriched in the high expression SLC38A1 phenotype (Supplementary Table 2). The most typically enriched signaling pathways are shown in Figure 7; analysis showed that multiple pathways that are related to tumor and immunity were differentially enriched in the high expression SLC38A1 phenotype.

3.5.2. Gene Coexpression and GO/KEGG Enrichment Analysis.
To further explore the potential mechanisms that might be mediated by SLC38A1 in HCC at the protein level, we conducted coexpression and GO/KEGG enrichment analysis, as based on the CPTAC database. According to a threshold set by |R| and p values, a total of 158 genes were found to be coexpressed with SLC38A1 and selected for subsequent GO/KEGG enrichment analysis (Supplementary Table 3). GO annotation revealed that 142 biological processes (BP), 48 molecular functions (MF), and 19 cellular component (CC) terms were significantly enriched (adjusted p value < 0.05). The top 10 GO terms are shown in Figure 8(a). These data suggested that the genes that were coexpressed with SLC38A1 may have a regulatory effect on
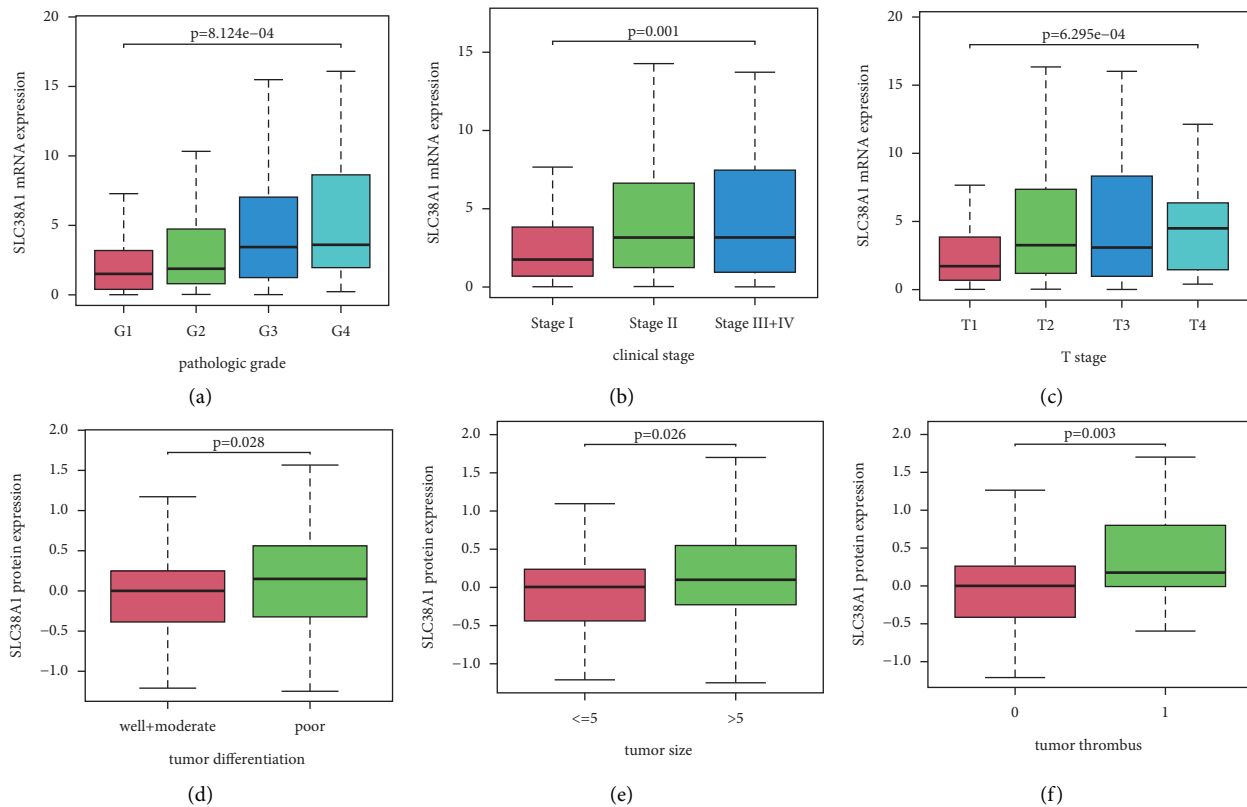
FIGURE 4: The association between SLC38A1 expression and clinicopathological characteristics. (a) Pathological grade, as determined from the TCGA database. (b) Clinical stage, as determined from the TCGA database. (c) T stage, as determined from the TCGA database. (d) Tumor differentiation, as determined from the CPTAC database. (e) Tumor size, as determined from the CPTAC database. (f) Tumor thrombus, as determined from the CPTAC database. The number of patients in the TCGA database that were in stage IV was very small; thus, patients with stages III and IV were pooled together for analysis. There was one patient in the well differentiation group derived from the CPTAC database; therefore, patients in the well differentiation and moderate differentiation groups were pooled for analysis.

HCC via mitochondrial matrix, pre-ribosome, oxidoreductase activity, and small molecule catabolic process. In addition, we identified 26 KEGG pathways that were significantly enriched (adjusted p value < 0.05), as shown in Figure 8(b). These highly enriched pathways included tryptophan metabolism, glycine, serine and threonine metabolism, valine, leucine and isoleucine degradation, and the PPAR signaling pathway.

3.6. The Expression of SLC38A1 Was Correlated with Tumor-Infiltrating Immune Cells (TIICs) and Immune Checkpoint Genes. To analyze the correlation between the expression levels of SLC38A1 and TIICs, we first calculated the proportion of 22 types of TIICs in HCC samples by CIBER-SORT analysis (Figure 9). As shown in Figures 10(a) and 10(b), we obtained 4 and 6 types of TIICs that were significantly associated with SLC38A1 expression, as based on the differential and correlation analysis, respectively. As shown in Venn diagrams (Figure 10(c)), we obtained 3 types of TIICs (CD8+ T cell, Macrophages M0, and Neutrophils) that were associated with SLC38A1 expression, as determined by differential and correlation analysis. To be specific, high expression levels of SLC38A1 were inversely proportional to the numbers of CD8+ T cells and directly

proportional to the numbers of macrophages M0 and neutrophils. Similarly, we used the differential analysis and correlation analysis to evaluate the relationships between SLC38A1 expression and immune checkpoints (PD-1, PD-L1, and CTLA-4). These analyses indicated that high expression levels of SLC38A1 were directly proportional to PD-1, PD-L1, and CTLA-4 (Figure 11).

4. Discussion

As a principal transporter of glutamine, SLC38A1 is selectively and physiologically expressed in normal human brain and placental tissues [8]. Studies have shown that SLC38A1 is overexpressed in malignant tumors and can promote the proliferative, invasive, and metastatic potentials of tumor cells [9–12]. However, prior to this study, the prognostic significance of SLC38A1 for patients with HCC was unknown. In the present study, we investigated the clinical significance of SLC38A1 by analyzing RNAseq and proteomic data. These public databases, along with IHC analysis of our own tissue samples, confirmed that the expression of SLC38A1 was upregulated in HCC. Both the mRNA and protein expression of SLC38A1 were associated with the clinicopathological characteristics and outcomes of HCC patients. In addition, we explored the correlations between

TABLE 1: The association between SLC38A1 expression and clinicopathological characteristics (logistic regression, TCGA database).

Clinicopathological characteristics	Total (N)	Odds ratio for SLC38A1 mRNA expression	p value
Age (years)			
>60 vs. ≤60	370	0.823 (0.546–1.237)	0.349
Sex			
Male vs. female	371	1.237 (0.801–1.915)	0.337
Pathological grade			
Grade II vs. grade I	232	1.527 (0.821–2.911)	0.187
Grade III vs. grade I	177	3.242 (1.683–6.411)	0.001*
Grade IV vs. grade I	67	3.789 (1.053–15.750)	0.048*
Clinical stage			
Stage II vs. stage I	257	2.104 (1.247–3.581)	0.006*
Stage III + IV[a] vs. stage I	261	2.380 (1.417–4.041)	0.001*
Tumor stage (T)			
T2 vs. T1	275	2.185 (1.320–3.647)	0.003*
T3 vs. T1	261	2.449 (1.435–4.233)	0.001*
T4 vs. T1	194	3.486 (1.091–13.260)	0.044*
Lymphatic metastasis			
Positive vs. negative	256	3.048 (0.384–62.071)	0.337
Distant metastasis			
Positive vs. negative	270	1.685E-07 (NA-2.860 E + 29)	0.983

Note. [a]Since the number of patients with stage IV was very small, we pooled patients with stage III and stage IV for analysis. *$p < 0.05$.

TABLE 2: The association between SLC38A1 expression and clinicopathological characteristics (logistic regression, CPTAC database).

Clinicopathological characteristics	Total (N)	Odds ratio for SLC38A1 protein expression	p value
Age (years)			
>60 vs. ≤60	152	0.523 (0.252–1.061)	0.076
Sex			
Male vs. female	152	1.181 (0.530–2.657)	0.684
Differentiation			
Poor vs. well + moderate[b]	152	2.619 (1.346–5.206)	0.005*
Cirrhosis			
Positive vs. negative	152	1.284 (0.642–2.586)	0.480
Size (cm)			
>5 vs. ≤5	152	1.447 (0.765–2.753)	0.257
Thrombus			
Positive vs. negative	152	2.237 (1.051–4.935)	0.040*
Lymphatic metastasis			
Positive vs. negative	152	1 (0.039–25.600)	1.000
Encapsulation			
Positive vs. negative	152	0.939 (0.466–1.887)	0.859

Note. [b]There was only one patient in the well differentiation group. Therefore, patients with well and moderate differentiation were pooled for analysis; *$p < 0.05$.

SLC38A1 expression and TIICs or immune checkpoints; these data suggested that the upregulated expression of SLC38A1 was associated with defective immune infiltration in HCC.

In the present study, we combined results from public databases with our own data acquired from IHC of tissue samples and confirmed that the expression levels of SLC38A1 were upregulated in HCC; this was consistent with the findings of previous studies [9, 22]. However, neither of these studies evaluated the clinical and prognostic significance of SLC38A1 expression in HCC patients. In the present study, we found that the upregulation of SLC38A1 expression predicted a worse prognosis for HCC patients.

Similarly, other studies have indicated that high levels of SLC38A1 expression represented an unfavorable prognostic indicator for human osteosarcoma, cholangiocarcinoma, gastric cancer, and acute myeloid leukemia [9–12, 23]. In addition, our study illustrated that the expression levels of SLC38A1 were positively associated with clinical stage, T stage, pathological grade, tumor size, and tumor thrombus, but were not significantly associated with M stage or N stage. Due to the small numbers of M1 and N1 patients in the TCGA database, it was not possible to define the precise association of SLC38A1 expression with lymphatic and distant metastasis. Therefore, it is necessary to perform further studies with larger sample sizes to confirm this

	pvalue	Hazard ratio
age	0.591	1.005(0.987–1.023)
sex	0.301	0.780(0.487–1.249)
grade	0.914	1.017(0.746–1.387)
stage	<0.001	1.865(1.456–2.388)
T	<0.001	1.804(1.434–2.270)
M	0.023	3.850(1.207–12.281)
N	0.328	2.022(0.494–8.276)
SLC38A1	<0.001	1.482(1.232–1.784)

(a)

	pvalue	Hazard ratio
Sex	0.366	0.741(0.386–1.421)
Age	0.058	0.976(0.952–1.001)
Differentiation	0.003	2.335(1.329–4.103)
Cirrhosis	0.666	1.150(0.609–2.172)
Size	<0.001	1.161(1.097–1.228)
Thrombus	0.014	2.112(1.167–3.823)
Encapsulation	0.987	1.005(0.540–1.870)
SLC38A1	<0.001	2.305(1.466–3.623)

(b)

	pvalue	Hazard ratio
age	0.370	1.009(0.990–1.029)
sex	0.788	1.073(0.642–1.795)
grade	0.914	1.019(0.728–1.426)
stage	0.842	1.112(0.393–3.141)
T	0.396	1.506(0.585–3.876)
M	0.284	2.137(0.533–8.564)
N	0.833	1.216(0.199–7.435)
SLC38A1	0.001	1.397(1.144–1.705)

(c)

	pvalue	Hazard ratio
Sex	0.248	0.671(0.340–1.322)
Age	0.192	0.982(0.957–1.009)
Differentiation	0.011	2.167(1.194–3.932)
Cirrhosis	0.363	1.363(0.700–2.653)
Size	<0.001	1.146(1.076–1.220)
Thrombus	0.900	0.958(0.492–1.866)
Encapsulation	0.501	0.803(0.424–1.521)
SLC38A1	0.029	1.766(1.061–2.940)

(d)

FIGURE 5: Univariate and multivariate Cox regression analysis of SLC38A1 expression and other clinicopathological characteristics. (a) Univariate cox regression analysis, as based on the TCGA database. (b) Univariate cox regression analysis, as based on the CPTAC database. (c) Multivariate cox regression analysis, as based on the TCGA database. (d) Multivariate cox regression analysis, as based on the CPTAC database.

finding. Moreover, our univariate and multivariate Cox regression analysis indicated that SLC38A1 expression was an independent predictor for prognosis in HCC patients. More importantly, the predictive accuracy of SLC38A1 expression was slightly better than that of the clinical stage. Collectively, these results strongly suggested that SLC38A1 expression is a good prognostic biomarker for HCC.

In order to further explore the potential mechanisms that might be mediated by SLC38A1 in HCC, we performed GSEA, coexpression analysis, and GO and KEGG enrichment analysis. GSEA results demonstrated that a phenotype characterized by high expression levels of SLC38A1 showed enrichment with tumor and immune-related pathways, including the JAK-STAT, Wnt, MAPK, mTOR ,and TGF-β signaling pathways. KEGG pathway enrichment analyses of genes that were coexpressed with SLC38A1 further indicated that SLC38A1 was involved in multiple metabolic pathways, the most important of which was amino acid metabolism; these findings were similar to those of a previous report.[5] Therefore, we concluded that SLC38A1 is involved in pathways related to substance metabolism, tumors, and immunity. However, the specific regulatory mechanisms involved needs to be investigated further.

Another major finding of this study was that the expression levels of SLC38A1 correlated with TIICs in HCC. Previous studies have shown that tumor-infiltrating lymphocytes can serve as independent predictors of survival in cancer patients [24, 25]. For this reason, we explored the correlation between SLC38A1 expression and immune infiltration in HCC. It is well established that CD8+ T cells are the main effector cells against tumors and stimulate cell death via the Fas-Fas ligand pathway or by releasing perforin granules to eliminate tumors [26]. A recent study confirmed that the number of CD8+T cells is closely associated with the prognosis of patients with a variety of tumors [27]. Furthermore, recent studies have shown that neutrophils can stimulate tumor angiogenesis and mediate immune suppression mechanisms to promote tumor growth and metastasis, and also represents a biomarker of tumor prognosis [28, 29]. In the present study, we found that high expression levels of SLC38A1 were inversely proportional to CD8+ T cells and directly proportional to macrophages M0 and neutrophils; this explained why high levels of SLC38A1 can predict a poor prognosis, at least in part. A series of immune checkpoints, including CTLA-4, PD-1, PD-L1, and lymphocyte activation gene 3 (LAG-3), have been
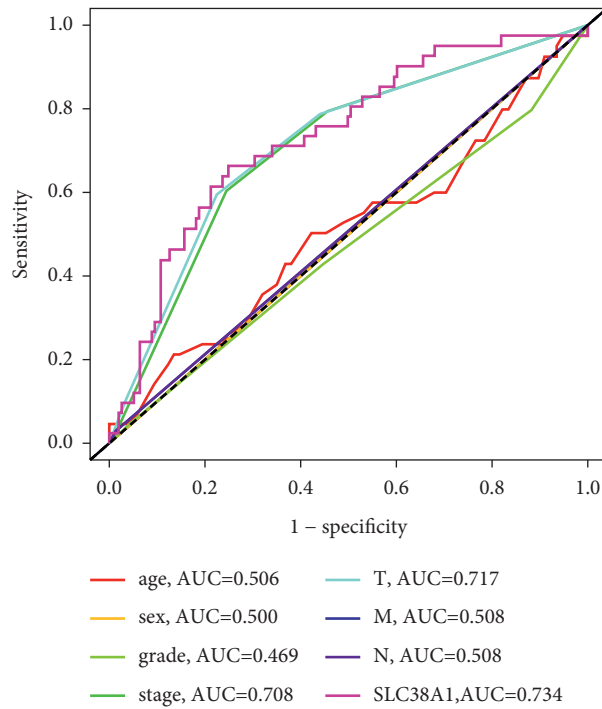
FIGURE 6: The AUCs of a range of prognostic predictors (including age, sex, grade, tumor stage, T stage, M stage, N stage, and SLC38A1). AUC, area under the curve.
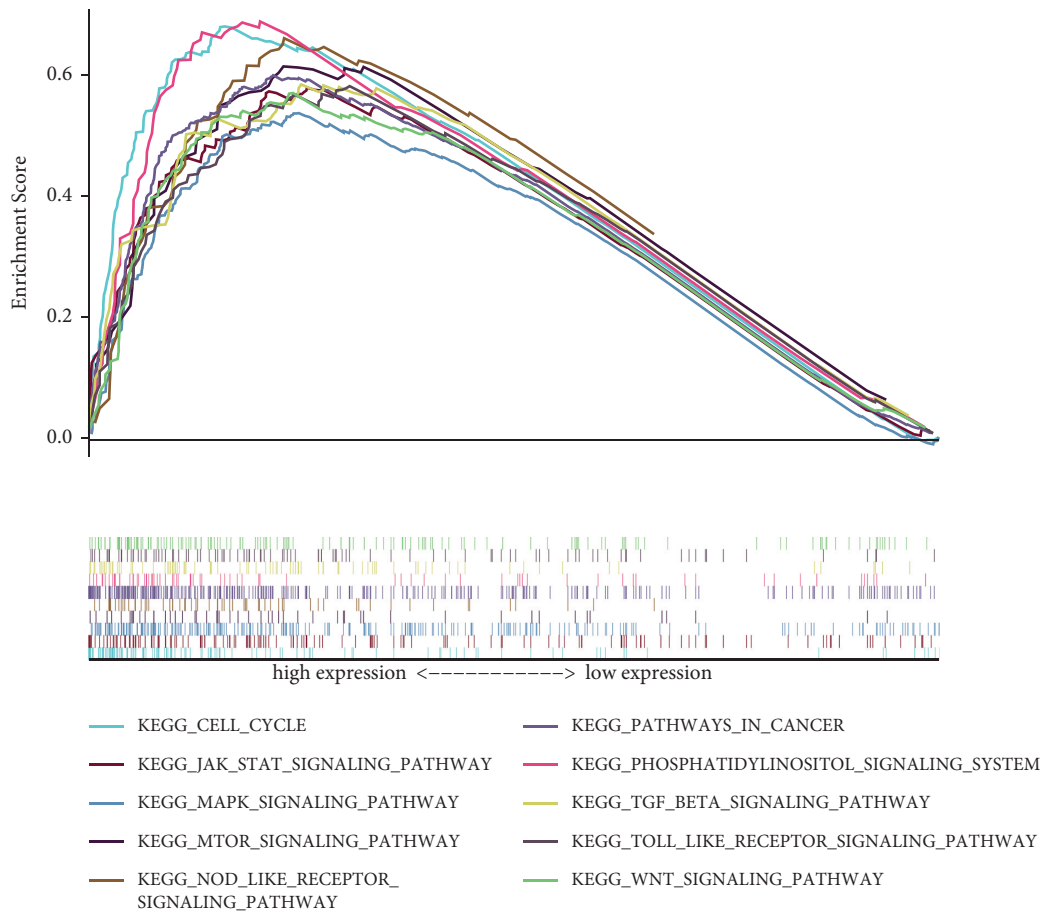
FIGURE 7: GSEA analysis of KEGG signaling pathways activated by high expression of SLC38A1 in HCC. GSEA, gene set enrichment analysis; KEGG, Kyoto Encyclopedia of Genes and Genomes.

(a)

(b)
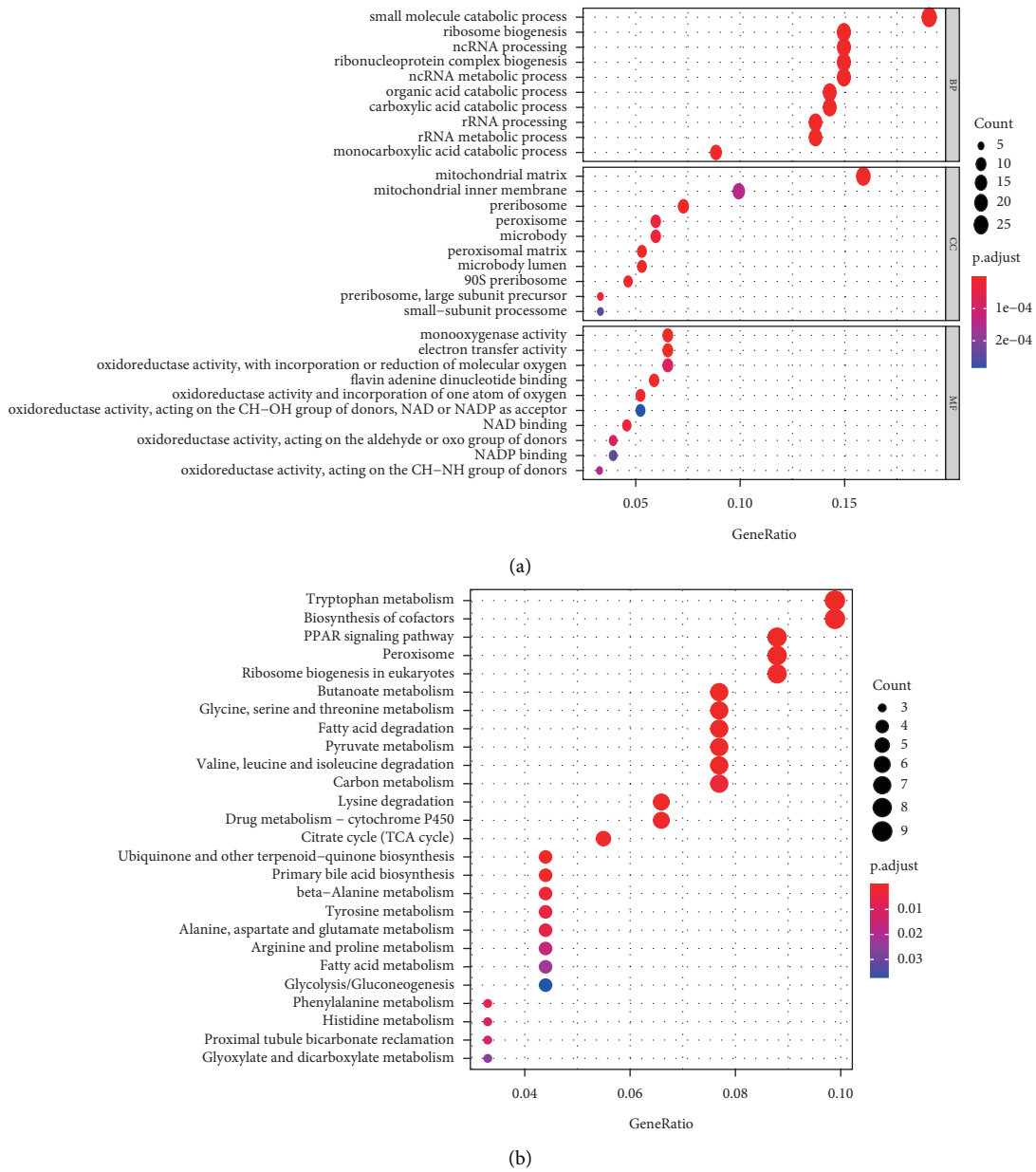
FIGURE 8: The top 10 GO terms and KEGG pathways related to coexpressed genes with SLC38A1. (a) GO terms (including BP, CC, and MF). (b) KEGG pathways. BP, biological process; CC, cellular component; MF, molecular function; GO, gene ontology; KEGG, Kyoto Encyclopedia of Genes and Genomes.

confirmed to be involved in the induction and maintenance of immune tolerance in HCC [30–32]. Moreover, immune checkpoint inhibitors have shown therapeutic potential for patients with advanced HCC in clinical trials [33, 34]. Therefore, we investigated the association between SLC38A1 expression and immune checkpoints and found that high expression levels of SLC38A1 were directly proportional to PD-1, PD-L1, and CTLA-4. This indicated that the poor outcomes of HCC patients with high levels of SLC38A1 expression may be attributable to the immunosuppressive microenvironment. Thus, we considered that SLC38A1 may have a potential impact on tumor immunology.

The main advantage of this study is that we comprehensively analyzed the prognostic significance of SLC38A1 expression at the RNA and protein levels; previous prognostic biomarkers based on bioinformatics mining were mainly focused on RNA levels. Furthermore, our study population included not only European and American populations but also Asian populations. Collectively, these factors increase the reliability and applicability of SLC38A1 as a prognostic biomarker for HCC patients. However, this study still has certain limitations that need to be considered. Firstly, there were clear differences in clinical characteristics between the
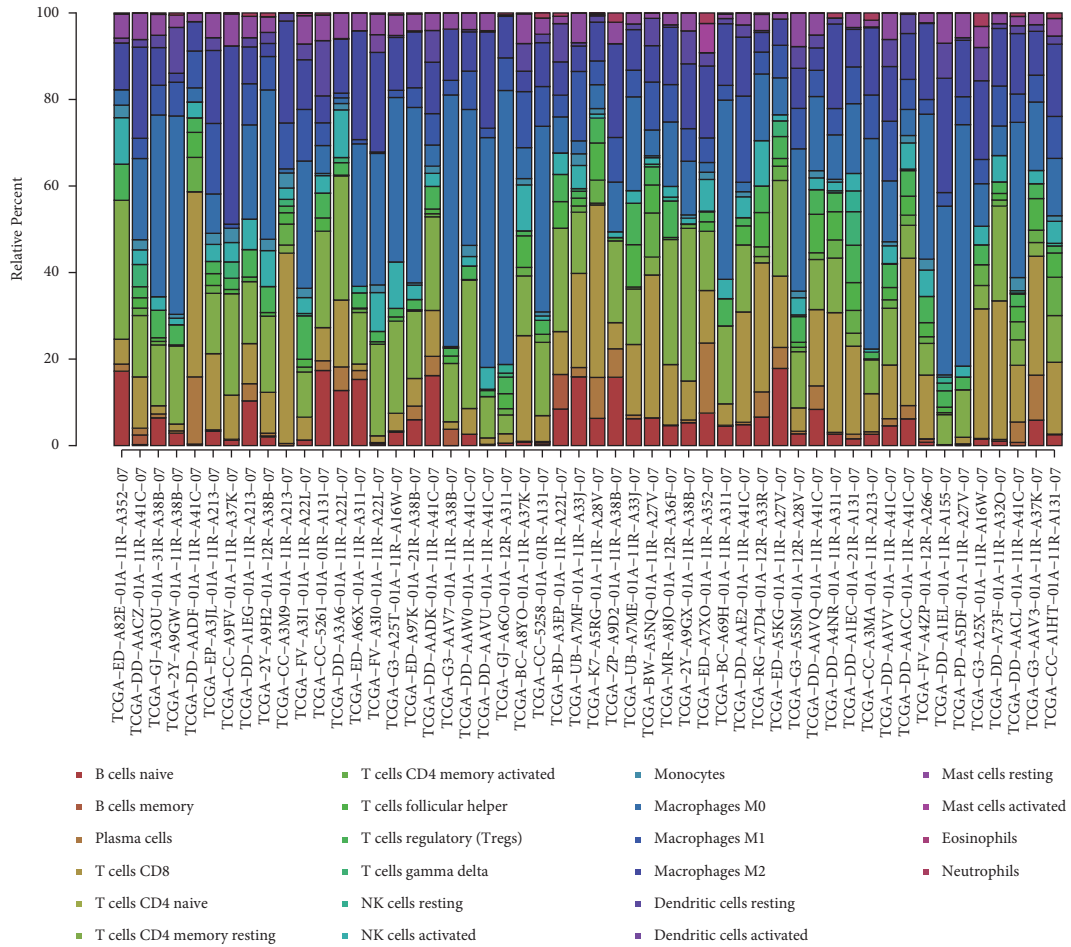
FIGURE 9: The proportion of 22 types of TIICs in HCC tumor samples. TIICs, tumor-infiltrating immune cells.

(a)
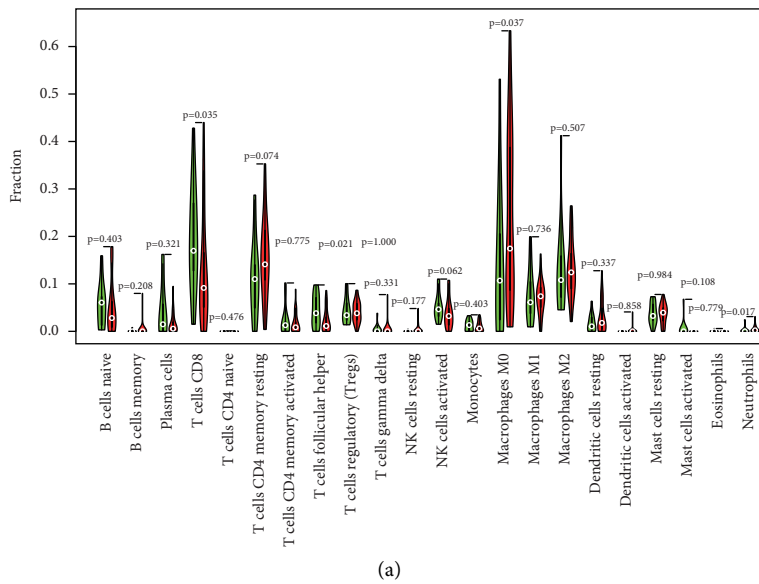
FIGURE 10: Continued.
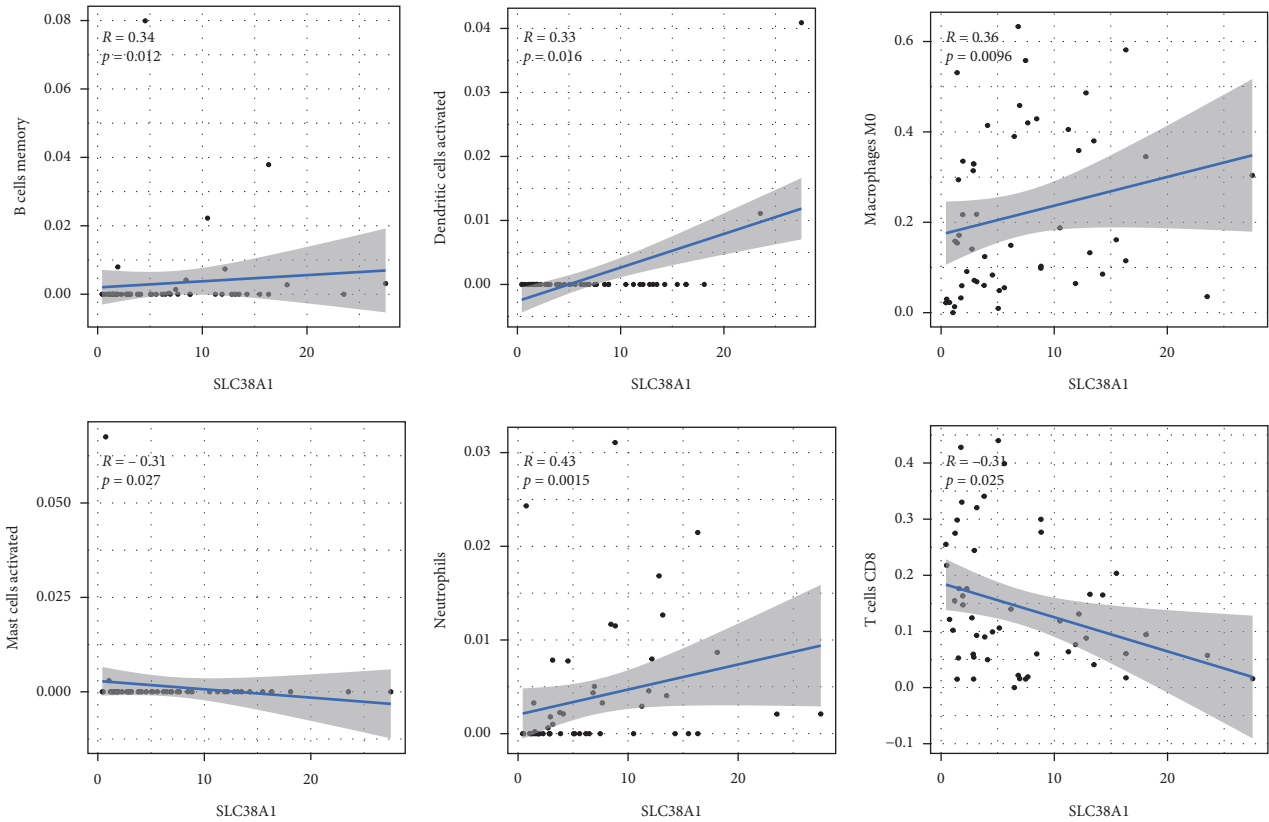
(b)
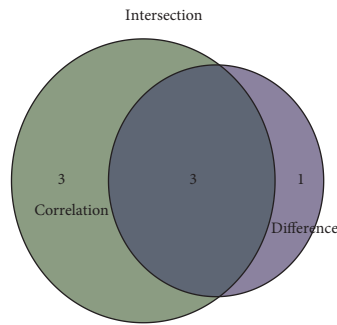
(c)

Figure 10: Correlation of SLC38A1 expression with TIICs. (a) Differential analysis of 22 TIICs between HCC tumor samples with high- and low-SLC38A1 expression levels. (b) Correlation analysis between SLC38A1 expression and the proportion of 6 TIICs ($p < 0.05$). (c) Venn diagrams showing 3 TIICs that were associated with the expression levels of SLC38A1, as determined by differential and correlation analysis. TIICs, tumor-infiltrating immune cells.
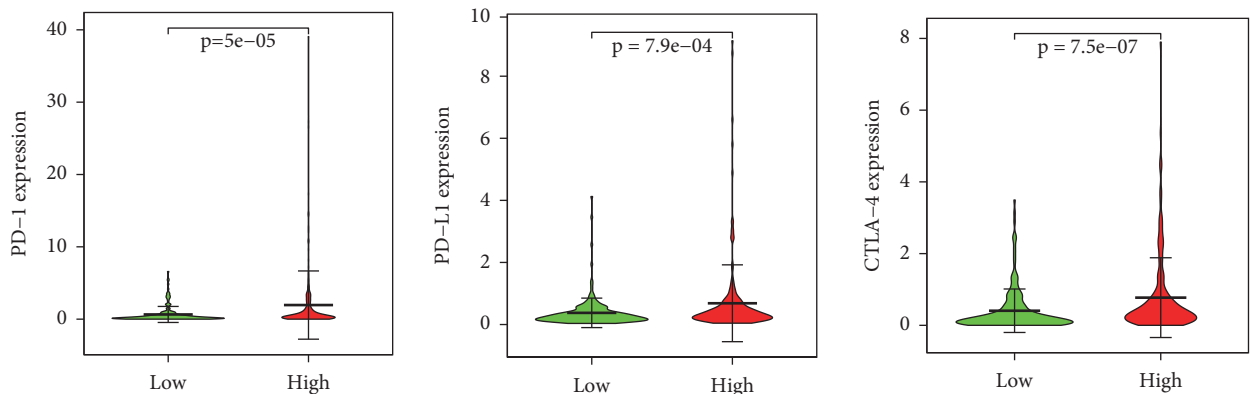
(a)

Figure 11: Continued.

(b)
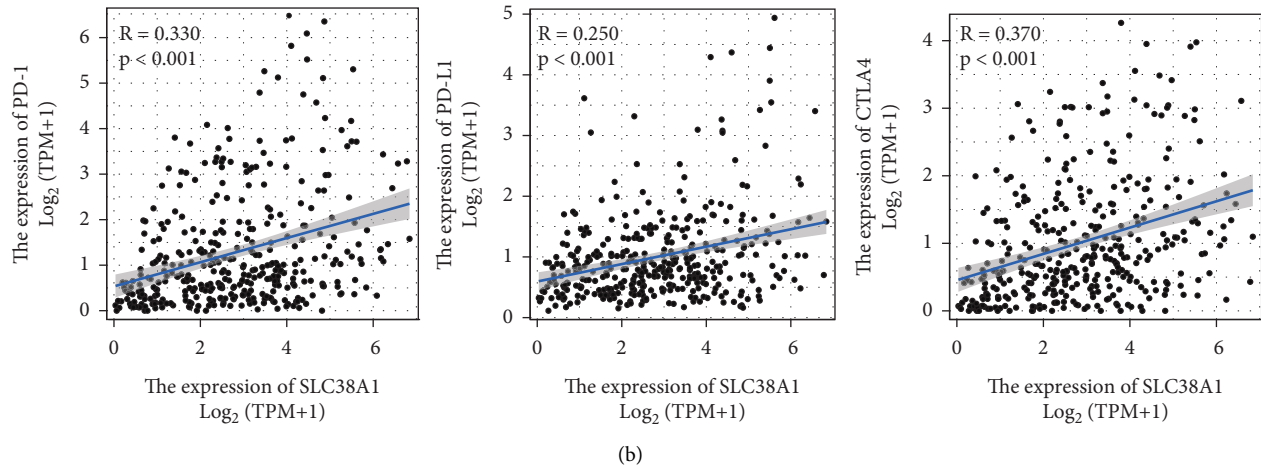
Figure 11: Correlation between SLC38A1 expression and immune checkpoint genes (PD-1, PD-L1, and CTLA-4). (a) Differential analysis of immune checkpoint genes with high and low expression levels of SLC38A1. (b) Correlation analysis between SLC38A1 expression and immune checkpoint genes.

TCGA and CPTAC databases. Secondly, the specific relationship between SLC38A1 expression and tumor immune infiltration requires further investigation.

5. Conclusions

In summary, we systematically analyzed the clinicopathological significance of SLC38A1 expression at the RNA and protein levels in HCC. Our study demonstrated that higher levels of SLC38A1 expression were associated with disease progression and a worse prognosis, as well as impaired immune infiltration in HCC.

Data Availability

The dataset of the public database can be found from the following websites: The *Cancer* Genome Atlas (TCGA) database: https://portal.gdc.cancer.gov/; The Clinical Proteomic Tumor Analysis Consortium (CPTAC) database: https://proteomics.cancer.gov/data-portal; The Oncomine database: https://www.oncomine.org/; The Hepatocellular Carcinoma Expression Atlas (HCCDB) database: http://lifeome.net/database/hccdb/home.html); and The Kaplan–Meier plotter database: http://kmplot.com/analysis/.

Disclosure

Yun Liu and Yong Yang should be considered co-first authors.

Conflicts of Interest

The authors declare that there are no conflicts of interest regarding the publication of this study.

Acknowledgments

Supplementary Materials

Supplementary Table 1: details of GEO series and ICGC dataset from the HCCDB database. Supplementary Table 2: gene sets enriched in phenotype high. Supplementary Table 3: coexpression genes of SLC38A1. (*Supplementary Materials*)

References

[1] F. Bray, J. Ferlay, I. Soerjomataram, R. L. Siegel, L. A. Torre, and A. Jemal, "Global cancer statistics 2018: GLOBOCAN estimates of incidence and mortality worldwide for 36 cancers in 185 countries," *CA: A Cancer Journal for Clinicians*, vol. 68, no. 6, pp. 394–424, 2018.

[2] J. L. Petrick, S. P. Kelly, S. F. Altekruse, K. A. McGlynn, and P. S. Rosenberg, "Future of hepatocellular carcinoma incidence in the United States forecast through 2030," *Journal of Clinical Oncology*, vol. 34, no. 15, pp. 1787–1794, 2016.

[3] M. Omata, A.-L. Cheng, N. Kokudo et al., "Asia-Pacific clinical practice guidelines on the management of hepatocellular carcinoma: a 2017 update," *Hepatology International*, vol. 11, no. 4, pp. 317–370, 2017.

[4] S. Liu, W. Zhao, X. li et al., "AGTRAP is a prognostic biomarker correlated with immune infiltration in hepatocellular carcinoma," *Frontiers in Oncology*, vol. 11, Article ID 713017, 2021.

[5] P. Kandasamy, G. Gyimesi, Y. Kanai, and M. A. Hediger, "Amino acid transporters revisited: new views in health and disease," *Trends in Biochemical Sciences*, vol. 43, no. 10, pp. 752–789, 2018.

[6] H. B. Schiöth, S. Roshanbin, M. G. A. Hägglund, and R. Fredriksson, "Evolutionary origin of amino acid transporter families SLC32, SLC36 and SLC38 and physiological, pathological and therapeutic aspects," *Molecular Aspects of Medicine*, vol. 34, no. 2-3, pp. 571–585, 2013.

[7] B. Mackenzie and J. D. Erickson, "Sodium-coupled neutral amino acid (system N/A) transporters of the SLC38 gene family," *Pflugers Archiv European Journal of Physiology*, vol. 447, no. 5, pp. 784–795, 2004.

[8] N. King, H. Lin, and M.-S. Suleiman, "Oxidative stress increases SNAT1 expression and stimulates cysteine uptake in freshly isolated rat cardiomyocytes," *Amino Acids*, vol. 40, no. 2, pp. 517–526, 2011.

[9] N. Kondoh, N. Imazeki, M. Arai et al., "Activation of a system a amino acid transporter, ATA1/SLC38A1, in human hepatocellular carcinoma and preneoplastic liver tissues," *International Journal of Oncology*, vol. 31, no. 1, pp. 81–87, 2007.

[10] M. Wang, Y. Liu, W. Fang et al., "Increased SNAT1 is a marker of human osteosarcoma and potential therapeutic target," *Oncotarget*, vol. 8, no. 45, pp. 78930–78939, 2017.

[11] W.-l. Yu, W.-m. Cong, Y. Zhang, Y. Chen, F. Wang, and G. Yu, "Overexpression of ATA1/SLC38A1 predicts future recurrence and death in Chinese patients with hilar cholangiocarcinoma," *Journal of Surgical Research*, vol. 171, no. 2, pp. 663–668, 2011.

[12] J. Xie, P. Li, H.-f. Gao, J.-x. Qian, L.-Y. Yuan, and J.-j. Wang, "Overexpression of SLC38A1 is associated with poorer prognosis in Chinese patients with gastric cancer," *BMC Gastroenterology*, vol. 14, no. 1, p. 70, 2014.

[13] D. R. Rhodes, S. Kalyana-Sundaram, V. Mahavisno et al., "Oncomine 3.0: genes, pathways, and networks in a collection of 18,000 cancer gene expression profiles," *Neoplasia*, vol. 9, no. 2, pp. 166–180, 2007.

[14] Q. Lian, S. Wang, G. Zhang et al., "HCCDB: a database of hepatocellular carcinoma expression atlas," *Genomics, Proteomics & Bioinformatics*, vol. 16, no. 4, pp. 269–275, 2018.

[15] Á. Nagy, G. Munkácsy, and B. Győrffy, "Pancancer survival analysis of cancer hallmark genes," *Scientific Reports*, vol. 11, no. 1, Article ID 6047, 2021.

[16] A. Subramanian, P. Tamayo, V. K. Mootha et al., "Gene set enrichment analysis: a knowledge-based approach for interpreting genome-wide expression profiles," *Proceedings of the National Academy of Sciences*, vol. 102, no. 43, pp. 15545–15550, 2005.

[17] G. Yu, L.-G. Wang, Y. Han, and Q.-Y. He, "ClusterProfiler: an R package for comparing biological themes among gene clusters," *OMICS: A Journal of Integrative Biology*, vol. 16, no. 5, pp. 284–287, 2012.

[18] A. M. Newman, C. L. Liu, M. R. Green et al., "Robust enumeration of cell subsets from tissue expression profiles," *Nature Methods*, vol. 12, no. 5, pp. 453–457, 2015.

[19] S. Roessler, H.-L. Jia, A. Budhu et al., "A unique metastasis gene signature enables prediction of tumor relapse in early-stage hepatocellular carcinoma patients," *Cancer Research*, vol. 70, no. 24, pp. 10202–10212, 2010.

[20] X. Chen, S. T. Cheung, S. So et al., "Gene expression patterns in human liver cancers," *Molecular Biology of the Cell*, vol. 13, no. 6, pp. 1929–1939, 2002.

[21] E. Wurmbach, Y.-b. Chen, G. Khitrov et al., "Genome-wide molecular profiles of HCV-induced dysplasia and hepatocellular carcinoma," *Hepatology*, vol. 45, no. 4, pp. 938–947, 2007.

[22] Q. Su and H. Wang, "Long non-coding RNA 01559 mediates the malignant phenotypes of hepatocellular carcinoma cells through targeting miR-511," *Clinics and Research in Hepatology and Gastroenterology*, vol. 45, no. 2, Article ID 101648, 2021.

[23] Y. Li, H. Shao, Z. Da, J. Pan, and B. Fu, "High expression of SLC38A1 predicts poor prognosis in patients with de novo

[24] J. C. Kong, G. R. Guerra, T. Pham et al., "Prognostic impact of tumor-infiltrating lymphocytes in primary and metastatic colorectal cancer: a systematic review and meta-analysis," *Diseases of the Colon & Rectum*, vol. 62, no. 4, pp. 498–508, 2019.

[25] F. Azimi, R. A. Scolyer, P. Rumcheva et al., "Tumor-infiltrating lymphocyte grade is an independent predictor of sentinel lymph node status and survival in patients with cutaneous melanoma," *Journal of Clinical Oncology*, vol. 30, no. 21, pp. 2678–2683, 2012.

[26] P. Golstein and G. M. Griffiths, "An early history of T cell-mediated cytotoxicity," *Nature Reviews Immunology*, vol. 18, no. 8, pp. 527–535, 2018.

[27] C. S. Jansen, N. Prokhnevska, V. A. Master et al., "An intra-tumoral niche maintains and differentiates stem-like CD8 T cells," *Nature*, vol. 576, no. 7787, pp. 465–470, 2019.

[28] M. E. Shaul and Z. G. Fridlender, "Tumour-associated neutrophils in patients with cancer," *Nature Reviews Clinical Oncology*, vol. 16, no. 10, pp. 601–620, 2019.

[29] A. Ocana, C. Nieto-Jiménez, A. Pandiella, and A. J. Templeton, "Neutrophils in cancer: prognostic role and therapeutic strategies," *Molecular Cancer*, vol. 16, no. 1, Article ID 137, 2017.

[30] A. A. Beek, G. Zhou, M. Doukas et al., "GITR ligation enhances functionality of tumor-infiltrating T cells in hepatocellular carcinoma," *International Journal of Cancer*, vol. 145, no. 4, pp. 1111–1124, 2019.

[31] G. Zhou, D. Sprengers, P. P. C. Boor et al., "Antibodies against immune checkpoint molecules restore functions of tumor-infiltrating t cells in hepatocellular carcinomas," *Gastroenterology*, vol. 153, no. 4, pp. 1107–1119, 2017.

[32] Y. Chen, R. R. Ramjiawan, T. Reiberger et al., "CXCR4 inhibition in tumor microenvironment facilitates anti-programmed death receptor-1 immunotherapy in sorafenib-treated hepatocellular carcinoma in mice," *Hepatology*, vol. 61, no. 5, pp. 1591–1602, 2015.

[33] A. G. Duffy, S. V. Ulahannan, O. Makorova-Rusher et al., "Tremelimumab in combination with ablation in patients with advanced hepatocellular carcinoma," *Journal of Hepatology*, vol. 66, no. 3, pp. 545–551, 2017.

[34] A. B. El-Khoueiry, B. Sangro, T. Yau et al., "Nivolumab in patients with advanced hepatocellular carcinoma (CheckMate 040): an open-label, non-comparative, phase 1/2 dose escalation and expansion trial," *The Lancet*, vol. 389, no. 10088, pp. 2492–2502, 2017.

acute myeloid leukemia," *Journal of Cellular Physiology*, vol. 234, no. 11, pp. 20322–20328, 2019.

Review Article

ceRNAs in Cancer: Mechanism and Functions in a Comprehensive Regulatory Network

Ni Yang ⓘ **, Kuo Liu** ⓘ **, Mengxuan Yang** ⓘ **, and Xiang Gao** ⓘ

Second Hospital of Hebei Medical University, Shijiazhuang 050000, China

Correspondence should be addressed to Xiang Gao; gaoxiang@hebmu.edu.cn

Noncoding RNAs have been shown with powerful ability in post-transcriptional regulation, enabling intertwined RNA crosstalk and global molecular interaction in a large amount of dysfunctional conditions including cancer. Competing endogenous RNAs (ceRNAs) are those competitively binding with shared microRNAs (miRNAs), freeing their counterparts from miRNA-induced degradation, thus actively influencing and connecting with each other. Constantly updated analytical approaches boost outstanding advancement achieved in this burgeoning hotspot in multilayered intracellular communication, providing new insights into pathogenesis and clinical treatment. Here, we summarize the mechanisms and correlated factors under this RNA interplay and deregulated transcription profile in neoplasm and tumor progression, underscoring the great significance of ceRNAs for diagnostic values, monitoring biomarkers, and prognosis evaluation in cancer.

1. Pervasive Noncoding RNAs in Genomic Scope

Numerous evidence has emerged regarding the noncoding properties of RNA transcripts over the past years, unraveling whose great capacity that goes far beyond the previously well-characterized genetic information carrier and indispensable messenger for protein synthesis to post-transcriptional regulation and multilayered sequence interactions, whereby extensively interweaved molecular crosstalk along with rapidly changing cellular environment composes a robust intracellular connection. The identified verification and importance of prevalent noncoding RNAs (ncRNAs) in evolutionary complexity of diverse organisms lies partially in the comparison, where up to 75%–95% of the human genome is transformed into RNA transcripts basically varying in length and functions, with actually less than 2%, quantitively 21,000 genes [1], attributed with protein-coding properties [2, 3], yet almost genome-wide translation has been confirmed in simply structured species such as unicellular yeast [4], and Caenorhabditis elegans possess about an equal amount of genes encoding a protein with human but a 30 times smaller genome [5]. Mingled with multiple contributing factors, various modes of transcription generate products including but not limited to antisense strands or noncoding intergenic transcripts, which were previously unrecognized and thought to be useless remainders of an immature expressing mechanism. Taking 200 base pairs as a boundary, noncoding transcripts are roughly divided into two categories corresponding with their size, namely small ncRNAs and long ncRNAs (lncRNAs) [6]. Small ncRNAs have been deeply functionalized, among which miRNAs enrolled in the intricate RNA-RNA regulation network are one of the most representative components and will be clarified later in detail, concerning their noteworthy roles in biochemical behaviors and pathophysiological conditions [3, 7, 8]. Conversely, presenting pleiotropic effects as guides, scaffolds, natural decoys, and sponges in large-scale molecular correlations in transcriptional, post-transcriptional, epigenetic, and gene-expressing events, lncRNAs have been reportedly viewed as "master regulator" [9], even so, those hitherto hidden approaches through which lncRNAs flexibly participate in cellular homeostasis stabilization and response to perturbation in development of plenty of diseases, herein exemplified by cancer, still await further exploration. Based on existing achievements underscoring the remarkable potential of

ncRNAs as regulating elements in carcinogenesis, we overview the profile of ncRNAs, their derived identity as ceRNAs in tumor pathogenesis, and objective conditions affecting their inner action, which facilitates the renewal of highly targeted predicting tools and lays a deeply rooted foundation for future research and clinical implications in biomarker detection, prognosis judgement, and therapeutic regimen selection.

2. ceRNA Hypothesis: Derivation and Extension

Transcribed mainly from introns of coding genes, with the rest from exons of coding genes as well as intronic and exonic regions of noncoding sequences [10], miRNAs are small single-stranded RNAs consisting of generally 19–23 nucleotides, centralizing ceRNAs to regulate and interplay with each other by recognizing miRNA response elements (MREs) of target transcripts [2, 11, 12]. miRNA biosynthesis is a sequential enzyme-dependent process, in which canonically transcribed precursor miRNAs (pre-miRNAs) in the nucleus, in tandem catalyzed by RNA polymerase and nuclear Drosha/DGCR8 complex, are released into the cytoplasm and cleaved into double-stranded miRNAs with appropriate length by Dice, and finally incorporated into Argonaute-loaded miRNA-induced silencing complexes (miRISC) after degeneration of complementary strands [6, 13], base pairing with targets under the direction of 6–8 nucleotides in miRNAs' 5′ ends [9]. Seed matches in target transcripts are required for binding with miRNAs, while perfect complementarity is not always necessary. MREs are commonly 2–8 nucleotides sited in coding sequences (CDS), 5′ untranslated regions (5′ UTRs), and mostly 3′ UTRs of several subsets of RNAs comprising lncRNAs, transcribed pseudogenes, circular RNAs (circRNAs), and mRNAs [14–16], which are subjected to inhibition on expression through either complete degradation or translation repression, respectively, occurring when in high or relatively low degrees complementary base pairs are matched between MREs and miRNAs [2, 3]. Some have pointed out that imperfect bindings, implying "bulged sponges" in seed regions, are more effective in soaking up miRNAs and serving as competing molecules partly because of the longer period of occupation; otherwise, miRNAs are released once the perfectly paired targets go through degradation [17]. As a mutual interaction, the availability and activity of miRNAs are impaired by their binding targets, some of which degrade them, while others sequester them from alternative sequences of interest [11, 18]. What's more, 3′ end modification of miRNAs and target RNA function in a mathematical titration principle also account for such reduction in miRNA levels [19]. Given the above, it is conceivable that miRNAs may act as axis center in complicated intracellular crosstalk in both homeostatic status and disturbed physiological milieux like cancer.

Theoretically, when various transcripts are targeted by the same miRNAs, an elevated transcription level of one side would alleviate miRNA-induced suppression on the other, leading to direct or indirect regulation on gene expression. Transfected into viral vectors, artificial sponges of specific miRNAs were exploited before natural targets came into view, which were transcribed by strong promoters and synthesized to bear repeated binding sites for aimed miRNAs, thus exhibiting fascinating effects on derepressing counterpart targets [20, 21], showing profound significance for RNA crosstalk, and more precisely, the formation of ceRNA hypothesis.

The first discovered natural sponge was lncRNA IPS1 found in *Arabidopsis thaliana*, which was observed to decoy phosphate starvation-induced miR-399 and subsequently help maintain the stability and abundance of its partner target PHO2 [22]. Unlike precedently clarified perfect complementarity in plants, the mismatched loop on the miRNA cleavage site made IPS1 bypass the impairment and competent for efficient binding [3, 22]. Following the uncovery of this phenomenon termed "target mimicry" [22], the parallel finding was disclosed in animal cells, where ectopic overexpression of MREs resulted in moderately declining miRNA levels and 1.5–2.5-fold accumulation of the targets [21]. Later in 2010, Herpesvirus saimiri transformed T cells were reported to express ncRNA H. saimiri U-rich RNAs (HSURs), which were correlated with miR-27 degradation and increased FOXO1 levels [23]. The underlying implication and mechanism of these promising discoveries were extended to the field of cancer when pseudogene PTENP1 was proved to share common miRNAs with its homologous coding RNA [24]. With the antecedent supporting evidence assembled, the ceRNA hypothesis was put forward in 2011, demonstrating that each miRNA has manifold RNA targets and most RNAs bear a wealth of MREs, thus endogenous coding and noncoding RNAs regulate and crosstalk with each other by competitively binding to the shared but limited miRNA pools [12]. In the same year, other three research reinforced the crucial role of ceRNAs in the molecular characterization of cancer cells [25–27].

Grouping all the noncoding RNAs and noncoding properties of mRNAs into a functional complexity, the ceRNA hypothesis essentially opens the window for a multilevel and trans-regulatory ceRNA network (ceRNET) over the transcriptome, where competition and interplay among all subsets of ceRNAs occur in direct, indirect, or secondary manners with the help of miRNAs, together shedding light on the biochemical mechanism and post-transcriptional-layered explanations for pathogenesis and progression of massive disordered conditions such as cancer. Moreover, correlation with other factors such as RBPs and transcription factors also influences ceRNAs' biological activities [28], and miRNAs similarly vie for potent binding with shared target pools [29]. Some suggested ceRNA concept to be expanded to whatever RNA crosstalk surrounding common regulators [6], while others by the same token proposed "ceRNome" as a notion referring to the integration of reciprocally tying RNA molecules in a comprehensive cellular environment [9], indicating that ceRNA crosstalk is in no way standalone but in a global post-transcriptional context.

3. Building Blocks of ceRNA

3.1. Pseudogenes. Previously regarded as nonfunctional relics of their ancestral genes due to detrimental mutations impeding them from being translated into explicit

phenotypes [2], pseudogenes are gradually performing as bona fide competitors for their cognate genes with highly homologous MRE overlaps. Independent epigenetic modifications in pseudogenes signify initiative and stable evolutionary conservation [2]. About 14,505 pseudogenes contribute to making up human genome according to GENCODE Release (version 24) [2], consisting of unprocessed pseudogenes originating from gene duplication, processed pseudogenes through reverse transcription, and de novo synthesized unitary pseudogenes with no coding partners [30], whose transcripts participate in gene regulation as antisense sequences or compelling miRNA decoys as a subset of lncRNAs in ubiquitously expressing and tumor-specific patterns [31].

3.2. lncRNAs. There are estimated approximately 17,910 lnRNAs varying in length from 0.2 to 100 kilobases [32], which display tissue and developmental complexity, align with functional and spatial diversity of chromatin modification, RNA processing in the nucleus, and gene coding management in cytoplasmic parts [33], counteracting the reportedly low abundance as competitive candidates for miRNA binding in given conditions [3]. More precisely, lncRNA X-inactive specific transcript (Xist) could act in cis to devitalize the entire chromosome [34], and HOX transcript antisense RNA (HOTAIR) function in trans to drive metastasis through gene expression regulation [35], and chromatin structure is remodeled by alternative splicing associated with metastasis-associated lung adenocarcinoma transcript 1 (MALAT1) [36]. The most studied lncRNA in hepatocellular carcinoma, highly upregulated in liver cancer (HULC), is able to disengage protein kinase catalytic β (PRKACB) from miR-372 restraint, therefore promoting cAMP response element-binding protein (CREB) phosphorylation and, in turn, amplifying HULC upregulation [37]. Besides, lncRNAs are of great importance in controlling cell differentiation and pluripotency maintenance with respect to the effects of long intergenic noncoding RNAs (lincRNAs) [38].

3.3. circRNAs. circRNAs are fairly abundant in mammalian cells, generated from nearly 20% of functional genes [39]. Self-circularization depends on covalent conjunction of $3'$ and $5'$ ends after "backsplicing," conferring high stability to these loop RNA structures compared with their linear counterparts, due to lack of free terminals and thereby resistance to exonuclease-induced degradation and miRNA-mediated repression [40]. circRNA ciRS-7 was identified to contain 60–70 MREs for miR-7 [40], acting as crucial regulators in cerebral development and tumorigenesis [40, 41]. Considerable evidence disclosed key roles of circRNAs as ceRNAs with dominant intracellular localization in malignancy progression [42], and the distinct stability makes them ideal biomarkers in body fluids such as blood or saliva for clinical assessment [43, 44].

3.4. mRNAs. Since more than 60% of human mRNAs harbor MREs according to computational prediction [45], it is unsurprising to postulate that the function of protein-coding RNAs is no more restricted to translation templates but propagated to active fine-tuners in ncRNA-mRNA and mRNA-mRNA crosstalk, which may give rise to accordant or opposite effects with their inherent encoding features. It has been widely studied that VAPA, CNOT6L, ZEB2, and VCAN mRNAs are ceRNAs for tumor suppressor PTEN mRNA, representing aberrant transcription levels and resulting in downregulation of PTEN mRNAs in a Dicer-dependent way in various cancer types such as colorectal cancer [25], breast carcinoma [46], and melanoma [26]. Similarly, other classically identified molecules include VCAN and CD44 with their competing RNAs, endowed with complex roles in cell proliferation, invasive behaviors, and some other malignant signatures in contexts of cancer [47, 48].

4. ceRNA Crosstalk Decipherment

Increasing computational, mathematical, and experimental tools have been posed for decoding ceRNA crosstalk and identifying putative candidates for their topology and dynamic fluctuation. Typical verifying process of ceRNA interactions successively includes corroborative tests such as RNA immunoprecipitation for miRNA-ceRNA binding, confirmation of positive correlation of transcription levels of ceRNAs, repeated miRNA-dependency tests through Dicer knock-out or MRE mutations, and finally epigenetic changes induced by up- or downregulation of ceRNAs in disrupted physiological conditions [6]. Prediction algorithms including PITA, TargetScan, miRanda, and rna22 have been validated efficient for seeking ceRNAs through recognition of MREs and scoring overlaps in quantified assessment, forming the database of predicted ceRNA interactions (ceRDB), yet the unclear targeting rules and incomplete complementarity brought out limitations in some cases [49]. With high-throughput sequencing of RNA isolated by crosslinking immunoprecipitation (HITS-CLIP) and photoactivatable ribonucleoside-enhanced crosslinking and immunoprecipitation (PAR-CLIP) introduced into wide use, RISC-bound targets are more efficiently and precisely identified [49–51]. Moreover, MS2-tagged RNA affinity purification (MS2-TRAP) makes it possible for context-specific verification [52]. Further elucidation of ncRNA regulation for each subtype includes PseudoFun for pseudogenes [53] and GDCRNATools for lncRNAs [54]. The combination of HITS-CLIP/PAR-CLIP with subcellular RNA imaging [5] and mass spectrometry-based RBP abundance measurement allows analysis of sublocalization and RBP binding [6]. Taken together, the Smart Cancer Survival Predictive System and the Gene Survival Analysis Screen System are brought up for individual prognostic evaluation and precise clinical supervision [55].

5. Molecular Bases for ceRNA Interaction

Mathematical, in silico, and laboratory approaches have been carried out as above enumerated, yielding conclusions that abundance of ceRNAs and miRNAs, subcellular

localization, the number of shared MREs, and many other indirect contributing factors are suggested to influence ceRNA-miRNA interaction efficiency.

Analyses for optimal cross-talk conditions showed that only when the stoichiometry of the interrelated ceRNA and miRNA falls in a narrow range of equivalence could significant cross-regulation occur [18, 56, 57]. Such swift mutual effects are initiated with a threshold-like behavior, accounting for miRNAs presenting both their roles as "switches" when target transcripts are highly repressed in low abundance and "fine-tuners" when ceRNA levels are floating around the threshold for sensitive regulation [58, 59], partly consistent with the assumption that higher amount of miRNAs for target ceRNAs exert stronger repressive effects [60]. Furthermore, with MREs in equal affinity for the shared miRNAs, the wider repertoire of ceRNAs targeted by the miRNA is, the weaker influence the miRNA would exert on each individual target [57]. In other words, distant ceRNAs in the same regulatory network bidirectionally detriment miRNAs' efficacy on each other. Notably, a quantitative assay for miR-122 and its ceRNA aldolase mRNA revealed that significant derepression for ceRNA rivals was only observed when aldolase mRNA experienced nonphysiological overexpression [59], indicating particular ceRNA crosstalk may be quite mild in normal conditions but prevalent in pathological contexts.

RNA-binding proteins (RBPs) are greatly involved in post-transcriptional regulation by means of RNA splicing, transport, and stability mediation. Except for MREs, there are RBP binding sites located in ceRNA sequences, whereby RBPs antagonize or cooperate with miRNAs by directly occupying specific binding sites or indirectly altering affinity to miRNAs through reordering the secondary structure of ceRNAs. With numerous binding locus neighboring or overlapping miRISC binding sites in 3′ UTR [61], RBP HuR largely stabilizes RNA transcripts, whereas AUF1 exerts synergistic effects with miRNAs on target energy [62]. Similarly, HuR recruits let-7 RISC for repression of transcriptional regulator c-Myc [63], and c-Myc is widely accepted in controlling miRNA transcription, including upregulation of oncogenic miR-17-92 cluster [64]. Expectedly, RNAs may be relocated into different subcellular distributions once loaded with RBPs, which also affects the efficacy of spatiotemporally mutual interaction.

Hydrolytic deamination of adenosine to inosine (A to I editing), most frequently existing in UTRs and intronic sequences [65], epitomizes widespread RNA editing events in post-transcriptional regulation. It has been validated predominant in the majority of pre-mRNAs relying on adenosine deaminase, and to create new seed regions and accordingly corresponding target spectrum for miRNAs, destroying or generating miRNA matching substrates in ceRNAs [66]. Other forms of RNA editing resulting in base insertion, deletion, and nucleotide substitution simultaneously enrich the variation and diversity of the ceRNA network.

ceRNA crosstalk embraces multilayered regulatory hallmarks. Aside from the aforementioned aspects, the abundance of argonaute also causes competition among miRNAs as a bottleneck in the enzyme catalyzing process of miRISC synthesis [67]. Single-nucleotide polymorphism (SNP) allows subtle nucleotide component differences in MREs sharing collective miRNA pools, and alternative splicing provides miRNAs with shortened 3′ UTRs in a variety of cancer cells [68], both embodied in the altered affinity of MREs for miRNA binding, with higher affinity possessing stronger binding capacity. Hence, the overall regulating network is presented in given conditions, where additional determinants are exactly taken into consideration.

6. ceRNAs in Cancer

Chromosomal rearrangement, point mutation, shortened 3′ UTR, and other alterations in chromosome structure are commonly seen in the cancer cell genome, as a consequence, dysregulation of the ceRNA network and closely linked tumorigenesis, cell proliferation, and resistance to conventional treatment occur in such circumstances (Table 1).

As has been well elucidated, a decreased level of pseudogene PTENP1 leads to inhibition of tumor suppressor PTEN in a miRNA-dependent manner in numerous cancer types. The antisense lncRNAs, asRNAa, and asRNAb, derived from PTENP1 locus, respectively, recruit epigenetic regulators to the PTEN promoter region, confining PTEN transcription, and stabilize PTENP1 to derepress PTEN from miRNA absorption [69]. Coincident with previously published materials, ceRNA rivals for PTEN mRNA also includes mRNAs, whose competition for a large number of miRNAs is weakened in given pathological conditions, thus disrupting the downstream anti-oncogenic PTEN/AKT/p53 pathway [70].

Recent evidence deepens the body of knowledge concerning circRNAs in cancer progression. The absence of NUDT21, an RNA splicing factor, causes downregulation of circRNAs in HCC occurrence [71], and UGUA elements were pointed out to be crucial for sequence cyclization through binding with NUDT21 to form a dimer. Microarray revealed cirr5615 as an effective sponge for miR-149-5p, and its upregulation results in worse clinical outcomes in CRC patients, through disinhibition of β-catenin stabilization regulator tankyrase (TNKS) [72]. Similar mechanisms and positive correlation are found between increased circTP63 and FOXM1 levels in lung cancer, linked by miR-873-3p [73]. A prognostic model of N stage in TNM classification and overexpression of circCRIM1 was established based on circCRIM1-miR-422a-FOXQ1 crosstalk in nasopharyngeal carcinoma, which is related to peripheral implantation, epithelial-mesenchymal transition (EMT), and impaired chemosensitivity [74].

Constantly emerging lncRNA protagonists also provide new avenues for refinement of deregulated ceRNA interplay in carcinoma development. Based on vast achievements in this field, integrated analysis has risen up luxuriantly, delving into tissue- and cancer-specific differentially expressed genes (DEGs), harnessing intensive databases such as the Cancer Genome Atlas (TCGA) and the Gene Expression Omnibus (GEO), with statistical methods

supporting bioinformatics analysis. Profile of lncRNA transcription has been outlined in a multitude of cancers such as HCC, breast cancer, glioblastoma, GC, and metastatic melanoma [75–80], providing promising biomarkers for prognostic evaluation and early-stage detection of these pathological changes.

Countless breakthrough in ceRNAs has undoubtedly sparkled diagnostic and curative potent towards cancer; what deserves extra attention, on the other hand, is that sometimes, it is the part of the integrated regulatory axis that paves the way for more outward-extending investigations. It has been revealed in 2018 that scaffold protein disabled-2 (DAB2), whose antineoplastic role was initially identified in ovarian cancer, was downregulated by miR-191 through binding with its MREs in 3′ UTR in response to estrogen stimulation, heralding promoted cellular viability, tumor growth, and poor long-term survival in patients with ER + breast cancer [81]. At the same time, the miR-203/SNAI2 axis emerged as a high-profile symbol in tumor stemness, EMT, and angiogenesis in prostate cancer, in which suppression of miR-203 on transcriptional inhibitor SNAI2 is relieved due to lessened miR-203 existence, rendering reanimation of the downstream oncogenic GSK-3β/β-CATENIN signal pathway by activated SNAI 2 [82]. Later in 2019, similar molecular activities, somewhat replenishing the former, were unveiled in tumorigenesis of lung adenocarcinoma (LUAD), where overexpressed lncRNA chromatin-associated RNA 10 (CAR10) and lncRNA histocompatibility leukocyte antigen complex P5 (HCP5), which was transcriptionally up-regulated by SMAD3 after TGFβ communication in advanced stages of LUAD, were both identified to prompt cell proliferation and metastasis exactly by means of miR-203/SNAI regulatory access [83, 84]. Such findings suggest a vast potential for future development with previous research.

7. Resistance to Immunotherapy and Chemotherapy

Despite endlessly upgraded triumphs in typical immunotherapies, such as monoclonal antibodies, immune checkpoint (IC) inhibitors, chimeric antigen receptor (CAR) genetically-modified T cell therapy, and genetic modification of T cell receptor (TCR), which are categorized into adoptive T cell therapy (ACT), tumor cells obstinately escape from internal or exogenously administered immune surveillance, through intrinsic, adaptive, or acquired accommodation, leading to malignant performance and nonresponse to immunotherapy. Cytotoxic T-lymphocyte-associated protein 4 (CTLA4) on T cells has been well studied as an immune checkpoint, which blocks T-cell-stimulating binding of CD28 and APC B7 molecules, inducing T cell inactivation [85]. Contrary regulatory trends of miR-29 and B7–H3, one of the eight isoforms of the B7 family, were confirmed in solid tumors such as neuroblastoma, sarcoma, cutaneous melanoma, and breast cancer [86–88]. Another commonly upregulated IC in cancers is PD-1, whose binding with its ligand PD-L1 induces T cell disability. Somatic mutation of guanine to cytosine in PD-L1 3′ UTR leads to altered MRE sequences in various

gastrointestinal cancers (GCs), freeing PD-L1 mRNA from the restriction of miR-570 [89, 90]. Additionally, an array of miRNAs have been found related to aberrant overexpression of PD-L1 in both solid and hematological cancers and to motivate chemoresistance and metastasis. lncRNA-miRNA-PD-L1 regulations are also broadly discovered in tumor growth, cell proliferation, and migration in GCs and nonsmall cell lung carcinoma (NSCLC) [91–94]. Possible explanations for resistance to IC inhibitor (ICI) immunotherapy reside in the heterogeneity of MHC loss and susceptibility to spontaneous mutations, with deteriorated recognition and immune response to abnormal stimuli.

The development of TCR-engineered T cell therapy and CAR-T cell therapy reflects and, to a great extent, stands for the longstanding exploration of adoptive T cell therapy. Granted as a breakthrough designation with CD19-targeting CAR-T cell therapy on CD19+ B cell hematological malignancies leading to complete or partial remission in clinical trials, cancer immunotherapy focuses on fully arousing or assisting the autologous immune system to exert intensified supervision and restriction on tumor progression, but in fact, immune evasion is always inevitable ascribed to the ever-changing tumor microenvironment, immunosuppressive cytokine pathways (e.g., IFNγ in PD-L1 expression, TGFβ in urothelial cancer, VEGF in producing myeloid-derived suppressor cells (MDSCs), Wnt/β-catenin signals in colorectal cancer, and lack of sensitizing cytokines such as IL-2, IL-12, and IL-15), impaired function or expression of antigen loading molecules and abnormal post-transcriptional background of ceRNAs, letting tumor cells subtly get away with immunological monitoring [95–100]. LncRNA MALAT1 drives dendritic cells (DCs) into tolerogenic types with the secretion of IL-10 and low-level expression of CD80 and MHC by acting as an miR-155 sponge [101]. Meanwhile, PD-L1 is overexpressed in the regulation of miR-195 on MALAT1 in diffuse large B-cell lymphoma and Linc00473 in pancreatic cancer [91, 102]. The above-mentioned lncRNA HOTAIR frees human leukocyte antigen-G (HLA-G) expression from miR-152, oppressing immune response through devitalizing NK cell activity in gastric cancer [103, 104]. CD8+ T cell fatigue and exhaustion, which is positively related with T cell immunoglobulin and mucin domain protein 3 (Tim-3), is a common route of immune escape in hepatic cell carcinoma and could be restored by inhibition of nuclear-enriched autosomal transcript 1 (NEAT1) to enhance Tim-3 capture via miR-155 [94]. Also, NEAT1 directly binds with DNMT1, a member of DNA methyltransferase family, with aberrant methylation in promoter regions leading to epigenetically downregulated antioncogene P53 expression and cGAS/STING pathway for T cell invigoration [105]. Here, we have merely touched on limited elements of ceRNA regulation in adoptive immunotherapy, while the understanding of therapeutic agents and regulatory hinges informs a feasible combination of T cell therapy with selected chemokines, cytokines, ICIs, and monoclonal

TABLE 1: ceRNAs in cancers.

Cancer	ceRNA	miRNA	Target	Reference
Breast cancer	CYP4Z2P-3′ UTR	miR-211, miR-197, miR-204	CYP4Z1	[111]
	FOXO1 3′ UTR	miR-9	E-cadherin	[112]
	VERSICAN 3′ UTR	miR-136, miR-199a-3p, miR-144	Rb1, PTEN	[46]
	lncRNA GAS5	miR-21	—	[113]
	linc-ROR	miR-205	ZEB2	[114]
		miR-145	ARF6	[115]
	lncRNA–CDC6	miR-215	CDC6	[116]
CC	lncRNA XLOC_006390	miR-331-3p, miR-338-3p	PKM2, EYA2	[117]
CRC	OCT4B mRNA	miR-145, miR-20a/b, miR-106a/b, miR-335	OCT4A	[118]
	circ-ITCH	miR-7, miR-17, miR-214	ITCH	[119]
	circ5615	miR-149-5p	TNKS	[72]
Endometrial cancer	linc-ROR	miR-145	—	[120]
GC	lncRNA GAPLINC	miR-211-3p	CD44	[121]
	lncRNA HOTAIR	miR-331-3p	HER2	[122]
	LncRNA MT1JP	miR-92a-3p	FBXW7	[123]
HCC	lncRNA CCAT1	let-7	HMGA2, c-Myc	[124]
	lncRNA HOTTIP	miR-125b	—	[125]
	lncRNA HULC	miR-372	PRKACB	[37]
	LINC00974	miR-642	KRT19	[126]
	lncRNA UCA1	miR-216b	FGFR1	[127]
	Pseudogene INTS6P1	miR-17-5p	INTS6	[128]
	PTENP1	miR-17, miR-19b, miR-20a	PTEN,	[129]
	lncRNA FAL1	miR-1236	AFP, ZEB1	[130]
Lung cancer	lncRMA LCAT1	miR-4715-5p	RAC1	[131]
LUSC	circTP63	miR-873-3p	FOXM1	[73]
NPC	circCRIM1	miR-422a	FOXQ1	[74]
	lncRNA FAM225A	miR-590-3p, miR-1275	ITGB3	[132]
	lncRNA PTPRG-AS1	miR-194-3p	PRC1	[133]
	lncRNA ZFAS1	miR-892b	LPAR1	[134]
NSCLC	AEG-1 3′ UTR	miR-30a	Vimentin, snail	[135]
OC	lnc-OC1	miR-34a, miR-34c	—	[136]
Prostate cancer	CNOT6L/VAPA	miR-17, miR-19a, miR-20a/b, miR-106a/b, miR-93	PTEN	[25]
	lncRNA PCAT1	miR-3667-3p	c-Myc	[137]
	K-RAS1P	—	K-RAS	[24]
	PTENP1	miR-17, miR-19, miR-21, miR-26, miR-214	PTEN	[24]
	lncRNA UCA1	miR143	MYO6	[138]

Abbreviation: CC: cervical cancer; CRC: colorectal cancer; GC: gastrointestinal cancer; HCC: hepatocellular carcinoma; LUSC: lung squamous cell carcinoma; NPC: nasopharyngeal carcinoma; NSCLC: nonsmall cell lung cancer. —: not available.

antibodies, foreboding accessible application and benefits of optional strategies in cancer treatment.

Chemoresistance is an Achilles heel for progression and unsatisfying prognosis of malignancy and is always accompanied by disadjust biological mechanisms including drug outflow, cell proliferation, distant migration, and EMT. One of the most exploited regulators in chemoresistance is lncPVT1-representing noncoding sequences transcribed from the cancer-prone 8q24 chromosome [106] (Table 2). lncPVT1 is empowered with three regulating approaches. First, it recruits modifiers such as EZH2 to epigenetically dampen tumor suppressors, including $p53$ in HCC [107], large tumor suppressor kinase 2 (LATS2) in NSCLC [108], and miR-195 [109]. Second, differential processing of lncPVT1 is referred to the generation of lncPVT1-derived miRNAs, taking miR-1204 in NSCLC for instance, which accelerates cell proliferation through targeting paired-like homeodomain 1 (PITX1) [110]. Finally and predominantly, lncPVT1 dysregulation in resistance to chemotherapeutic agents towards a myriad of cancers reconciles its tremendous vitality as a ceRNA.

TABLE 2: ceRNAs in chemotherapy resistance.

ceRNA	miRNA	Target	Chemotherapeutic agent	Cancer	Reference
LncPVT1	miR-195	SMAD3	Paclitaxel	CC	[139]
	miR-216b	Beclin-1	Cisplatin	NSCLC	[140]
	miR-152	c-MET	Gemcitabine	Osteosarcoma	[141]
	miR-1207-5p/3p	SMAD	Gemcitabine	PC	[142]
	miR-143	Hexokinase 2	—	GBC	[143]
	miR-186-5p	YAP1	—	HCC	[144]
lncRNA HOTAIR	miR-17-5p	Beclin1	Sunitinib	Renal cancer	[145]
lncRNA HOXA-AS2	miR-520c-3p	S100A4	Adriamycin	AML	[146]
lncRNA GAS5	miR-221	—	Gemcitabine	PC	[147]

Abbreviation: CC: cervical cancer; NSCLC: nonsmall cell lung cancer; PC: pancreatic cancer; GBC: gallbladder cancer; HCC: hepatocellular carcinoma; AML: acute myelocytic leukemia. —: not available.

8. Conclusion

In this review, we present a genome-wide molecular interaction dominated by ncRNAs in a deep-going extent of post-transcriptional regulation regarding different types of cancer, where detailed mechanisms of the dynamic network, powerful predicting tools, and typical ceRNA crosstalk in pathogenesis, progression, and drug resistance in cancer have all together sketched out an encouraging blueprint for in-depth scientific research and translation into clinical application. Still, we have to acknowledge that despite extensive efforts endeavored into broadening our understanding of this realm, there is much more Terra incognita remaining to be carved out. Primarily, with most of the current research carried out on the overall cell-cluster level, intratumor heterogeneity among cancer cells has long been neglected, which is also crucial for neoplasia and therapeutic resistance. Here, we lay emphasis on two points of concern. First, even if numerous regulating nodes have been implicated as prospective targets for clinical therapy, accurate manipulation on these hubs without the involvement of other irrelevant locus waits for delicate Polish. Given that each single molecular tends to be the junction of, or to be indirectly covered by separate regulatory pathways with synergistic, antagonistic, or unrelated functions, controllable and unidirectional interventions would furthest avoid adverse reactions and achieve desired outcomes. Second, phenotypes observed through lowered expression or overexpression of single ceRNA/miRNA axis may need to be dialectically viewed, as its significance could be overmuch exaggerated under counteraction of other seemingly nonessential issues when conducting the research, or it is so tightly dragged by many other unclarified interlinks that enforced changes on the target axis alone is too weak to stand out in physiological conditions. There is no denying that booming advance in ceRNA network provides an exciting starting point for clinical practice and future research in cancer.

Data Availability

References in this review were mainly retrieved from PubMed, ClinicalKey, and OVID and were downloaded from respective websites (https://pubmed.ncbi.nlm.nih.gov/, http://www.clinicalkey.com, and http://ovidsp.ovid.com/) and http://www.yz365.com/.

Conflicts of Interest

The authors declare that there are no conflicts of interest.

Authors' Contributions

Xiang Gao proposed the topic; Ni Yang, Kuo Liu, and Mengxuan Yang retrieved and analyzed the literature. Ni Yang drafted the manuscript; Kuo Liu, Mengxuan Yang, and Xiang Gao helped in revision. All the authors have read through and approved the article.

References

[1] P.-J. Volders, K. Helsens, X. Wang et al., "LNCipedia: a database for annotated human lncRNA transcript sequences and structures," *Nucleic Acids Research*, vol. 41, no. D1, pp. D246–D251, 2013.

[2] Y. An, K. L. Furber, and S. Ji, "Pseudogenes regulate parental gene expressionviaceRNA network," *Journal of Cellular and Molecular Medicine*, vol. 21, no. 1, pp. 185–192, 2017.

[3] Y. Tay, J. Rinn, and P. P. Pandolfi, "The multilayered complexity of ceRNA crosstalk and competition," *Nature*, vol. 505, no. 7483, pp. 344–352, 2014.

[4] T. Gutschner and S. Diederichs, "The hallmarks of cancer a long non-coding RNA point of view," *RNA Biology*, vol. 9, no. 6, pp. 703–719, 2012.

[5] J. S. Mattick, "The genetic signatures of noncoding RNAs," *PLoS Genetics*, vol. 5, no. 4, Article ID e1000459, 2009.

[6] Y. Wang, J. Hou, D. He et al., "The emerging function and mechanism of ceRNAs in cancer," *Trends in Genetics*, vol. 32, no. 4, pp. 211–224, 2016.

[7] R. Vishnubalaji, H. Shaath, E. Elkord, and N. M. Alajez, "Long non-coding RNA (lncRNA) transcriptional landscape in breast cancer identifies LINC01614 as non-favorable prognostic biomarker regulated by TGF beta and focal adhesion kinase (FAK) signaling," *Cell Death Discovery*, vol. 5, p. 109, 2019.

[8] M. Matsui and D. R. Corey, "Non-coding RNAs as drug targets," *Nature Reviews Drug Discovery*, vol. 16, no. 3, pp. 167–179, 2017.

[9] R. Abdollahzadeh, A. Daraei, Y. Mansoori, M. Sepahvand, M. M. Amoli, and J. Tavakkoly-Bazzaz, "Competing endogenous RNA (ceRNA) cross talk and language in ceRNA regulatory networks: a new look at hallmarks of breast

cancer," *Journal of Cellular Physiology*, vol. 234, no. 7, pp. 10080–10100, 2019.

[10] A. Rodriguez, S. Griffiths-Jones, J. L. Ashurst, and A. Bradley, "Identification of mammalian microRNA host genes and transcription units," *Genome Research*, vol. 14, no. 10A, pp. 1902–1910, 2004.

[11] J. Qu, M. Li, W. Zhong, and C. Hu, "Competing endogenous RNA in cancer: a new pattern of gene expression regulation," *International Journal of Clinical and Experimental Medicine*, vol. 8, no. 10, pp. 17110–17116, 2015.

[12] L. Salmena, L. Poliseno, Y. Tay, L. Kats, and P. P. Pandolfi, "A ceRNA hypothesis: the rosetta stone of a hidden RNA language?" *Cell*, vol. 146, no. 3, pp. 353–358, 2011.

[13] R. C. Wilson, A. Tambe, M. A. Kidwell, C. L. Noland, C. P. Schneider, and J. A. Doudna, "Dicer-TRBP complex formation ensures accurate mammalian microRNA biogenesis," *Molecular Cell*, vol. 57, no. 3, pp. 397–407, 2015.

[14] M. Maldotti, D. Incarnato, F. Neri et al., "The long intergenic non-coding RNA CCR492 functions as a let-7 competitive endogenous RNA to regulate c-Myc expression," *Biochimica et Biophysica Acta (BBA)—Gene Regulatory Mechanisms*, vol. 1859, no. 10, pp. 1322–1332, 2016.

[15] D. P. Bartel, "MicroRNAs: target recognition and regulatory functions," *Cell*, vol. 136, no. 2, pp. 215–233, 2009.

[16] M. D. Paraskevopoulou, G. Georgakilas, N. Kostoulas et al., "DIANA-LncBase: experimentally verified and computationally predicted microRNA targets on long non-coding RNAs," *Nucleic Acids Research*, vol. 41, no. D1, pp. D239–D245, 2013.

[17] B. D. Brown and L. Naldini, "INNOVATION exploiting and antagonizing microRNA regulation for therapeutic and experimental applications," *Nature Reviews Genetics*, vol. 10, no. 8, pp. 578–585, 2009.

[18] M. Figliuzzi, E. Marinari, and A. De Martino, "MicroRNAs as a selective channel of communication between competing RNAs: a steady-state theory," *Biophysical Journal*, vol. 104, no. 5, pp. 1203–1213, 2013.

[19] H. Seitz, "Redefining microRNA targets," *Current Biology*, vol. 19, no. 10, pp. 870–873, 2009.

[20] B. D. Brown, B. Gentner, A. Cantore et al., "Endogenous microRNA can be broadly exploited to regulate transgene expression according to tissue, lineage and differentiation state," *Nature Biotechnology*, vol. 25, no. 12, pp. 1457–1467, 2007.

[21] M. S. Ebert, J. R. Neilson, and P. A. Sharp, "MicroRNA sponges: competitive inhibitors of small RNAs in mammalian cells," *Nature Methods*, vol. 4, no. 9, pp. 721–726, 2007.

[22] J. M. Franco-Zorrilla, A. Valli, M. Todesco et al., "Target mimicry provides a new mechanism for regulation of microRNA activity," *Nature Genetics*, vol. 39, no. 8, pp. 1033–1037, 2007.

[23] D. Cazalla, T. Yario, and J. A. Steitz, "Down-regulation of a host microRNA by a herpesvirus saimiri noncoding RNA," *Science*, vol. 328, no. 5985, pp. 1563–1566, 2010.

[24] L. Poliseno, L. Salmena, J. Zhang, B. Carver, W. J. Haveman, and P. P. Pandolfi, "A coding-independent function of gene and pseudogene mRNAs regulates tumour biology," *Nature*, vol. 465, no. 7301, pp. 1033–1038, 2010.

[25] Y. Tay, L. Kats, L. Salmena et al., "Coding-independent regulation of the tumor suppressor PTEN by competing endogenous mRNAs," *Cell*, vol. 147, no. 2, pp. 344–357, 2011.

[26] F. A. Karreth, Y. Tay, D. Perna et al., "In vivo identification of tumor-suppressive PTEN ceRNAs in an oncogenic BRAF-induced mouse model of melanoma," *Cell*, vol. 147, no. 2, pp. 382–395, 2011.

[27] P. Sumazin, X. Yang, H.-S. Chiu et al., "An extensive microRNA-mediated network of RNA-RNA interactions regulates established oncogenic pathways in glioblastoma," *Cell*, vol. 147, no. 2, pp. 370–381, 2011.

[28] P. Paci, T. Colombo, and L. Farina, "Computational analysis identifies a sponge interaction network between long non-coding RNAs and messenger RNAs in human breast cancer," *BMC Systems Biology*, vol. 8, p. 83, 2014.

[29] M. Nitzan, A. Steiman-Shimony, Y. Altuvia, O. Biham, and H. Margalit, "Interactions between distant ceRNAs in regulatory networks," *Biophysical Journal*, vol. 106, no. 10, pp. 2254–2266, 2014.

[30] L. Poliseno, "Pseudogenes: newly discovered players in human cancer," *Science Signaling*, vol. 5, p. 242, 2012.

[31] J. D. Welch, J. Baran-Gale, C. M. Perou, P. Sethupathy, and J. F. Prins, "Pseudogenes transcribed in breast invasive carcinoma show subtype-specific expression and ceRNA potential," *BMC Genomics*, vol. 16, p. 113, 2015.

[32] C. P. Ponting, P. L. Oliver, and W. Reik, "Evolution and functions of long noncoding RNAs," *Cell*, vol. 136, no. 4, pp. 629–641, 2009.

[33] M. N. Cabili, M. C. Dunagin, P. D. McClanahan et al., "Localization and abundance analysis of human lncRNAs at single-cell and single-molecule resolution," *Genome Biology*, vol. 16, p. 20, 2015.

[34] G. D. Penny, G. F. Kay, S. A. Sheardown, S. Rastan, and N. Brockdorff, "Requirement for xist in X chromosome inactivation," *Nature*, vol. 379, no. 6561, pp. 131–137, 1996.

[35] R. A. Gupta, N. Shah, K. C. Wang et al., "Long non-coding RNA HOTAIR reprograms chromatin state to promote cancer metastasis," *Nature*, vol. 464, no. 7291, pp. 1071–1076, 2010.

[36] V. Tripathi, J. D. Ellis, Z. Shen et al., "The nuclear-retained noncoding RNA MALAT1 regulates alternative splicing by modulating SR splicing factor phosphorylation," *Molecular Cell*, vol. 39, no. 6, pp. 925–938, 2010.

[37] J. Wang, X. Liu, H. Wu et al., "CREB up-regulates long noncoding RNA, HULC expression through interaction with microRNA-372 in liver cancer," *Nucleic Acids Research*, vol. 38, no. 16, pp. 5366–5383, 2010.

[38] Y. Zhang, G. Liao, J. Bai et al., "Identifying cancer driver lncRNAs bridged by functional effectors through integrating multi-omics data in human cancers," *Molecular Therapy—Nucleic Acids*, vol. 17, pp. 362–373, 2019.

[39] J. U. Guo, V. Agarwal, H. Guo, and D. P. Bartel, "Expanded identification and characterization of mammalian circular RNAs," *Genome Biology*, vol. 15, no. 7, p. 409, 2014.

[40] S. Memczak, M. Jens, A. Elefsinioti et al., "Circular RNAs are a large class of animal RNAs with regulatory potency," *Nature*, vol. 495, no. 7441, pp. 333–338, 2013.

[41] T. B. Hansen, J. Kjems, and C. K. Damgaard, "Circular RNA and miR-7 in cancer," *Cancer Research*, vol. 73, no. 18, pp. 5609–5612, 2013.

[42] L. S. Kristensen, T. B. Hansen, M. T. Venø, and J. Kjems, "Circular RNAs in cancer: opportunities and challenges in the field," *Oncogene*, vol. 37, no. 5, pp. 555–565, 2018.

[43] J. H. Bahn, Q. Zhang, F. Li et al., "The landscape of MicroRNA, piwi-interacting RNA, and circular RNA in human saliva," *Clinical Chemistry*, vol. 61, no. 1, pp. 221–230, 2015.

[44] M. Galasso, G. Costantino, L. Pasquali et al., "Profiling of the predicted circular RNAs in ductal in situ and invasive breast

cancer: a pilot study," *International Journal of Genomics*, vol. 2016, Article ID 4503840, 7 pages, 2016.

[45] F. A. Karreth, U. Ala, P. Provero, and P. P. Pandolfi, "Pseudogenes as competitive endogenous RNAs: target prediction and validation," *Methods in Molecular Biology*, vol. 1167, pp. 199–212, 2014.

[46] D. Y. Lee, Z. Jeyapalan, L. Fang et al., "Expression of versican 3′-untranslated region modulates endogenous microRNA functions," *PLoS One*, vol. 5, no. 10, Article ID e13599, 2010.

[47] L. Fang, W. W. Du, X. Yang et al., "Versican 3′-untranslated region (3′-UTR) functions as a ceRNA in inducing the development of hepatocellular carcinoma by regulating miRNA activity," *The FASEB Journal*, vol. 27, no. 3, pp. 907–919, 2013.

[48] Z. Jeyapalan, Z. Deng, T. Shatseva, L. Fang, C. He, and B. B. Yang, "Expression of CD44 3′-untranslated region regulates endogenous microRNA functions in tumorigenesis and angiogenesis," *Nucleic Acids Research*, vol. 39, no. 8, pp. 3026–3041, 2011.

[49] M. Thomas, J. Lieberman, and A. Lal, "Desperately seeking microRNA targets," *Nature Structural & Molecular Biology*, vol. 17, no. 10, pp. 1169–1174, 2010.

[50] S. W. Chi, J. B. Zang, A. Mele, and R. B. Darnell, "Argonaute HITS-CLIP decodes microRNA-mRNA interaction maps," *Nature*, vol. 460, no. 7254, pp. 479–486, 2009.

[51] M. Hafner, M. Landthaler, L. Burger et al., "Transcriptome-wide identification of RNA-binding protein and MicroRNA target sites by PAR-CLIP," *Cell*, vol. 141, no. 1, pp. 129–141, 2010.

[52] J.-H. Yoon, S. Srikantan, and M. Gorospe, "MS2-TRAP (MS2-tagged RNA affinity purification): tagging RNA to identify associated miRNAs," *Methods*, vol. 58, no. 2, pp. 81–87, 2012.

[53] T. S. Johnson, S. Li, E. Franz et al., "PseudoFuN: deriving functional potentials of pseudogenes from integrative relationships with genes and microRNAs across 32 cancers," *GigaScience*, vol. 8, no. 5, p. giz046, 2019.

[54] R. Li, H. Qu, S. Wang et al., "GDCRNATools: an R/bioconductor package for integrative analysis of lncRNA, miRNA and mRNA data in GDC," *Bioinformatics*, vol. 34, no. 14, pp. 2515–2517, 2018.

[55] Z. Zhang, T. He, L. Huang et al., "Two precision medicine predictive tools for six malignant solid tumors: from gene-based research to clinical application," *Journal of Translational Medicine*, vol. 17, no. 1, p. 405, 2019.

[56] Y. Yuan, B. Liu, P. Xie et al., "Model-guided quantitative analysis of microRNA-mediated regulation on competing endogenous RNAs using a synthetic gene circuit," *Proceedings of the National Academy of Sciences*, vol. 112, no. 10, pp. 3158–3163, 2015.

[57] U. Ala, F. A. Karreth, C. Bosia et al., "Integrated transcriptional and competitive endogenous RNA networks are cross-regulated in permissive molecular environments," *Proceedings of the National Academy of Sciences*, vol. 110, no. 18, pp. 7154–7159, 2013.

[58] S. Mukherji, M. S. Ebert, G. X. Y. Zheng, J. S. Tsang, P. A. Sharp, and A. van Oudenaarden, "MicroRNAs can generate thresholds in target gene expression," *Nature Genetics*, vol. 43, no. 9, pp. 854–859, 2011.

[59] R. Denzler, V. Agarwal, J. Stefano, D. P. Bartel, and M. Stoffel, "Assessing the ceRNA hypothesis with quantitative measurements of miRNA and target abundance," *Molecular Cell*, vol. 54, no. 5, pp. 766–776, 2014.

[60] J. Zhang, L. Liu, T. Xu et al., "miRspongeR: an R/bioconductor package for the identification and analysis of miRNA sponge interaction networks and modules," *BMC Bioinformatics*, vol. 20, p. 235, 2019.

[61] N. Mukherjee, D. L. Corcoran, J. D. Nusbaum et al., "Integrative regulatory mapping indicates that the RNA-binding protein HuR couples pre-mRNA processing and mRNA stability," *Molecular Cell*, vol. 43, no. 3, pp. 327–339, 2011.

[62] A. Barker, M. R. Epis, C. J. Porter et al., "Sequence requirements for RNA binding by HuR and AUF1," *Journal of Biochemistry*, vol. 151, no. 4, pp. 423–437, 2012.

[63] H. H. Kim, Y. Kuwano, S. Srikantan, E. K. Lee, J. L. Martindale, and M. Gorospe, "HuR recruits let-7/RISC to repress c-Myc expression," *Genes & Development*, vol. 23, no. 15, pp. 1743–1748, 2009.

[64] T.-C. Chang, D. Yu, Y.-S. Lee et al., "Widespread microRNA repression by Myc contributes to tumorigenesis," *Nature Genetics*, vol. 40, no. 1, pp. 43–50, 2008.

[65] A. Athanasiadis, A. Rich, and S. Maas, "Widespread A-to-I RNA editing of Alu-containing mRNAs in the human transcriptome," *PLoS Biology*, vol. 2, no. 12, p. e391, 2004.

[66] X. Qi, D.-H. Zhang, N. Wu, J.-H. Xiao, X. Wang, and W. Ma, "ceRNA in cancer: possible functions and clinical implications," *Journal of Medical Genetics*, vol. 52, no. 10, pp. 710–718, 2015.

[67] G. Meister, "Argonaute proteins: functional insights and emerging roles," *Nature Reviews Genetics*, vol. 14, no. 7, pp. 447–459, 2013.

[68] C. Mayr and D. P. Bartel, "Widespread shortening of 3′UTRs by alternative cleavage and polyadenylation activates oncogenes in cancer cells," *Cell*, vol. 138, no. 4, pp. 673–684, 2009.

[69] A. de Giorgio, J. Krell, V. Harding, J. Stebbing, and L. Castellano, "Emerging roles of competing endogenous RNAs in cancer: insights from the regulation of PTEN," *Molecular and Cellular Biology*, vol. 33, no. 20, pp. 3976–3982, 2013.

[70] R.-K. Li, J. Gao, L.-H. Guo, G.-Q. Huang, and W.-H. Luo, "PTENP1 acts as a ceRNA to regulate PTEN by sponging miR-19b and explores the biological role of PTENP1 in breast cancer," *Cancer Gene Therapy*, vol. 24, no. 7, pp. 309–315, 2017.

[71] X. Li, J. Ding, X. Wang, Z. Cheng, and Q. Zhu, "NUDT21 regulates circRNA cyclization and ceRNA crosstalk in hepatocellular carcinoma," *Oncogene*, vol. 39, no. 4, pp. 891–904, 2020.

[72] Z. Ma, C. Han, W. Xia et al., "circ5615 functions as a ceRNA to promote colorectal cancer progression by upregulating TNKS," *Cell Death & Disease*, vol. 11, no. 5, p. 356, 2020.

[73] Z. Cheng, C. Yu, S. Cui et al., "circTP63 functions as a ceRNA to promote lung squamous cell carcinoma progression by upregulating FOXM1," *Nature Communications*, vol. 10, p. 3200, 2019.

[74] X. Hong, N. Liu, Y. Liang et al., "Circular RNA CRIM1 functions as a ceRNA to promote nasopharyngeal carcinoma metastasis and docetaxel chemoresistance through upregulating FOXQ1," *Molecular Cancer*, vol. 19, no. 1, p. 33, 2020.

[75] Y. Bai, J. Long, Z. Liu et al., "Comprehensive analysis of a ceRNA network reveals potential prognostic cytoplasmic lncRNAs involved in HCC progression," *Journal of Cellular Physiology*, vol. 234, no. 10, pp. 18837–18848, 2019.

[76] Z. Liu, X. Wang, G. Yang et al., "Construction of lncRNA-associated ceRNA networks to identify prognostic lncRNA

biomarkers for glioblastoma," *Journal of Cellular Biochemistry*, vol. 121, no. 7, pp. 3502–3515, 2020.

[77] M. Qi, B. Yu, H. Yu, and F. Li, "Integrated analysis of a ceRNA network reveals potential prognostic lncRNAs in gastric cancer," *Cancer Medicine*, vol. 9, no. 5, pp. 1798–1817, 2020.

[78] Y. Yao, T. Zhang, L. Qi et al., "Integrated analysis of co-expression and ceRNA network identifies five lncRNAs as prognostic markers for breast cancer," *Journal of Cellular and Molecular Medicine*, vol. 23, no. 12, pp. 8410–8419, 2019.

[79] X. Wu, Z. Sui, H. Zhang, Y. Wang, and Z. Yu, "Integrated analysis of lncRNA-mediated ceRNA network in lung adenocarcinoma," *Frontiers in Oncology*, vol. 10, Article ID 554759, 2020.

[80] L.-X. Wang, C. Wan, Z.-B. Dong, B.-H. Wang, H.-Y. Liu, and Y. Li, "Integrative analysis of long noncoding RNA (lncRNA), microRNA (miRNA) and mRNA expression and construction of a competing endogenous RNA (ceRNA) network in metastatic melanoma," *Medical Science Monitor*, vol. 25, pp. 2896–2907, 2019.

[81] X. Tian and Z. Zhang, "miR-191/DAB2 axis regulates the tumorigenicity of estrogen receptor-positive breast cancer," *IUBMB Life*, vol. 70, no. 1, pp. 71–80, 2018.

[82] X. Tian, F. Tao, B. Zhang, J.-T. Dong, and Z. Zhang, "The miR-203/SNAI2 axis regulates prostate tumor growth, migration, angiogenesis and stemness potentially by modulating GSK-3β/β-CATENIN signal pathway," *IUBMB Life*, vol. 70, no. 3, pp. 224–236, 2018.

[83] X. Ge, G.-Y. Li, L. Jiang et al., "Long noncoding RNA CAR10 promotes lung adenocarcinoma metastasis via miR-203/30/SNAI axis," *Oncogene*, vol. 38, no. 16, pp. 3061–3076, 2019.

[84] L. Jiang, R. Wang, L. Fang et al., "HCP5 is a SMAD3-responsive long non-coding RNA that promotes lung adenocarcinoma metastasis via miR-203/SNAI axis," *Theranostics*, vol. 9, no. 9, pp. 2460–2474, 2019.

[85] R. Vishnubalaji, H. Shaath, R. Elango, and N. M. Alajez, "Noncoding RNAs as potential mediators of resistance to cancer immunotherapy," *Seminars in Cancer Biology*, vol. 65, pp. 65–79, 2020.

[86] H. Xu, I. Y. Cheung, H.-F. Guo, and N.-K. V. Cheung, "MicroRNA miR-29 modulates expression of immunoinhibitory molecule B7-H3: potential implications for immune based therapy of human solid tumors," *Cancer Research*, vol. 69, no. 15, pp. 6275–6281, 2009.

[87] J. Wang, K. K. Chong, Y. Nakamura et al., "B7-H3 associated with tumor progression and epigenetic regulatory activity in cutaneous melanoma," *Journal of Investigative Dermatology*, vol. 133, no. 8, pp. 2050–2058, 2013.

[88] M. K. Nygren, C. Tekle, V. A. Ingebrigtsen et al., "Identifying microRNAs regulating B7-H3 in breast cancer: the clinical impact of microRNA-29c," *British Journal of Cancer*, vol. 110, no. 8, pp. 2072–2080, 2014.

[89] W. Wang, J. Sun, F. Li et al., "A frequent somatic mutation in CD274 3′-UTR leads to protein over-expression in gastric cancer by disrupting miR-570 binding," *Human Mutation*, vol. 33, no. 3, pp. 480–484, 2012.

[90] W. Wang, F. Li, Y. Mao et al., "A miR-570 binding site polymorphism in the B7-H1 gene is associated with the risk of gastric adenocarcinoma," *Human Genetics*, vol. 132, no. 6, pp. 641–648, 2013.

[91] W. Y. Zhou, M. M. Zhang, C. Liu, Y. Kang, J. O. Wang, and X. H. Yang, "Long noncoding RNA LINC00473 drives the progression of pancreatic cancer via upregulating programmed death-ligand 1 by sponging microRNA-195-5p,"

[92] S. Wei, K. Wang, X. Huang, Z. Zhao, and Z. Zhao, "LncRNA MALAT1 contributes to non-small cell lung cancer progression via modulating miR-200a-3p/programmed death-ligand 1 axis," *International Journal of Immunopathology and Pharmacology*, vol. 33, Article ID 2058738419859699, 2019.

[93] C.-J. Wang, C.-C. Zhu, J. Xu et al., "The lncRNA UCA1 promotes proliferation, migration, immune escape and inhibits apoptosis in gastric cancer by sponging anti-tumor miRNAs," *Molecular Cancer*, vol. 18, p. 115, 2019.

[94] K. Yan, Y. Fu, N. Zhu et al., "Repression of lncRNA NEAT1 enhances the antitumor activity of CD8+T cells against hepatocellular carcinoma via regulating miR-155/Tim-3," *The International Journal of Biochemistry & Cell Biology*, vol. 110, pp. 1–8, 2019.

[95] K. DePeaux and G. M. Delgoffe, "Metabolic barriers to cancer immunotherapy," *Nature Reviews Immunology*, 2021.

[96] P. S. Hegde and D. S. Chen, "Top 10 challenges in cancer immunotherapy," *Immunity*, vol. 52, no. 1, pp. 17–35, 2020.

[97] Y. Li, T. Jiang, W. Zhou et al., "Pan-cancer characterization of immune-related lncRNAs identifies potential oncogenic biomarkers," *Nature Communications*, vol. 11, no. 1, p. 1000, 2020.

[98] B.-L. Zhang, D.-Y. Qin, Z.-M. Mo et al., "Hurdles of CAR-T cell-based cancer immunotherapy directed against solid tumors," *Science China Life Sciences*, vol. 59, no. 4, pp. 340–348, 2016.

[99] K. Yamamoto, A. Venida, J. Yano et al., "Autophagy promotes immune evasion of pancreatic cancer by degrading MHC-I," *Nature*, vol. 581, no. 7806, pp. 100–105, 2020.

[100] S. Jhunjhunwala, C. Hammer, and L. Delamarre, "Antigen presentation in cancer: insights into tumour immunogenicity and immune evasion," *Nature Reviews Cancer*, vol. 21, no. 5, pp. 298–312, 2021.

[101] J. Wu, H. Zhang, Y. Zheng et al., "The long noncoding RNA MALAT1 induces tolerogenic dendritic cells and regulatory T cells via miR155/dendritic cell-specific intercellular adhesion molecule-3 grabbing nonintegrin/IL10 axis," *Frontiers in Immunology*, vol. 9, p. 1847, 2018.

[102] Q.-M. Wang, G.-Y. Lian, Y. Song, Y.-F. Huang, and Y. Gong, "LncRNA MALAT1 promotes tumorigenesis and immune escape of diffuse large B cell lymphoma by sponging miR-195," *Life Sciences*, vol. 231, Article ID 116335, 2019.

[103] V. Pistoia, F. Morandi, X. Wang, and S. Ferrone, "Soluble HLA-G: are they clinically relevant?" *Seminars in Cancer Biology*, vol. 17, no. 6, pp. 469–479, 2007.

[104] B. Song, Z. Guan, F. Liu, D. Sun, K. Wang, and H. Qu, "Long non-coding RNA HOTAIR promotes HLA-G expression via inhibiting miR-152 in gastric cancer cells," *Biochemical and Biophysical Research Communications*, vol. 464, no. 3, pp. 807–813, 2015.

[105] F. Ma, Y.-Y. Lei, M.-G. Ding, L.-H. Luo, Y.-C. Xie, and X.-L. Liu, "LncRNA NEAT1 interacted with DNMT1 to regulate malignant phenotype of cancer cell and cytotoxic T cell infiltration via epigenetic inhibition of p53, cGAS, and STING in lung cancer," *Frontiers in Genetics*, vol. 11, p. 250, 2020.

[106] Y.-Y. Tseng, B. S. Moriarity, W. Gong et al., "PVT1 dependence in cancer with MYC copy-number increase," *Nature*, vol. 512, no. 7512, pp. 82–86, 2014.

[107] J. Guo, C. Hao, C. Wang, and L. Li, "Long noncoding RNA PVT1 modulates hepatocellular carcinoma cell proliferation

and apoptosis by recruiting EZH2," *Cancer Cell International*, vol. 18, p. 98, 2018.

[108] L. Wan, M. Sun, G.-J. Liu et al., "Long noncoding RNA PVT1 promotes non-small cell lung cancer cell proliferation through epigenetically regulating LATS2 expression," *Molecular Cancer Therapeutics*, vol. 15, no. 5, pp. 1082–1094, 2016.

[109] O. O. Ogunwobi and A. Kumar, "Chemoresistance mediated by ceRNA networks associated with the PVT1 locus," *Frontiers in Oncology*, vol. 9, p. 834, 2019.

[110] W. Jiang, Y. He, Y. Shi et al., "MicroRNA-1204 promotes cell proliferation by regulating PITX1 in non-small-cell lung cancer," *Cell Biology International*, vol. 43, no. 3, pp. 253–264, 2019.

[111] L. Zheng, X. Li, Y. Gu, X. Lv, and T. Xi, "The 3′UTR of the pseudogene CYP4Z2P promotes tumor angiogenesis in breast cancer by acting as a ceRNA for CYP4Z1," *Breast Cancer Research and Treatment*, vol. 150, no. 1, pp. 105–118, 2015.

[112] J. Yang, T. Li, C. Gao et al., "FOXO1 3′UTR functions as a ceRNA in repressing the metastases of breast cancer cells via regulating miRNA activity," *FEBS Letters*, vol. 588, no. 17, pp. 3218–3224, 2014.

[113] Z. Zhang, Z. Zhu, K. Watabe et al., "Negative regulation of lncRNA GAS5 by miR-21," *Cell Death & Differentiation*, vol. 20, no. 11, pp. 1558–1568, 2013.

[114] J.-H. Yuan, F. Yang, F. Wang et al., "A long noncoding RNA activated by TGF-β promotes the invasion-metastasis cascade in hepatocellular carcinoma," *Cancer Cell*, vol. 25, no. 5, pp. 666–681, 2014.

[115] G. Eades, B. Wolfson, Y. Zhang, Q. Li, Y. Yao, and Q. Zhou, "lincRNA-RoR and miR-145 regulate invasion in triple-negative breast cancer via targeting ARF6," *Molecular Cancer Research*, vol. 13, no. 2, pp. 330–338, 2015.

[116] X. Kong, Y. Duan, Y. Sang et al., "LncRNA-CDC6 promotes breast cancer progression and function as ceRNA to target CDC6 by sponging microRNA-215," *Journal of Cellular Physiology*, vol. 234, no. 6, pp. 9105–9117, 2019.

[117] X. Luan and Y. Wang, "LncRNA XLOC_006390 facilitates cervical cancer tumorigenesis and metastasis as a ceRNA against miR-331-3p and miR-338-3p," *Journal of Gynecologic Oncology*, vol. 29, no. 6, p. e95, 2018.

[118] D. Li, Z.-K. Yang, J.-Y. Bu et al., "OCT4B modulates OCT4A expression as ceRNA in tumor cells," *Oncology Reports*, vol. 33, no. 5, pp. 2622–2630, 2015.

[119] G. Huang, H. Zhu, Y. Shi, W. Wu, H. Cai, and X. Chen, "Cir-ITCH plays an inhibitory role in colorectal cancer by regulating the wnt/beta-catenin pathway," *PLoS One*, vol. 10, no. 6, Article ID e0131225, 2015.

[120] X. Zhou, Q. Gao, J. Wang, X. Zhang, K. Liu, and Z. Duan, "Linc-RNA-RoR acts as a "sponge" against mediation of the differentiation of endometrial cancer stem cells by microRNA-145," *Gynecologic Oncology*, vol. 133, no. 2, pp. 333–339, 2014.

[121] Y. Hu, J. Wang, J. Qian, X. Kong, J. Tang, and Y. Wang, "Long noncoding RNA GAPLINC regulates CD44-dependent cell invasiveness and associates with poor prognosis of gastric cancer," *Cancer Research*, vol. 74, pp. 6890–6902, 2014.

[122] X. H. Liu, M. Sun, F. Q. Nie et al., "Lnc RNA HOTAIR functions as a competing endogenous RNA to regulate HER2 expression by sponging miR-331-3p in gastric cancer," *Molecular Cancer*, vol. 13, p. 92, 2014.

[123] G. Zhang, S. Li, J. Lu et al., "LncRNA MT1JP functions as a ceRNA in regulating FBXW7 through competitively binding to miR-92a-3p in gastric cancer," *Molecular Cancer*, vol. 17, p. 87, 2018.

[124] L. Deng, S. B. Yang, F. F. Xu, and J. H. Zhang, "Long noncoding RNA CCAT1 promotes hepatocellular carcinoma progression by functioning as let-7 sponge," *Journal of Experimental & Clinical Cancer Research: Climate Research*, vol. 34, p. 18, 2015.

[125] F. H. C. Tsang, S. L. K. Au, L. Wei et al., "Long non-coding RNA HOTTIP is frequently up-regulated in hepatocellular carcinoma and is targeted by tumour suppressive miR-125b," *Liver International*, vol. 35, no. 5, pp. 1597–1606, 2014.

[126] J. Tang, H. Zhuo, X. Zhang et al., "A novel biomarker Linc00974 interacting with KRT19 promotes proliferation and metastasis in hepatocellular carcinoma," *Cell Death & Disease*, vol. 5, p. e1549, 2014.

[127] F. Wang, H.-Q. Ying, B.-S. He et al., "Upregulated lncRNA-UCA1 contributes to progression of hepatocellular carcinoma through inhibition of miR-216b and activation of FGFR1/ERK signaling pathway," *Oncotarget*, vol. 6, no. 10, pp. 7899–7917, 2015.

[128] H. Peng, M. Ishida, L. Li et al., "Pseudogene INTS6P1 regulates its cognate gene INTS6 through competitive binding of miR-17-5p in hepatocellular carcinoma," *Oncotarget*, vol. 6, no. 8, pp. 5666–5677, 2015.

[129] C.-L. Chen, Y.-W. Tseng, J.-C. Wu et al., "Suppression of hepatocellular carcinoma by baculovirus-mediated expression of long non-coding RNA PTENP1 and MicroRNA regulation," *Biomaterials*, vol. 44, pp. 71–81, 2015.

[130] B. Li, R. Mao, C. Liu, W. Zhang, Y. Tang, and Z. Guo, "LncRNA FAL1 promotes cell proliferation and migration by acting as a CeRNA of miR-1236 in hepatocellular carcinoma cells," *Life Sciences*, vol. 197, pp. 122–129, 2018.

[131] J. Yang, Q. Qiu, X. Qian et al., "Long noncoding RNA LCAT1 functions as a ceRNA to regulate RAC1 function by sponging miR-4715-5p in lung cancer," *Molecular Cancer*, vol. 18, no. 1, p. 171, 2019.

[132] Z.-Q. Zheng, Z.-X. Li, G.-Q. Zhou et al., "Long noncoding RNA FAM225A promotes nasopharyngeal carcinoma tumorigenesis and metastasis by acting as ceRNA to sponge miR-590-3p/miR-1275 and upregulate ITGB3," *Cancer Research*, vol. 79, no. 18, pp. 4612–4626, 2019.

[133] L. Yi, L. Ouyang, S. Wang, S. S. Li, and X. M. Yang, "Long noncoding RNA PTPRG-AS1 acts as a microRNA-194-3p sponge to regulate radiosensitivity and metastasis of nasopharyngeal carcinoma cells via PRC1," *Journal of Cellular Physiology*, vol. 234, no. 10, pp. 19088–19102, 2019.

[134] J. Peng, F. Liu, H. Zheng, Q. Wu, and S. Liu, "Long non-coding RNA ZFAS1 promotes tumorigenesis and metastasis in nasopharyngeal carcinoma by sponging miR-892b to upregulate LPAR1 expression," *Journal of Cellular and Molecular Medicine*, vol. 24, no. 2, pp. 1437–1450, 2020.

[135] K. Liu, L. Guo, Y. Guo et al., "AEG-1 3′-untranslated region functions as a ceRNA in inducing epithelial-mesenchymal transition of human non-small cell lung cancer by regulating miR-30a activity," *European Journal of Cell Biology*, vol. 94, no. 1, pp. 22–31, 2015.

[136] F. Tao, X. Tian, M. Lu, and Z. Zhang, "A novel lncRNA, Lnc-OC1, promotes ovarian cancer cell proliferation and migration by sponging miR-34a and miR-34c," *Journal of Genetics and Genomics*, vol. 45, no. 3, pp. 137–145, 2018.

[137] J. R. Prensner, W. Chen, S. Han et al., "The long non-coding RNA PCAT-1 promotes prostate cancer cell proliferation through cMyc," *Neoplasia*, vol. 16, no. 11, pp. 900–908, 2014.

[138] Y. Yu, F. Gao, Q. He, G. Li, and G. Ding, "lncRNA UCA1 functions as a ceRNA to promote prostate cancer progression via sponging miR143," *Molecular Therapy—Nucleic Acids*, vol. 19, pp. 751–758, 2020.

[139] C.-J. Shen, Y.-M. Cheng, and C.-L. Wang, "LncRNA PVT1 epigenetically silences miR-195 and modulates EMT and chemoresistance in cervical cancer cells," *Journal of Drug Targeting*, vol. 25, no. 7, pp. 637–644, 2017.

[140] L. Chen, X. Han, Z. Hu, and L. Chen, "The PVT1/miR-216b/beclin-1 regulates cisplatin sensitivity of NSCLC cells via modulating autophagy and apoptosis," *Cancer Chemotherapy and Pharmacology*, vol. 83, no. 5, pp. 921–931, 2019.

[141] E. Palmerini, R. L. Jones, E. Marchesi et al., "Gemcitabine and docetaxel in relapsed and unresectable high-grade osteosarcoma and spindle cell sarcoma of bone," *BMC Cancer*, vol. 16, p. 280, 2016.

[142] X. Zhang, W. Feng, J. Zhang et al., "Long non-coding RNA PVT1 promotes epithelial-mesenchymal transition via the TGF-/smad pathway in pancreatic cancer cells," *Oncology Reports*, vol. 40, no. 2, pp. 1093–1102, 2018.

[143] J. Chen, Y. Yu, H. Li et al., "Long non-coding RNA PVT1 promotes tumor progression by regulating the miR-143/HK2 axis in gallbladder cancer," *Molecular Cancer*, vol. 18, p. 33, 2019.

[144] T. Lan, X. Yan, Z. Li et al., "Long non-coding RNA PVT I serves as a competing endogenous RNA for miR-I86-5p to promote the tumorigenesis and metastasis of hepatocellular carcinoma," *Tumor Biology*, vol. 39, no. 6, pp. 1–11, Article ID 705338, 2017.

[145] D. Li, C. Li, Y. Chen et al., "LncRNA HOTAIR induces sunitinib resistance in renal cancer by acting as a competing endogenous RNA to regulate autophagy of renal cells," *Cancer Cell International*, vol. 20, no. 1, p. 338, 2020.

[146] X. Dong, Z. Fang, M. Yu et al., "Knockdown of long non-coding RNA HOXA-AS2 suppresses chemoresistance of acute myeloid leukemia via the miR-520c-3p/S100A4 axis," *Cellular Physiology and Biochemistry*, vol. 51, no. 2, pp. 886–896, 2018.

[147] B. Liu, S. Wu, J. Ma et al., "lncRNA GAS5 reverses EMT and tumor stem cell-mediated gemcitabine resistance and metastasis by targeting miR-221/SOCS3 in pancreatic cancer," *Molecular Therapy—Nucleic Acids*, vol. 13, pp. 472–482, 2018.

Research Article

Identification of Differentially Expressed Circular RNAs as miRNA Sponges in Lung Adenocarcinoma

Yuechao Liu,[1] Xin Wang,[1] Lulu Bi,[1] Hongbo Huo,[1] Shi Yan,[1] Yimeng Cui,[1] Yaowen Cui,[1] Ruixue Gu,[1] Dexin Jia,[1] Shuai Zhang,[1] Li Cai ⓘ,[1] Xiaomei Li ⓘ,[2] and Ying Xing ⓘ[1]

[1]*The Fourth Department of Medical Oncology, Harbin Medical University Cancer Hospital, 150 Haping Road, Harbin 150040, China*
[2]*Department of Pathology, Harbin Medical University Cancer Hospital, 150 Haping Road, Harbin 150040, China*

Correspondence should be addressed to Li Cai; caili@ems.hrbmu.edu.cn, Xiaomei Li; fanliwenqi@163.com, and Ying Xing; xingying0618@163.com

Received 12 June 2021; Revised 17 August 2021; Accepted 23 August 2021; Published 10 September 2021

Academic Editor: Zhiqian Zhang

Background. Circular RNAs (circRNAs) may function as the decoys for microRNAs (miRNAs) or proteins, the templates for translation, and the sources of pseudogene generation. The purpose of this study is to determine the diagnostic circRNAs, which are related to lung adenocarcinoma (LUAD), that adsorb miRNAs on the basis of the competing endogenous RNA (ceRNA) hypothesis. *Methods.* The differentially expressed circRNAs (DEcircRNAs) in LUAD were revealed by the microarray data (GSE101586 and GSE101684) that were obtained from the Gene Expression Omnibus (GEO) database. The miRNAs that were targeted by the DEcircRNAs were predicted with the CircInteractome, and the target mRNAs of the miRNAs were found by the miRDB and the TargetScan. The ceRNA network was built by the Cytoscape. The potential biological roles and the regulatory mechanisms of the circRNAs were investigated by the Gene Ontology (GO) enrichment analysis and the Kyoto Encyclopedia of Genes and Genomes (KEGG) analysis. The expression of the host genes of circRNAs was examined by the Ualcan. The survival analysis was performed by the Kaplan–Meier plotter. *Results.* In comparison with normal lung tissues, LUAD tissues contained 7 overlapping cancer-specific DEcircRNAs with 294 miRNA response elements (MREs). Among the 7 DEcircRNAs, 3 circRNAs (hsa_circ_0072088, hsa_circ_0003528, and hsa_circ_0008274) were upregulated and 4 circRNAs (hsa_circ_0003162, hsa_circ_0029426, hsa_circ_0049271, and hsa_circ_0043256) were downregulated. A circRNA-miRNA-mRNA regulatory network, which included 33 differentially expressed miRNAs (DEmiRNAs) and 2007 differentially expressed mRNAs (DEmRNAs), was constructed. These mRNAs were enriched in the biological function of cell-cell adhesion, response to hypoxia, and stem cell differentiation and were involved in the PI3K-Akt signaling, HIF-1 signaling, and cAMP signaling pathways. *Conclusion.* Our results indicated that 7 DEcircRNAs could have diagnostic value for LUAD. Additionally, the circRNAs-mediated ceRNA network might provide a novel perspective into unraveling the pathogenesis and progression of LUAD.

1. Introduction

Lung cancer is the second most commonly diagnosed cancer and the primary cause of cancer-related death worldwide [1]. In 2020, over 2.2 million new lung cancer cases and 1.8 million lung-cancer-related deaths were estimated [1]. Non-small-cell lung cancer (NSCLC) cases account for 85% of lung cancer, and the most common histological type of NSCLC is lung adenocarcinoma (LUAD) [2]. In spite of the improvement in chemotherapy and radiotherapy, the 5-year

survival rate of LUAD remains below 20% [3]. Therefore, it is critical to clarify the underlying mechanisms and therapeutic targets of LUAD, which are beneficial for the diagnosis and prognostic evaluation [4].

An increasing amount of evidence has shown that noncoding RNAs such as long noncoding RNAs (lncRNAs), pseudogenic RNAs, and circular RNAs (circRNAs) may act as competing endogenous RNAs (ceRNAs) by competitively binding to several miRNAs [5, 6]. Compared with the traditional liner RNAs, circular RNAs (circRNAs) have a

completely closed-loop structure [7]. CircRNAs have been identified to be the miRNA sponges involved in cancer development [8–10]. CircRNAs and mRNAs compete for binding to the limited targeting miRNAs via plentiful miRNA binding sites (MREs) regions to construct a ceRNA regulatory network [11]. When mRNAs competitively bind to miRNAs, the translation process is interrupted and the stability of miRNAs is compromised [12–14]. However, circRNAs remain stable and resist the degradation by RNA exonucleases [11].

Interestingly, ceRNA regulatory networks are dysregulated and are closely related to the occurrence and progression of different types of cancers, including LUAD [11, 15–17]. For example, a previous study revealed that circRNA-ENO1 played a crucial role in glycolysis and tumor progression of LUAD by promoting the expression of its host gene ENO1 [18]. In addition, circ_EPB41L2 played a protective role by repressing proliferation, migration, and invasion through regulating CDH4 and miR-211-5p in LUAD cells [19]. Moreover, in vivo studies indicated that the overexpression of circ_EPB41L2 inhibited tumor growth by regulating miR-211-5p and CDH4 [19]. Furthermore, bioinformatics analysis, which depends on the rise of high-throughput sequencing technology, has been widely used in the research on the etiology and the underlying mechanism of cancers. To explore the tumor markers with prognostic significance, researchers need to build a comprehensive ceRNA regulatory network through the in-depth analysis of public databases. Although many bioinformatics studies have been conducted on ceRNAs, novel circRNA molecules and ceRNA networks are worth further investigation [20–22]. Further research on the ceRNA network will help to explore novel diagnostic and treatment methods of LUAD.

In the present study, we collected the expression profiles of circRNAs (GSE101586 and GSE101684), miRNAs (GSE135918 and TCGA-LUAD), and mRNAs (TCGA-LUAD) of LUAD. Seven differentially expressed and cancer-specific circRNAs in LUAD were identified by bioinformatic analysis. A circRNA-miRNA-mRNA regulatory network was constructed. Furthermore, we performed functional enrichment analysis to reveal the potential biological function and mechanism of the circRNAs, which might provide new insights into the diagnosis and treatment of LUAD.

2. Methods

2.1. Research Process Design.
The experimental design and the specific implementation scheme of the study are shown in Figure 1.

2.2. Collection of the Data from Public Database.
The Gene Expression Omnibus (GEO, https://www.ncbi.nlm.nih.gov/geo/) is a database widely applied in many fields. It involves the noncoding RNA analysis, the comparative genomic analysis, the proteomics analysis, the single nucleotide polymorphism genome analysis, and the DNA methylation status analysis. We searched for the microarray data in the GEO dataset by inputting "lung adenocarcinoma" and "circRNA" keywords. The inclusion and exclusion criteria were (1) human LUAD tissues and the adjacent normal human lung tissues, (2) microarray expression profiling of circRNA, and (3) data annotation platform and the original data matrix. Two datasets (GSE101586 and GSE101684) that satisfied the screening criteria were obtained and downloaded.

2.3. Data Processing.
The base 2 logarithm ($\log_2$) transformation was used to transform the expression value of circRNAs and the R software was used to interpret the raw microarray data. For similar circRNAs in the expression matrix, we took the average expression value of the duplicates. The information on the probe annotation of the circRNAs was downloaded from GPL19978 and GPL21825 platform files. The detailed annotation of the probe, the sample, and the platform was obtained from GEO database. We standardized original expression data by the $\log_2$ transformed. We used an R package for the differentiation analysis of the microarray data and set the thresholds of $|\log_2 \text{(fold-change)}| > 1$ and $P < 0.05$ to determine the DEcircRNAs in each dataset. Then, we retained the DEcircRNAs and removed the circRNAs that were not differentially expressed.

2.4. Identification of DEcircRNAs.
When multiple probes were mapped to a certain Agilent ID, the corresponding mean value was selected. The Perl scripting was used to convert the Agilent ID to gene names. To standardize the matrix information and analyze the differential gene expression among models, we used the limma package to normalize the raw microarray data. Whereafter, the fold-change and the P value were used to determine the differentially expressed genes in the 2 datasets, the screening criteria of which were $|\log_2 \text{(fold-change)}| > 1$ and P value <0.05. We used the CircBase database to obtain the host genes related to the circRNAs [23].

2.5. Prediction of CircRNA-MicroRNA-Target Gene Networks.
The CircBase database (circbase.org/) and cancer-specific circRNAs database (CSCD, https://gb.whu.edu.cn/CSCD/) were used to predict MREs of the circRNAs that provided information on the circRNAs from multiple perspectives, including the location of circRNAs on chromosomes, the length variation of the circRNAs, and the interaction between the circRNAs and miRNAs. Specific miRNA targets were predicted based on the MicroRNA Target Prediction Database (miRDB, http://mirdb.org/) and the TargetScan (http://www.targetscan.org/vert_71/). The overlapping genes of the three databases were selected as host genes. The prognostic value of host genes were investigated by the Kaplan–Meier plotter.

2.6. GO Enrichment Analysis.
In order to understand the potential function of the circRNAs, we performed the GO enrichment analysis of target genes by DAVID (https://david.ncifcrf.gov/home.jsp). GO analysis included the
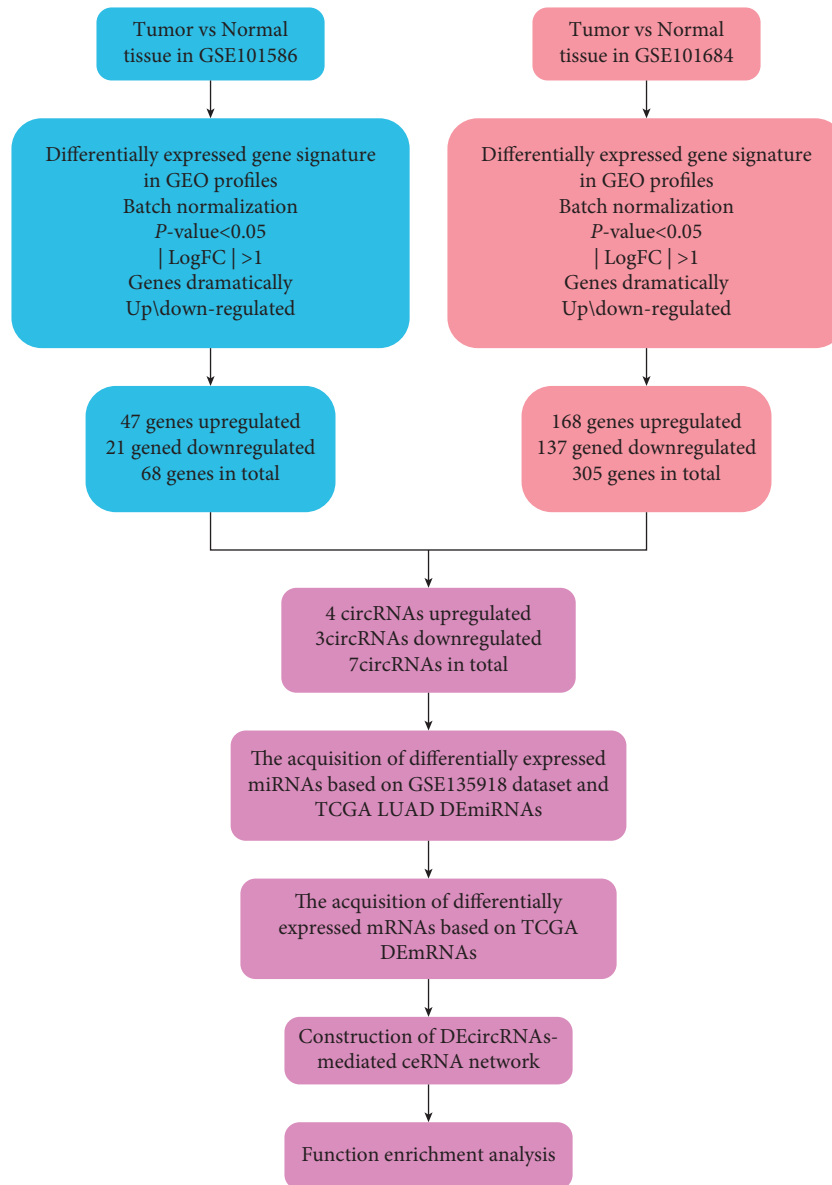
FIGURE 1: Flowchart for bioinformatics analysis of this study.

analysis of cellular components (CC), molecular functions (MF), and biological processes (BP). Each category of the GO analysis explained the different biological function of the genes. We used Sangerbox (http://www.sangerbox.com/) to visualize the results of the GO enrichment analysis.

3. Results

3.1. Identification of DEcircRNAs. We downloaded and analyzed the GSE101586 and GSE101684 microarray data by the GEO2R tool to identify the DEcircRNAs between paired NSCLC tissues and adjacent nontumor tissues. The basic information on these 2 datasets is illustrated in Table 1. We obtained 68 DEcircRNAs that included 47 upregulated and 21 downregulated circRNAs on the basis of GSE101586 dataset and 305 DEcircRNAs that consisted of 168 upregulated and 137 downregulated circRNAs on the basis of the

GSE101684 dataset (Figures 2(a) and 2(b), *P* value < 0.05 and absolute value of fold-change >1). We provided two volcano plots to visualize the DEcircRNAs (Figures 2(c) and 2(d)). The Venn diagram shown in Figure 2(e) displays the 10 overlapping DEcircRNAs between the two datasets.

The cancer-specific circRNA database (CSCD, http://gb. whu.edu.cn/CSCD) is a useful circRNA database to deduce whether particular circRNAs are cancer-specific [24]. The 7 differentially expressed and cancer-specific circRNAs in LUAD are presented in Figure 2(f).

3.2. Characterization of DEcircRNAs. As shown in Figures 3(a) and 3(b), 3 circRNAs (hsa_circ_0072088, hsa_circ_0003528, and hsa_circ_0008274) were upregulated and 4 circRNAs (hsa_circ_0003162, hsa_circ_0029426, hsa_circ_0049271, and hsa_circ_0043256) were

TABLE 1: The information of GSE101586 and GSE101684 datasets obtained from the GEO database.

Reference	Tissue	GEO	Platform	Normal	Tumor	Upregulated gene	Downregulated gene
Qiu M. et al., 2017	LUAD	GSE101586	GPL19978	5	5	47	21
Xu M. et al., 2019	LUAD	GSE101684	GPL21825	4	4	168	137
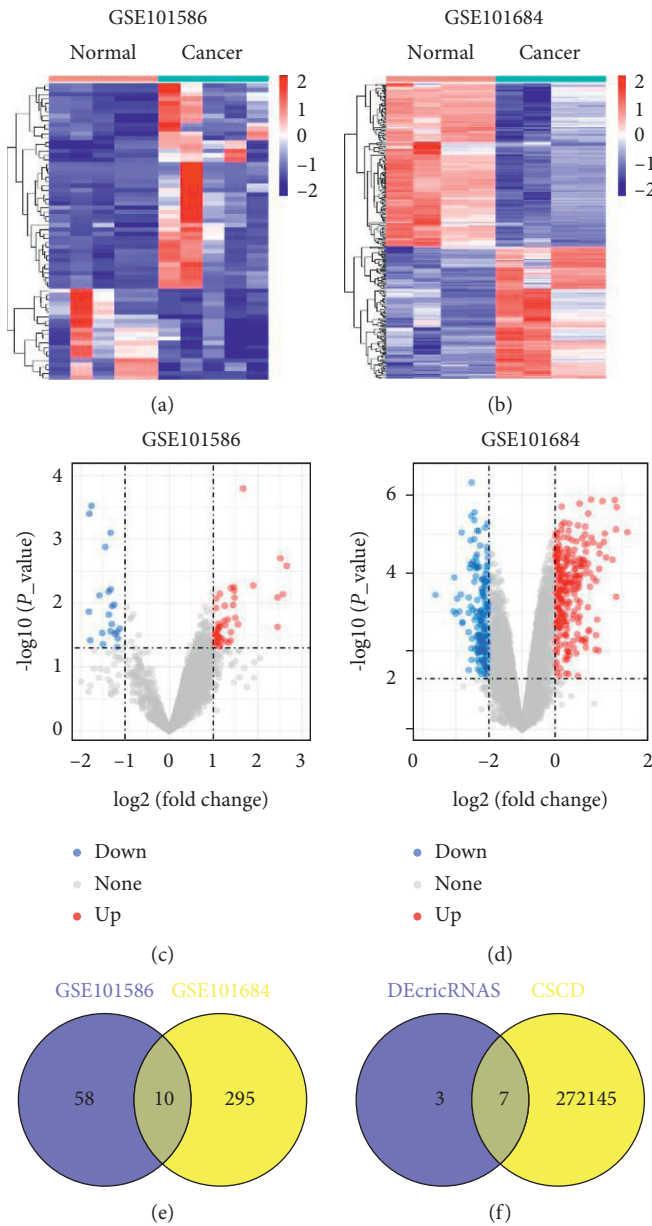
FIGURE 2: Identification of differentially expressed circRNAs in LUAD. (a, b) Hierarchical clustering heat map of the DEcircRNAs of LUAD samples compared with normal lung samples from GSE101586 and GSE101684, with absolute fold-changes >1 and P value < 0.05 as significant. (c, d) The volcano maps showed the number and distribution of the DEcircRNAs. The red dots represent the upregulated circRNAs and the blue dots indicate the downregulated circRNAs. (e) Venn diagram of the intersection of DEcircRNAs in GSE101586 and GSE101684 datasets. (f) Venn diagram of the intersection of differentially expressed and cancer-specific circRNAs based on Cancer-Specific CircRNA Database (CSCD, http://gb.whu.edu.cn/CSCD).

downregulated. In this study, we used the CircBase database to determine the location, genomic length, strand, and gene symbol of the 7 DEcircRNAs. The basic characteristics of the DEcircRNAs are listed in Table 2.

Moreover, the structural patterns of the 7 circRNAs from the CSCD database are shown in Figure 3(c). 294 MREs were predicted for the cancer-specific DEcircRNA candidates. Specifically, we found that hsa_circ_0072088 harbored 32 MREs, hsa_circ_0003528 harbored 57 MREs, hsa_circ_0008274 harbored 51 MREs, hsa_circ_0049271 harbored 38 MREs, hsa_circ_0003162 harbored 42 MREs, hsa_circ_0029426 harbored 28 MREs, and hsa_circ_0043256 harbored 48 MREs. These findings suggested that the DEcircRNAs were potential miRNA sponges (Figure 3(c)).

The DEcircRNAs were the partial fragments transcribed by the host genes. Next, we examined the expression and diagnostic and prognostic significance of the host genes of these 7 cancer-specific DEcircRNAs. The host genes of hsa_circ_0049271, hsa_circ_0029426, and hsa_circ_0072088 had diagnostic and prognostic significance (Supplementary Figure S1).

3.3. The Determination of Differentially Expressed miRNAs and Differentially Expressed mRNAs.

On the basis of the GSE135918 dataset, we determined out 624 differentially expressed miRNAs (DEmiRNAs) in LUAD. CircInteractome database was used to predict the miRNAs targeted by the 7 DEcircRNAs, and 114 miRNAs were found. Figure 4(a) illustrated GSE135918 dataset contained 2693 miRNAs, with 624 DEmiRNAs. On the other hand, the TCGA-LUAD dataset contained 2197 miRNAs and 362 DEmiRNAs (Figure 4(b)). 33 DEmiRNAs that were related to the DEcircRNAs were found by Venn analysis (Figure 4(c)). Then, by the miRDB and TargetScan databases, we searched for the target mRNAs of the DEmiRNAs targeted by the 7 DEcircRNAs. A total of 7622 target genes were bound to the 33 DEmiRNAs. On the basis of the TCGA-LUAD database, 2007 out of 7622 mRNAs were found to be differentially expressed (Figure 4(d)).

3.4. Construction of a ceRNA Network.

In previous sections, we obtained 7 DEcircRNAs, 33 DEmiRNAs, and 2007 DEmRNAs and elucidated the interaction among the DEcircRNAs, the DEmiRNAs, and the DEmRNAs. Next, we used Cytoscape 3.8.2 to visualize the circRNA-miRNA-mRNA regulatory network (Figures 5(a) and 5(b) and Supplementary Table 1).

3.5. Functional Enrichment Analysis.

The potential biological roles and regulatory mechanisms of circRNAs were investigated using GO enrichment analysis and Kyoto Encyclopedia of Genes and Genomes (KEGG) analysis. The
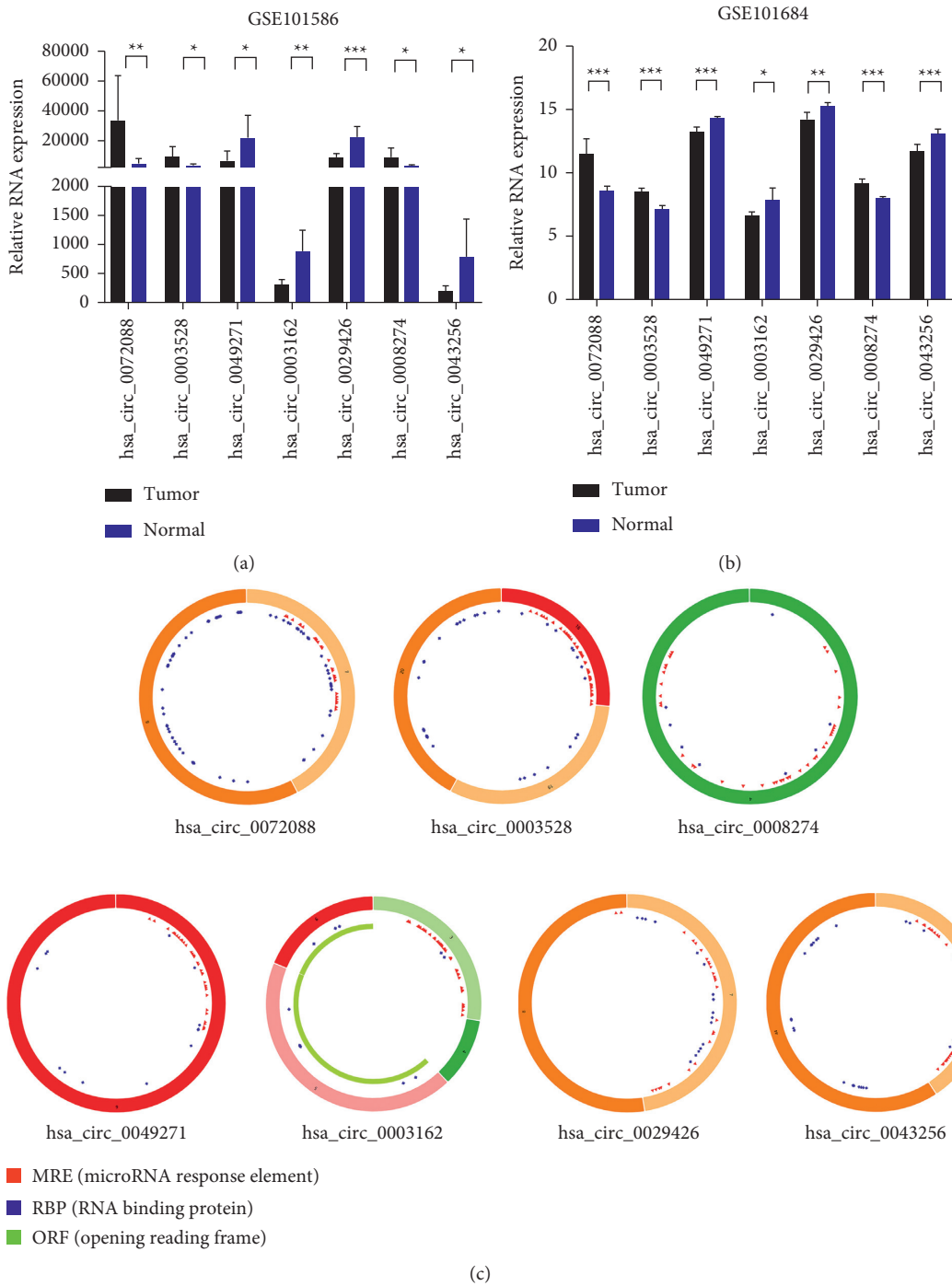
(a)

(b)

(c)

FIGURE 3: Characterization of DEcircRNAs. (a, b) The expression levels of DEcircRNAs in human LUAD tissues and normal lung samples were analyzed based on GSE101586 and GSE101684 datasets. The differences were compared by paired t-test. Mean ± SEM, $n = 3$, $^*P < 0.05$; $^{**}P < 0.01$; $^{***}P < 0.001$. (c) Structural patterns of the 7 circRNAs: hsa_circ_0072088, hsa_circ_0003528, hsa_circ_0008274, hsa_-circ_0049271, hsa_circ_0003162, hsa_circ_0029426, and hsa_circ_0043256. The green part represents the open reading frame (ORF) of circRNAs. The blue part is the place where circRNA binds to the proteins. The red small triangle represents the binding position of the circRNA to the miRNA.

mRNAs were enriched in the biological function of cell-cell adhesion, response to hypoxia, and stem cell differentiation (Figure 6(a) and Supplementary Figure S2(a)). Moreover, the mRNAs were involved in the PI3K-Akt signaling, HIF-1 signaling, and cAMP signaling pathways (Figure 6(b) and Supplementary Figure S2(b)).

TABLE 2: The information of the 7 cancer-specific DEcircRNAs.

Genes total	Up-/downregulated	Position	Genomic length	Gene symbol	Strand
hsa_circ_0029426	Down	chr12 : 131357380-131357465	85	RAN	+
hsa_circ_0043256	Down	chr17 : 35604934-35609962	5028	ACACA	−
hsa_circ_0049271	Down	chr19 : 10610070-10610756	686	KEAP1	−
hsa_circ_0003162	Down	chr7 : 33185853-33217203	31350	BBS9	+
hsa_circ_0003528	Up	chr5 : 134032815-134044578	11763	SEC24A	+
hsa_circ_0072088	Up	chr5 : 32379220-32388780	9560	ZFR	−
hsa_circ_0008274	Up	chr13 : 96485180-96489456	4276	UGGT2	−

(a)

(b)

(c)

(d)
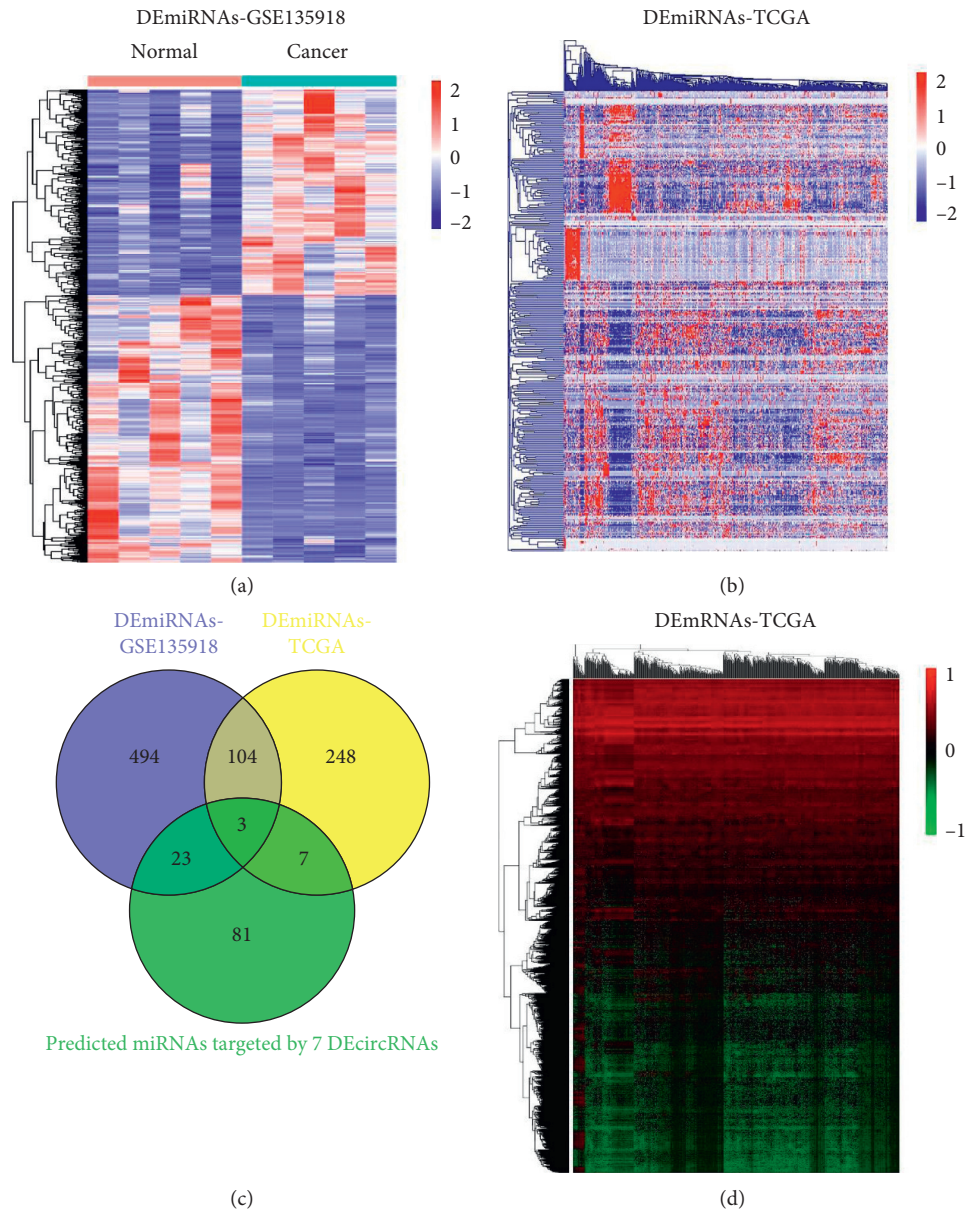
FIGURE 4: Identification of differentially expressed miRNAs and mRNAs. (a, b) Hierarchical clustering heat map of the DEmiRNAs of LUAD samples compared with normal lung samples from GSE135918 dataset (a) and TCGA-LUAD dataset (b). (c) Venn diagram of the union of DEmiRNAs in GSE135918 dataset and TCGA-LUAD dataset. (d) Hierarchical clustering heat map of the DEmRNAs of LUAD samples compared with normal lung samples based on TCGA-LUAD dataset.
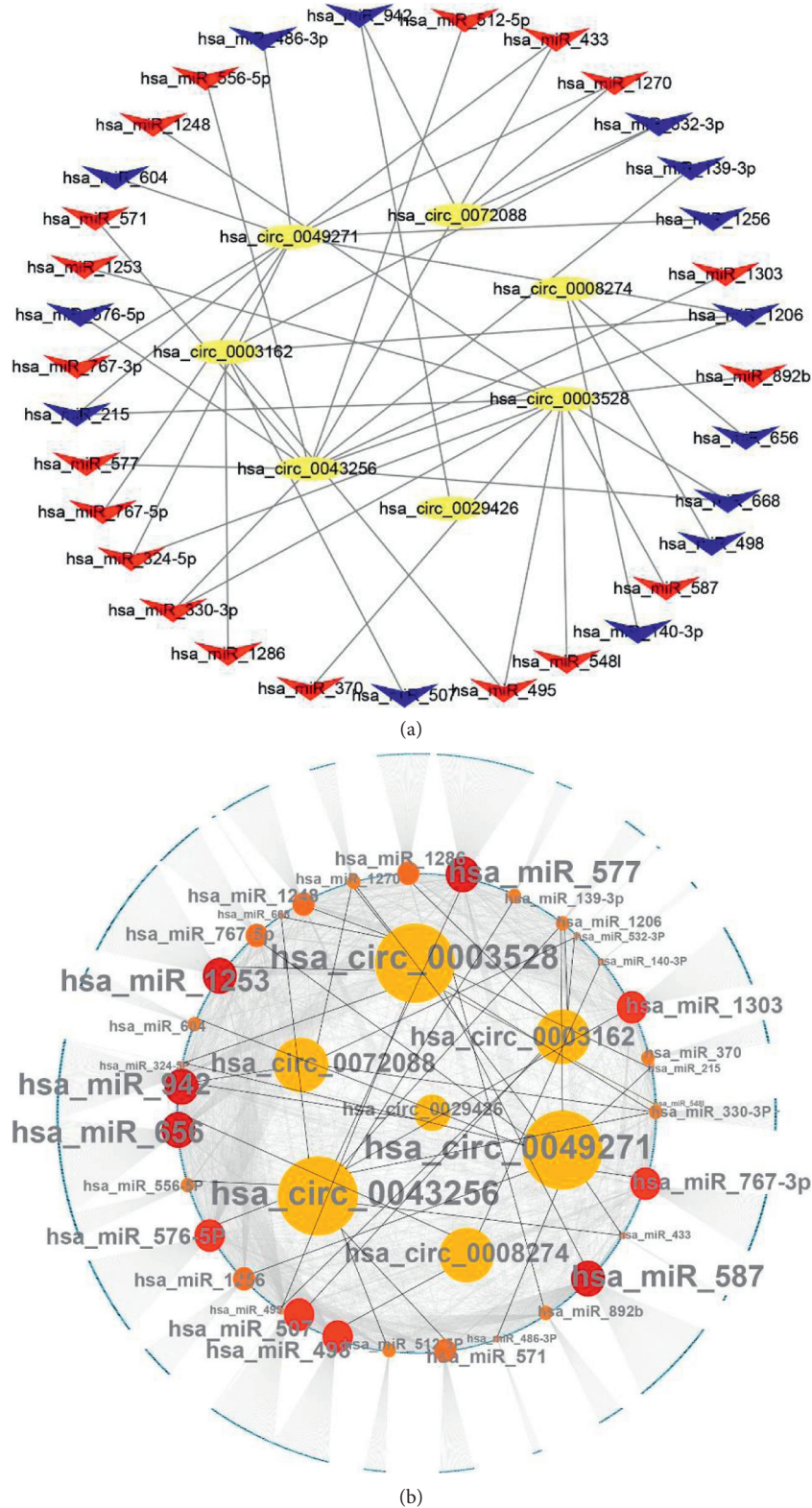
(a)

(b)

FIGURE 5: Construction of circRNA-miRNA-mRNA networks. (a) The relationship between 7 DEcircRNAs and their interacting DEmiRNAs ($n = 33$). Red, upregulation. Blue, downregulation. (b) circRNA-miRNA-mRNA regulatory networks using their interactions with Cytoscape software (version 3.8.2). Sizes of circles represent the weight of connection of circRNAs and miRNAs. The black lines connect circRNAs with miRNAs. The grey lines connect miRNAs with mRNAs.
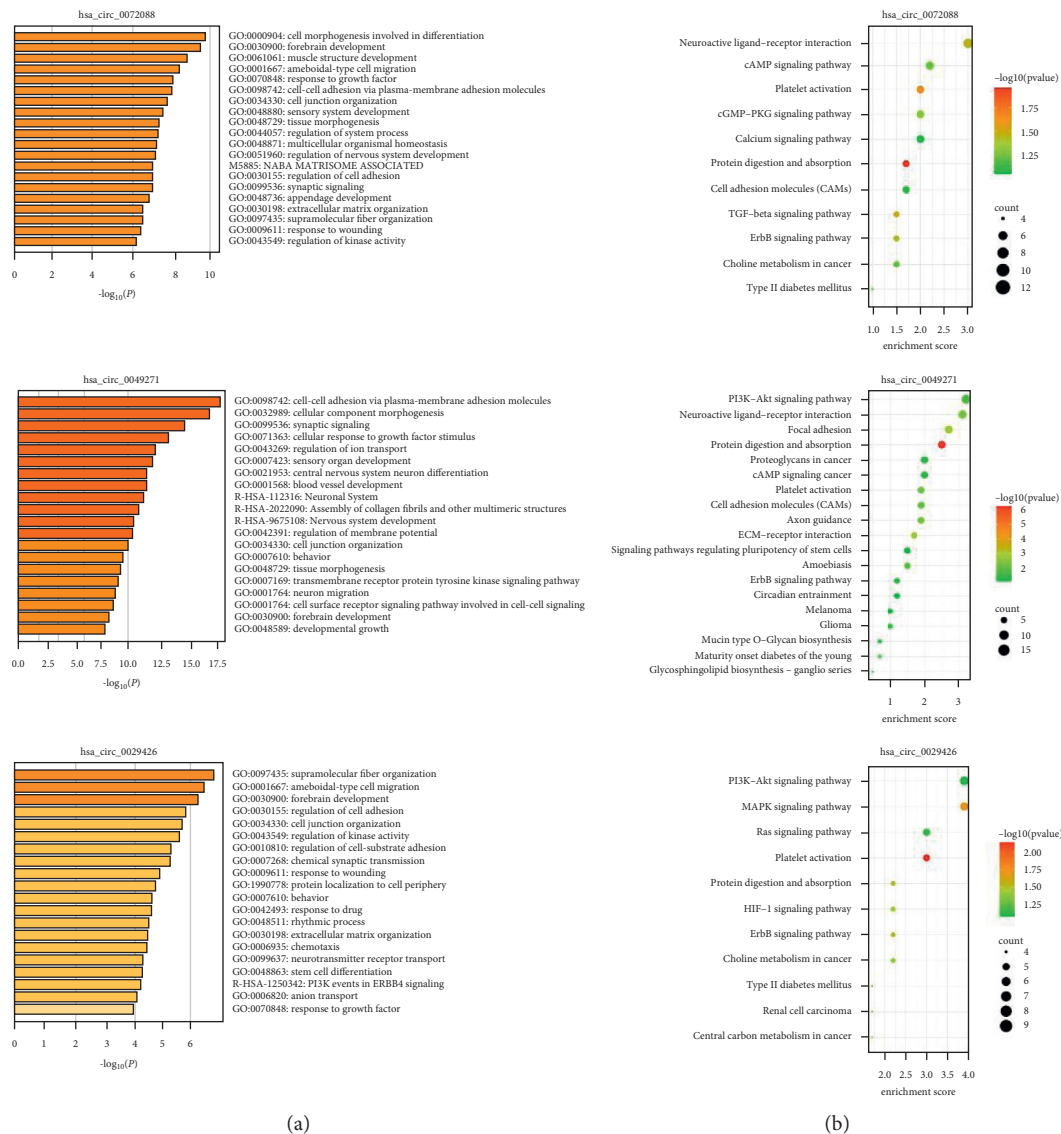
(a)　　　　　　　　　　　　　　　(b)

Figure 6: Functional enrichment analysis of targeted mRNA. (a) GO enrichment analysis and (b) KEGG pathway enrichment analysis of DEmRNAs of hsa_circ_0072088, hsa_circ_0049271, and hsa_circ_0029426.

4. Discussion

In view of the high mortality and the extremely low survival rate of LUAD, the determination of the specific biomarkers for the diagnosis and the treatment of LUAD remains critical [4, 25]. Previous studies found that noncoding RNAs, especially circRNAs, contribute to the malignant progression (the metastasis, proliferation, and tumor growth) of multiple types of cancer [26–30]. CircRNAs have high stability due to the unique covalent closed-loop structure that allows the circRNAs to resist the RNase R degradation [31]. Many studies reported that the ceRNA regulatory networks that were constructed by circRNAs contained substantial diagnosis and prognostic value. In our study, we comprehensively analyzed the ceRNA network for reliable diagnostic markers. Similarly, Li et al. [32] selected the combination of GSE101586, GSE101684, and GSE112214 and identified the

DEcircRNAs in the patients with early-stage NSCLC. By utilizing the CSCD, we identified that the differentially expressed and cancer-specific cirRNAs in LUAD were potential miRNA sponges for the first time.

Subsequently, the function enrichment analysis of mRNAs suggested the relevant biological function and pathways for LUAD. Our study revealed that the target mRNAs selected from the ceRNA network were enriched in the biological function of cell-cell adhesion, response to hypoxia, and stem cell differentiation. Moreover, the target mRNAs were involved in the PI3K-Akt signaling, HIF-1 signaling, and cAMP signaling pathways. Then, we applied bioinformatics analysis to explore the structure of circRNAs and used CircBase and CSCD database to figure out the location, genomic length, strand, and gene symbol of the circRNAs. The cancer-specific circRNAs that exhibited the MRE, the RNA binding protein (RBP), and the open reading

frame (ORF) were determined to be ceRNAs. MREs are observed on lncRNAs, circRNAs, and protein-coding mRNAs, which can compete for the miRNAs, form a ceRNA regulatory network, and absorb RBPs [12]. A large amount of evidence identified that noncoding RNAs played a role in regulating gene expression at both the transcriptional and posttranscriptional level by the physical interaction with RBPs or other noncoding RNAs [33]. On the other hand, RBPs contribute to circRNA biogenesis of exons circularization through narrowing the distance between the donor site and the receptor site by binding to the introns on the flank regions [34]. Additionally, ORF advances the translation of engineered circRNAs [35].

Out of the 7 DEcircRNAs identified in this study, 3 DEcircRNAs had been reported in previous studies [36, 37]. Hsa_circ_0072088 was identified as a ceRNA of miR-377-5p via upregulating NOVA2 to expedite the proliferation and metastasis of NSCLC [36]. Moreover, hsa_circ_0008274 and hsa_circ_0043256 that were derived from the ceRNA network were reported to be involved in the cancer progression [37]. Bioinformatics-related analysis suggested the significance of the understanding of the potential mechanisms of circRNAs-miRNAs-target gene network [10, 38–40].

Although we have described the significance of the ceRNA network in the clinical diagnosis of LUAD, the investigation of the prognostic value and clinical parameters is urgently needed to validate our findings in the samples from the patients with clinical LUAD. Moreover, molecular experiments need to be conducted to validate the biological function and the molecular mechanisms of the identified genes in LUAD cell lines.

5. Conclusions

In summary, by bioinformatics analysis, we identified 3 significantly upregulated circRNAs and 4 significantly downregulated circRNAs from public databases, which indicated the potential of the DEcircRNAs for the noninvasive biomarkers for the LUAD diagnosis. In future study, the biological function and the molecular regulatory mechanisms of the DEcircRNAs need to be experimentally validated.

Data Availability

All data generated or analyzed during this study are included in this published article and its supplementary information files.

Conflicts of Interest

The authors declare that they have no conflicts of interest.

Authors' Contributions

Yuechao Liu, Xin Wang, and Lulu Bi contributed equally to this work.

Supplementary Materials

Supplementary Figure S1: the diagnostic and prognostic significance of the host gene. (a) The expression of the host genes of hsa_circ_0049271, hsa_circ_0029426, and hsa_circ_0072088 in The Cancer Genome Atlas (TCGA)-LUAD dataset. (b) Survival analysis for the host genes of the three circRNAs in LUAD patients was performed using the Kaplan–Meier plotter. $^{*}P < 0.05$; $^{**}P < 0.01$; $^{***}P < 0.001$. Supplementary Figure S2: (a) GO enrichment analysis and (b) KEGG pathway enrichment analysis of DEmRNAs of hsa_circ_0003162, hsa_circ_0003528, hsa_circ_0008274, and hsa_circ_0043256. Supplementary Table 1: the construction of a circRNA-miRNA-mRNA regulatory network. (*Supplementary Materials*)

References

[1] H. Sung, J. Ferlay, R. L. Siegel et al., "Global cancer statistics 2020: GLOBOCAN estimates of incidence and mortality worldwide for 36 cancers in 185 countries," *CA: A Cancer Journal for Clinicians*, vol. 71, no. 3, pp. 209–249, 2021.

[2] B. D. Hutchinson, G. S. Shroff, M. T. Truong, and J. P. Ko, "Spectrum of lung adenocarcinoma," *Seminars in Ultrasound, CT and MRI*, vol. 40, no. 3, pp. 255–264, 2019.

[3] C. H. Y. Cheung and H.-F. Juan, "Quantitative proteomics in lung cancer," *Journal of Biomedical Science*, vol. 24, no. 1, p. 37, 2017.

[4] D. Greto, M. Loi, F. Terziani et al., "A matched cohort study of radio-chemotherapy versus radiotherapy alone in soft tissue sarcoma patients," *La radiologia medica*, vol. 124, no. 4, pp. 301–308, 2019.

[5] X. Qi, D.-H. Zhang, N. Wu, J.-H. Xiao, X. Wang, and W. Ma, "ceRNA in cancer: possible functions and clinical implications," *Journal of Medical Genetics*, vol. 52, no. 10, pp. 710–718, 2015.

[6] F. Tao, X. Tian, M. Lu, and Z. Zhang, "A novel lncRNA, Lnc-OC1, promotes ovarian cancer cell proliferation and migration by sponging miR-34a and miR-34c," *Journal of Genetics and Genomics*, vol. 45, no. 3, pp. 137–145, 2018.

[7] W. R. Jeck and N. E. Sharpless, "Detecting and characterizing circular RNAs," *Nature Biotechnology*, vol. 32, no. 5, pp. 453–461, 2014.

[8] A. C. Panda, "Circular RNAs act as miRNA sponges," *Advances in Experimental Medicine and Biology*, vol. 1087, pp. 67–79, 2018.

[9] X. Cai, L. Lin, Q. Zhang, W. Wu, and A. Su, "Bioinformatics analysis of the circRNA-miRNA-mRNA network for non-

small cell lung cancer," *Journal of International Medical Research*, vol. 48, 2020.

[10] L. Yu and Y. Liu, "circRNA_0016624 could sponge miR-98 to regulate BMP2 expression in postmenopausal osteoporosis," *Biochemical and Biophysical Research Communications*, vol. 516, no. 2, pp. 546–550, 2019.

[11] Z.-Z. Liang, C. Guo, M.-M. Zou, P. Meng, and T.-T. Zhang, "circRNA-miRNA-mRNA regulatory network in human lung cancer: An update," *Cancer Cell International*, vol. 20, no. 1, p. 173, 2020.

[12] Y. Cheng, Y. Su, S. Wang et al., "Identification of circRNA-lncRNA-miRNA-mRNA competitive endogenous RNA network as novel prognostic markers for acute myeloid leukemia," *Genes (Basel)*, vol. 11, 2020.

[13] X. Tian and Z. Zhang, "miR-191/DAB2 axis regulates the tumorigenicity of estrogen receptor-positive breast cancer," *IUBMB Life*, vol. 70, no. 1, pp. 71–80, 2018.

[14] X. Tian, F. Tao, B. Zhang, J.-T. Dong, and Z. Zhang, "The miR-203/SNAI2 axis regulates prostate tumor growth, migration, angiogenesis and stemness potentially by modulating GSK-3β/β-CATENIN signal pathway," *IUBMB Life*, vol. 70, no. 3, pp. 224–236, 2018.

[15] L. Qiu, X. Tan, J. Lin et al., "CDC27 induces metastasis and invasion in colorectal cancer via the promotion of epithelial-to-mesenchymal transition," *Journal of Cancer*, vol. 8, no. 13, pp. 2626–2635, 2017.

[16] S. Wang, Y. Zhang, Q. Cai et al., "Circular RNA FOXP1 promotes tumor progression and Warburg effect in gallbladder cancer by regulating PKLR expression," *Molecular Cancer*, vol. 18, no. 1, p. 145, 2019.

[17] Y. Sang, B. Chen, X. Song et al., "circRNA_0025202 regulates tamoxifen sensitivity and tumor progression via regulating the miR-182-5p/FOXO3a Axis in breast cancer," *Molecular Therapy*, vol. 27, no. 9, pp. 1638–1652, 2019.

[18] J. Zhou, S. Zhang, Z. Chen, Z. He, Y. Xu, and Z. Li, "CircRNA-ENO1 promoted glycolysis and tumor progression in lung adenocarcinoma through upregulating its host gene ENO1," *Cell Death & Disease*, vol. 10, no. 12, p. 885, 2019.

[19] S. J. Zhang, J. Ma, J. C. Wu, Z. Z. Hao, Y. N. Zhang., and Y. J Zhang, "CircRNA EPB41L2 inhibits tumorigenicity of lung adenocarcinoma through regulating CDH4 by miR-211-5p," *European Review for Medical and Pharmacological Sciences*, vol. 24, pp. 3749–3760, 2020.

[20] Y. Zhong, Y. Du, X. Yang et al., "Circular RNAs function as ceRNAs to regulate and control human cancer progression," *Molecular Cancer*, vol. 17, no. 1, p. 79, 2018.

[21] R.-S. Zhou, E.-X. Zhang, Q.-F. Sun et al., "Integrated analysis of lncRNA-miRNA-mRNA ceRNA network in squamous cell carcinoma of tongue," *BMC Cancer*, vol. 19, no. 1, p. 779, 2019.

[22] R. Yang, L. Xing, M. Wang, H. Chi, L. Zhang, and J. Chen, "Comprehensive analysis of differentially expressed profiles of lncRNAs/mRNAs and miRNAs with associated ceRNA networks in triple-negative breast cancer," *Cellular Physiology and Biochemistry*, vol. 50, no. 2, pp. 473–488, 2018.

[23] P. Glazar, P. Papavasileiou, and N. Rajewsky, "circBase: A database for circular RNAs," *RNA*, vol. 20, pp. 1666–1670, 2014.

[24] S. Xia, J. Feng, K. Chen et al., "CSCD: A database for cancer-specific circular RNAs," *Nucleic Acids Research*, vol. 46, no. D1, pp. D925–d929, 2018.

[25] J. Liang, H. Li, J. Han et al., "Mex3a interacts with LAMA2 to promote lung adenocarcinoma metastasis via PI3K/AKT pathway," *Cell Death & Disease*, vol. 11, no. 8, p. 614, 2020.

[26] Q. Huang, H. Guo, S. Wang et al., "A novel circular RNA, circXPO1, promotes lung adenocarcinoma progression by interacting with IGF2BP1," *Cell Death & Disease*, vol. 11, no. 12, p. 1031, 2020.

[27] M. Yu, Y. Tian, M. Wu et al., "A comparison of mRNA and circRNA expression between squamous cell carcinoma and adenocarcinoma of the lungs," *Genetics and Molecular Biology*, vol. 43, Article ID e20200054, 2020.

[28] Z. Liu, Y. Zhou, G. Liang et al., "Circular RNA hsa_circ_001783 regulates breast cancer progression via sponging miR-200c-3p," *Cell Death & Disease*, vol. 10, no. 2, p. 55, 2019.

[29] L. Wang, H. Long, Q. Zheng, X. Bo, X. Xiao, and B. Li, "Circular RNA circRHOT1 promotes hepatocellular carcinoma progression by initiation of NR2F6 expression," *Molecular Cancer*, vol. 18, no. 1, p. 119, 2019.

[30] T. Lu, T. Qiu, B. Han et al., "Circular RNA circCSNK1G3 induces HOXA10 signaling and promotes the growth and metastasis of lung adenocarcinoma cells through hsa-miR-143-3p sponging," *Cellular Oncology*, vol. 44, no. 2, pp. 297–310, 2021.

[31] F. Saaoud, C. Drummer I.V., Y. Shao et al., "Circular RNAs are a novel type of non-coding RNAs in ROS regulation, cardiovascular metabolic inflammations and cancers," *Pharmacology & Therapeutics*, vol. 220, p. 107715, 2021.

[32] L. Li, D. Sun, X. Li, B. Yang, and W. Zhang, "Identification of key circRNAs in non-small cell lung cancer," *The American Journal of the Medical Sciences*, vol. 361, no. 1, pp. 98–105, 2021.

[33] M. Turner, A. Galloway, and E. Vigorito, "Noncoding RNA and its associated proteins as regulatory elements of the immune system," *Nature Immunology*, vol. 15, no. 6, pp. 484–491, 2014.

[34] X. Zhao, Y. Cai, and J. Xu, "Circular RNAs: biogenesis, mechanism, and function in human cancers," *International Journal of Molecular Sciences*, vol. 20, 2019.

[35] N. Abe, K. Matsumoto, M. Nishihara et al., "Rolling circle translation of circular RNA in living human cells," *Scientific Reports*, vol. 5, no. 1, Article ID 16435, 2015.

[36] Z. Tan, F. Cao, B. Jia, and L. Xia, "Circ_0072088 promotes the development of non-small cell lung cancer via the miR -377-5p/NOVA2 axis," *Thoracic Cancer*, vol. 11, no. 8, pp. 2224–2236, 2020.

[37] L. Liang, L. Zhang, J. Zhang, S. Bai, and H. Fu, "Identification of circRNA-miRNA-mRNA networks for exploring the fundamental mechanism in lung adenocarcinoma," *Onco-Targets and Therapy*, vol. 13, pp. 2945–2955, 2020.

[38] G. Yang, Y. Zhang, and J. Yang, "Identification of potentially functional CircRNA-miRNA-mRNA regulatory network in gastric carcinoma using bioinformatics analysis," *Medical Science Monitor*, vol. 25, pp. 8777–8796, 2019.

[39] Q. Lu, T. Liu, H. Feng et al., "Circular RNA circSLC8A1 acts as a sponge of miR-130b/miR-494 in suppressing bladder cancer progression via regulating PTEN," *Molecular Cancer*, vol. 18, no. 1, p. 111, 2019.

[40] Y. Tian, Y. Xing, Z. Zhang, R. Peng, L. Zhang, and Y. Sun, "Bioinformatics analysis of key genes and circRNA-miRNA-mRNA regulatory network in gastric cancer," *BioMed Research International*, vol. 2020, Article ID 2862701, 2020.

Research Article

Long Noncoding RNA MALAT1 Interacts with miR-124-3p to Modulate Osteosarcoma Progression by Targeting SphK1

Bin Liu [ID],[1,2] **Xinli Zhan** [ID],[1] **and Chong Liu** [ID][1]

[1]*Department of Spine Osteopathic Surgery, The First Affiliated Hospital of Guangxi Medical University, Nanning 530022, Guangxi, China*
[2]*Department of Spine Surgery, Hunan Provincial People's Hospital (The First Affiliated Hospital of Hunan Normal University), Changsha 410005, Hunan, China*

Correspondence should be addressed to Xinli Zhan; zhanxinli@stu.gxmu.edu.cn

Introduction. Long noncoding RNAs (lncRNAs) have been implicated in a variety of biological functions, including tumor proliferation, apoptosis, progression, and metastasis. lncRNA metastasis-associated lung adenocarcinoma transcript 1 (MALAT1) is overexpressed in various cancers, as well as osteosarcoma (OS); however, its underlying mechanism in OS is poorly understood. This investigation aims to elucidate the mechanisms of MALAT1 in OS proliferation and migration and to provide theoretical grounding for further targeted therapy in OS. *Methods.* In the present study, we applied qRT-PCR to assess the MALAT1 expression in OS tissues and cell lines. The effects of MALAT1 and miR-124-3p on OS cell proliferation and migration were studied by CCK-8 and scratch assays. Cell cycle and apoptosis were tested using a flow cytometer. The competing relationship between MALAT1 and miR-124-3p was confirmed by dual-luciferase reporter assay. *Results.* MALAT1 was overexpressed in OS cell lines and tissue specimens, and knockdown of MALAT1 significantly inhibited cell proliferation and migration and increased cell apoptosis and the percentage of G0/G1 phase. Furthermore, MALAT1 could directly bind to miR-124-3p and inhibit miR-124-3p expression. Moreover, MALAT1 overexpression significantly relieved the inhibition on OS cell proliferation mediated by miR-124-3p overexpression, which involved the derepression of sphingosine kinase 1 (SphK1). *Conclusions.* We propose that lncRNA MALAT1 interacts with miR-124-3p to modulate OS progression by targeting SphK1. Hence, we identified a novel MALAT1/miR-124-3p/SphK1 signaling pathway in the regulation of OS biological behaviors.

1. Introduction

Osteosarcoma (OS) is a common primary bone tumor with predilection in children and adolescents, the incidence of which has been ranked as the highest of all primary malignant bone tumor types [1]. OS is characterized by high degree of malignancy and early metastasis. Many patients with OS already have advanced disease with distant metastases at the time of initial presentation, and thus it poses great challenges to clinical practitioners. OS has a dismal prognosis after metastasis has occurred although the 5-year survival of treated OS patients has significantly increased in the past decades. Recent breakthroughs in the use of targeted therapies in the management of malignant tumors, such as leukemia and lung cancer, bring beneficial inspiration for OS

treatment. Thus, it is essential to explore the molecular mechanisms underlying OS tumorigenesis and progression and to identify clinically relevant biomarkers and targets for OS.

Although 93% of human genome can be transcribed into RNAs, only 2% of these RNAs can be translated to proteins. The rest of 98% of the RNAs are noncoding RNA (ncRNA) with limited or no protein-coding capacity. Among them, long noncoding RNAs (lncRNAs) are a class of RNA molecules with lengths in the range of 200–100,000 nucleotides and engaged in diverse biological processes. Increasing evidence has suggested that lncRNAs can participate in gene expression, including epigenetic regulation, transcription regulation, and posttranscriptional regulation, thus playing a pivotal role in cancer development

and progression. Previous studies show that metastasis associated lung adenocarcinoma transcript 1 (MALAT1) is related to the occurrence, development, metastasis, and prognosis of multiple tumor types, including OS [2]. MALAT1 is highly expressed in OS primary tissues and cell lines, and downregulation of MALAT1 decreases proliferation, migration, invasion, and epithelial-mesenchymal transition (EMT) in OS cells. In addition, inhibition of MALAT1 can lead to cell cycle arrest and apoptosis [3–5]. However, the molecular mechanism underlying MALAT1 regulation on OS is not clear enough.

MicroRNAs (miRNAs) are a class of endogenous noncoding single-stranded RNA molecules with lengths in the range of 18–24 nucleotides. They can degrade mRNAs or inhibit mRNAs translation by binding to the $3'$-untranslated regions ($3'$-UTR) of the target mRNA, resulting in downregulation of target gene expression. In the latest years, increasing attention has now been paid to the role of miRNAs in tumor initiation and progression [6]. Previous studies indicate that miR-124-3p is a tumor suppressor miR due to its low expression in a variety of cancers and that it may inhibit proliferation, migration, and invasion of cancer cells by suppressing different targets [7, 8]. However, the specific mechanism of miR-124-3p in OS is still obscure.

It has been reported that MALAT1 can competitively bind with miRNAs, thus indirectly regulating miRNA-target expression. This competitive binding to miRNAs is also called miRNA sponges [9, 10]. In the present study, we identified the overexpression of MALAT1 in OS and its oncogenic role in OS development. Moreover, our research validated that MALAT1 could bind to miR-124-3p, thereby competing directly with sphingosine kinase 1 (SphK1) as endogenous molecular sponges. This study identified the MALAT1/miR-124-3p/SphK1 pathway in human OS for the first time.

2. Materials and Methods

2.1. Specimen Collection.
Fresh tumor specimens were surgically isolated from OS patients who were treated in Hunan Provincial People's Hospital. Adjacent healthy tissues were also taken from these patients with OS to serve as control tissue. All specimens were pathologically confirmed as OS. All of the specimens were immediately snap-frozen in liquid nitrogen and stored at −80°C until use. All study procedures conformed to the ethical standards of the Declaration of Helsinki. Approval for the study was obtained from the hospital ethics committee (approval number 2019-S14), and informed consent was obtained from all individuals.

2.2. Cell Source and Culturation.
Human osteoblast cell line (HfoB1.19) and human OS cell lines (MG63, U2OS, and Saos-2) were all purchased from Procell Life Science & Technology Co., Ltd. (Wuhan, China).

Cell culture: HfoB1.19 cells, MG63, U2OS, and Saos-2 OS cells were cultured in DMEM medium supplemented with 10% fetal bovine serum (FBS). The media were purchased from Procell Life Science & Technology Corporation (Wuhan, China), and the FBS were purchased from Hyclone (South Logan, UT, USA). The medium contained penicillin (100 U/mL) and streptomycin (100 U/mL). All cell lines were grown in a 37°C incubator with 5% CO_2.

2.3. Binding Site Prediction for MALAT1, miR-124-3p, and SphK1.
Binding sites between MALAT1 and miR-124-3p were predicted with online prediction software starBase V2 (http://starbase.sysu.edu.cn/starbase2/), while binding sites between miR-124-3p and SphK1 were predicted with online prediction software TargetScan (http://www.targetscan.org/vert_72/).

2.4. RNA Extraction and Quantitative Real-Time Polymerase Chain Reaction (qRT-PCR).
Total RNA extraction was performed using MiniBEST Universal RNA Extraction Kit (Cat.#9767) (Takara, Dalian, China) according to the manufacturer's instructions. An amount of 1.5288 μg of RNA was reverse transcribed into cDNA by using a Reverse Transcriptase kit (Primescript RT reagent kit with gDNA Eraser perfect real time). Standard qRT-PCR reactions were performed on the ABI 12K Real-Time PCR System instrument, and mRNA levels were quantified using a SYBR-Green Mix Kit (LightCycler 480 SYBER Green I Master, Roche).

miRNA extraction was performed using miRNeasy Micro Kit (QIAGEN, Valencia, CA, USA) according to the manufacturer's instructions. RNA was reverse transcribed into cDNA and then subjected to a qRT-PCR assay.

All primers were purchased from Jima Pharmaceutical Company (Shanghai, China), and all primer sequences are available in Table 1. Relative expression levels were calculated as ratios normalized against the endogenous control (GAPDH or U6 snRNA). The relative fold changes of candidate genes were analyzed using the $2^{-\Delta\Delta CT}$ method.

2.5. Cell Transfection.
Three small interfering RNA (siRNA) targeting MALAT1 sequences were designed, and the sequence with the best suppressive effect was selected and used in further studies to minimize off-target effects. Lipofectamine RNAiMAX Reagent (Life Technologies, Carlsbad, CA) was used for the transfection of various siRNA constructs into OS cells, and for luciferase reporter assay, Lipofectamine 2000 Reagent was used for the cotransfection of pmirGLO-MALAT1/SphK1-WT or pmirGLO-MALAT1/SphK1-MUT and miR-124-3p mimic or mimic-NC into HEK 293T cells. siRNA targeting MALAT1 (si-MALAT1), siRNA targeting SphK1 (si-SphK1), scrambled negative control (si-NC), miR-124-3p, miR-124-3p mimic, and NC mimics were all purchased from Jima Pharmaceutical Company (Shanghai, China).

2.6. Cell Counting Kit-8 (CCK-8) Assay.
A CCK-8 assay was used to detect cell proliferation. 24 h after transfection, cells in the logarithmic growth phase were seeded in 96-well plates, with 5000 cells per well, and three replicates

Table 1: Primer sequence of PCR.

Gene name		5′-3′ sequence	Size (bp)
MALAT1	Forward	ACTGTAATGCTGGGTGGGAA	168
	Reverse	CATTGGAGATCAGCTTCCGC	
SphK1	Forward	TGACCAACTGCACGCTATTG	159
	Reverse	CCAGACGCCGATACTTCTCA	
GAPDH	Forward	TCAAGAAGGTGGTGAAGCAGG	115
	Reverse	TCAAAGGTGGAGGAGTGGGT	
miR-124-3p	Stemloop	GTCGTATCCAGTGCAGGGTCCGAGGTATTCGCACTGGATACGACTTGGCATT	
	F-PCR	TGCGCTAAGGCACGCGGTGAAT	
U6	Stemloop	GAATTTGCGTGTCATCCTTG	
	Forward	GCTTCGGCAGCACATATACTAAAAT	
	Reverse	CGCTTCACGAATTTGCGTGTCAT	

were set in each group. Cells were cultured at 5% CO2, 37°C in an incubator. After an additional 4 h incubation with 10 μL CCK-8 reagent, the optical density (OD) at the 450 nm wavelength (OD450) was measured using an EnSpire Multimode Plate Reader (PerkinElmer, Woodbridge, ON, Canada) at 1, 2, 3, and 4 days after transfection.

2.7. Scratch Assay. A scratch assay was applied to evaluate the migration of human osteoblast cell line and OS cell lines. Two parallel lines were drawn on back of the 6-well plates with a marker pen before cell seeding, and the cells were seeded in 6-well plate after digesting. We used a 10 μl pipette tip to gently draw lines on the plate when cells covered the bottom of the plate, and the width of each scratch should be as close to identical as possible. After rinsing the plate with PBS buffer for three times to remove cell debris produced by the scratching, the cells were photographed (0 h). Next, pictures were taken at 6 h, 24 h, and 48 h incubation, respectively. Finally, the pictures were collected for analysis.

2.8. Cell Cycle and Apoptosis Assay. Cell cycle phase distribution was measured and analyzed with CytoFLEX flow cytometer (Beckman Coulter). Cells were transiently transfected with siRNA after overnight incubation, and OS cells were collected at 48 h after transfection and washed with PBS. Then, the collected cells were fixed by 70% ethanol overnight at 4°C. Finally, DNA dye liquor was added for flow cytometry detection after ethanol removing and PBS washing. Data were collected and analyzed with the CytExpert v.2.3 software (Beckman Coulter).

Cell apoptosis was analyzed using the Annexin V-PI apoptosis detection kit (A211, Vazyme, Nanjing, China). The cells were transfected with a specific siRNA (6×10^4 cells per well in a 24-well plate). The transfected OS cells were harvested and washed with PBS. Then, cells were resuspended in 100 μl of Annexin Binding Buffer and incubated with 5 μl of Annexin FITC and 5 μl of PI for 15 min. The solutions were protected from light and incubated at room temperature. Finally, we examined cell apoptosis after adding 150 μl Annexin Binding Buffer.

2.9. Dual-Luciferase Reporter Assay. The luciferase assays were carried out using Dual-Luciferase Reporter Assay System (Promega, Madison, WI, USA). Cells were collected and lysed for luciferase detection according to the manufacturer's instructions at 48 h after cotransfection.

2.10. Western Blotting. Cells were lysed using RIPA buffer (Beyotime Biotechnology, Shanghai, China). Following lysis, cells were mixed with $5 \times$ SDS loading buffer and boiled for 5 min at 100°C. The proteins were separated by 10% SDS-PAGE and transferred onto PVDF membranes. Then, membranes were blocked with 5% milk/TBST for 1 h and subsequently incubated with primary antibodies at 4°C overnight, and secondary antibodies were diluted in 5% milk/TBST at room temperature for 1 h. The protein expressions were analyzed using an enhanced chemiluminescence (ECL) reagent and ChemiDoc™ XRS + imaging system System (Bio-Rad, CA, USA), and GAPDH served as internal reference.

2.11. Statistical Analysis. All statistical analyses were performed with SPSS software (version 22.0). Values are presented as the mean ± SD, and each experiment was repeated at least three times. The Fisher analysis, independent sample *t*-test, and one-way analysis of variance (ANOVA) were used as appropriate. *p* values less than 0.05 were considered statistically significant. All graphs were prepared using GraphPad Prism 7.0 software (GraphPad Software, San Diego, USA) and Adobe Illustrator (Adobe, San Jose, CA).

3. Results

3.1. LncRNA MALAT1 Plays an Important Role in Progression of OS. The effect of lncRNA MALAT1 on OS development and progression was investigated. The qRT-PCR results showed that MALAT1 was elevated in human OS specimens compared to adjacent healthy tissues ($p < 0.01$) (Figure 1(a)). We further explored the association between MALAT1 expression and clinical pathologic parameters. Based on the MALAT1 expression median value, OS patients were divided into two groups: high and low MALAT1 expression groups. Our data suggested that high MALAT1 expression was correlated with advanced clinical stage and distant
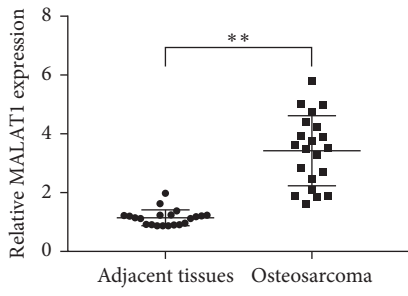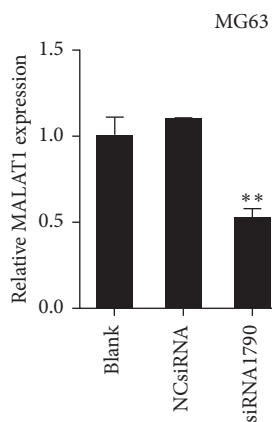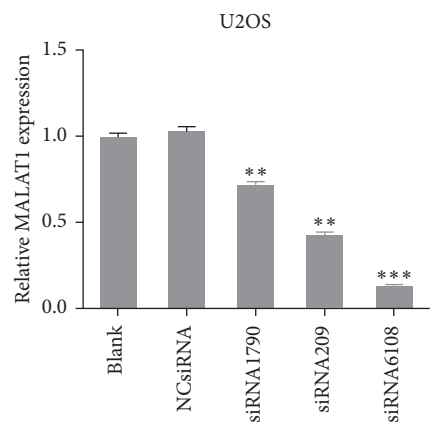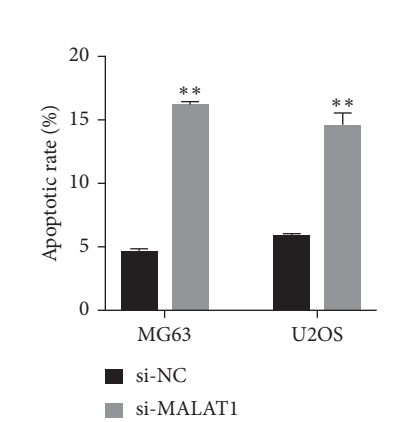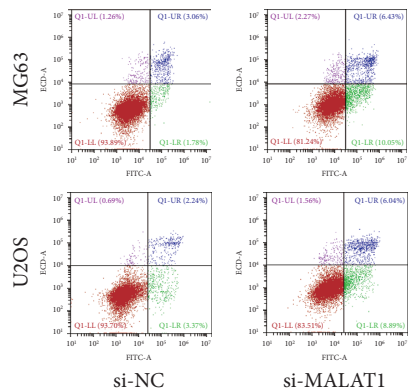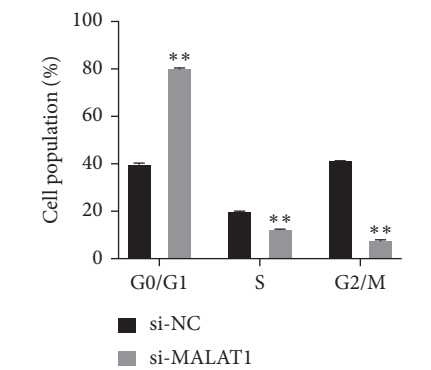
(a)
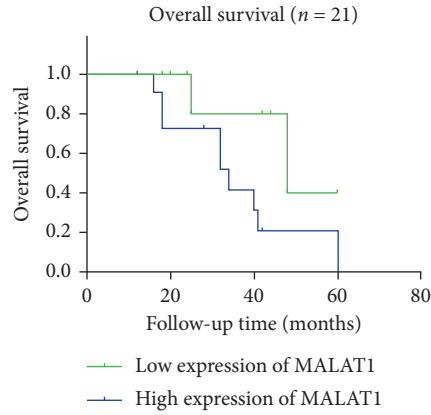
(b)
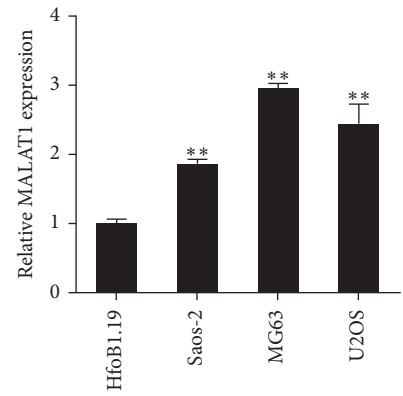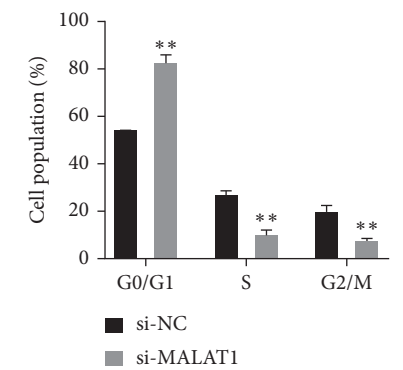

(c)

(d)

(e)

(f)

(g)
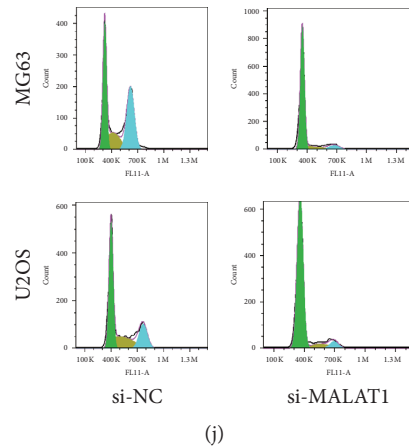

(h)

(i)

Figure 1: Continued.

(j)

FIGURE 1: (a) Long noncoding RNA metastasis associated lung adenocarcinoma transcript 1 (MALAT1) was upregulated in osteosarcoma (OS) tissues. (b) Survival curve revealed that high MALAT1 expression was associated with a poorer overall survival in OS patients. (c) MALAT1 was upregulated in OS cell lines. The three OS cell lines Saos-2, MG63, and U2OS all had a higher level of MALAT1 expression than the normal osteoblast cell line HfoB1.19. (d, e) MALAT1 knockdown was achieved by MALAT1 small interfering RNA (si-MALAT1), especially in siRNA6108 group. (f, g) Knockdown of MALAT1 increased ratios of apoptotic cells, compared with the si-NC (negative control) group. (h–j) MALAT1 silence increased the percentage of OS cell lines in G0/G1 phase, compared to the si-NC group in MG63 and U2OS cells. $^*p < 0.01$.

metastasis (Table 2; $p < 0.05$). Moreover, the analysis of the survival curve revealed that high MALAT1 expression was associated with poorer overall survival in OS patients (Figure 1(b); $p < 0.05$).

Next, we measured MALAT1 expression in different OS cell lines (MG63, U2OS, and Saos-2) and human osteoblast cell line (HfoB1.19) using qRT-PCR. The results showed that MALAT1 was significantly upregulated in all the OS cell lines, particularly in MG63 and U2OS ($p < 0.05$) (Figure 1(c)). Therefore, MG63 and U2OS cell lines were selected for subsequent experimentations. Together, it was suggested that MALAT1 may significantly associated with OS development and progression.

To ensure that OS cells were effectively and specifically blocked, cells were transfected with either a control scrambled siRNA (NC-siRNA) or the MALAT1-specific siRNA (siRNA1790, siRNA209, and siRNA6108). Compared with the NC-siRNA group, MALAT1 expression was decreased in siRNA groups, especially in siRNA6108 group (Figures 1(d) and 1(e)). Thus, siRNA6108 was selected for the following experiments.

To explore the association of MALAT1 expression with OS cell cycle and apoptosis, MALAT1 siRNA (si-MALAT1) and negative control (si-NC) were transfected into two OS cell lines: MG63 and U2OS. Compared with the si-NC group, ratios of apoptotic cells were increased in cells transfected with si-MALAT1 as measured by flow cytometry analysis (Figures 1(f) and 1(g)), while MALAT1 silence increased the percentage of OS cell lines in G0/G1 phase (Figures 1(h)–1(j)). Cell proliferation and migration were determined by CCK-8 and scratch assays, respectively. When compared with the si-NC group, knockdown of MALAT1 relatively decreased the cell viability of both MG63 and U2OS cells for up to 4 days (Figures 2(a) and 2(b)). Knockdown of MALAT1 also reduced the relative migration distance in both MG63 and U2OS cells (Figures 2(c)–2(e)).

Together, the above data indicated that si-MALAT1 could extremely downregulate expression level of MALAT1 and that MALAT1 decreases the percentage of G0/G1 phase, inhibits apoptosis, and promotes cell proliferation and migration in human OS cells.

3.2. Negative Regulation Relationship between miR-124-3p and MALAT1 in OS. Accumulating evidence has suggested that lncRNAs could function as miRNA sponges and inhibit miRNAs activity. Does MALAT1 also regulate miRNAs in the form of sponge molecule in OS? First, we searched for miRNAs with complementary base pairing with MALAT1 using the online software Starbase v2.0, and a complementary binding site between miR-124-3p and the 3′-UTR of MALAT1 (Figure 3(d)) was identified. Next, we concentrated on miR-124-3p, a tumor suppressor involved in cancer cell proliferation and migration.

We found a negative linear relationship between the expression of miR-124-3p and MALAT1 in OS tissue (Figure 3(a)). The qRT-PCR assay showed that miR-124-3p expression was increased in the si-MALAT1 group when compared with the si-NC group (Figure 3(b)), while MALAT1 expression was decreased in the miR-124-3p overexpression group when compared with the negative control (NC) group (Figure 3(c)). Together, the above data suggested that expression of miR-124-3p is negatively correlated with expression of MALAT1 in OS cells.

We explored the targeted binding relationship between miR-124-3p and MALAT1 using dual luciferase assay in further experiments. We cloned the predicted miR-124-3p binding site of MALAT1 (MALAT1-WT) and a mutated binding site (MALAT1-MUT) into a luciferase reporter plasmid. Luciferase activity was assayed 24 h after transient cotransfection. The results showed that miR-124-3p mimic significantly decreased the luciferase activities of

TABLE 2: Correlation between MALAT1 expression and clinical pathologic parameters of OS.

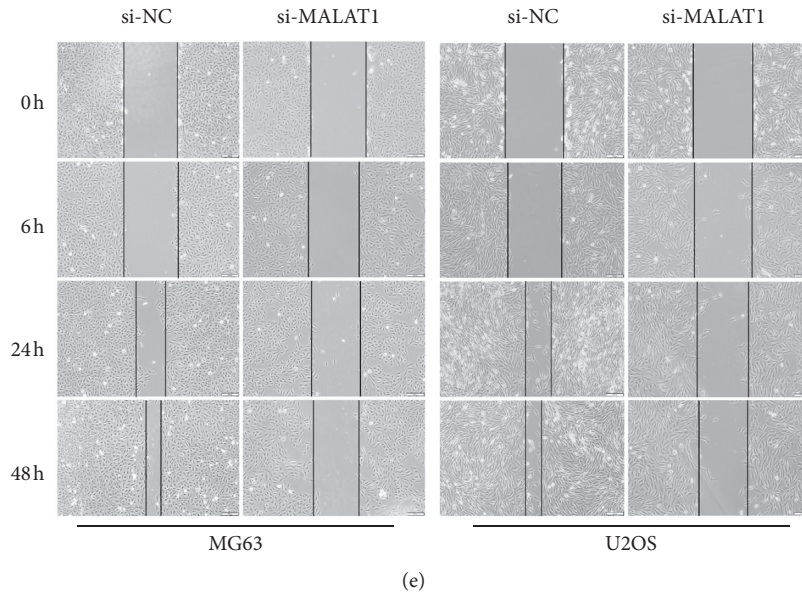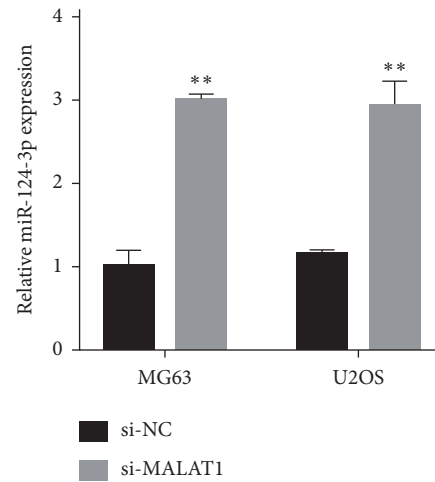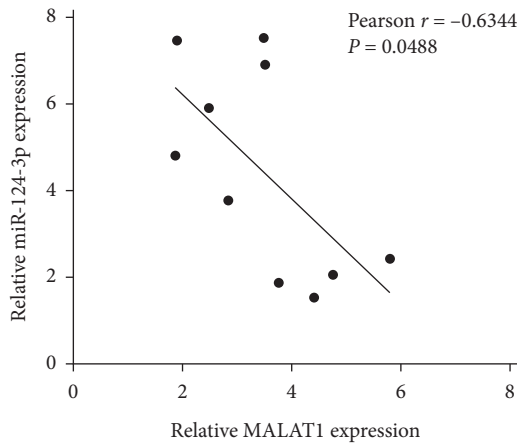| Clinicopathological features	Group	MALAT1 expression		p value
		Low	High	
Gender	Male	4	6	1.000
	Female	5	6	
Age (years)	<20	4	7	0.670
	≥20	5	5	
Anatomic location	Tibia/femur	7	8	0.659
	Elsewhere	2	4	
Clinical stage	I/IIA	6	2	0.032
	IIB/III	3	10	
Distant metastasis	Yes	2	11	0.002
	No	7	1	

(a)

(b)

(c)

(d)

FIGURE 2: Continued.

(e)
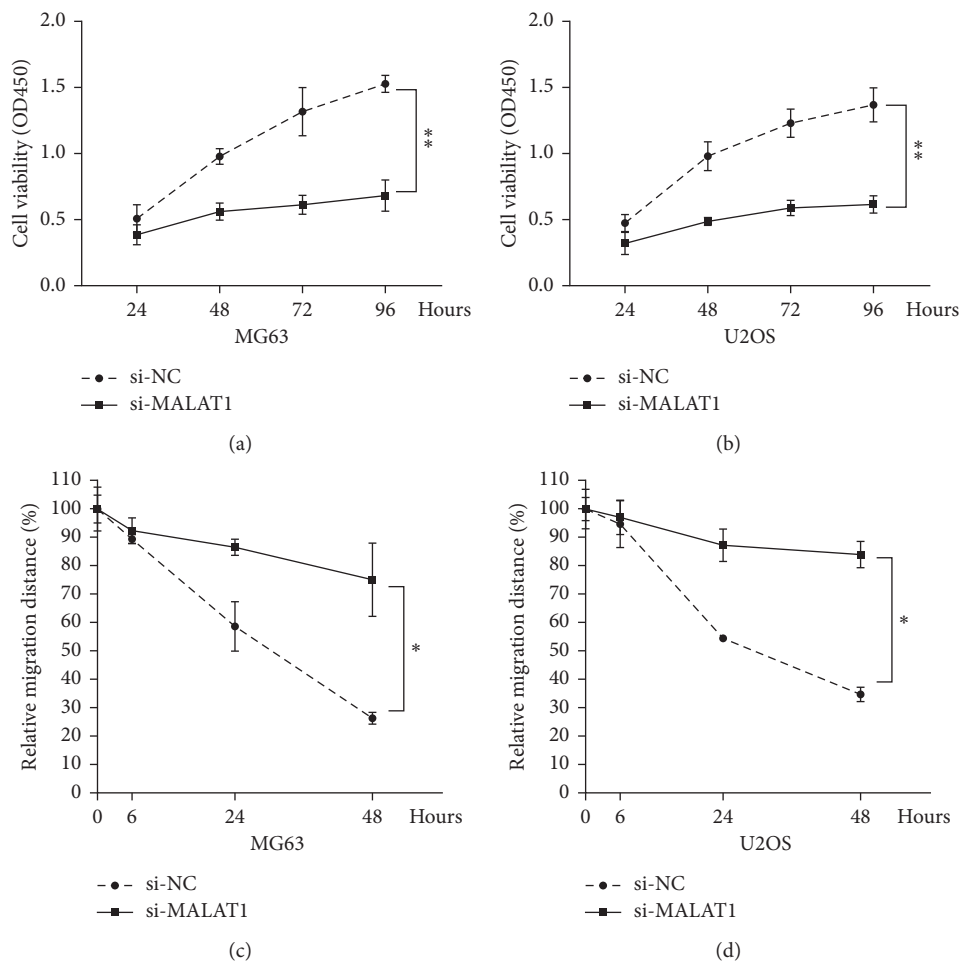
FIGURE 2: MALAT1 is associated with OS cells proliferation and migration. (a, b) CCK-8 assay showed that knockdown of MALAT1 decreased the cell viability of both MG63 and U2OS cells for up to 4 days, compared with the si-NC group. (c–e) Cell migration in MG63 and U2OS cells transfected with si-MALAT1 or si-NC was detected by scratch assay and is shown both pictorially and graphically. Compared to the si-NC group, knockdown of MALAT1 reduced the relative migration distance in both MG63 and U2OS cells for up to 48 hours. $^{*}p < 0.05$ and $^{**}p < 0.01$.
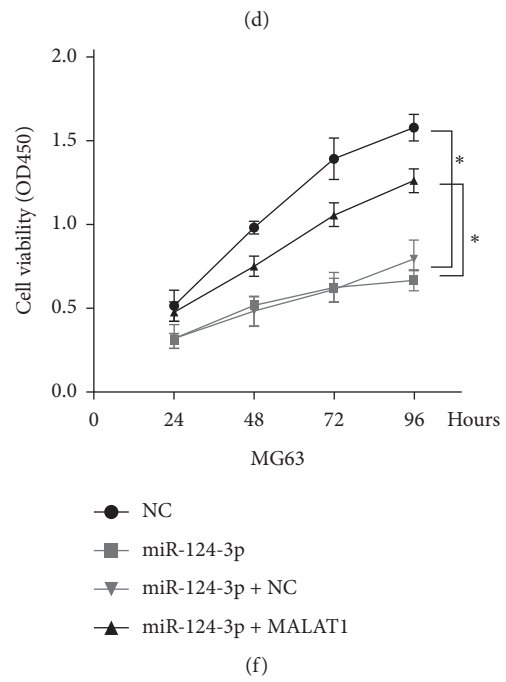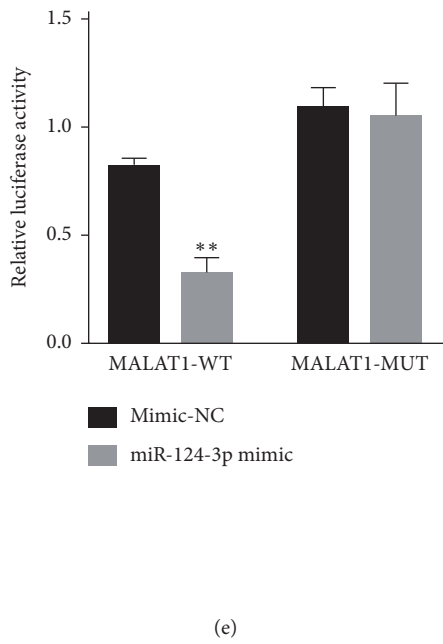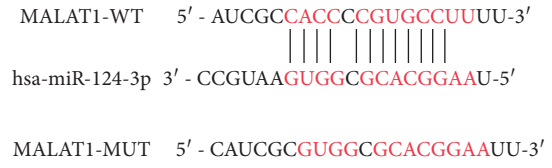

(a)

(b)

FIGURE 3: Continued.

MALAT1-WT   5′ - AUCGCCACCCCGUGCCUUUU-3′

hsa-miR-124-3p 3′ - CCGUAAGUGGCGCACGGAAU-5′

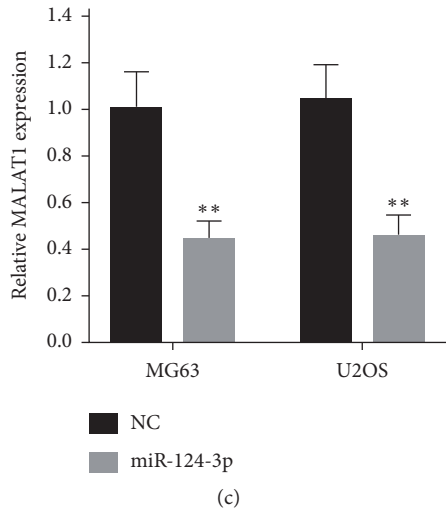MALAT1-MUT   5′ - CAUCGCGUGGCGCACGGAAUU-3′

(c)
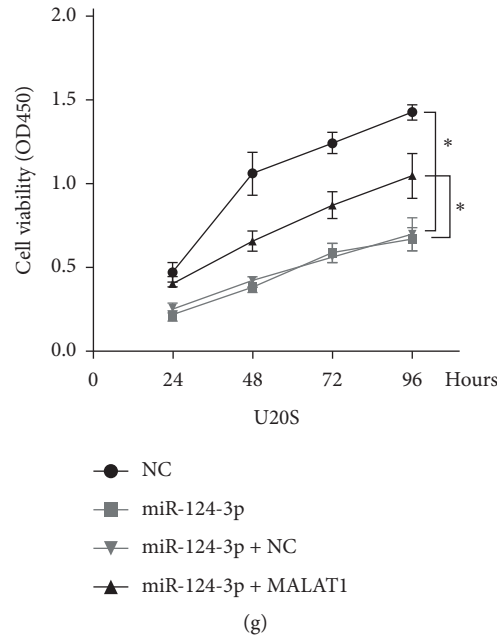
(d)

(e)

(f)

Figure 3: Continued.

(g)

Figure 3: MALAT1 is associated with microRNA-124-3p (miR-124-3p) expression in OS tissues. (a) An inverse correlation between MALAT1 and miR-124-3p expression was observed in OS tissues. (b) Real-time PCR assay showed that knockdown of MALAT1 (si-MALAT1) caused upregulation of miR-124-3p in the MG63 and U2OS cell lines. (c) MALAT1 expression was decreased in response to miR-124-3p overexpression, compared with the miR-NC (NC) group. (d) Generation of MALAT1-WT and MALAT1-MUT containing luciferase reporter vectors by sequentially mutating the predicted miR-124-3p binding site in the MALAT1 3′-untranslated region (3′-UTR). (e) The MALAT1-WT/MALAT1-MUT vectors and miR-NC/miR-124-3p mimics were cotransfected into human embryonic kidney (HEK) 293T cells, respectively. miR-124-3p mimic significantly decreased the luciferase activities of MALAT1-WT compared with mimic-NC. Cotransfection with miR-124-3p mimic and MALAT1-MUT did not alter luciferase activities either. (f, g) MG63 and U2OS cells were transfected with NC, miR-124-3p, miR-124-3p + NC, or miR-124-3p + MALAT1. Cell viability was determined by CCK-8 assay in transfected MG63 and U2OS cells at 24, 48, 72, and 96 h. Results showed that MALAT1 overturns the miR-124-3p induced inhibitory effect on proliferation of OS cells. Data are presented as mean ± SD of three independent experiments. $^{*}p < 0.05$ and $^{**}p < 0.01$.
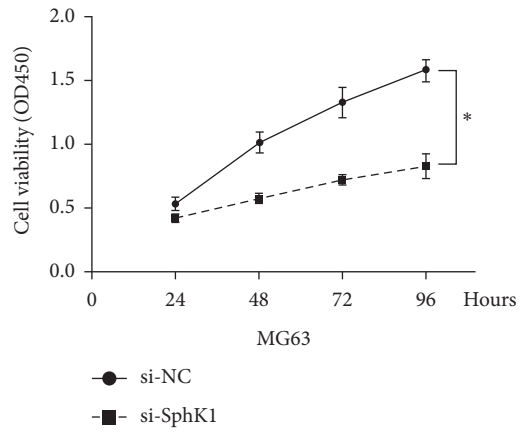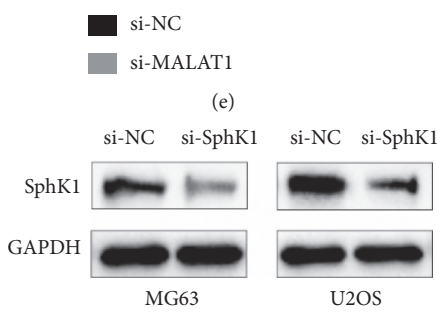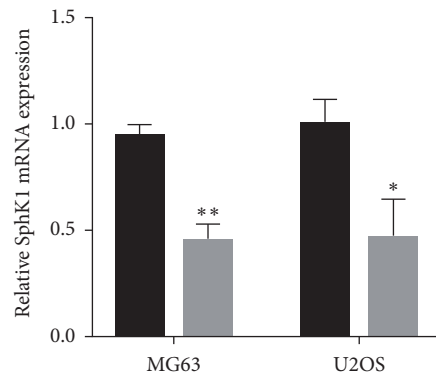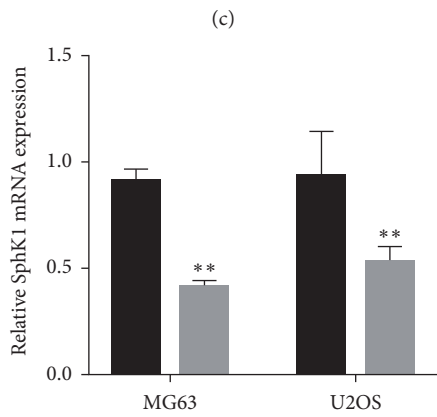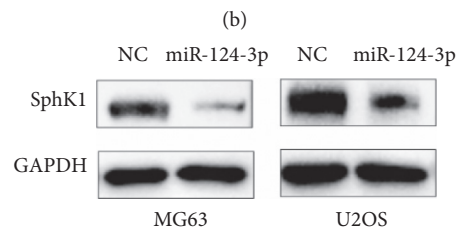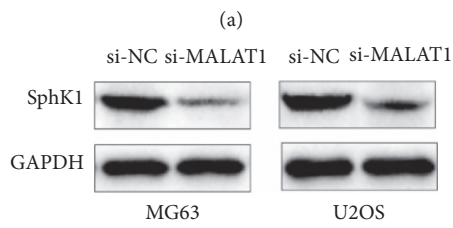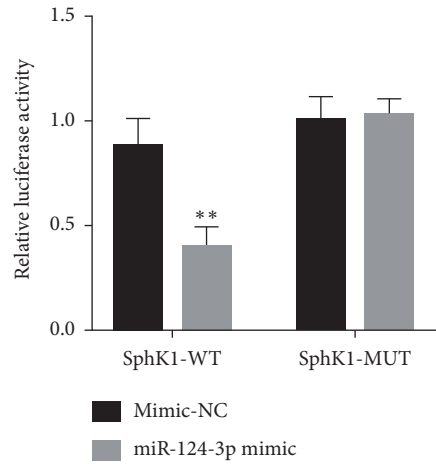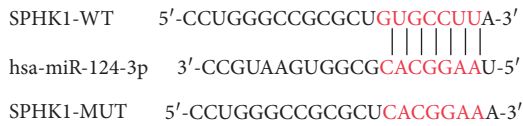
MALAT1-WT compared with mimic-NC. Cotransfection with miR-124-3p mimic and MALAT1-MUT did not alter luciferase activities either (Figure 3(e)). Together, these data suggested that miR-124-3p could directly bind to MALAT1 and decrease its expression.

To confirm the biological function of this targeted binding relationship, we observed the cell viability of MG63 and U2OS cells transfected with NC, miR-124-3p, miR-124-3p + NC, or miR-124-3p + MALAT1. CCK-8 results showed that miR-124-3p overexpression significantly inhibited cell viability in MG63 and U2OS cells when compared with the NC transfected group, whereas MALAT1 alleviated the inhibitory effect (Figures 3(f) and 3(g)). Collectively, the results indicated that targeted binding relationship between miR-124-3p and MALAT1 might present functional regulatory effect except for expression alterations.

3.3. Identifying the Regulatory Relationship between MALAT1, miR-124-3p, and SphK1. Further analysis was conducted with a focus on the relationship between miR-14-3p and Sphk1. First, we predicted the binding sites between miR-124-3p and SphK1 using online prediction software TargetScan (Figure 4(a)). Then, we validated the targeted binding relationship between miR-124-3p and SphK1 using dual luciferase assay. We cloned the predicted miR-124-3p

binding site of SphK1 (SphK1-WT) and a mutated binding site (SphK1-MUT) into a luciferase reporter plasmid. Luciferase activity was assayed 24 h after transient cotransfection. The results showed that miR-124-3p mimic significantly decreased the luciferase activities of SphK1-WT compared with mimic-NC. Cotransfection with miR-124-3p mimic and SphK1-MUT did not alter luciferase activities either (Figure 4(b)). Together, these data suggested that miR-124-3p could directly bind to SphK1 and decrease its expression.

To identify the regulatory relationship between MALAT1, miR-124-3p, and SphK1, we first explored the effect of miR-124-3p and MALAT1 on Sphk1 mRNA/protein expression in human OS cells. Sphk1 was downregulated by the knockdown of MALAT1 and overexpression of miR-124-3p, as demonstrated by Western blot (Figures 4(c) and 4(d)). Similar results were also observed in mRNA levels (Figures 4(e) and 4(f)). We next evaluated the effects of SphK1 on OS cells. Western blot results showed that si-SphK1 obviously decreased the SphK1 expression in MG63 and U2OS cells when compared with the si-NC group (Figure 4(g)). CCK-8 assays revealed that OS cells viability was decreased in response to SphK1 inhibition by si-SphK1 (Figures 4(h) and 4(i)). Together, these results suggested that SphK1 promotes proliferation in OS cells, and MALAT1 may interact with

SPHK1-WT   5′-CCUGGGCCGCGCU GUGCCUU A-3′
hsa-miR-124-3p   3′-CCGUAAGUGGCG CACGGAA U-5′
SPHK1-MUT   5′-CCUGGGCCGCGCU CACGGAA A-3′

(a)

(b)

(c)

(d)

(e)

(f)
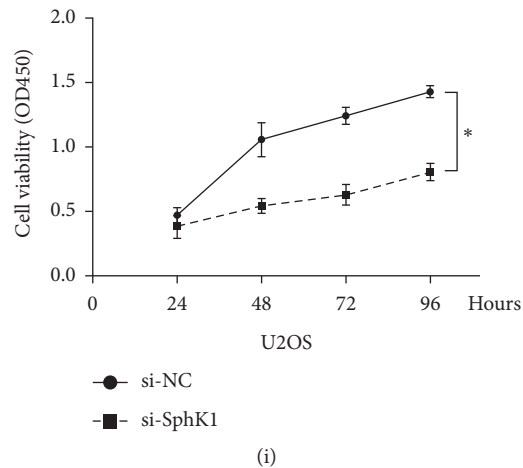

(g)

(h)

Figure 4: Continued.

(i)

Figure 4: Identifying the regulatory relationship between MALAT1, miR-124-3p, and SphK1. (a) The putative binding sequences of miR-124-3p and 3′-UTR of SPHK1. (b) The SphK1-WT/SphK1-MUT vectors and miR-NC/miR-124-3p mimics were cotransfected into 293T cells, respectively. miR-124-3p mimic significantly decreased the luciferase activities of SphK1-WT compared with mimic-NC. Cotransfection with miR-124-3p mimic and SphK1-MUT did not alter luciferase activities either. (c, d) Western blot assay showed that the expression of SphK1 was downregulated by knockdown of MALAT1 and miR-124-3p overexpression in both MG63 and U2OS cells. (e, f) Real-time PCR assay also showed similar results in both MG63 and U2OS cell lines. (g) SphK1 knockdown was achieved by si-SphK1 as demonstrated by Western blot assay. (h, i) CCK-8 assay results showed that SphK1 inhibition by si-SphK1 reduced the proliferation of OS cells. Data are presented as mean ± SD of three independent experiments. *$p < 0.05$ and **$p < 0.01$.

miR-124-3p to modulate OS progression by targeting SphK1.

4. Discussion

In recent years, numerous studies demonstrated that lncRNAs play a pivotal role in cancer development and progression, including breast cancer [11], gallbladder cancer [12], prostate cancer [13], and other malignancies, as well as OS [14]. Considering that biological behaviors of malignancies can be regulated by lncRNAs, they may be a potential therapeutic target in patients with malignant tumor.

lncRNA MALAT1 expression has been demonstrated increased in human OS, and it was shown to regulate the proliferation, invasion, and metastasis of OS cells via several signaling pathways [3, 4, 15, 16]. Moreover, lncRNA MALAT1 was shown to be an independent prognostic factor in OS [17]. In the present study, we demonstrated that lncRNA MALAT1 was markedly upregulated in OS tissues and cell lines when compared with adjacent healthy tissues and normal cell lines. We also found that knockdown of MALAT1 decreased proliferation and migration in OS cells. These results were concordant with the findings of previous studies, and it suggested MALAT1 could serve as a potential target for OS treatment.

As a member of miR-124 family, miR-124-3p could inhibit cell proliferation, and dysregulation of miR-124-3p has been demonstrated to be involved in tumorigenesis and progression in multiple tumor types, including breast cancer [7], bladder cancer [18], non-small cell lung cancer [19], and prostate cancer [20], as well as OS. Huang demonstrated that miR-124-3p was downregulated in OS, functioning as a tumor suppressor by attenuating OS cell proliferation and invasion. Moreover, miR-124-3p was associated with the

adverse clinical and pathological features observed in OS [21]. Our previous study also found that miR-124-3p could function as a tumor suppressor in OS by targeting ROCK1 [22]. However, the underlying mechanism of miR-124-3p inhibiting OS remained unclear, requiring further study and exploration.

To explore the correlation between MALAT1 and miR-124-3p, we performed bioinformatics analysis, and the result demonstrated a putative binding site in MALAT1 for miR-124-3p. Next, a luciferase assay indicated that miR-124-3p indeed could bind to MALAT1 directly by the putative miRNA response element. In addition, MALAT1 knockdown led to an elevated miR-320b expression, while miR-124-3p overexpression suppressed MALAT1 expression. These results indicated the negative regulatory relationship between MALAT1 and miR-124-3p. Further experimental results revealed that MALAT1 could alleviate the proliferation inhibition mediated by miR-124-3p, suggesting negative regulation of miR-124-3p by the MALAT1 could regulate biological behavior in OS cells.

The sphingosine kinase 1 (SphK1) is a key regulator of the balance between pro-death sphingosine and ceramide and pro-survival sphingosine-1-phosphate (S1P). The role of SphK1 in the regulation of cell cycle progression through the G1/S phase has been well documented. As an oncogenic kinase, it exhibits high expression in many types of tumors, including breast cancer, colon cancer, lung cancer, ovarian cancer, gastric cancer, uterine cancer, renal cancer [23, 24], and acute leukemia [25], as well as OS [26]. Patients with SphK1 overexpression are often with poor prognosis [27]. Previous studies showed that the expression of SphK1 was significantly increased in OS tissues, and SphK1 proved to be a critical oncogene of OS, and it could promote growth of OS and endorsed its resistance against chemotherapeutic drugs

[26]. Further study suggested that SphK1 participated in the development of doxorubicin resistance and contributed to glycolysis in OS cells by regulating HIF-1α expression [28]. In the present study, the CCK-8 assay showed that a downregulated expression of SphK1 reduced the proliferation of OS cells, which in turn proved that SphK1 promoted the proliferation of OS cells.

However, the relationship between SphK1, MALAT1, and miR-124-3p in OS is currently unclear. On the basis of proving the negative-regulation relationship between MALAT1 and miR-124-3p, we further identified that SphK1 was a potential target of miR-124-3p using a bioinformatics tool. Luciferase reporter assay and regulatory analysis in this study showed that miR-124-3p downregulated the expression level of SphK1. We also observed that overexpression of miR-124-3p or knockdown of MALAT1 both led to a significantly reduced SphK1 expression.

In recent years, a new RNA regulation mechanism—competing endogenous RNA (ceRNA)—has been proposed [29]. In this mechanism, RNAs can compete with each other miRNAs to bind with miRNAs, thereby regulating downstream RNAs, achieving posttranscriptional regulation, and participating in the regulation of biological behaviors of OS. For example, our previous study suggested that lncRNA HOXA11-AS acts as an endogenous sponge by directly binding miR-124-3p and decreasing the expression of miR-124-3p and then exerts an oncogene function in OS [22].

In the present study, we found that the expression of SphK1 was significantly downregulated after MALAT1 knockout and miR-124-3p overexpression. Combined with the negative regulatory relationship between MALAT1 and miR-124-3p, we believed that SphK1 expression is positively correlated with MALAT1 expression and negatively correlated with miR-124-3p expression.

Together, we speculated that MALAT1 acted as an endogenous sponge by directly binding to miR-124-3p and consequently decreasing the expression of miR-124-3p. Also, we found that MALAT1 may regulate OS progression by affecting miR-124-3p targeting SphK1 expression, indicating that MALAT1 functioned as a ceRNA to regulate SphK1 expression by sponging miR-124-3p in OS.

5. Conclusions

Overall, the present study demonstrated that MALAT1 overexpression facilitates cell proliferation and migration in OS. More importantly, our data revealed a novel MALAT1/miR-124-3p/SphK1 regulatory pathway in OS cells. Among them, MALAT1 could act as a competing endogenous RNA to bind miR-124-3p, then potentially promoting OS progression via targeting SphK1.

Abbreviations

OS: Osteosarcoma
MALAT1: Metastasis associated lung adenocarcinoma transcript 1
LncRNA: Long noncoding RNA
SphK1: Sphingosine kinase 1.

Data Availability

Data and materials would be made available upon request.

Ethical Approval

The present study was approved by the ethical review committee of Hunan Provincial People's Hospital (approval number 2019-S14).

Conflicts of Interest

The authors declare no conflicts of interest with respect to the research, authorship, and/or publication of this article.

Authors' Contributions

LB wrote the manuscript and performed most of the experiments. ZXL and LC assisted in performing the experiments. LB and ZXL sponsored and designed the study. All authors read and approved the final manuscript.

Acknowledgments

References

[1] L. Mirabello, R. J. Troisi, and S. A. Savage, "Osteosarcoma incidence and survival rates from 1973 to 2004: data from the surveillance," *Epidemiology, and End Results Program*, vol. 115, no. 7, pp. 1531–1543, 2010.

[2] T. Gutschner, M. Hämmerle, and S. Diederichs, "MALAT1—a paradigm for long noncoding RNA function in cancer," *Journal of Molecular Medicine*, vol. 91, no. 7, pp. 791–801, 2013.

[3] X. Cai, Y. Liu, W. Yang et al., "Long noncoding RNA MALAT1 as a potential therapeutic target in osteosarcoma," *Journal of Orthopaedic Research*, vol. 34, no. 6, pp. 932–941, 2016.

[4] Y. Zhang, Q. Dai, F. Zeng, and H. Liu, "MALAT1 promotes the proliferation and metastasis of osteosarcoma cells by activating the Rac1/JNK pathway via targeting MiR-509," *Oncology Research*, 2017.

[5] Q. Li, X. Pan, X. Wang et al., "Long noncoding RNA MALAT1 promotes cell proliferation through suppressing miR-205 and promoting SMAD4 expression in osteosarcoma," *Oncotarget*, vol. 8, no. 63, pp. 106648–106660, 2017.

[6] W. Dorothee, A. Mario, M. C. Carlo, and G. Romano, "MicroRNA and cancer—a brief overview," *Advances in Biological Regulation*, vol. 57, pp. 1–9, 2015.

[7] Y. Wang, L. Chen, Z. Wu et al., "miR-124-3p functions as a tumor suppressor in breast cancer by targeting CBL," *BMC Cancer*, vol. 16, no. 1, p. 826, 2016.

[8] X. Chen, R. Mao, W. Su et al., "Circular RNA circHIPK3 modulates autophagy via MIR124-3p-STAT3-PRKAA/AMPKα signaling in STK11 mutant lung cancer," *Autopathy*, vol. 16, no. 4, pp. 659–671, 2019.

[9] S. Chen, M. Wang, H. Yang et al., "LncRNA TUG1 sponges microRNA-9 to promote neurons apoptosis by up-regulated

Bcl2l11 under ischemia," *Biochemical and Biophysical Research Communications*, vol. 485, no. 1, pp. 167–173, 2017.

[10] X. S. Wu, F. Wang, H. F. Li et al., "Lnc RNA—PAGBC acts as a micro RNA sponge and promotes gallbladder tumorigenesis," *EMBO Reports*, vol. 18, no. 10, pp. 1837–1853, 2017.

[11] L. Aifu, L. Chunlai, X. Zhen et al., "The LINK-A lncRNA activates normoxic HIF1α signalling in triple-negative breast cancer," *Nature Cell Biology*, vol. 18, no. 2, pp. 213–224, 2016.

[12] M.-Z. Ma, B.-F. Chu, Y. Zhang et al., "Long non-coding RNA CCAT1 promotes gallbladder cancer development via negative modulation of miRNA-218-5p," *Cell Death and Disease*, vol. 6, no. 1, p. e1583, 2015.

[13] A. Misawa, K. I. Takayama, T. Urano, and S. Inoue, "Androgen-induced lncRNA SOCS2-AS1 promotes cell growth and inhibits apoptosis in prostate cancer cells," *Journal of Biological Chemistry*, vol. 291, no. 34, pp. 17861–17880, 2016.

[14] W. Li, P. Xie, and W.-H. Ruan, "Overexpression of lncRNA UCA1 promotes osteosarcoma progression and correlates with poor prognosis," *Journal of Bone Oncology*, vol. 5, no. 2, pp. 80–85, 2016.

[15] Y. Dong, G. Liang, B. Yuan et al., "MALAT1 promotes the proliferation and metastasis of osteosarcoma cells by activating the PI3K/Akt pathway," *Tumor Biology*, vol. 36, no. 3, pp. 1477–1486, 2015.

[16] R. Dong, Z. Hao, F. Sang, and J.-L. Zhao, "MALAT1 induces osteosarcoma progression by targeting miR-206/CDK9 axis," *Journal of Cellular Physiology*, vol. 234, no. 1, pp. 950–957, 2019.

[17] M. Liu, P. Yang, G. Mao et al., "Long non-coding RNA MALAT1 as a valuable biomarker for prognosis in osteosarcoma: a systematic review and meta-analysis," *International Journal of Surgery*, vol. 72, pp. 206–213, 2019.

[18] R. B. Zo and L. Ziwen, "MiR-124-3p suppresses bladder cancer by targeting DNA methyltransferase 3B," *Journal of Cellular Physiology*, vol. 234, no. 1, pp. 464–474, 2019.

[19] L. X. Tang, G. H. Chen, H. Li, P He, Y Zhang, and X.-W. Xu, "Long non-coding RNA OGFRP1 regulates LYPD3 expression by sponging miR-124-3p and promotes non-small cell lung cancer progression," *Biochemical and Biophysical Research Communications*, vol. 505, no. 2, pp. 578–585, 2018.

[20] K. Yan, L. Hou, T. Liu et al., "lncRNA OGFRP1 functions as a ceRNA to promote the progression of prostate cancer by regulating SARM1 level via miR-124-3p," *Aging*, vol. 12, no. 10, pp. 8880–8892, 2020.

[21] J. Huang, Y. Liang, M. Xu, J. Xiong, D. Wang, and Q. Ding, "MicroRNA124 acts as a tumorsuppressive miRNA by inhibiting the expression of Snail2 in osteosarcoma," *Oncology Letters*, vol. 15, no. 4, pp. 4979–4987, 2018.

[22] M. Cui, J. Wang, Q. Li et al., "Long non-coding RNA HOXA11-AS functions as a competing endogenous RNA to regulate ROCK1 expression by sponging miR-124-3p in osteosarcoma," *Biomedicine & Pharmacotherapy*, vol. 92, pp. 437–444, 2017.

[23] K. J. French, R. S. Schrecengost, B. D. Lee et al., "Discovery and evaluation of inhibitors of human sphingosine kinase," *Cancer Research*, vol. 63, no. 18, pp. 5962–5969, 2003.

[24] K. R. Johnson, K. Y. Johnson, H. G. Crellin et al., "Immunohistochemical distribution of sphingosine kinase 1 in normal and tumor lung tissue," *Journal of Histochemistry & Cytochemistry*, vol. 53, no. 9, pp. 1159–1166, 2005.

[25] S. Sobue, T. Iwasaki, C. Sugisaki et al., "Quantitative RT-PCR analysis of sphingolipid metabolic enzymes in acute leukemia and myelodysplastic syndromes," *Leukemia*, vol. 20, no. 11, pp. 2042–2046, 2006.

[26] C. Yao, S. Wu, D. Li et al., "Co-administration phenoxodiol with doxorubicin synergistically inhibit the activity of sphingosine kinase-1 (SphK1), a potential oncogene of osteosarcoma, to suppress osteosarcoma cell growth both in vivo and in vitro," *Molecular Oncology*, vol. 6, no. 4, pp. 392–404, 2012.

[27] M. Xiao-Dong, Z. Zhan-Song, Q. Jian-Hong, S. Wen-Hao, W. Qu, and X. Jun, "Increased SPHK1 expression is associated with poor prognosis in bladder cancer," *Tumour Biology*, vol. 35, no. 3, pp. 2075–2080, 2014.

[28] X. Ren and C. Su, "Sphingosine kinase 1 contributes to doxorubicin resistance and glycolysis in osteosarcoma," *Molecular Medicine Reports*, vol. 22, pp. 2183–2190, 2020.

[29] Y. Tay, J. Rinn, and P. P. Pandolfi, "The multilayered complexity of ceRNA crosstalk and competition," *Nature*, vol. 505, no. 7483, pp. 344–352, 2014.

Research Article

Chidamide and Radiotherapy Synergistically Induce Cell Apoptosis and Suppress Tumor Growth and Cancer Stemness by Regulating the MiR-375-EIF4G3 Axis in Lung Squamous Cell Carcinomas

Xu Huang [ID],[1,2] **Nan Bi** [ID],[1] **Jingbo Wang** [ID],[1] **Hua Ren** [ID],[1] **Desi Pan** [ID],[3] **Xianping Lu** [ID],[3] **and Luhua Wang** [ID][1,4]

[1]*Department of Radiation Oncology, National Cancer Center, Cancer Hospital,*
 Chinese Academy of Medical Sciences and Peking Union Medical College, Beijing 100021, China
[2]*Department of Radiation Oncology, Harbin Medical University Cancer Hospital, Harbin, Heilongjiang 150040, China*
[3]*Shenzhen Chipscreen Biosciences, Shenzhen 518057, China*
[4]*Department of Radiation Oncology, National Cancer Center, Cancer Hospital & Shenzhen Hospital,*
 Chinese Academy of Medical Sciences and Peking Union Medical College, Shenzhen 518000, China

Correspondence should be addressed to Luhua Wang; wlhwq2@126.com

As a selective histone deacetylase (HDAC) inhibitor developed in China, chidamide has been applied for the treatment of refractory peripheral T-cell lymphoma (PTCL) and multiple solid tumors, including lung cancer. However, the underlying mechanisms are not well elucidated. In our present study, we found that chidamide and radiation acted synergistically to suppress cell and xenograft growth of lung squamous cell carcinoma cells by inducing cell apoptosis. Moreover, chidamide alone or a combination of chidamide and radiation treatment inhibited cancer cell stemness. miRNA microarray analysis demonstrated that miR-375 was the highest upregulated microRNA (miRNA) in NCI-2170 and NCI-H226 cells treated with chidamide alone or treated with chidamide plus radiation, compared with normal control. Inhibition of miR-375 attenuated the promoting effect of chidamide alone and chidamide plus radiation-induced NCI-2170 and NCI-H226 cell apoptosis and reverted the suppression of cancer stemness caused by chidamide alone or chidamide plus radiation treatment. Moreover, EIF4G3, a scaffold protein in the translation initiation complex, was found to be a direct target of miR-375 based on the luciferase reporter assay and western blot analysis. Interestingly, both chidamide alone and chidamide plus radiation treatments suppressed the mRNA and protein expression of EIF4G3. Silence of EIF4G3 also induced cell apoptosis and suppressed tumor growth in NCI-2170 and NCI-H226 cells. These data suggest that chidamide shows a synergistic effect with radiation therapy on lung squamous cell carcinomas by modulating the miR-375-EIF4G3 axis, which may afford an effective strategy to overcome the drug resistance of chidamide in clinical cancer therapy.

1. Introduction

Lung cancer is one of the leading causes of cancer-associated deaths all over the world, with a high metastatic potential [1]. Lung cancer can be divided into two main groups: small-cell lung cancers (SCLCs) and non-small-cell lung cancers (NSCLCs) [2]. NSCLCs account for 85% of lung cancer and can be further classified into four subtypes according to their

histological and molecular features: lung large-cell carcinomas (LCLCs), lung neuroendocrine tumors (LungNETs), lung adenocarcinomas (LUADs), and lung squamous cell carcinomas (LSCCs) [3]. LSCCs are the main type of NSCLC showing strong malignancy. Although advanced treatment strategies and technologies such as surgical treatment, radiotherapy, and chemotherapy have been developed rapidly, the five-year survival rate among patients with LSCC remains very

poor with increased risk of recurrence [4]. Therefore, it is urgently needed to furtherly understand the molecular mechanisms underlying LSCC initiation and progression and to seek effective methods for early detection and treatment.

Chidamide, a selective inhibitor of HDAC1, 2, 3, and 10 developed wholly in China, has been entered into clinical trials both in the United States and China. In December 2014, chidamide has been approved by the China Food and Drug Administration (CFDA) as a treatment strategy for peripheral T-cell lymphoma (PTCL) [5]. Interestingly, accumulating studies have demonstrated that chidamide shows an effective antitumor activity in multiple solid tumors, including liver cancer, colon carcinoma, and lung cancer [6–11]. In lung cancer, Hu et al. have performed a phase I trial of chidamide combined with paclitaxel and carboplatin in patients with advanced NSCLC and found that a combination treatment of chidamide and paclitaxel or carboplatin was tolerated without unanticipated toxicities or pharmacokinetic interactions [6]. Chidamide has also been reported to enhance the suppressive effect of platinum on NSCLCs [11]. However, the underlying mechanisms through which chidamide suppresses lung cancer are unclear.

MicroRNAs (miRNAs) represent a class of noncoding short RNAs with 19–24 nucleotides in length, which was highly conserved in eukaryotes. miRNAs play an important role in regulating multiple physiological and pathological processes by binding to the $3'$-untranslated regions ($3'$-UTRs) of target genes [12, 13]. Dysregulation of miRNA has been implicated in the initiation and progression of a wide range of cancers, including liver, gastric, breast, lung, and colorectal cancers. For instance, Tian et al. found that silence of miR-203 promotes tumor cell growth and invasion by upregulating the SNAI2 in prostate cancer [14]. miR-22 inhibits breast cancer cell proliferation and increases paclitaxel sensitivity by suppressing N-RAS [15]. Aberrant expression of miRNAs has also been observed in lung cancer. For example, downregulation of miR-98-5p in NSCLC suppresses NSCLC proliferation and metastasis by targeting TGFBR1 [16]. miR-5195-3p inhibits cell proliferation, migration, and invasion in human NSCLC by targeting MYO6 [17].

Among these cancer-related miRNAs, miR-375 was initially identified as a critical regulator of insulin secretion and a novel therapeutic target for diabetes treatment [18]. Further studies have demonstrated that miR-375 participates in various cancer types by targeting several critical target genes including ATG7, AEG-1, YAP1, SP1, IGF1R, JAK2, and PDK1 [19]. The deregulation of miR-375 in tumors can be caused by a variety of mechanisms such as aberrant promoter methylation [20–22]. Deregulation of miR-375 can also be used as a biomarker for cancer prediction and diagnosis [23, 24]. In lung cancer, Jin et al. have reported that miR-375 expression was obviously increased in lung adenocarcinoma and SCLCs but reduced in LSCCs [25]. However, the exact role of miR-375 in lung cancer, especially in LSCCs, is not fully understood.

In the present study, we found that a combination of chidamide and radiation treatment promoted synergistic cytotoxicity and suppressed tumor stemness in LSCCs. Importantly, miR-375 was upregulated in NCI-2170 and NCI-H226 cells treated with chidamide alone or with chidamide plus radiation, compared with normal control. In addition, suppression of miR-375 attenuated chidamide alone and chidamide plus radiation-induced NCI-2170 and NCI-H226 cell apoptosis and suppressed tumor growth and stemness. Moreover, EIF4G3 was identified as a direct target of miR-375. Interestingly, both chidamide alone and chidamide plus radiation treatments suppressed the mRNA and protein expression of EIF4G3. Silence of EIF4G3 also induced cell apoptosis and suppressed tumor growth in NCI-2170 and NCI-H226 cells. These data suggest that chidamide shows a synergistic effect with radiation therapy on lung squamous cell carcinomas by modulating the miR-375-EIF4G3 axis.

2. Materials and Methods

2.1. Cell Cultures and Treatment. Human lung squamous cell carcinoma NCI-H2170 and NCI-H226 cells were obtained from ATCC (Manassas, VA, USA) and maintained in DMEM (Invitrogen, Carlsbad, CA, USA) with 10% fetal bovine serum (FBS; GIBCO, Waltham, MA, USA) and 1% penicillin/streptomycin (Beyotime, Shanghai, China) at $37°C$ in a 5% CO_2 incubator. Chidamide (BioVision, Milpitas, CA, USA) was diluted in dimethyl sulfoxide (DMSO; Sigma-Aldrich, Shanghai, China). Cells were exposed to 300 nM of chidamide for 24 h or/and 6 MV X-ray radiation using a linear accelerator (Elekta; Stockholm, Sweden) at single doses of 0, 1, 2, and 4 Gy.

2.2. miRNA Mimic, Inhibitor, and siRNA Transfection. Cells were cultured to about 75% confluence before transfection. Control mimic, miR-375 mimic, control siRNA, and EIF4G3 siRNA were transfected into cells using Lipofectamine RNAiMAX Reagent (Thermo Fisher Scientific, Waltham, MA, USA) following the manufacturer's manual. Forty-eight hours after transfection, the cells were applied for the following experiment. The siRNA oligos were synthesized by Santa Cruz (CA, USA).

2.3. Cell Proliferation. Cell Counting Kit-8 was applied to determine the proliferation rate of NCI-H2170 and NCI-H226 cells with indicated treatment as previously described. Briefly, two thousand treated cells were plated into 96-well plates. Then, CCK-8 solution was added at the harvest time and incubated for an additional 30 min. The absorbance was determined at 450 nm on the microplate reader (Molecular Devices, Walpole, MA, USA).

2.4. Apoptosis Assay. Apoptosis assay was performed by Annexin V/PI double staining using the Annexin V-FITC apoptosis detection kit (BD Biosciences, Pharmingen, CA, USA) following the standard manual. Briefly, treated cells were washed with cold 1x PBS and resuspended in 1x binding buffer. Five μl of FITC-labeled Annexin V and 5 μl

of propidium iodide (PI) were added to the suspended cells and gently mixed, following by the incubation at room temperature for 15 min in dark. At last, the samples were detected on the flow cytometer (BD Biosciences).

2.5. miRNA Microarray.
miRNA microarray was performed as previously described [26].

2.6. Real-Time RT-PCR.
Real-time RT-PCR was performed as previously described [27]. The primers used for real-time PCR detection were as follows: 5′-GTCGTATCCAGTGCAG GGTCCGAGGTATTCGCACTGGATACGACGGTTTG-3′ (miR-375 reverse transcription), 5′-GTGCAGGGTCCG AGGT-3′ (miR-375, forward), 5′-GCGCGACGAGCCCC TCGCT-3′ (miR-375, reverse), 5′-CTCGCTTCGGCAG-CACA-3′ (U6, forward), 5′-AACGCTTCACGAATTTGCGT-3′ (U6, reverse), 5′-CCACAGCGCCATGTTGGAT-3′ (EIF 4G3, forward), 5′-GATCTTTATCCCCCTCCCCG-3′ (EIF4G 3, reverse), 5′-GCACCGTCAAGGCTGAGAAC-3′ (GAPDH, forward), and 5′-ATGGTGGTGAAGACGCCAGT-3′ (GAP DH, reverse).

2.7. Luciferase Reporter Assay.
The luciferase reporter assay was determined using the psi-CHECK2 dual-luciferase system (Promega, Madison, WI, USA) following the standard manual. The QuickMutation™ Site-Directed Mutagenesis Kit (Beyotime, Shanghai, China) was applied for construction of EIF4G3 3′-UTR reporter plasmids with a mutant miR-375 binding site. Primer sequences used for construction of these plasmids were as follows: 5′-GCGCGATCGCAACTTCAAATACACAAAATG-3′ (EIF4 G3-WT, forward), 5′-GCGTTTAAACCTGTCCAAAGGA GAAGTCAC-3′ (EIF4G3-WT, reverse); 5′-AGGCTTGT AAATACATACTTGTTTTATTTAAAAAAAC-3′ (EIF4G3 -Mut1, forward), 5′-GTTTTTTTTAAATAAAACAAGTATG TATTTACAAGCCT-3′ (EIF4G3-Mut1, reverse); 5′- CAC TTTGAAAATATAAACTTGTTTTAAAGACAAAC-3′ (EI F4G3-Mut2, forward), and 5′-GTTTGTCTTTAAAACA AGTTTATATTTTCAAAGTG-3′ (EIF4G3-Mut2, reverse).

2.8. Western Blot Analysis to Determine Protein Expression.
Western blot analysis was performed as previously described [28]. The primary antibodies were as follows: anti-EIF4G3 (AV40487; Sigma, Shanghai, China), anti-Bax (ab182733; Abcam), anti-BCL2 (#2872; Cell Signaling Technology), and anti-β-actin (AF0003; Beyotime).

2.9. ALDEFLUOR Assay and Flow Cytometry.
The ALDE-FLUOR Kit (Stemcell Technologies) was used for ALDH$^+$ cell analyses according to the manufacturer's manual. For each sample, one-half of cells was treated with 50 mM of diethylaminobenzaldehyde (DEAB) to define negative gates.

2.10. Sphere Formation Assay.
Sphere formation assay was determined as previously described [29].

2.11. Xenograft Mouse Model.
Treated cells were subcutaneously injected into both sides of flank areas of 6–8-week-old BALB/c nude mice for 42 days. Tumor volumes were measured using the following equation: $0.5 \times \text{length} \times \text{width}^2$ each other day after palpable tumors appeared. The study protocol was approved by the Animal Care and Use committee of Harbin Medical University.

2.12. Immunohistochemistry.
Immunohistochemistry assay was performed as previously described [30].

2.13. Statistical Analysis.
All data were expressed as mean ± standard deviation (SD). Statistical analysis was performed using the software GraphPad Prism 5. Student's t-test was used to determine the statistical differences, in which $p < 0.05$ was considered to be significant.

3. Results

3.1. Both Chidamide Alone and Chidamide Plus Radiation Combinational Treatment Synergistically Promote Cell Apoptosis and Suppressed Cancer Cell Stemness in NCI-H2170 and NCI-226 Cells. Initially, to determine the effect of chidamide on cellular proliferation in LSCC cells, we treated NCI-H2170 and NCI-226 cells with 300 nM of chidamide for 24 h or/and 6 mV X-ray radiation using a linear accelerator at single doses of 0, 1, 2, and 4 Gy. The results indicated that chidamide, radiotherapy, and their combinational treatment inhibited cell proliferation in NCI-H2170 and NCI-H226 cells (Figures 1(a)–1(c)). Next, to explore the possible mechanism underlying chidamide-regulating proliferation of LSCC cells, we intended to testify whether cellular apoptosis could be contributed to the synergistic anticancer effect of chidamide and radiation on LSCC. After treating the NCI-H2170 and NCI-226 cells with 300 nM of chidamide for 24 h and/or with 2 Gy radiation, the effect of chidamide, radiotherapy, and their combinational treatment on cell apoptosis was determined by flow cytometry. Both the early and late apoptosis rates were significantly increased in cells treated with chidamide, radiotherapy, and their combination (Figures 1(d)–1(f)). The results demonstrate that chidamide and radiation synergistically inhibit LSCC cell proliferation potentially via inducing cellular apoptosis.

It has been known that cancer stem cells (also named cancer-initiating cells or cancer stem-like cells) play a central role in tumor progression, metastasis, recurrence, and chemotherapy resistance. Herein, we also detect the effect of chidamide on lung cancer stemness. Results of sphere formation assay demonstrated that the sizes and number of spheres were suppressed by chidamide alone or a combination treatment of chidamide and radiation (Figures 2(a)–2(j)). To determine the population of cancer stem cells, ALDEFLUOR assay was performed. The results demonstrated that chidamide alone or a combination treatment of chidamide and radiation reduced the population of ALDH$^+$ cells (Figures 2(k)–2(m)).

(a)

(b)
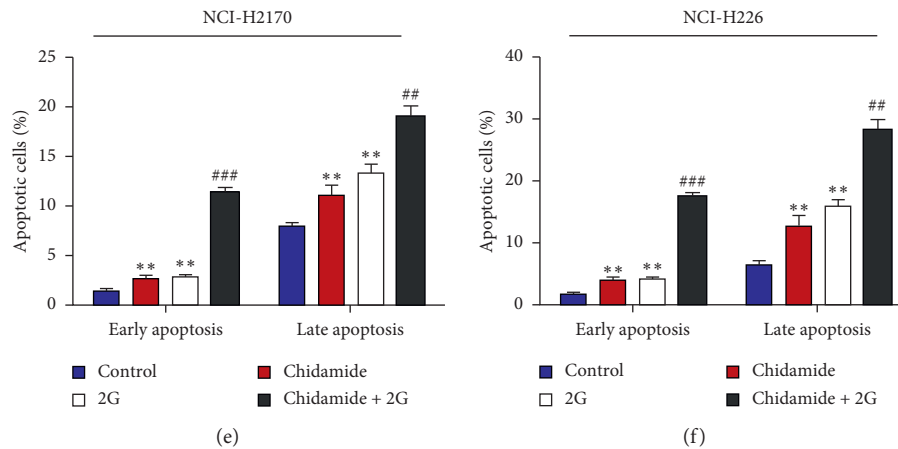

(c)
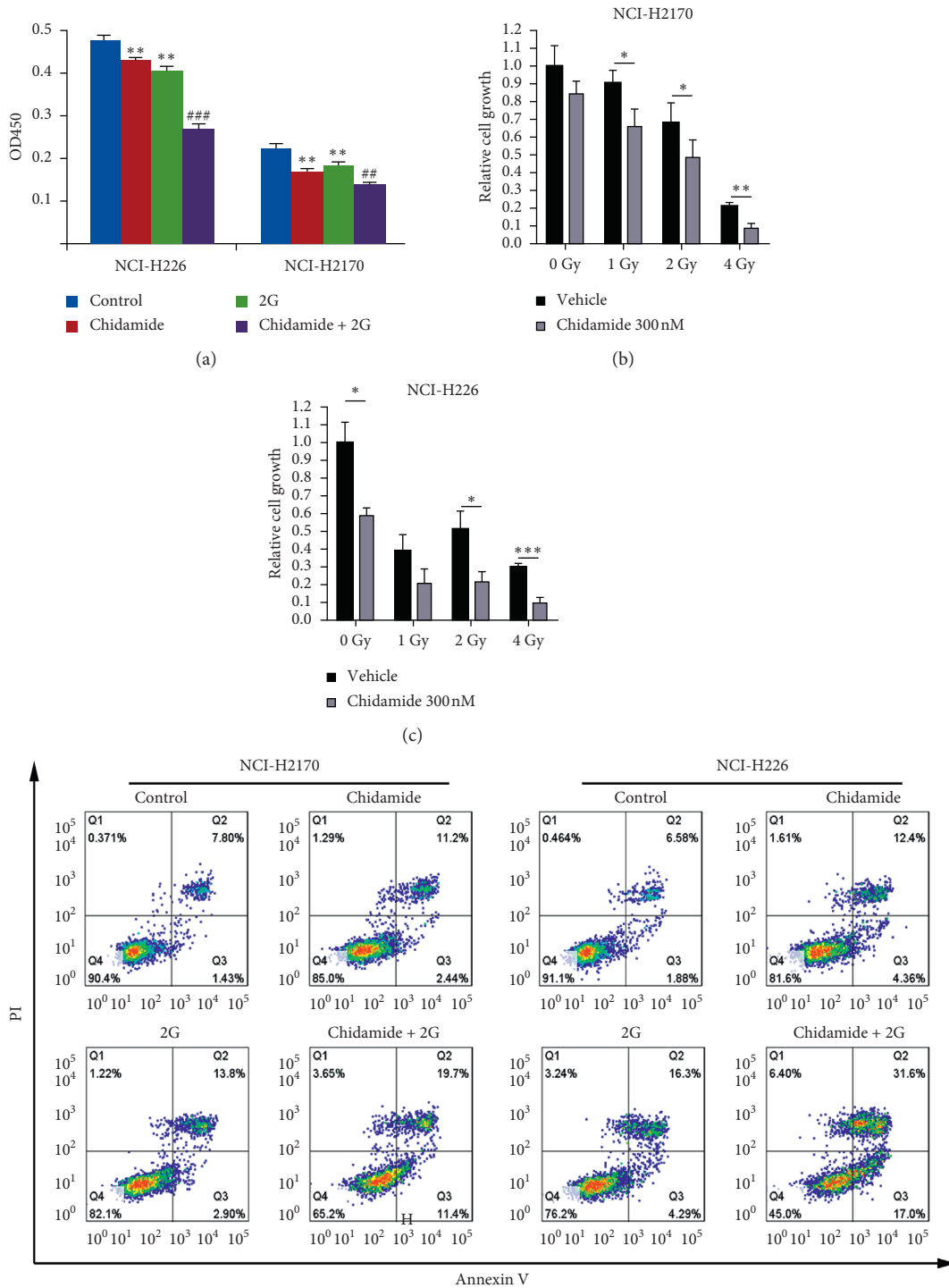
(d)

FIGURE 1: Continued.

FIGURE 1: Chidamide or chidamide combined with radiation synergistically promotes apoptosis in NCI-H2170 and NCI-H226 cells. (a) CCK8 assay to determine the cell viability of NCI-H2170 and NCI-H226 cells with chidamide (300 nM), radiation (2 Gy), and their combinational treatment, respectively. (b-c) The proliferation rate of NCI-H2170 (b) and NCI-H226 (c) cells with chidamide (300 nM) combined with radiation treatment at single doses of 0, 1, 2, and 4 Gy. (d)–(f) Annexin V-PI double staining to determine the apoptosis rate of NCI-H2170 and NCI-H226 cells with chidamide (300 nM), radiation (2 Gy), and their combinational treatment.

3.2. Chidamide Alone or a Combinational Treatment with Chidamide and Radiation Upregulates miR-375 Expression.

Next, we sought to elucidate the molecular mechanism underlying antitumor activity of chidamide. As miRNAs play a critical role in tumorigenesis, we hence focused on the expression profile alterations of miRNAs. The Affymetrix miRNA 2.0 Array was applied to identify differentially expressed miRNAs in NCI-H2170 and NCI-H226 cells in response to chidamide, radiotherapy, and their combinational treatment. Among the upregulated miRNAs, miR-375 showed the most remarkable fold (Figure 3(a)). Moreover, real-time PCR results also validated that both chidamide and chidamide plus radiation combinational treatment elevated the expression of miR-375 in NCI-H2170 and NCI-H226 cells (Figure 3(b)). Interestingly, radiation alone could not upregulate miR-375 expression, which indicates a crucial role of miR-375 in mediating the antitumor activity of chidamide against LSCC.

3.3. Suppression of miR-375 Reverses the Promoting Effect of Chidamide on LSCC Cell Apoptosis and Attenuates Reduction of Cancer Stem Cells Caused by Chidamide.

To delineate the role of miR-375 in the chidamide-induced LSCC cell apoptosis, we transfected NCI-H2170 and NCI-H226 cells with control inhibitor and miR-375 inhibitor following chidamide, radiation, and their combinational treatment, respectively. CCK8 assay was performed to measure the proliferation rate in these treated cells. As shown in Figures 4(a) and 4(b), transfection of miR-375 inhibitor effectively suppressed the expression of miR-375 both in NCI-H2170 (Figure 4(a)) and NCI-H226 (Figure 4(b)) cells. Moreover, miR-375 inhibition significantly reelevated the proliferation rates of NCI-H2170 and NCI-H226 cells, which were suppressed by chidamide or chidamide plus radiation combinational treatment (Figures 4(c) and 4(d)). In addition, both the chidamide

and chidamide plus radiation combinational treatment-induced cell apoptosis were rescued by miR-375 inhibitor (Figures 4(e)–4(j)). To further address the underlying mechanism, western blot analyses were performed to detect the expression of BAX and BCL2 in these treated cells. Data from the western blot analysis revealed that both chidamide and chidamide plus radiation combinational treatment upregulated the protein expression of BAX and downregulated BCL2 protein level, which were diminished by the transfection of miR-375 inhibitor (Figure 4(k)). Moreover, inhibition of miR-375 also reversed the population of ALDH$^+$ cells suppressed by chidamide alone or chidamide and radiation combinational treatment (Figures 5(a) and 5(b)).

3.4. Chidamide Reduces Xenograft Growth by Elevating miR-375 Expression In Vivo.

Our *in vitro* results demonstrated that chidamide inhibited LSCC cell proliferation and induced cell apoptosis via upregulation of miR-375 expression. Here we sought to further investigate the *in vivo* antitumor activity of chidamide. Xenograft nude mice were established by subcutaneous inoculation of treated NCI-H2170 cells. The results indicated that the cells treated with chidamide or chidamide plus radiation generated smaller tumors than control (Figures 6(a)–6(c)). Meanwhile, as Figures 6(d)–6(f) show, transfection with miR-375 reelevated the tumor growth rate suppressed by chidamide or chidamide plus radiation combinational treatment. In addition, these results were confirmed by *TUNEL* staining (Figures 6(g)–6(j)).

3.5. EIF4G3 Is a Direct Target of miR-375.

Furthermore, we identified the target genes of miR-375 using TargetScan online software (http://www.targetscan.org/vert_72/). Among the numerous targets, eukaryotic translation initiation factor 4 gamma 3 (EIF4G3) was selected as the
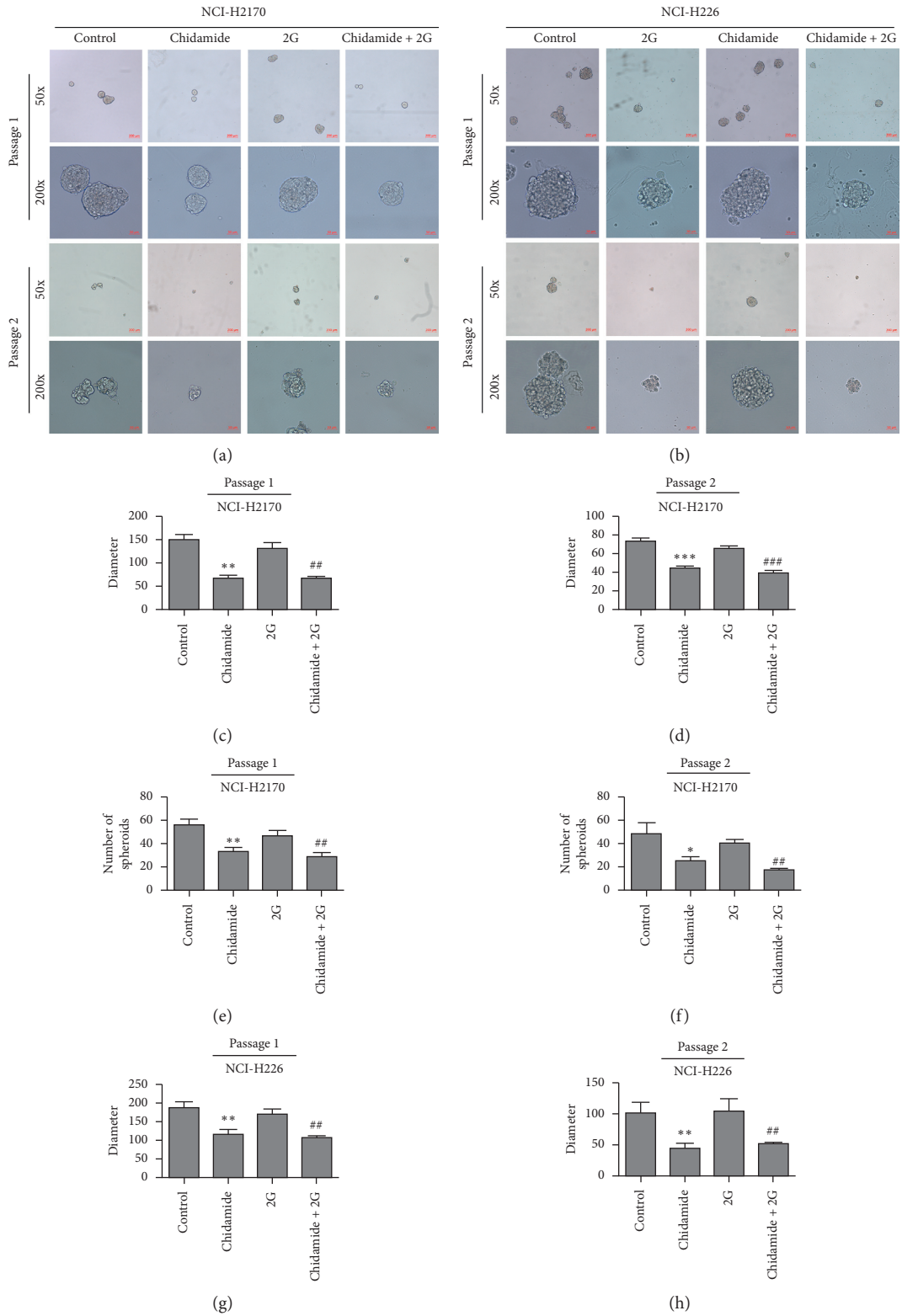
(a)

(b)

(c)

(d)

(e)

(f)

(g)

(h)

FIGURE 2: Continued.
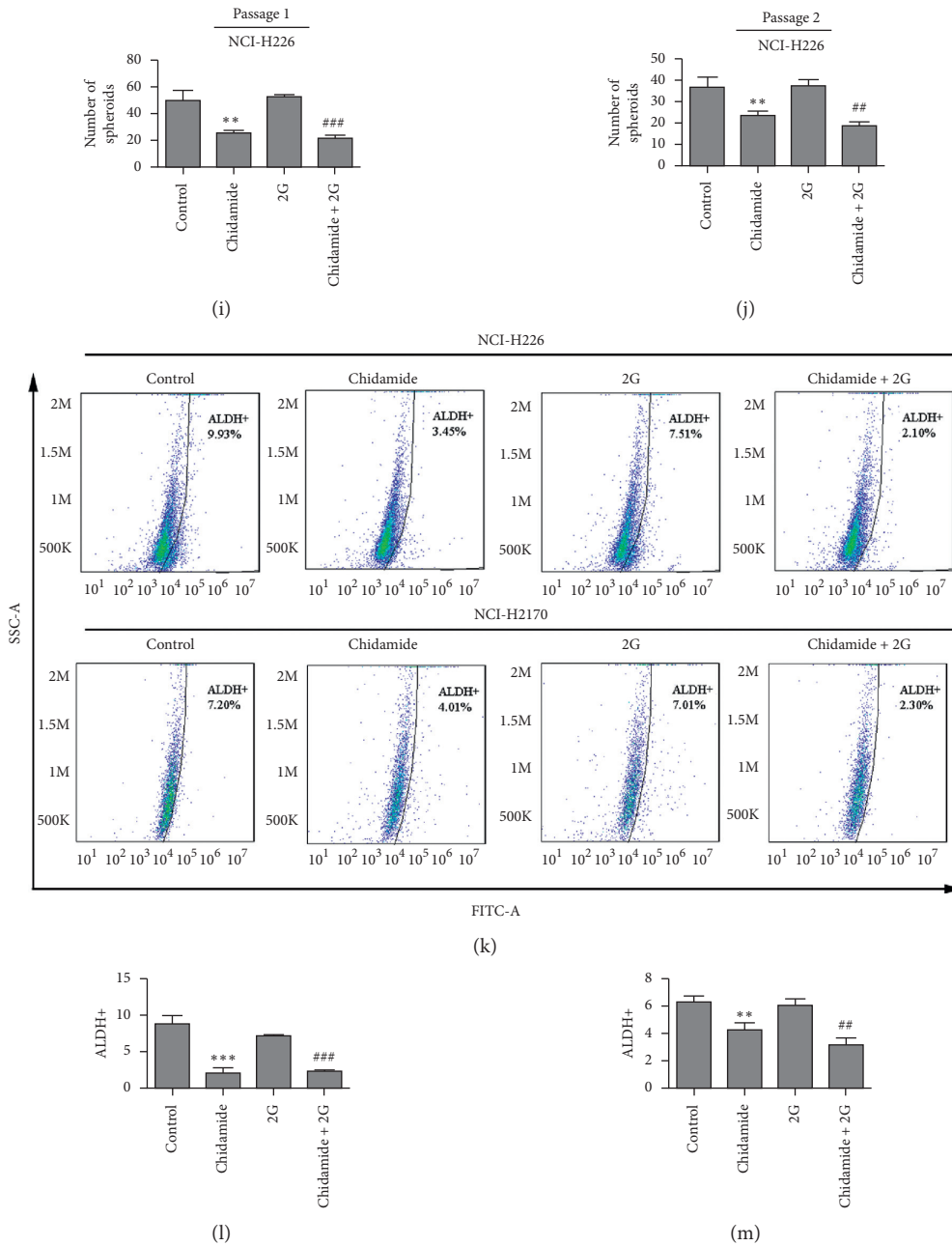
(i)

(j)

(k)

(l)

(m)

Figure 2: Chidamide or chidamide combined with radiation treatment suppressed cancer stemness in NCI-H2170 and NCI-H226 cells. (a–j) Sphere formation assay to determine the self-renewal capacities of NCI-H2170 and NCI-H226 cells treated with chidamide alone or a combination of chidamide and radiation. The sphere sizes and number were calculated in Figures 2(c)–2(j). (k–m) Treated cells with chidamide alone (300 nM) or combined with radiation treatment were subjected to ALDEFLUOR assay and the population of ALDH$^+$ cells were counted by flow cytometry. Statistical significance was determined by Student's t-test and indicated by $^*p < 0.05$; $^{**}p < 0.01$; and $^{***}p < 0.001$ (vs. control); $^{##}p < 0.01$; $^{###}p < 0.001$ (vs. Gy).

candidate target gene for miR-375 for further analysis, as its 3′-UTR contains two conserved binding regions of miR-375. The binding sites between miRNA-375 and EIF4G3 are shown in Figure 7(a). To clarify whether EIF4G3 is a direct target of miR-375, a dual-luciferase reporter assay was applied to determine the luciferase activities of EIF4G3 3′-UTR. As shown in Figure 7(b), transfection of miR-375 mimic significantly reduced the luciferase activity of the wild-type 3′-UTR of EIF4G3 compared with the control mimic-transfected cells (Figure 7(b)). However, less significant differences were found between cells transfected with control mimic and the miR-375 mimic when cotransfected with the mutated 3′-UTR of EIF4G3 (Figure 7(b)). Additionally, results of western blotting revealed that miRNA-375 significantly downregulated EIF4G3 (Figure 7(c)).
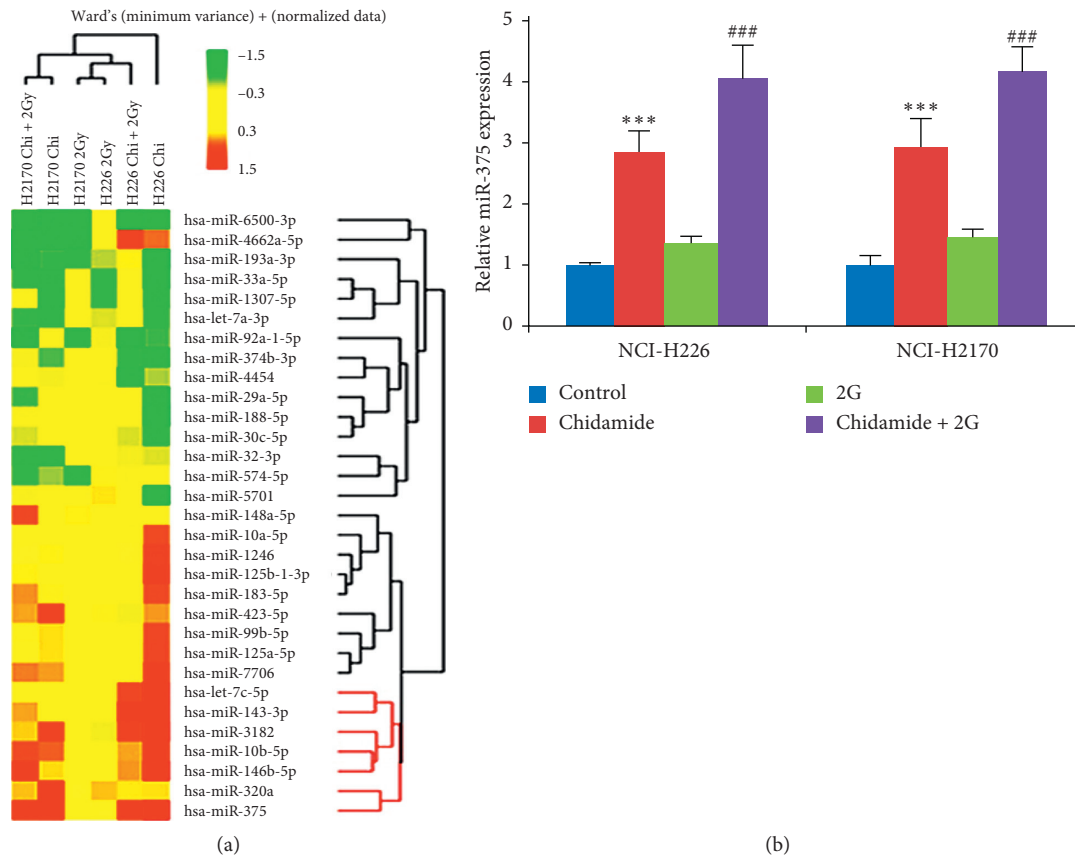
(a)

(b)

FIGURE 3: Chidamide alone or chidamide and radiation combinational treatment upregulates miR-375 in NCI-H2170 and NCI-H226 cells. (a) miRNA microarray to identify the differential expressed miRNAs in NCI-H2170 and NCI-H226 cells subjected to radiation (2 Gy), chidamide (300 nM), and their combinational treatment. (b) Real-time PCR to determine the expression of miR-375 in NCI-H2170 and NCI-H226 cells with indicated treatment. Statistical significance was determined by Student's t-test and indicated by $^*p < 0.05$; $^{**}p < 0.01$; and $^{***}p < 0.001$ (vs. control); $^{##}p < 0.01$; $^{###}p < 0.001$ (vs. Gy).

3.6. Silence of EIF4G3 Promotes Cell Apoptosis and Suppresses Xenograft Growth in NCI-H2170 and NCI-H226 Cells. To determine the role of EIF4G3 in the biological behaviors of LSCC cells, we first detected the expression of EIF4G3 in NCI-H2170 and NCI-H226 cells treated with chidamide or chidamide plus radiation combinational treatment. The results demonstrated that both chidamide and chidamide plus radiation combinational treatment suppressed EIF4G3 expression both at the mRNA and protein levels (Figures 7(d)–7(f)). Next, we silenced the expression of EIF4G3 in NCI-H2170 and NCI-H226 cells and found that silence of EIF4G3 significantly induced cell apoptosis (Figures 7(g)–7(i)). Moreover, silence of EIF4G3 in NCI-H2170 cells obviously suppressed xenograft growth (Figures 7(j)–7(l)).

Taken together, our study systematically demonstrates that chidamide and radiation synergistically promote LSCC cell apoptosis and suppressed tumor growth and stemness by modulating the miR-375-EIF4G3 axis.

4. Discussion

The HDAC inhibitors can be used for various diseases, some of which have entered clinical trials. In cancer, HDAC inhibitors are becoming promising novel tumor therapeutic

drugs exerting anticancer function across a wide range of cancers, especially in leukemia. Chidamide, an orally active novel HDAC inhibitor of the benzamide class, selectively inhibits HDAC1, HDAC2, HDAC3, as well as HDAC10. In pancreatic cancers, chidamide augments gemcitabine-induced cell growth arrest and apoptosis by downregulating the antiapoptotic gene MCL-1 [31]. Chidamide has been tested extensively for its tumor inhibitory activity. In colon cancer cells, chidamide suppresses cell proliferation and induces cell cycle arrest by inhibiting the PI3K/AKT and RAS/MAPK signaling pathways. In non-small-cell lung cancer cell lines, chidamide and carboplatin synergistically induce cell growth arrest [11]. In the present study, we demonstrated that chidamide-induced cellular growth inhibition of NCI-H2170 and NCI-H226 LSCC cells and it synergistically augmented radiation-induced cell apoptosis. Previous reported studies have demonstrated that HDAC inhibitors show significant single-agent anticancer activity in T-cell lymphomas. Consistent with these results, our data also show that chidamide alone induces cell apoptosis and suppresses tumor growth in LSCC.

Although previously published data also demonstrate chidamide induces cell apoptosis, the underlying mechanism is not very clear. Our data showed that both chidamide
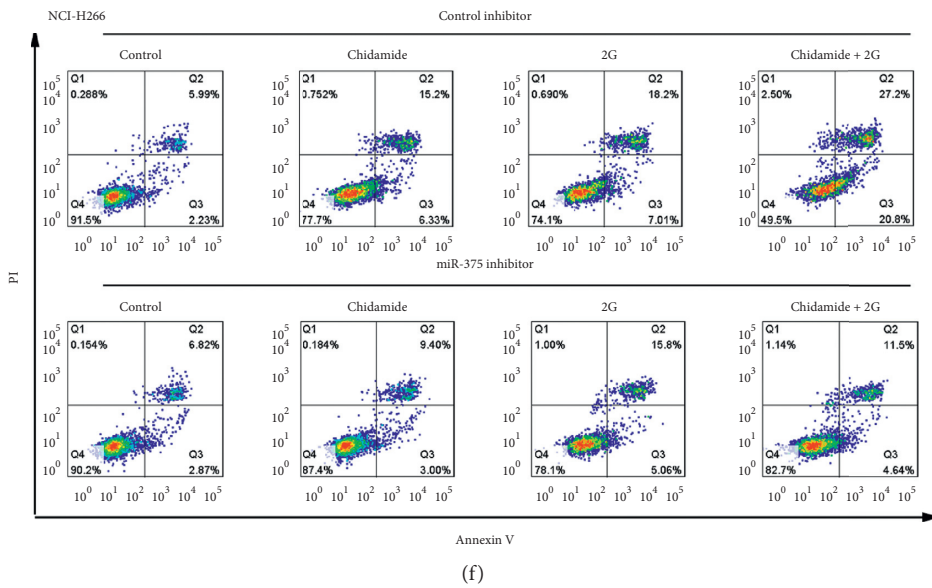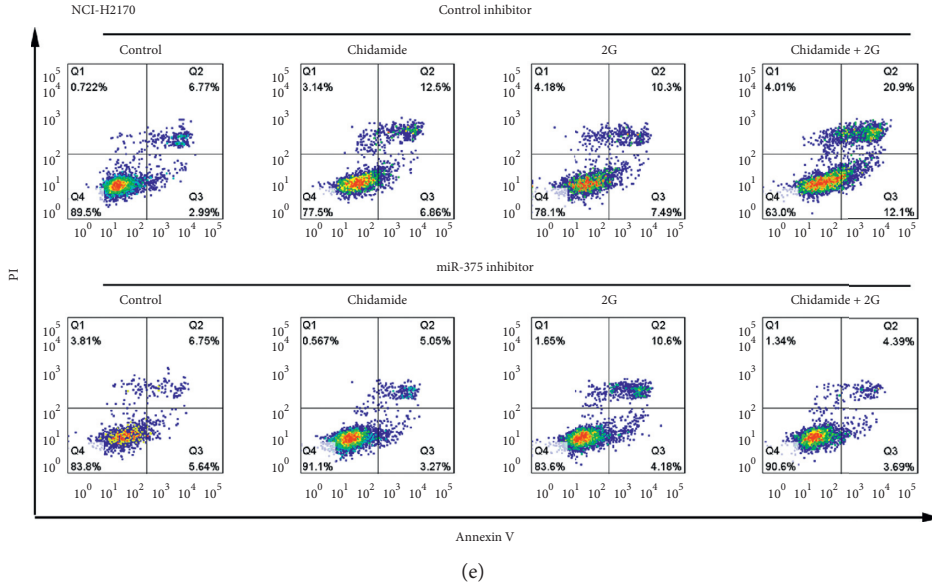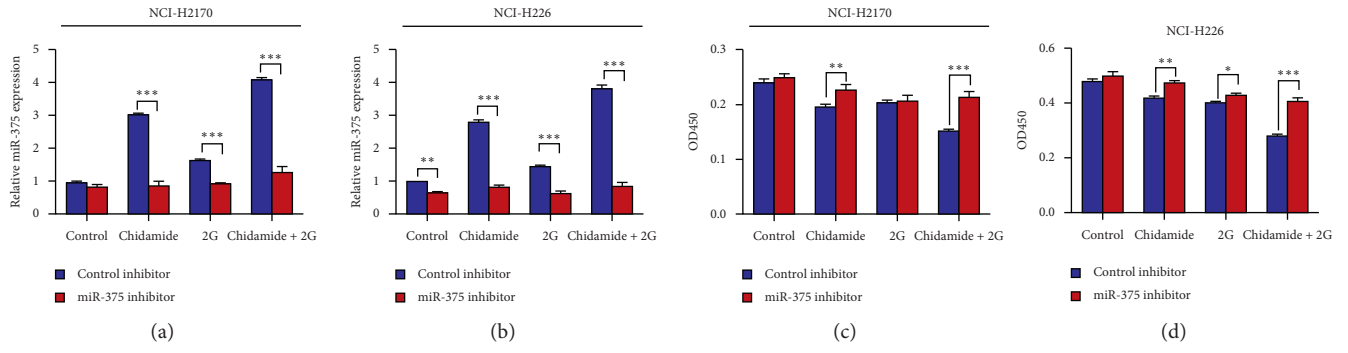
(a)

(b)

(c)

(d)

(e)

(f)

FIGURE 4: Continued.
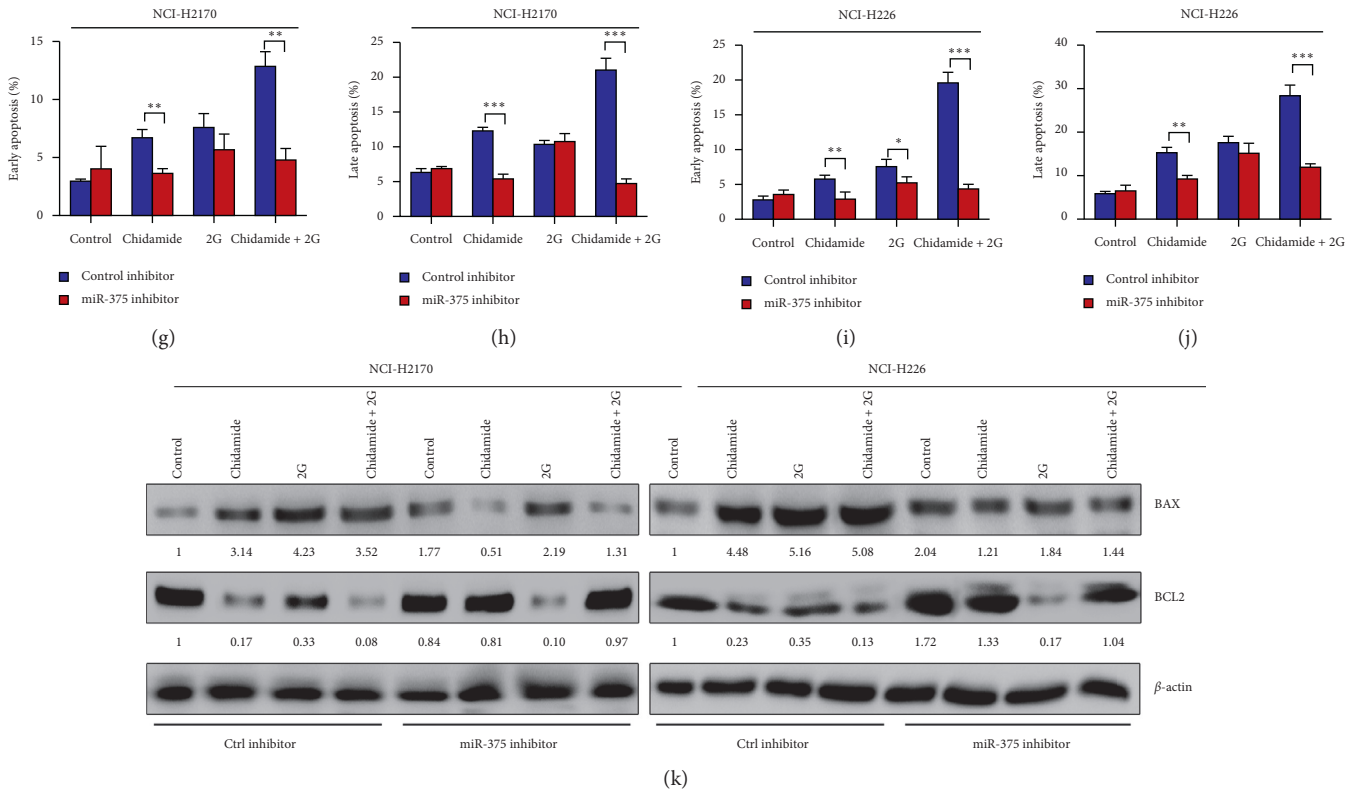
(g) (h) (i) (j)

(k)

FIGURE 4: Suppression of miR-375 reversed chidamide and chidamide plus radiation combinational treatment-induced apoptosis in NCI-H2170 and NCI-H226 cells. (a) Real-time PCR to determine the expression of miR-375 in control mimic and miR-375 mimic-transfected NCI-H2170 and NCI-H226 cells with radiation (2 Gy), chidamide (300 nM), and their combinational treatment, respectively. (b) CCK8 assay to evaluate the cell viability of NCI-H2170 and NCI-H226 cells with indicated treatment. (c–j) Annexin V-PI double staining to determine the apoptosis rate of NCI-H2170 and NCI-H226 cells with indicated treatment. (k) The expression of proapoptotic protein BAX and antiapoptotic protein BCL2 in NCI-H2170 and NCI-H226 cells with indicated treatment, determined by western blot analysis. All the data were statistically analyzed by Student's t-test. $^*p < 0.05$; $^{**}p < 0.01$; and $^{***}p < 0.001$.
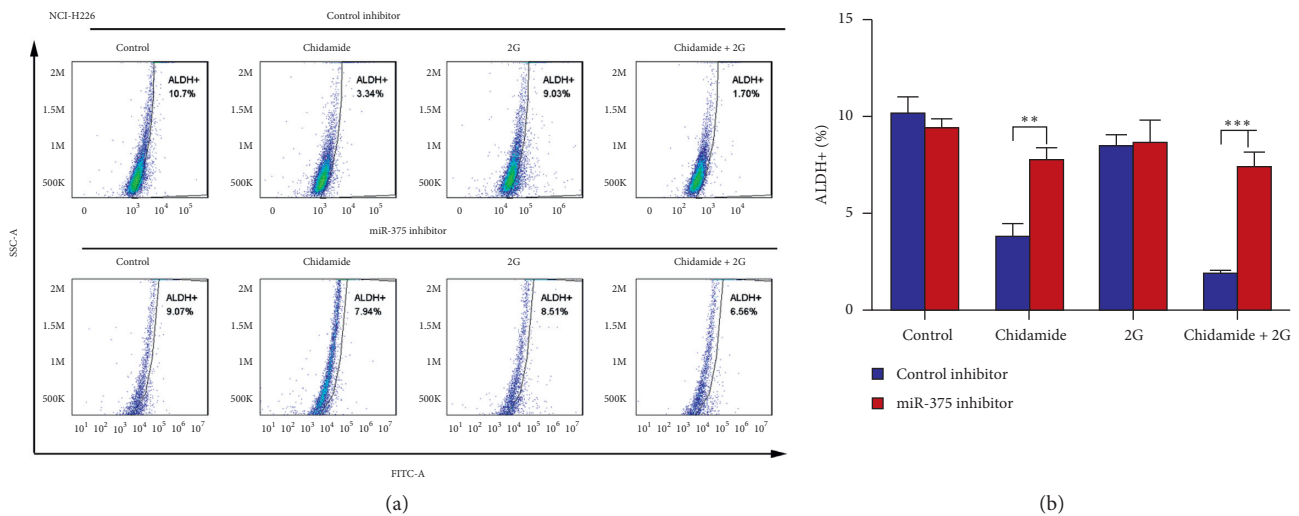

(a) (b)

FIGURE 5: Inhibition of miR-375 attenuated chidamide and chidamide plus radiation combinational treatment-induced suppression of cancer stemness in NCI-H2170 and NCI-H226 cells. (a) ALDEFLUOR assay was performed to evaluate the population of ALDH$^+$ cells of NCI-H2170 and NCI-H226 cells with indicated treatment and the representative images were shown. (b) Statistic analysis of ALDH$^+$ populations of NCI-H2170 and NCI-H226 cells with indicated treatment. All the data were statistically analyzed by Student's t-test. $^*p < 0.05$; $^{**}p < 0.01$; and $^{***}p < 0.001$.
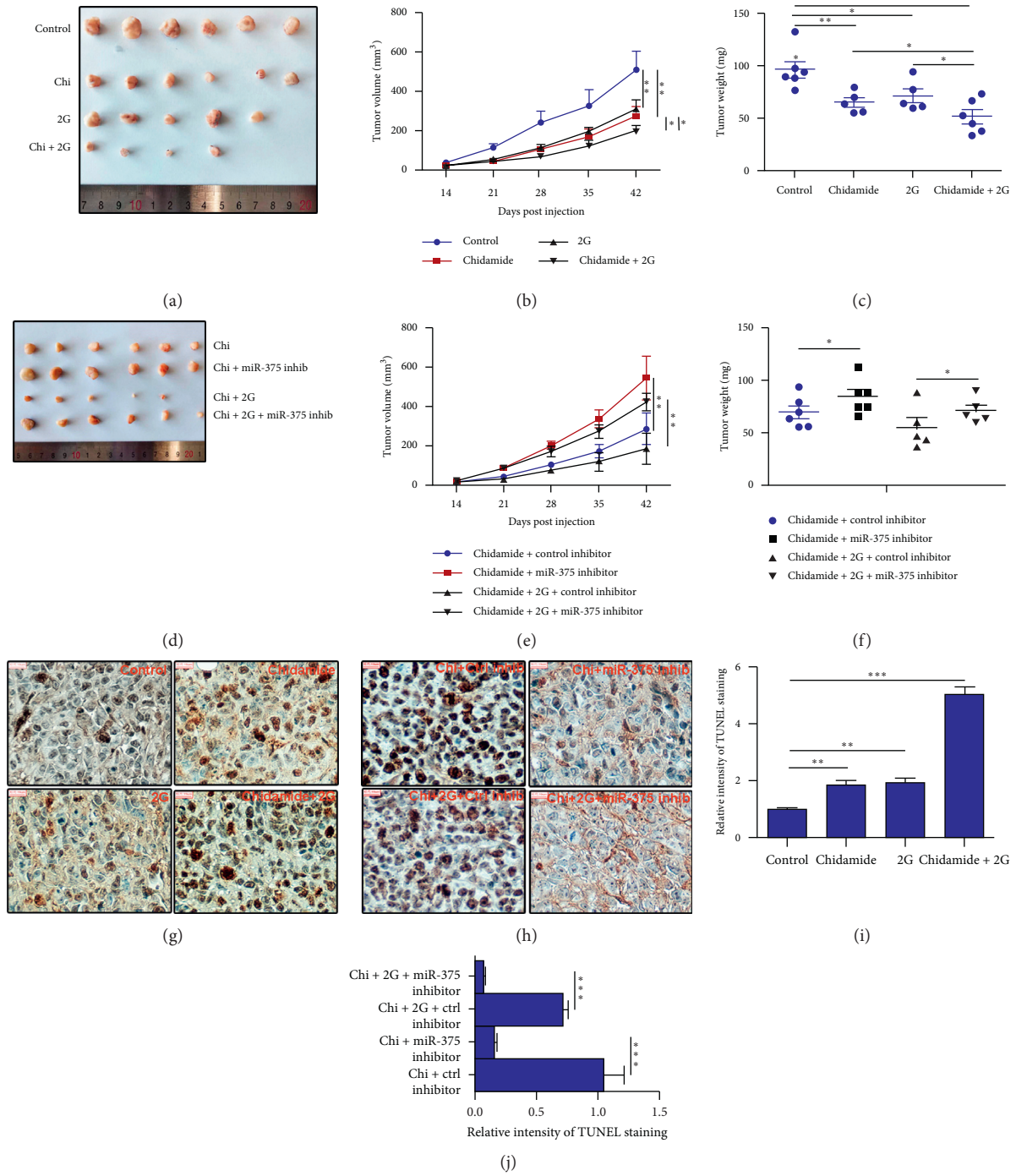
(a)

(b)

(c)

(d)

(e)

(f)

(g)

(h)

(i)

(j)

Figure 6: miR-375 inhibition rescued chidamide and chidamide plus radiation combinational treatment-induced tumor growth arrest in NCI-H2170 and NCI-H226 cells, respectively. (a–c) Chidamide, radiation, and their combinational treatment inhibited tumor growth in NCI-H2170 cells. Tumor growth curves and tumor weight analysis are shown in Figures 3(b) and 3(c), respectively. (d–f) Suppression of miR-375 reversed chidamide and chidamide plus radiation combinational treatment-induced tumor growth arrest in NCI-H2170 and NCI-H226 cells, respectively. Tumor growth curves and tumor weight analysis are shown in Figures 3(e) and 3(f), respectively. (g-h) *TUNEL* staining to demonstrate the cell apoptosis rate in indicated xenograft tissues. (i-j) The relative intensity of TUNEL staining in (g) and (h). Scale bars: 100 μm. All the data were statistically analyzed by Student's t-test. $^{*}p < 0.05$; $^{**}p < 0.01$.

(a)

(b)

(c)

(d)

(e)

(f)

(g)

FIGURE 7: Continued.
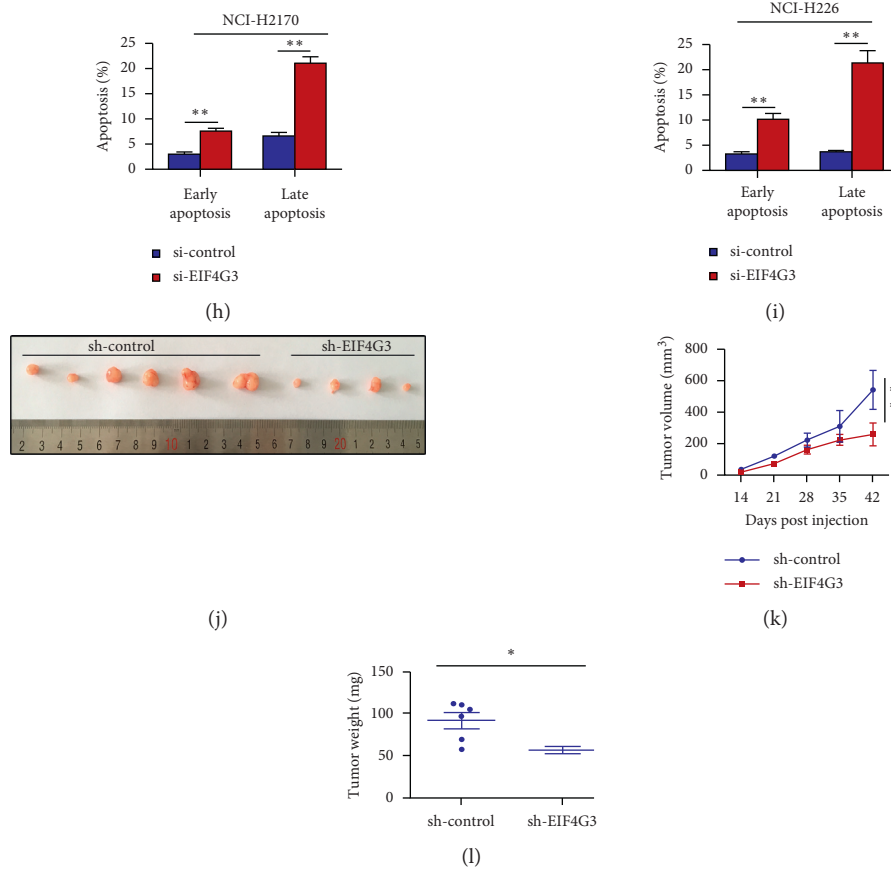
(h)

(i)

(j)

(k)

(l)

Figure 7: EIF4G3 is a direct target of miR-375. (a) Schematic view to present putative miR-375 binding sites in the 3′UTR region of EIF4G3. The mutant sequences are shown below. (b) Luciferase reporter assay to assess the effect of miR-375 on the transcription of Renilla luciferase with 3′UTR of EIF4G3 expression. Data were shown as means ± SEM. Each group was performed in six biological replicates. $^*p < 0.05$; $^{**}p < 0.01$. (c) Western blot analysis to determine the protein expression of EIF4G3 in NCI-H2170 and NCI-H226 cells transfected with miR-375 mimic at the concentration of 0 nM, 50 nM, and 100 nM, respectively. (d)-(e) Detection of the mRNA expression of EIF4G3 in NCI-H2170 and NCI-H226 cells with indicated treatment. (f) Western blot analysis to detect the expression of EIF4G3 in the indicated groups. (g–i) The apoptosis rate of NCI-H2170 and NCI-H226 cells transfected with 100 nM of EIF4G3 siRNA, compared with control. (j–l) EIF4G3 inhibition significantly suppresses tumor growth *in vivo* in NCI-H2170 cells. Tumor growth curves and tumor weight analysis are shown in Figures 5(h) and 5(i), respectively. All the data were statistically analyzed by Student's t-test. $^*p < 0.05$; $^{**}p < 0.01$; and $^{***}p < 0.001$.

and chidamide plus radiation combinational treatment induced the expression of endogenous miR-375 in NCI-H2170 and NCI-H226 cells. Moreover, rescue experiments indicated that the apoptosis-promoting function of chidamide depended on the upregulation of miR-375 expression. In addition, the scaffold protein EIF4G3 was identified as a direct target of miR-375 and the suppression of EIF4G3 induced cell apoptosis and inhibited tumor growth in NCI-2170 and NCI-H226 cells. These data conclude that chidamide exhibits a synergistic effect with radiation therapy on LSCC by modulating the miR-375-EIF4G3 axis. Our finding may represent a universal mechanism underlying the synergistic antitumor interactions between HDAC inhibitors and DNA damaging agents in tumorigenesis, which should be confirmed in our future studies.

In the study of NCI-H2170 and NCI-H226 cell lines, it has been found that chidamide, radiation, and their combinational treatment could exert an anti-LSCC effect. However, unlike chidamide and chidamide plus radiation combinational treatment, radiation alone could not upregulate the expression of miR-375 and downregulate the expression of EIF4G3. These results suggest the miR-375/EIF4G3 axis may not be involved in the regulation of radiotherapy alone-induced cell apoptosis. On the other hand, acquired drug resistance frequently occurred to destroy effective therapy with chemotherapeutic agents, leading to an unsatisfactory clinical outcome. Therefore, HDAC inhibitor combined with radiation at different dose might have multiple targets and pathways to induce cell apoptosis.

In conclusion, our results systematically explored the role of miR-375/EIF4G3 axis in chidamide-induced LSCC apoptosis and tumor growth arrest, which may afford an effective strategy to overcome the drug resistance of chidamide in clinical cancer therapy.

Abbreviations

miRNA: MicroRNA
HDAC: Histone deacetylase
PTCL: Peripheral T-cell lymphoma
LSCC: Lung squamous cell carcinomas
SCLC: Small-cell lung cancer
NSCLC: Non-small-cell lung cancer
LCLC: Lung large-cell carcinoma
LungNET: Lung neuroendocrine tumor
LUAD: Lung adenocarcinoma
3′-UTRs: Untranslated regions
EIF4G3:   Eukaryotic translation initiation factor 4 gamma 3
FBS: Fetal bovine serum
ATCC: American Type Culture Collection
DMEM: Dulbecco's Modified Eagle Medium
DMSO: Dimethyl sulfoxide.

Data Availability

The data used to support the findings of this study are available from the corresponding author upon request.

Conflicts of Interest

All the authors declare that they have no conflicts of interest regarding the publication of this paper.

Acknowledgments

References

[1] M. Wu, G. Wang, W. Tian, Y. Deng, and Y. Xu, "MiRNA-based therapeutics for lung cancer," *Current Pharmaceutical Design*, vol. 23, no. 39, pp. 5989–5996, 2018.

[2] X.-C. Wang, L.-Q. Du, H. Zhang et al., "Expression of miRNA-130a in nonsmall cell lung cancer," *The American Journal of the Medical Sciences*, vol. 340, no. 5, pp. 385–388, 2010.

[3] C. Zhao, F. Lu, H. Chen et al., "Clinical significance of circulating miRNA detection in lung cancer," *Medical Oncology*, vol. 33, p. 41, 2016.

[4] X. Li, H.-l. Wang, X. Peng, H.-f. Zhou, and X. Wang, "miR-1297 mediates PTEN expression and contributes to cell progression in LSCC," *Biochemical and Biophysical Research Communications*, vol. 427, no. 2, pp. 254–260, 2012.

[5] Y. Xu, P. Zhang, and Y. Liu, "Chidamide tablets: HDAC inhibition to treat lymphoma," *Drugs of Today*, vol. 53, no. 3, pp. 167–176, 2017.

[6] X. Hu, L. Wang, L. Wang et al., "A phase I trial of an oral subtype-selective histone deacetylase inhibitor, chidamide, in combination with paclitaxel and carboplatin in patients with advanced non-small cell lung cancer," *Chinese Journal of Cancer Research*, vol. 28, no. 4, pp. 444–451, 2016.

[7] S.-H. Lin, B.-Y. Wang, C.-H. Lin et al., "Chidamide alleviates TGF-β-induced epithelial-mesenchymal transition in lung cancer cell lines," *Molecular Biology Reports*, vol. 43, no. 7, pp. 687–695, 2016.

[8] L. Liu, B. Chen, S. Qin et al., "A novel histone deacetylase inhibitor chidamide induces apoptosis of human colon cancer cells," *Biochemical and Biophysical Research Communications*, vol. 392, no. 2, pp. 190–195, 2010.

[9] L. Liu, S. Qiu, Y. Liu et al., "Chidamide and 5-flurouracil show a synergistic antitumor effect on human colon cancer xenografts in nude mice," *Neoplasma*, vol. 63, pp. 193–200, 2016.

[10] S. Luo, K. Ma, H. Zhu et al., "Molecular, biological characterization and drug sensitivity of chidamide-resistant non-small cell lung cancer cells," *Oncology Letters*, vol. 14, pp. 6869–6875, 2017.

[11] Y. Zhou, D.-S. Pan, S. Shan et al., "Non-toxic dose chidamide synergistically enhances platinum-induced DNA damage responses and apoptosis in non-small-cell lung cancer cells," *Biomedicine & Pharmacotherapy*, vol. 68, no. 4, pp. 483–491, 2014.

[12] A. Markou, M. Zavridou, and E. S. Lianidou, "miRNA-21 as a novel therapeutic target in lung cancer," *Lung Cancer (Auckland, N.Z.)*, vol. 7, pp. 19–27, 2016.

[13] R. Rupaimoole, G. A. Calin, G. Lopez-Berestein, and A. K. Sood, "miRNA deregulation in cancer cells and the tumor microenvironment," *Cancer Discovery*, vol. 6, no. 3, pp. 235–246, 2016.

[14] X. Tian, F. Tao, B. Zhang, J.-T. Dong, and Z. Zhang, "The miR-203/SNAI2 axis regulates prostate tumor growth, migration, angiogenesis and stemness potentially by modulating GSK-3β/β-CATENIN signal pathway," *IUBMB Life*, vol. 70, no. 3, pp. 224–236, 2018.

[15] Y. K. Song, Y. Wang, Y. Y. Wen, P. Zhao, and Z. J. Bian, "MicroRNA-22 suppresses breast cancer cell growth and increases paclitaxel sensitivity by targeting NRAS," *Technology in Cancer Research & Treatment*, vol. 17, 2018.

[16] F. Jiang, Q. Yu, Y. Chu et al., "MicroRNA-98-5p inhibits proliferation and metastasis in non-small cell lung cancer by targeting TGFBR1," *International Journal of Oncology*, vol. 54, 2018.

[17] Q. Yang, "MicroRNA-5195-3p plays a suppressive role in cell proliferation, migration and invasion by targeting MYO6 in human non-small cell lung cancer," *Bioscience, Biotechnology, and Biochemistry*, vol. 83, no. 2, pp. 212–220, 2018.

[18] M. N. Poy, L. Eliasson, J. Krutzfeldt et al., "A pancreatic islet-specific microRNA regulates insulin secretion," *Nature*, vol. 432, no. 7014, pp. 226–230, 2004.

[19] J.-W. Yan, J.-S. Lin, and X.-X. He, "The emerging role of miR-375 in cancer," *International Journal of Cancer*, vol. 135, no. 5, pp. 1011–1018, 2014.

[20] M. Chu, Y. Chang, P. Li, Y. Guo, K. Zhang, and W. Gao, "Androgen receptor is negatively correlated with the methylation-mediated transcriptional repression of miR-375 in human prostate cancer cells," *Oncology Reports*, vol. 31, no. 1, pp. 34–40, 2014.

[21] M. Hao, W. Zhao, L. Zhang, H. Wang, and X. Yang, "Low folate levels are associated with methylation-mediated transcriptional repression of miR-203 and miR-375 during cervical carcinogenesis," *Oncology Letters*, vol. 11, no. 6, pp. 3863–3869, 2016.

[22] S. L. Liu, Y. F. Sui, and M. Z. Lin, "MiR-375 is epigenetically downregulated due to promoter methylation and modulates

multi-drug resistance in breast cancer cells via targeting YBX1," *European Review for Medical and Pharmacological Sciences*, vol. 20, pp. 3223–3229, 2016.

[23] H. Yu, L. Jiang, C. Sun et al., "Decreased circulating miR-375: a potential biomarker for patients with non-small-cell lung cancer," *Gene*, vol. 534, no. 1, pp. 60–65, 2013.

[24] W.-H. Zhang, J.-H. Gui, C.-Z. Wang et al., "The identification of miR-375 as a potential biomarker in distal gastric adenocarcinoma," *Oncology Research Featuring Preclinical and Clinical Cancer Therapeutics*, vol. 20, no. 4, pp. 139–147, 2012.

[25] Y. Jin, Y. Liu, J. Zhang et al., "The expression of miR-375 is associated with carcinogenesis in three subtypes of lung cancer," *PLoS One*, vol. 10, Article ID e0144187, 2015.

[26] Y. S. Ma, Z. W. Lv, F. Yu et al., "MicroRNA-302a/d inhibits the self-renewal capability and cell cycle entry of liver cancer stem cells by targeting the E2F7/AKT axis," *Journal of Experimental & Clinical Cancer Research*, vol. 37, p. 252, 2018.

[27] C. Sun, X. Zhang, Y. Chen, Q. Jia, J. Yang, and Y. Shu, "MicroRNA-365 suppresses cell growth and invasion in esophageal squamous cell carcinoma by modulating phosphoserine aminotransferase 1," *Cancer Management and Research*, vol. 10, pp. 4581–4590, 2018.

[28] J. Chu, Y. Li, X. Fan et al., "MiR-4319 suppress the malignancy of triple-negative breast cancer by regulating self-renewal and tumorigenesis of stem cells," *Cellular Physiology and Biochemistry*, vol. 48, no. 2, pp. 593–604, 2018.

[29] E. Gheytanchi, M. Naseri, F. Karimi-Busheri et al., "Morphological and molecular characteristics of spheroid formation in HT-29 and Caco-2 colorectal cancer cell lines," *Cancer Cell International*, vol. 21, p. 204, 2021.

[30] M. Colombel, S. Filleur, P. Fournier et al., "Androgens repress the expression of the angiogenesis inhibitor thrombospondin-1 in normal and neoplastic prostate," *Cancer Research*, vol. 65, pp. 300–308, 2005.

[31] Z. Qiao, S. Ren, W. Li et al., "Chidamide, a novel histone deacetylase inhibitor, synergistically enhances gemcitabine cytotoxicity in pancreatic cancer cells," *Biochemical and Biophysical Research Communications*, vol. 434, no. 1, pp. 95–101, 2013.